LA-UR-02-4760

ABSTRACT

EDM Collaboration Meeting

These viewgraphs are a record of the meeting held on July 19-20, 2002, for planning the EDM experiment.

The LANSCE experiment to search for the electric dipole moment (EDM) of the neutron proposes a sensitivity of 4 x 10**-28 e-cm. It uses the cold neutron beam from a coupled liquid hydrogen moderator and a 10-cm x 10-cm supermirror guide to illuminate a superthermal 4He source. Systematic errors are suppressed by the addition of trace amounts of 3He as a magnetometer. See the following web site for more information: http://p25ext.lanl.gov/edm/edm.html

LOS ALAMOS NATIONAL LABORATORY
3 9338 01038 2595

EDM Collaboration Meeting
July 19-20, 2002
Los Alamos, NM

Agenda for EDM Meeting
July 19-20, 2002

July 19

09:00 - Welcome - John McClelland (Los Alamos)
09:10 - Statement of purpose - Martin Cooper (Los Alamos)
09:20 - DOE reaction to the pre-proposal - Martin Cooper (Los Alamos)
09:30 - EDM project development in the next 1.5 years - Steve Lamoreaux (Los Alamos)
10:00 - Discussion
10:15 - A new measurement at NIST of the neutron storage time in a TPB coated cell - Jen-Chieh Peng (Illinois)
10:30 - Discussion

10:45 - Coffee

11:15 - New ideas regarding light collection and backgrounds - Paul Huffman (NIST)
11:30 - Discussion
11:45 - How well can we identify neutron beta decays? - Bob Golub (HMI)
12:00 - Discussion
12:15 - Monte-Carlo studies - Martin Cooper (Los Alamos)
12:30 - Discussion

12:45 - Lunch

13:45 - Fitting into LANSCE ER-2 - Jan Boissevain (Los Alamos)
14:00 - Discussion
14:15 - Tour of LANSCE ER-2 and Building 10 Lab - Seppo Penttila (Los Alamos)
15:15 - Separating the purifier from the dilution refrigerator, an alternate design - Paul Huffman (NIST)
15:30 - Discussion

15:45 - Coffee

16:15 - Proposed tests of SQUIDs - Michelle Espy (Los Alamos)
16:30 - Discussion
16:45 - Shortening the magnet by better matching of boundary conditions; magnetic shielding issues - Brad Filippone (Caltech)
17:00 - Discussion
17:15 - Modifications of the apparatus to incorporate the dressed-spin technique - Bob Golub (HMI)
17:30 - Discussion

19:00 - Dinner at ...

July 20

09:00 - Update on the HV-test apparatus - Debbie Clark (Los Alamos)
09:15 - Discussion
09:30 - Measuring the Kerr effect at crogenic temperatures - Alex Sushkov (UC-Berkeley)
09:45 - Discussion
10:00 - Update on the polarized 3He source - Justin Torgerson (LANL)
10:15 - Discussion

10:30 - Coffee

11:00 - Experiences with hexapole state selectors - Janos Fuzi (Budapest)
11:30 - Discussion
11:45 - Experiments relavent to transporting 3He into the superfluid He and the 3He polarization lifetime - Mike Hayden (Simon-Fraser)
12:15 - Discussion

12:30 - Lunch

14:00 - Determining the projects to be undertaken at each institution - moderated by Steve Lamoreaux (Los Alamos)

15:15 - Coffee

15:45 - Future telephone conference calls - moderated by Martin Cooper (Los Alamos)
16:00 - Development of a financial strategy - moderated by Martin Cooper (Los Alamos)
16:45 - Adjourn

Welcome
John McClelland (Los Alamos)

Statement of purpose
Martin Cooper (Los Alamos)

MECHANICS

Agenda

Dinner at 7:00 PM (19:00) at the Central Avenue Grill

- Located on Central Avenue (1 block north of Trinity) across from the post office
- Must pre-order your meal and beverage by circling your choices and putting down your name

Sign into our visitor log during first coffee break

Attendance list

Telephone, FAX, and E-mail list plus institutional addresses

Turn in you badges to me at end of the meeting (Debbie will keep them)

PURPOSE

Exchange scientific ideas
Establish the R&D plan for the experiment
•Speakers should list tasks on blackboard
Establish who will work on what for the next 1.5 years
Open dialogue on long term commitments
Open dialogue on a funding plan

DOE reaction to the pre-proposal
Martin Cooper (Los Alamos)

DOE REACTION TO THE PRE-PROPOSAL

Jehanne Simon-Gillo / Gene Henry 18 July 2002

Next week in writing

Nice job on the physics case

Many external comments on how exciting the project is

Additions to make a real proposal

- Table of technical risks and how we are dealing with them
- Safety issues
- Order of magnitude and source of operating funds
- Potential commitment of physicists
- Facility modifications - their character and costs
- More detailed cost estimates -

--Rough breakdown into R&D, engineering,construction, pre-ops,TEC, and TPC

--Realistic contingency analysis-a repetitive effort for CDR

DOE REACTION TO THE PRE-PROPOSAL

Jehanne Simon-Gillo / Gene Henry 18 July 2002

- Milestones not understandable - "ready" means what, e.g. designed, constructed, installed, commissioned
- Breakout the cost of people from the cost of equipment

We should continue to work on the proposal

FY'05 funding still a possibility

We will need the upgraded proposal to establish "mission need"

Peter Rosen will want the upgrade for believability

Two conditions to proceed:

- Sorting out of the SNS beamline
- Integrated strategy for national neutron-physics program endorsed by the community

  Community should take the initiative (in the form of a conference?)

EDM project development in the next 1.5 years

Steve Lamoreaux (Los Alamos)

The Neutron EDM Project over the Next 1.5 Years

S.K. Lamoreaux

1. Magnetic shielding; ferromagnetic vs. superconducting

   a. magnetic field generation
   b. RF coil
   c. Johnson noise etc. from materials

2. Studies of scintillation
   a. background
   b. cross effects (leakage currents, other cross effects with Larmor precession)
   c. event identification

3. Polarization of He-3

4. Transport and Storage of Polarized He-3

5. High Voltage Tests

   a. radiation effects
   b. wall coating stability
   c. measurements of field strength, uniformity
   d. effects on scintillation
   e. capacitive voltage multiplier

6. Cold neutron beam optics

7. General cryogenic design

8. Tests of SQUIDS in realistic environments

9. Investigation of incorporation of dress spin technique

10. 3-He diffusion at low concentrations

ASAP Tasks.

1. Ferromagnetic cryogenic Shields
2. ^3He + Transport T_2, T_1
3. Aftepulse study,
4. HV effects on scintillations
5. HV effects on cell

General Technical Study

1. Measurement of E field
   Dima et al. UCB
2. Valves
3. Cross effects in scintillation/
   Larmor precession
4. UCN polarization lifetime in cell
5. Stray charge in cell
6. ^3He diffusion at low concentration
   Spin diffusion
   Temp gradient effects
7. Monte Carlo study of polarization
   Splitting guide
8. Study of backgrounds
9. RF Coil
10. Other wall coatings, Neon etc.
11. Study with Mike Hayden's technique
    + SQUIDS
    → Preliminary study in full apparatus

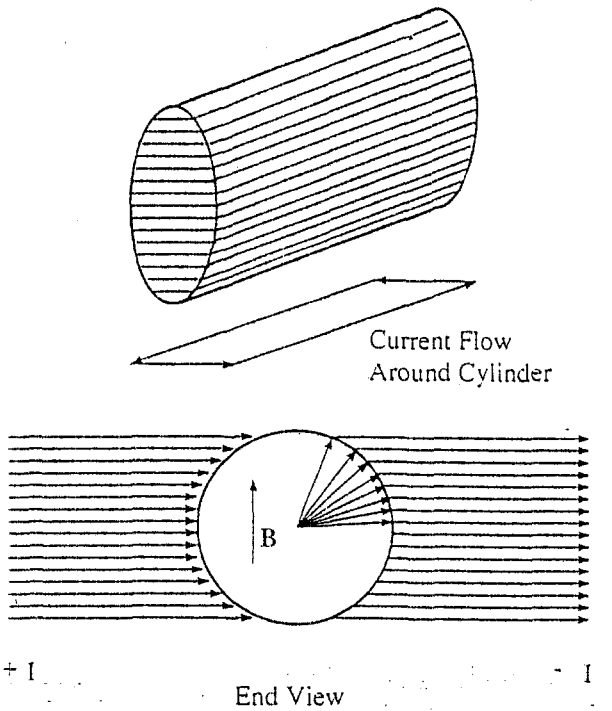

FIG. 1: Cosine magnetic field winding.

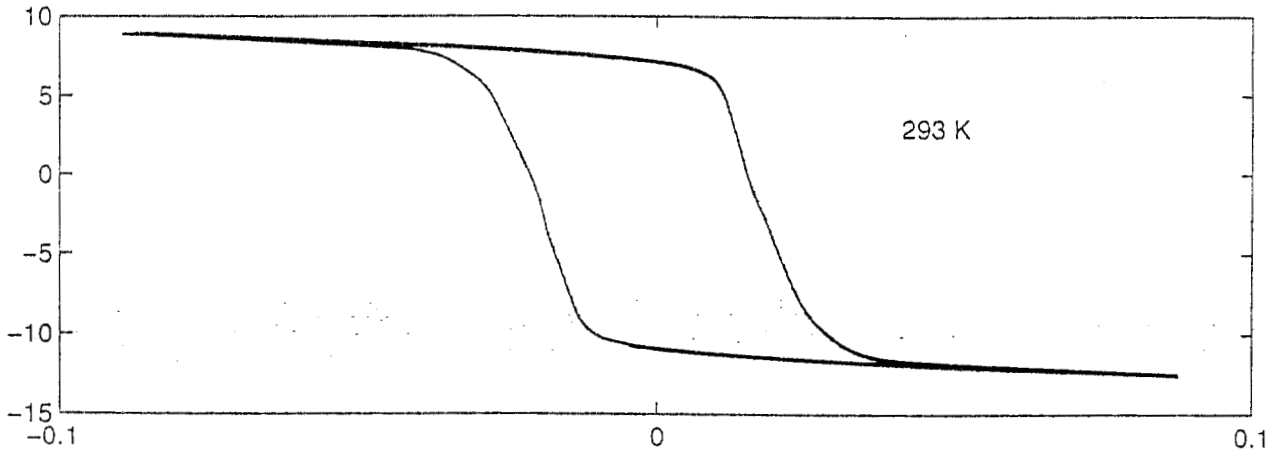
10
5
0
-5
-10
-15
-0.1
0
0.1
293 K

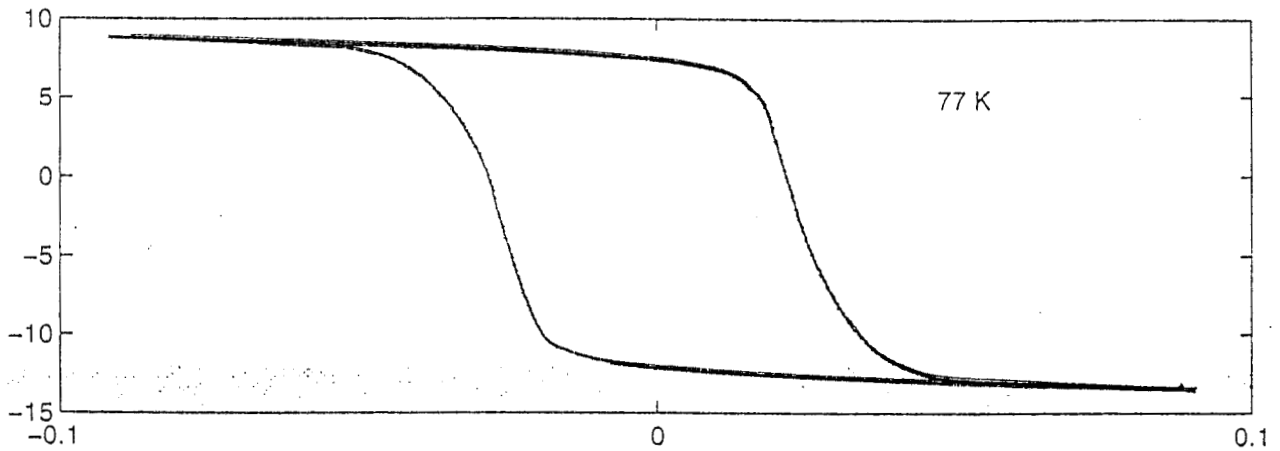
10
5
0
-5
-10
-15
-0.1
0
0.1
77 K

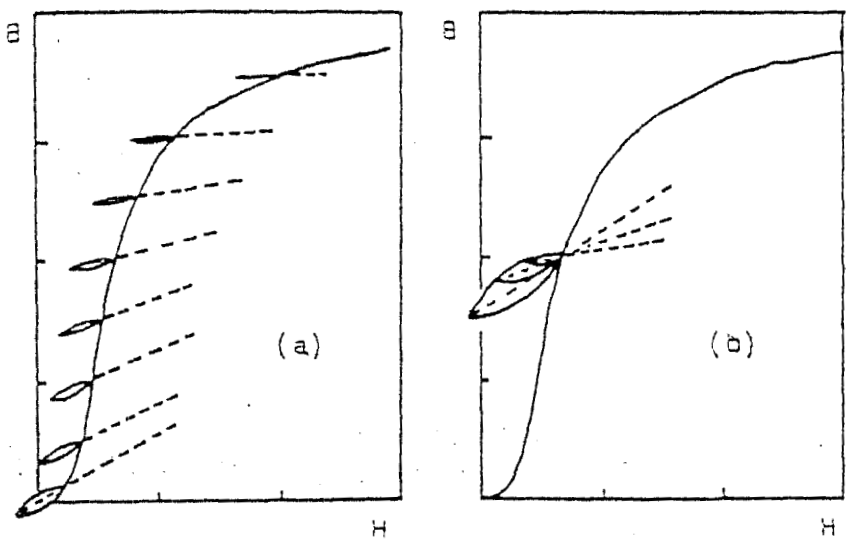

FIG 2·4 : Behaviour of minor hysteresis loops with (a) steady field, H_m, and, (b) the perturbation amplitude, H_1.

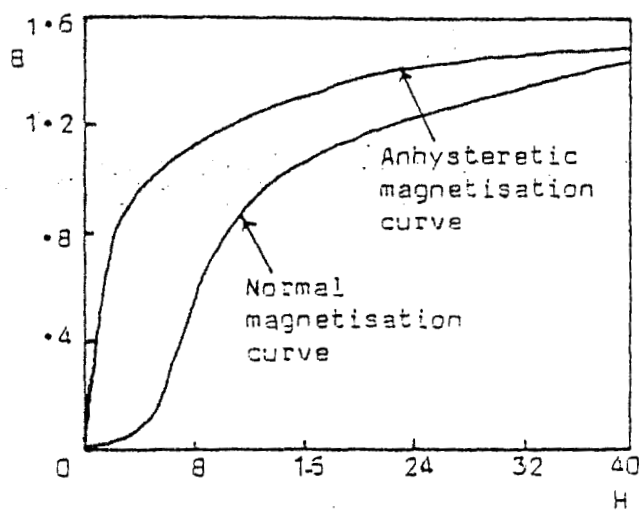

FIG 2·5 : Anhysteretic magnetisation curve (for iron).

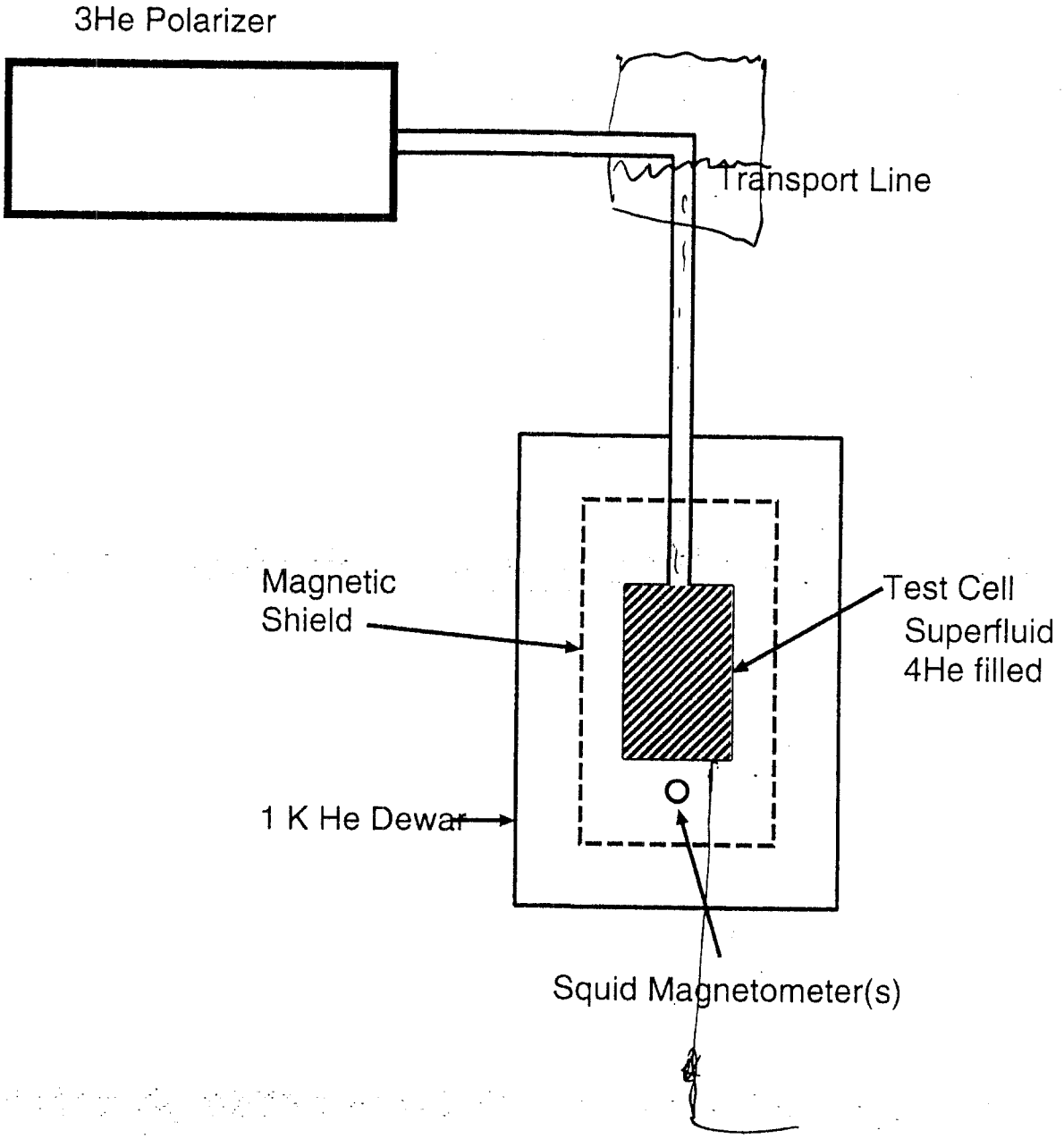

$D \propto T^{-7}$

.2K

$DL^2 = \tau$

Johnson Noise

$\delta \gg t$

$$\left[j_l(\vec{r})\, j_k(\vec{r}\,') \right]_\omega = \left(\frac{kT}{\pi} \right) \sigma\, \delta_{ik}\, \delta(\vec{r}-\vec{r}\,')$$

Rytov
Lifshitz

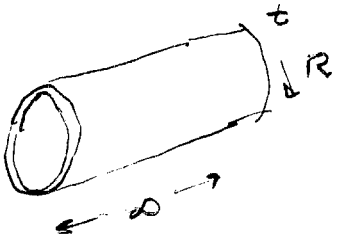

$$B_\omega^2(r) = \frac{kT}{\pi} \sigma \left[\frac{\mu_0}{4\pi} \right]^2 \int \frac{1}{(r-r')^4}\, dV$$

$$= \frac{kT}{\pi} \sigma \left[\frac{\mu_0}{4\pi} \right]^2 \int_R^{R+t} 2\pi r'\, dr' \int_{-\infty}^{\infty} \frac{1}{((r-r')^2 + z^2)^2}\, dz$$

take $r = 0$

$$B_\omega^2(0) = \frac{kT}{\pi} \sigma \left[\frac{\mu_0}{4\pi} \right]^2 \frac{\pi^2}{R^2}\, t$$

$R = 30$ cm Cu $\sigma = 6 \times 10^7 \frac{\mho}{cm}$

$t = 1$ cm

$$\sqrt{B_\omega^2(0)} = \sqrt{T} \times 1.2 \times 10^{-11}\ G/\sqrt{rad/s}$$

$$= 50\ \mu\Phi_0/cm^2$$

$$\times \frac{1}{\sqrt{3}}$$

A new measurement at NIST of the neutron storage time in a TPB coated cell

Jen-Chieh Peng (Illinois)

UCN PRODUCTION AND STORAGE AT NIST

Jen-Chieh Peng
University of Illinois
Los Alamos, July 19, 2002

Outline

- Summary of existing measurements at NIST
- Ideas for a new NIST measurement

UCN PRODUCTION IN ^4He

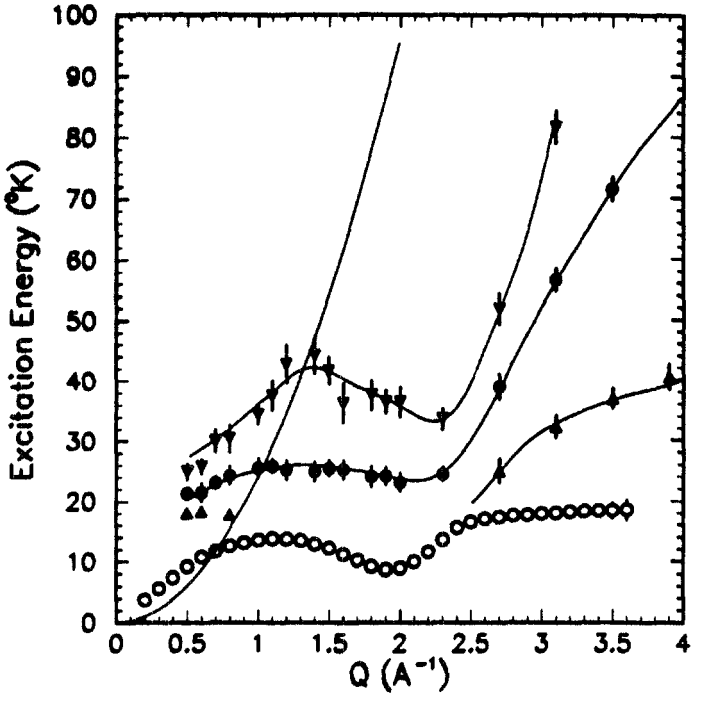

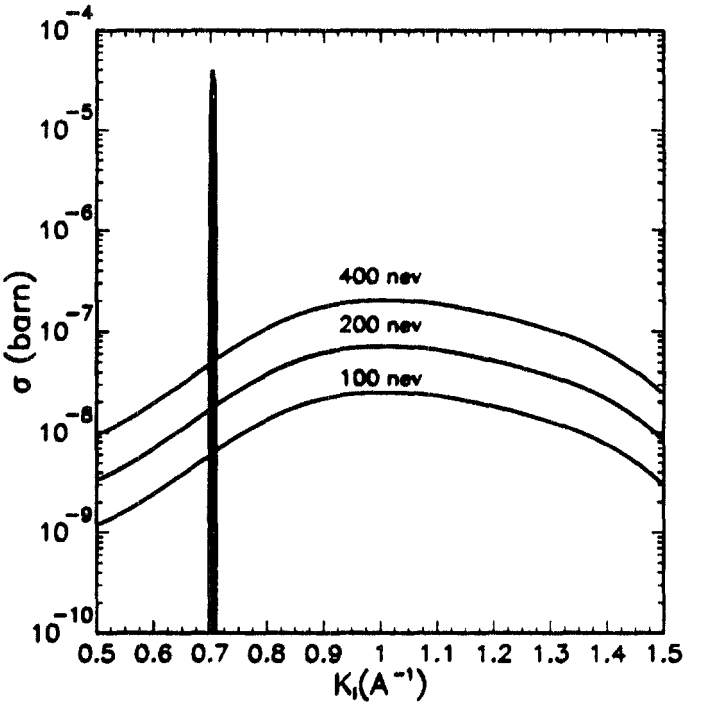

UCN production rate was recently verified at NIST

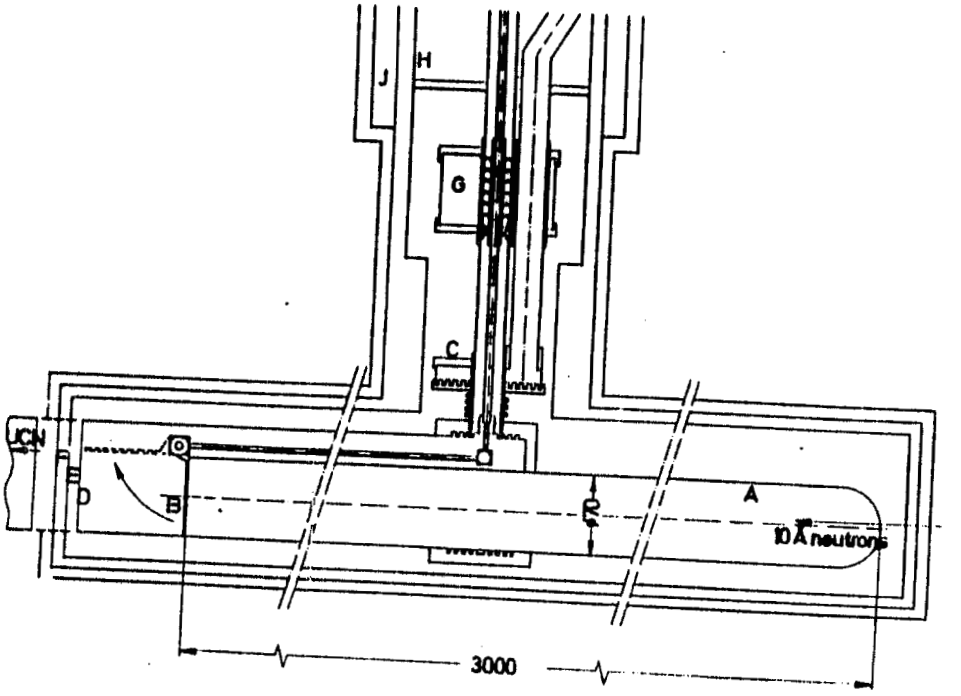
J
H
G
C
UCN
D
B
R
A
10 Å neutrons
3000

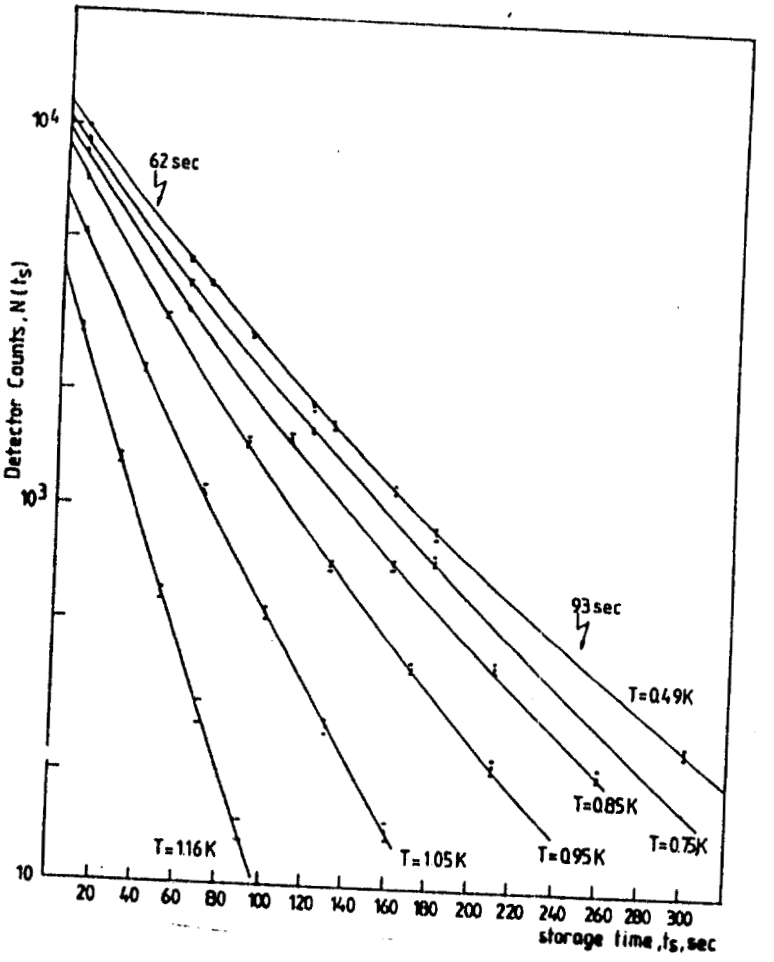
Detector Counts, N(ts)
storage time, ts, sec
62 sec
93 sec
T=0.49K
T=0.85K
T=0.75K
T=1.16K
T=1.05K
T=0.95K
10
10³
10⁴
20
40
60
80
100
120
140
160
180
200
220
240
260
280
300

UCN Losses in Superfluid ^4He Bottle

1. Neutron beta decay

2. Wall absorption

3. Upscattering in superfluid ^4He

   - Single-phonon upscattering rate $\propto e^{-1/KT}$
   - Multi-phonon upscattering rate $\propto T^7$

4. $n - ^3He$ absorption

$$n + ^3He \rightarrow p + t + 764KeV$$

total spin	σ_{abs} at $v = 5m/sec$
$J = 0$	$\sim 4.8 \times 10^6$ barns
$J = 1$	~ 0

- The natural abundance of $^3He/^4He$ ($\sim 10^{-7}$) implies an absorption time of $\sim$ 0.4 s

- Purified ^4He with $^3He/^4He < 10^{-11}$ is required

UCN Production in Superfluid ^4He

Magnetic Trapping of UCN
(Nature 403 (2000) 62)

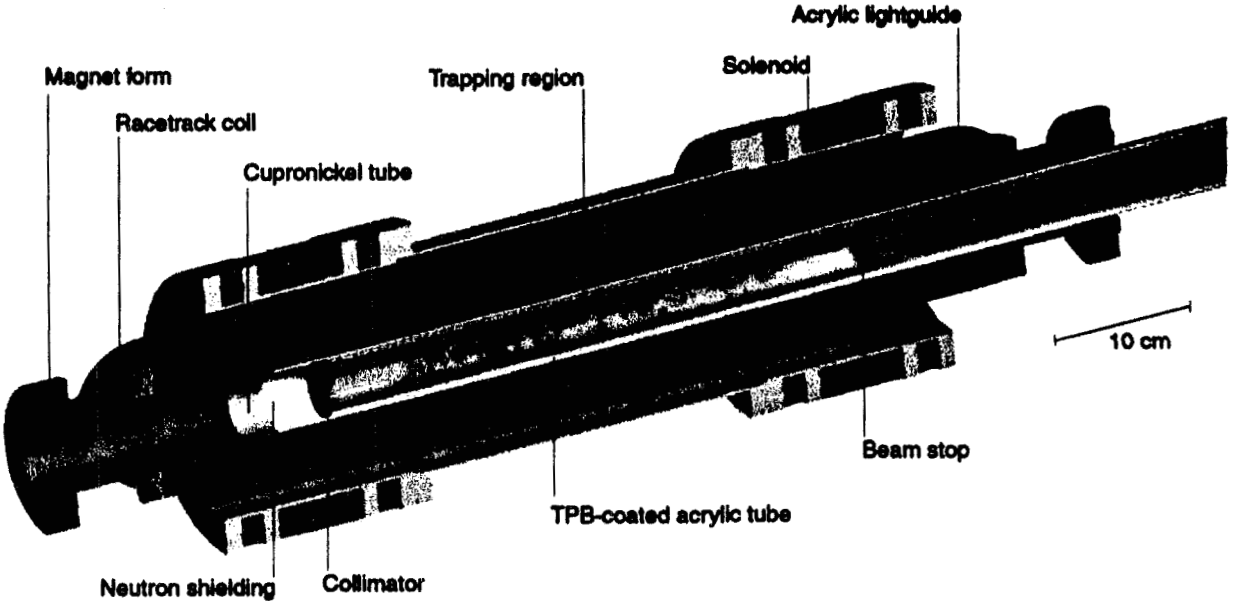

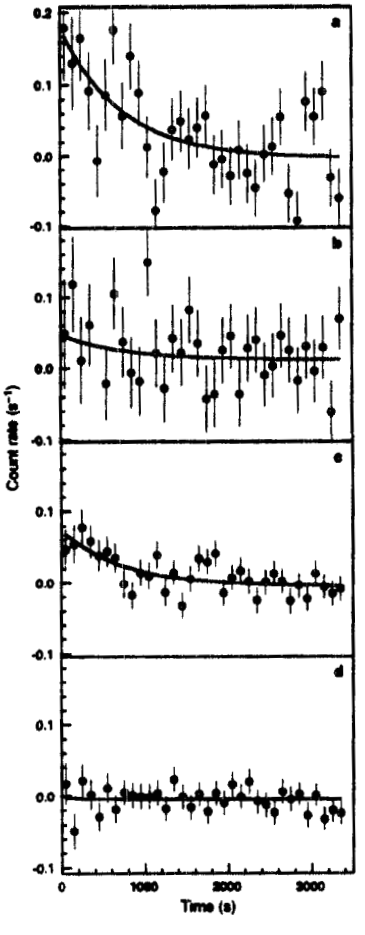

560 ± 160 UCNs trapped per cycle (observed)

480 ± 100 UCNs trapped per cycle (predicted)

Measured neutron lifetime:

750^{+330}_{-200} seconds

Peak UCN signal: 0.2/s
Peak Bkgrnd: 6.0/s

Neutron flux at NIST

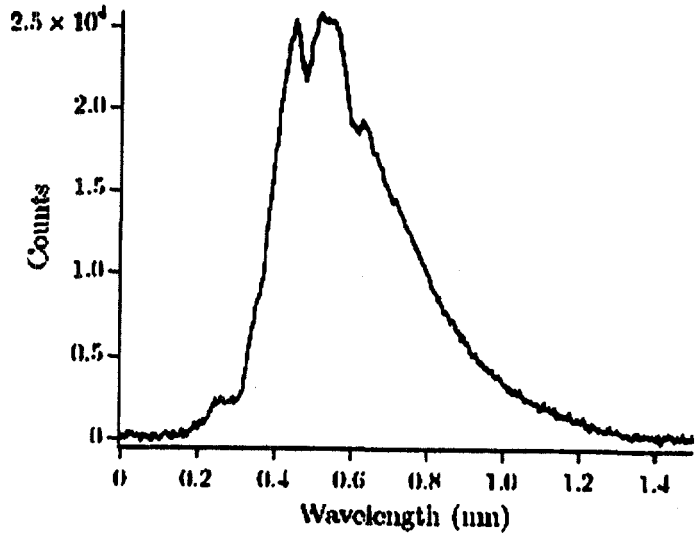

$$\frac{d\phi}{d\lambda} = 1.62 \times 10^6 \; n \; cm^{-2} \; s^{-1} \; K^{-1}$$

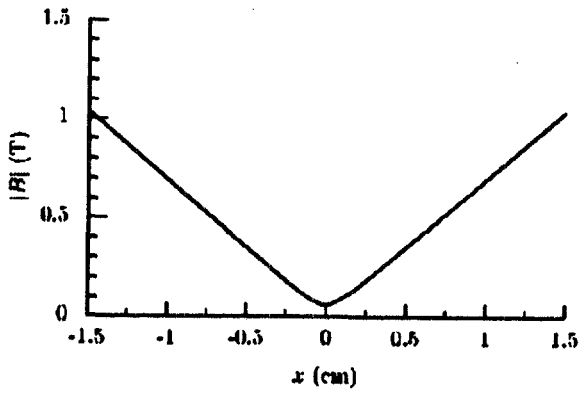

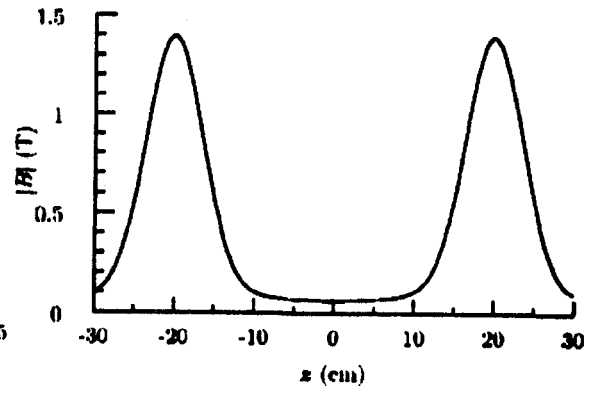

Net depth of B field trap = 1.04 Telsla

Trap UCN's of $E < 60$ nev with the correct spin orientation

PROPOSED NIST MEASUREMENTS

1. Use the new monochromatic neutron beam centered around 8.9 $\AA$
   - $\sim$ 80 percent transmission of 8.9 $\AA$ neutrons
   - A factor of 20 reduction of background-producing neutrons

2. Install a UCN storage cell coated with deuterated TPB
   - UCN confining potential is raised from $\sim$ 60 nev to $\sim$ 200 nev
   - UCN production rate is $\propto U^{3/2}$

3. Measure $n \rightarrow pe^{-}\bar{\nu}$ signals and upscattering UCN's as a function of ^4He temperature

GOALS

1. Study UCN production rate
2. Determine rates of UCN losses due to wall interaction and upscattering
3. Study of background

Monochromatic Neutron Beam at NIST

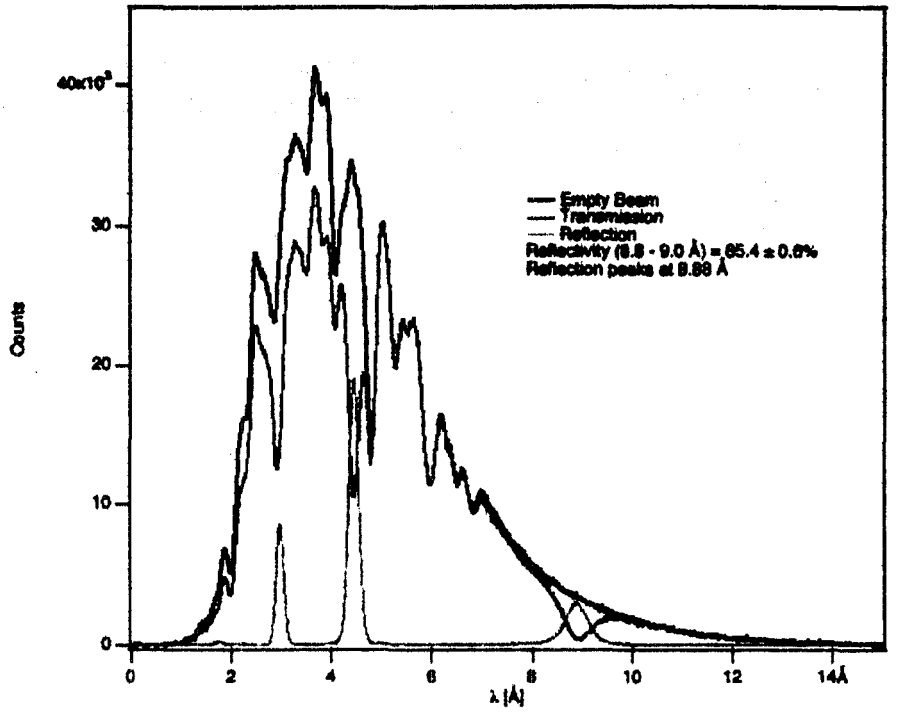

After adding graphite filter

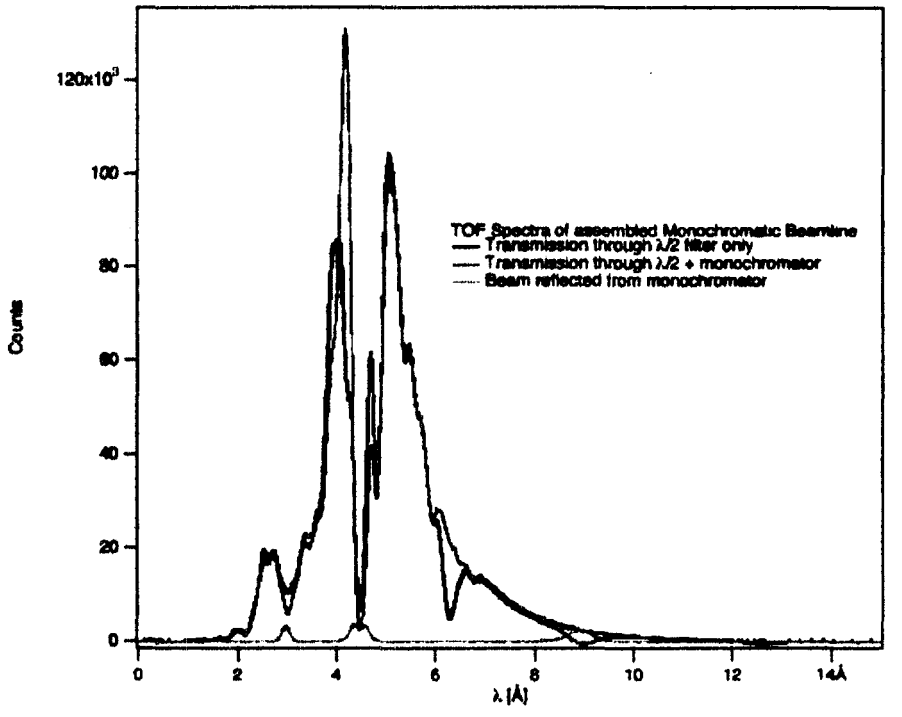

Estimated rate for UCN signal

- Neutron flux: $\frac{d\phi}{d\lambda} = 1.3 \times 10^6\ n/cm^2/s/K$
- UCN prod. rate $= \frac{d\phi}{d\lambda} \times 10^{-7}\ UCN/cm^3/s =$ 0.13 $UCN/cm^3/s$
- Cell size: $40cm \times 3.2cm$ diameter cylinder: 320 cm^3
- UCN production rate $\sim$ 40 UCN/s
- Effective storage time of UCN: $\sim$ 100 – $500sec$
- detector efficiency $\sim$ 30 percent
- Initial UCN detection rate of 1.2 - 6 per second

Background reduction

- Monochromatic beam near 8.9$\AA$
- Transparent beam stop and better light transmission for higher threshhold to reject background

New ideas regarding light collection and backgrounds

Paul Huffman (NIST)

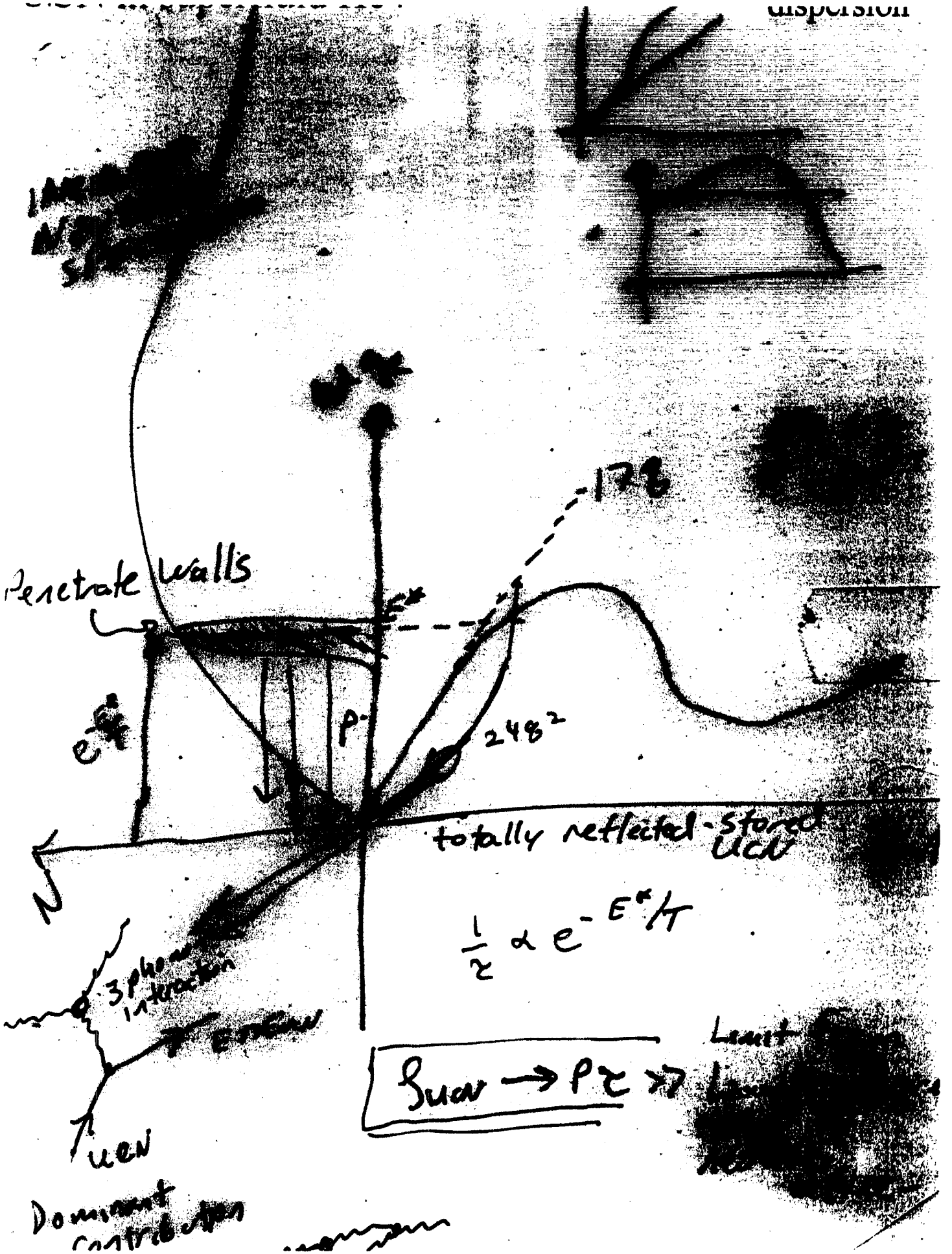
dispersion
Penetrate walls
E^*
$e^{-E^*/T}$
p
248^2
178
totally reflected - stored UCN
N
$\frac{1}{\tau} \propto e^{-E^*/T}$
3 phonon interaction
UCN
Dominant contribution
$\rho_{UCN} \rightarrow p\tau \gg$
Limit

Detection of Neutron Capture

$$n + {}^3He \rightarrow p + {}^3H + 764\ \text{keV}$$

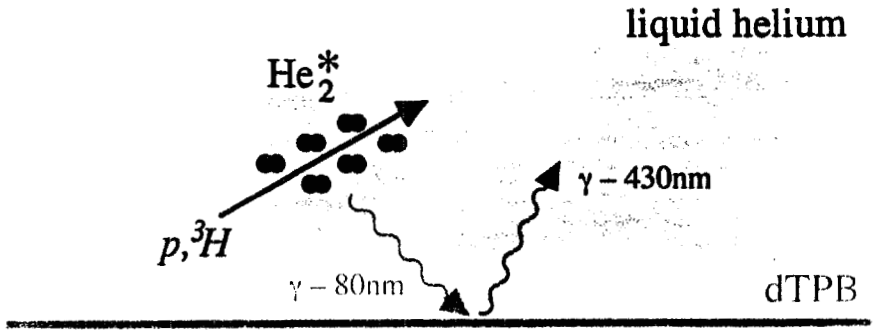

- Recoil proton and/or triton creates an ionization track in the helium.
- Helium ions form excited He_2* molecules (ns time scale) in both singlet and triplet states.
- He_2* singlet molecules decay, producing a large prompt (< 20 ns) emission of extreme ultraviolet (EUV) light.
- EUV light (80 nm) converted to blue using the organic fluor dTPB (deuterated tetraphenyl butadiene).

Light Guide Detection System

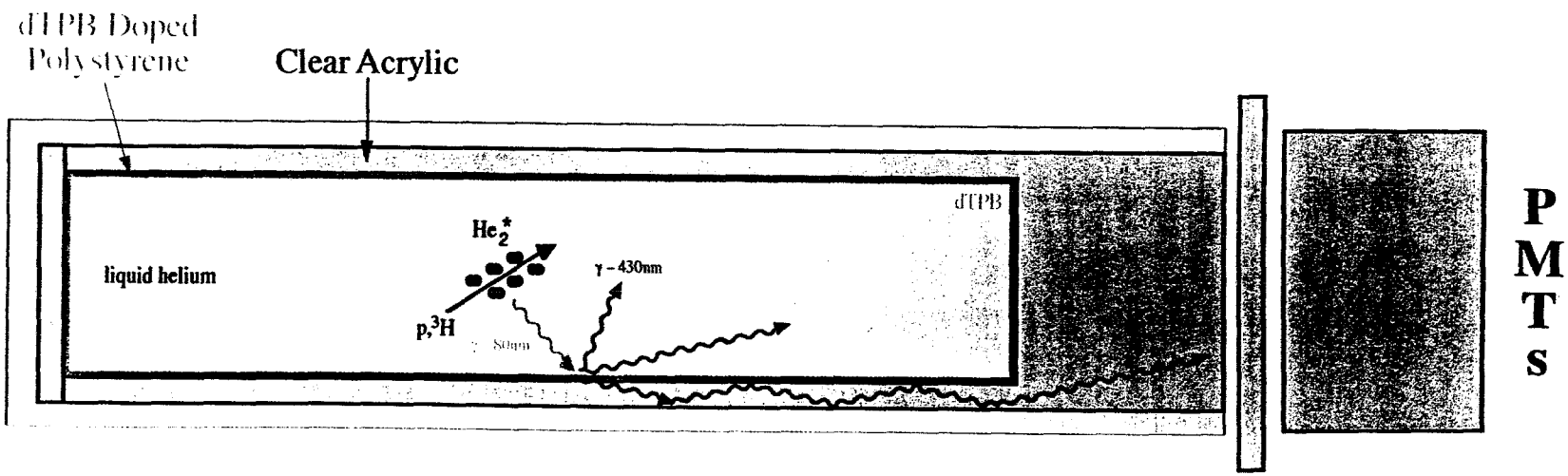

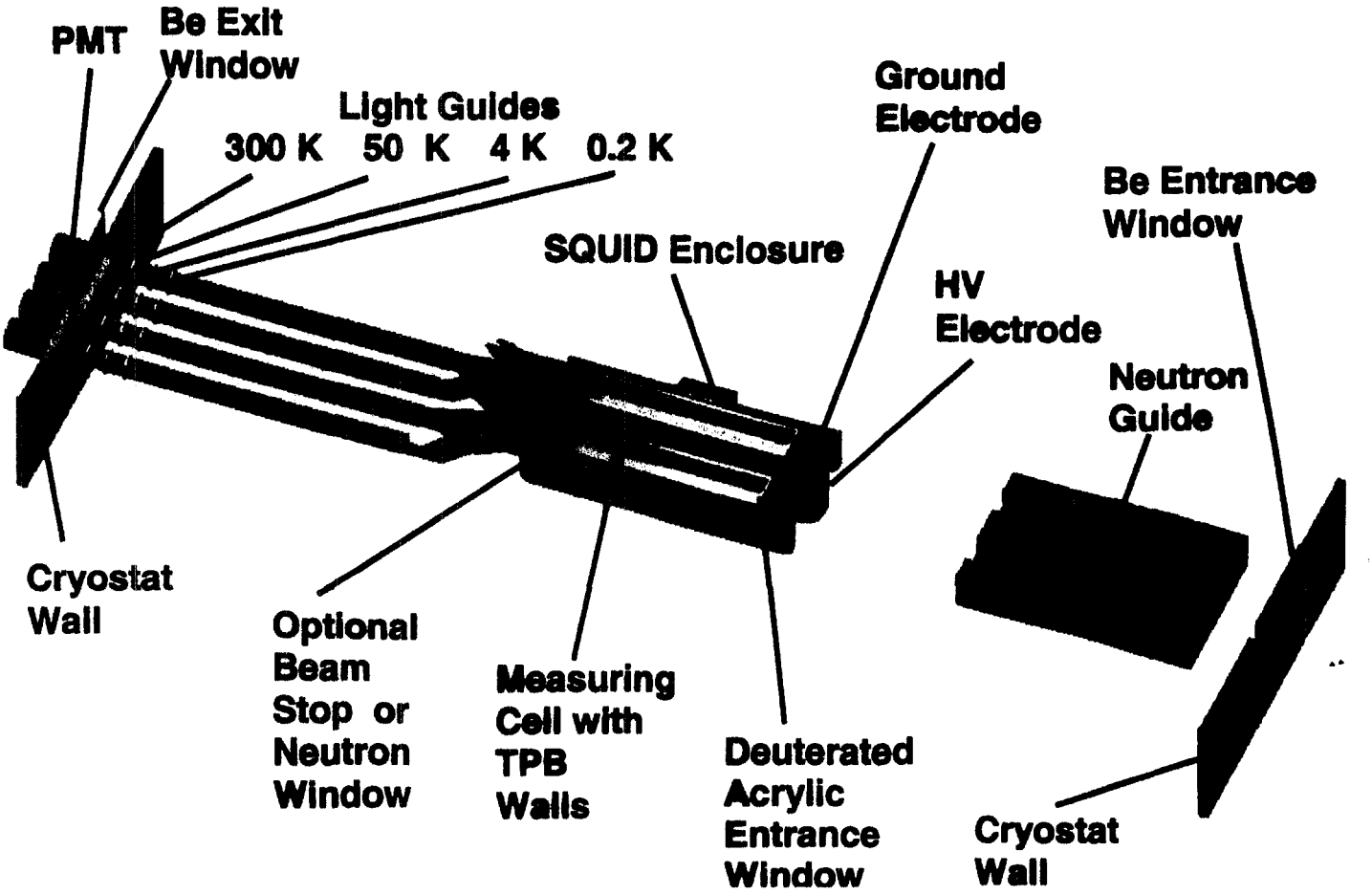
PMT
Be Exit Window
Light Guides
300 K
50 K
4 K
0.2 K
Ground Electrode
Be Entrance Window
SQUID Enclosure
HV Electrode
Neutron Guide
Cryostat Wall
Optional Beam Stop or Neutron Window
Measuring Cell with TPB Walls
Deuterated Acrylic Entrance Window
Cryostat Wall

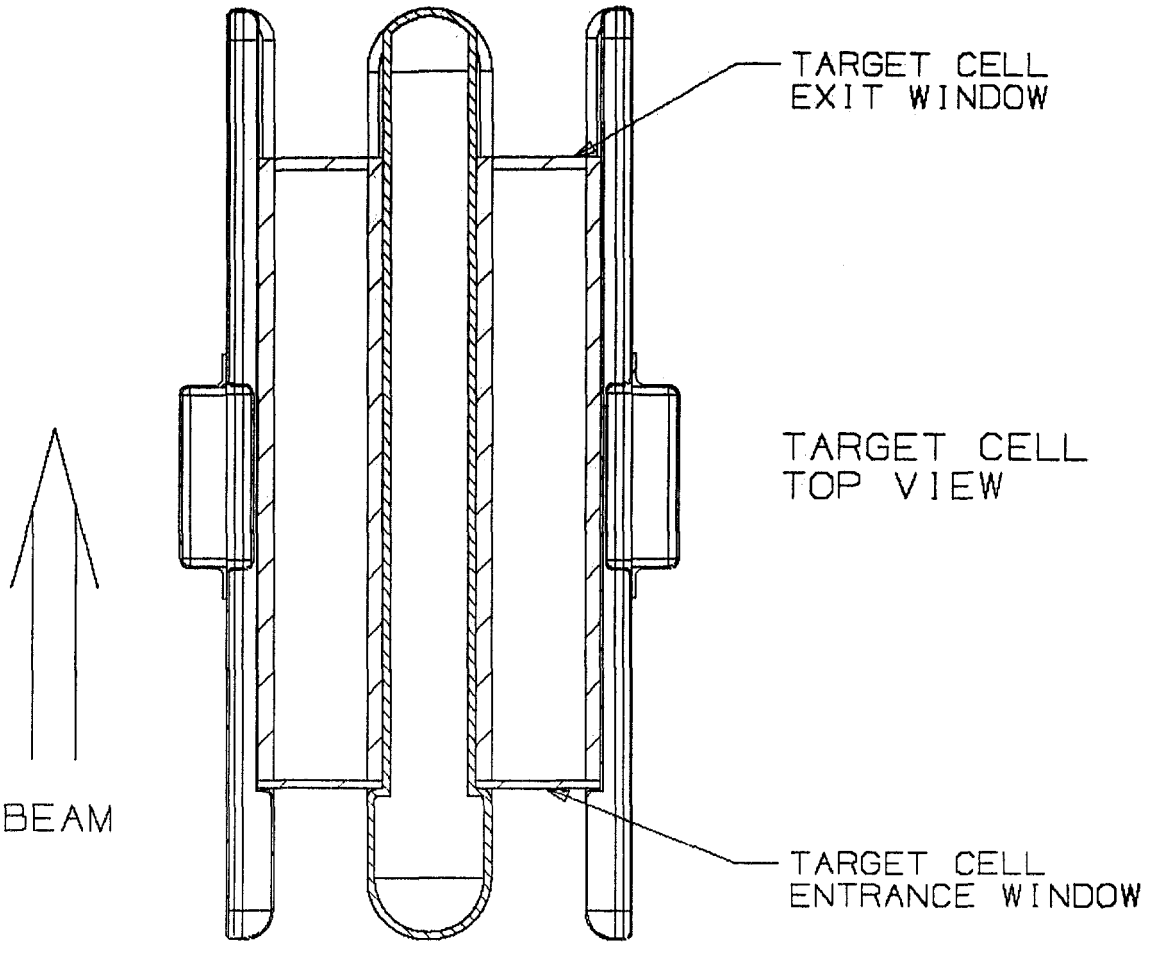
TARGET CELL
EXIT WINDOW
TARGET CELL
TOP VIEW
BEAM
TARGET CELL
ENTRANCE WINDOW

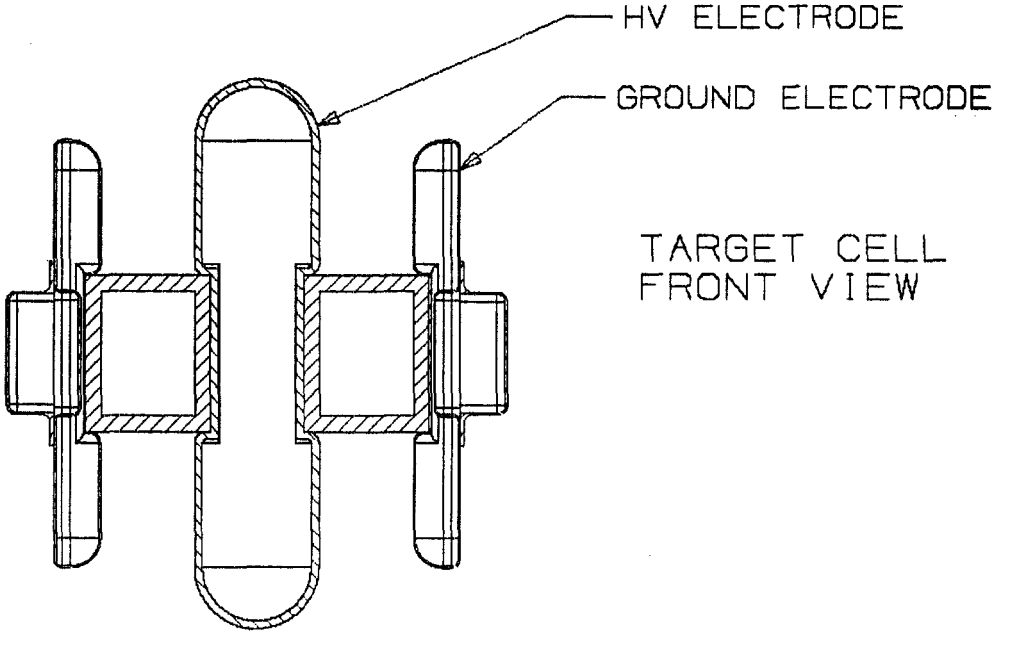
HV ELECTRODE
GROUND ELECTRODE
TARGET CELL
FRONT VIEW

BEAM STOP

1). Placement of beam stop

2). Material (clear, opaque)

3). Pass thru design?

LIGHT GUIDES

1). How many? (≥ 2)

2) Breaks at 4K, 50K, etc...

ENTRANCE WINDOW

1). How much scattering?

2). Thickness

3) Need to make & test

CELL WALLS

1). How thick?

2). dTPB coatings (thickness, concentrations, application technique)

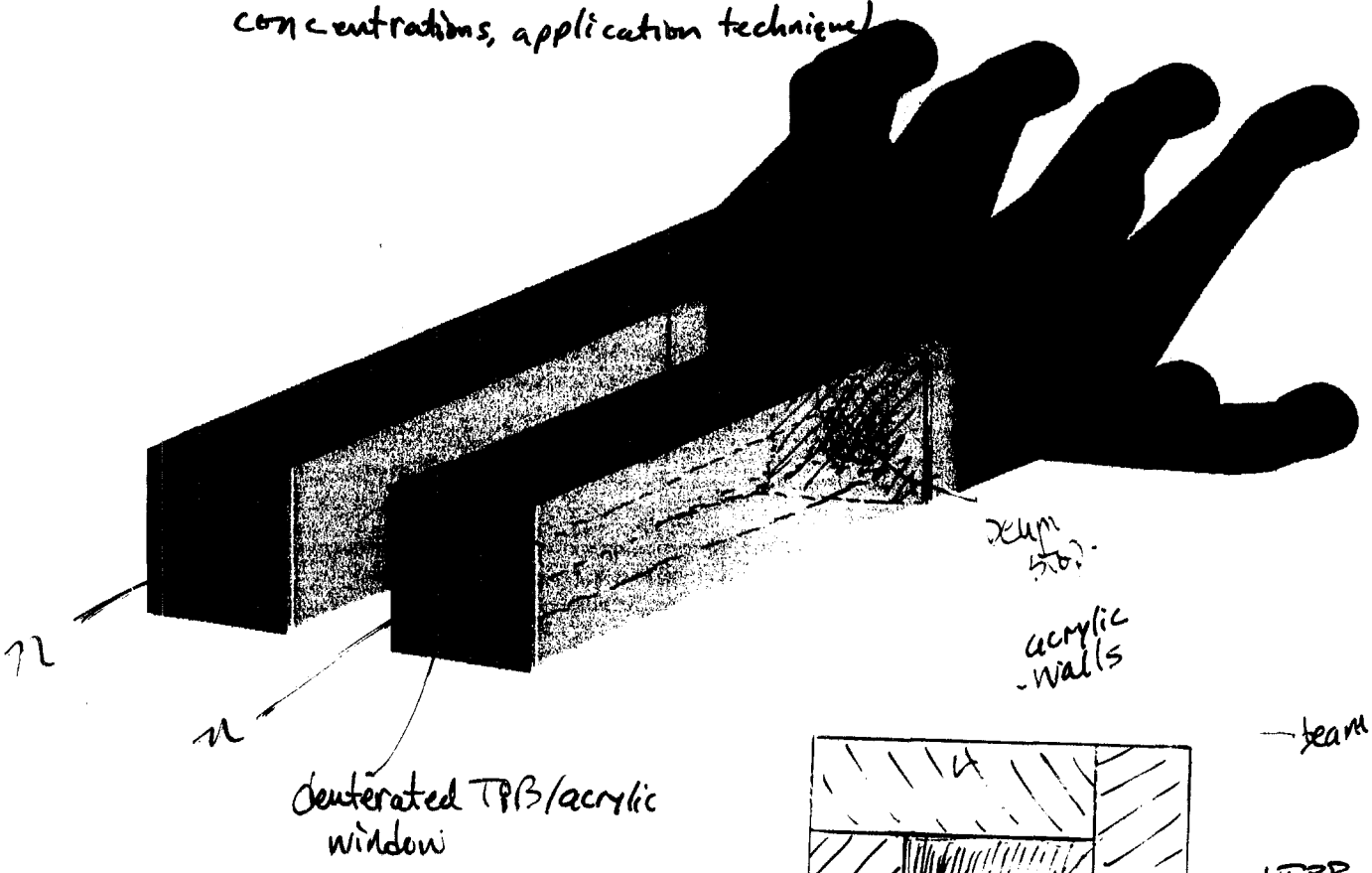

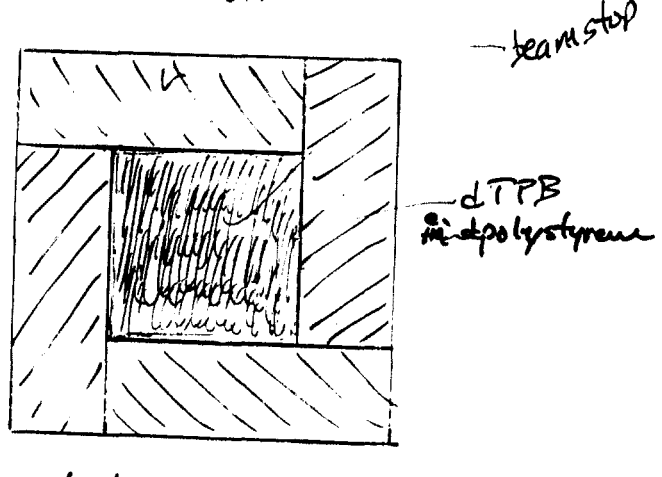

not to scale

Where do we stop the beam?

a). End of cell

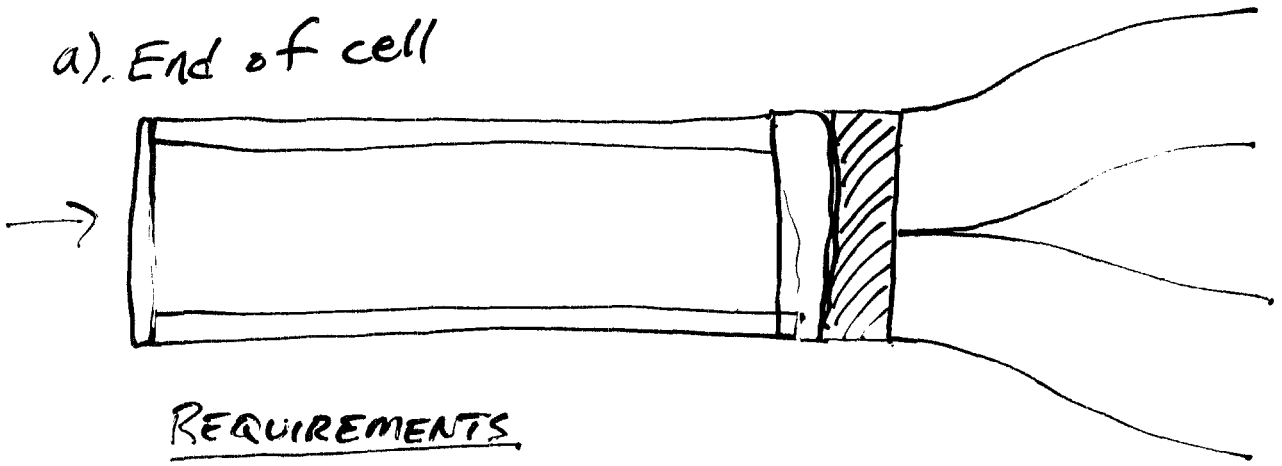

REQUIREMENTS

1). Clear

2). Minimal luminescence

Advantages

1). Considerably more light
- amt. depends on wall thickness, but could be a factor of 2-3 more

2). Could consider evaporated TPB which gives ~x3 more light. Must be tested in this geometry.

MATERIALS OF CHOICE

B_2O_3

b). Beam passes thru.

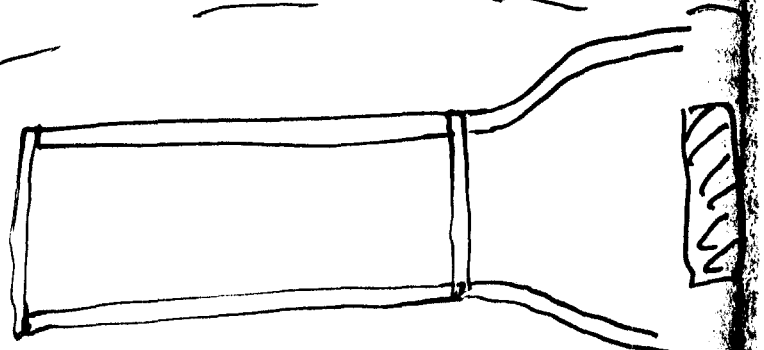

DISADVANTAGES

1). lower light collection effic. - relies on total internal reflection within the walls

MATERIALS OF CHOICE

B_4C, BN (shielded in graphite), etc...

DETECTION EFFICIENCY.

Parameters

1). wall thickness

2). surface quality of dTPB/polystyrene coatings

3). dTPB concentration

- know efficiency for TPB - is it the same?

4). # of PMT's

- need at least two/cell for coincidence detection

5). Light extraction from apparatus.

- need breaks in light guides for thermal isolation
- acrylic is poor thermal conductor - need other windows to minimize black-body radiation

TESTS MUST BE DONE TO OPT. THESE FOR OUR SETUP!

BEAM STOP:

Materials: ^3He, Boron, Lithium, Cadmium, Gd. compounds.

~~^3He~~ - too complex to deal with
- probably most attractive otherwise
  (no luminescence, impurities, activation, etc... &, CLEAR!)

should re-visit
- ~~Cd~~ - some isotopes activate into β emitters $\tau_{1/2} \sim$ hours
- ~~Gd~~ - same as Cd.

Li - produces $T \rightarrow {}^3He$
- bad for lifetime measurement - probably ok here.

B - produces ~~an~~ α & prompt γ

LiF, BN, B_2O_3, B_4C

LiF & BN luminescence

LiF & B_2O_3 optically clear, but hydroscopic

B_4C (hot pressed) - expensive, not easily machined

All cryogenically OK
All can be obtained with low impurity elements

All have some activation problems

Light guides

In setup. not to scale!

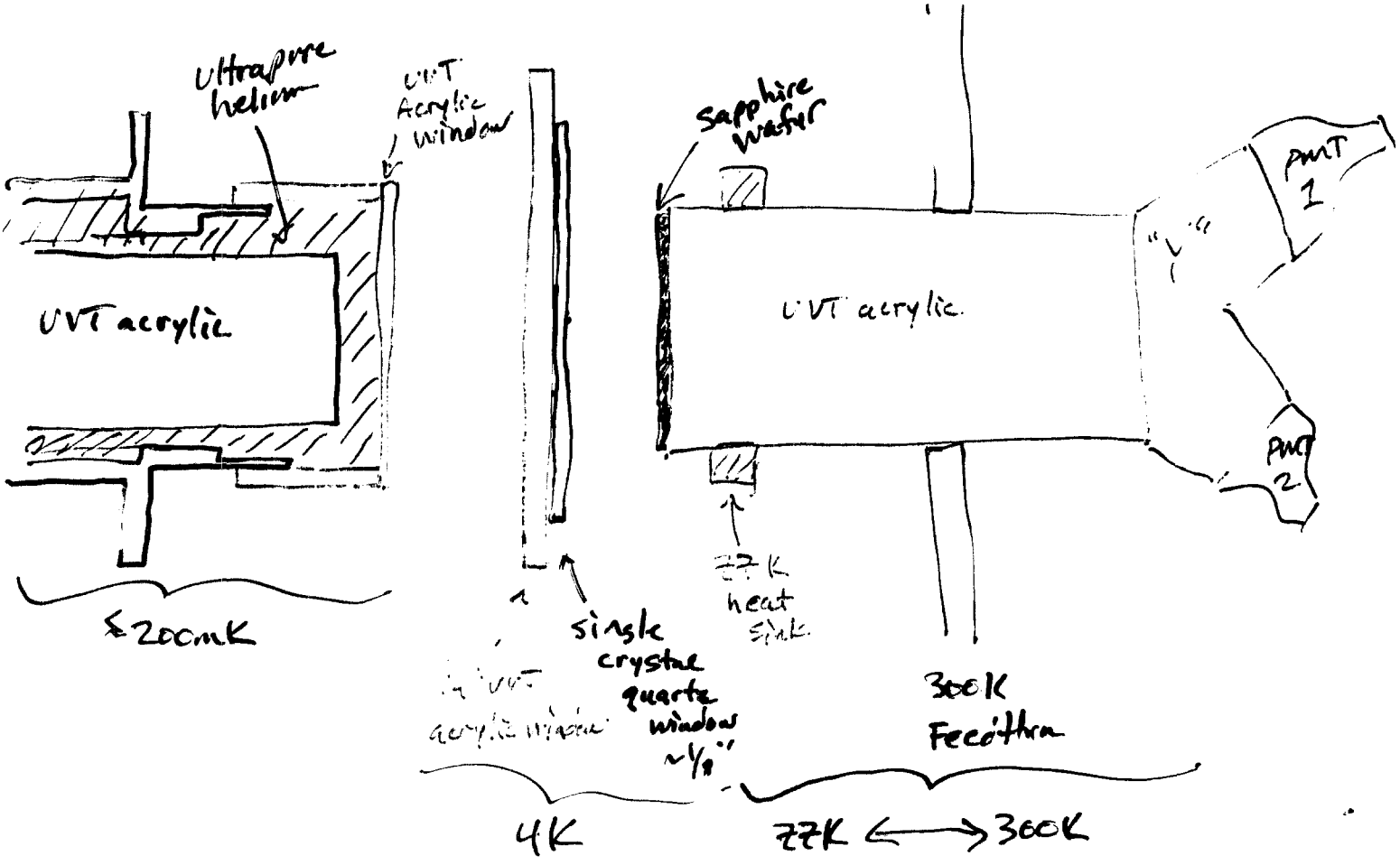

Problems to consider

1). 300 → 77K lightguide

poor thermal conductivity ⇒ center of lightguide is "warm"
⇒ large blackbody heat load onto 4K ⇒ high helium boiloff

Sapphire window used as thermal anchor

2) 77K Blackbody to cell

quartz window carries away most of heat & blackbody
acrylic provides vacuum seal & blocks remaining blackbody.
(acrylic alone won't work due to poor thermal conductivity)

LiF

F activates - ^{20}F, $\tau_{1/2} = 11$ sec.

short, but a lot of it!

can it cause gain shift problems in PMT?

Boron / Lithium loaded glasses

has both ^6Li and ^{16}O.

$$n + {}^6Li \rightarrow T + \alpha$$

$$T + {}^{16}O \rightarrow n + {}^{18}F$$

positron emission

$\tau_{1/2} = 1.8h$

$$\alpha + {}^{10}B \rightarrow n + {}^{13}N$$

positron decay

$\tau_{1/2} = 10$ min

Boron compounds

$$n + {}^{10}B \rightarrow \alpha + {}^7Li$$

$$\alpha + {}^{10}B \rightarrow n + {}^{13}N$$

positron decay

$\tau_{1/2} = 10$ min

10^7 n/s

$\Rightarrow$ ~20 ^{13}N produced / second $\times 1000$ s $\approx 1 \times 10^4$ ^{13}N

$\Rightarrow$ 15 Hz of events!

NEED TO DECIDE HOW MUCH ACTIVACTION/BACKGROUNDS WE CAN LIVE WITH.

EXPECT ~ 10 Hz just from surroundings.

How well can we identify neutron beta decays?

Bob Golub (HMI)

Detection of Neutrons in Liquid Helium

Neutrons inside the superfluid helium can be detected via the energetic charged particles which are produced in the beta decay:

$$n \longrightarrow p + e^- + \bar{\nu} + 783\ \text{keV}$$

or with a dilute solution of ^3He inside the ^4He volume:

$$n + {}^3He \longrightarrow p + {}^3H + 764\ \text{keV}$$

Travelling through the helium these charged particles loose their kinetic energy which is partially converted into scintillation light.

→ Scintillations with highest intensity in vacuum ultraviolet region (VUV) of the optical spectrum.

Using a fluorescent wavelength shifter the VUV scintillation light is converted into visible light which can easily be detected by a photomultiplier.

$$\text{VUV} \xrightarrow[\text{shifter}]{\text{wavelength}} \text{visible light} \longrightarrow \text{photomultiplier tube}$$

Sketch of the experimental apparatus

Liquid Helium Experiments

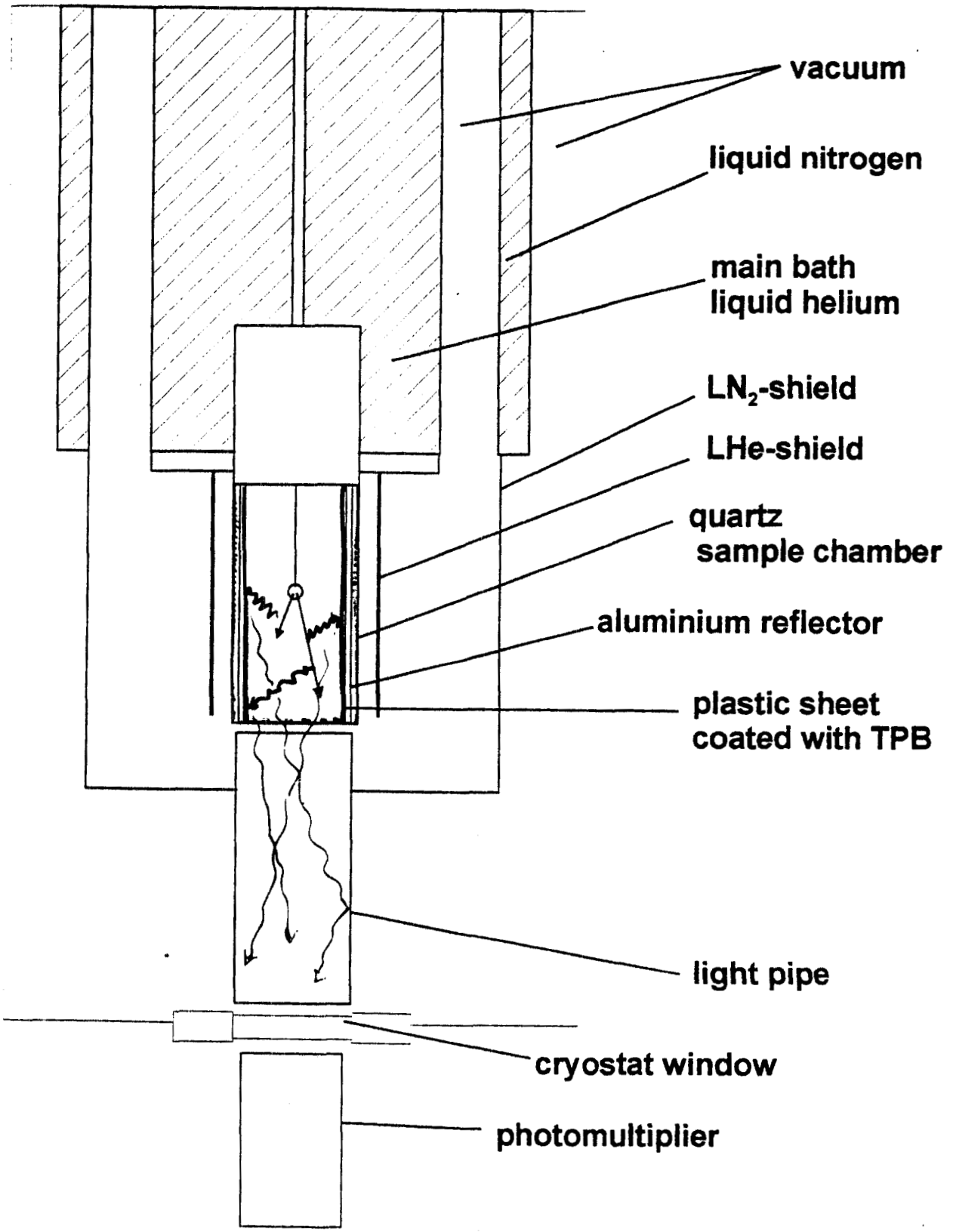

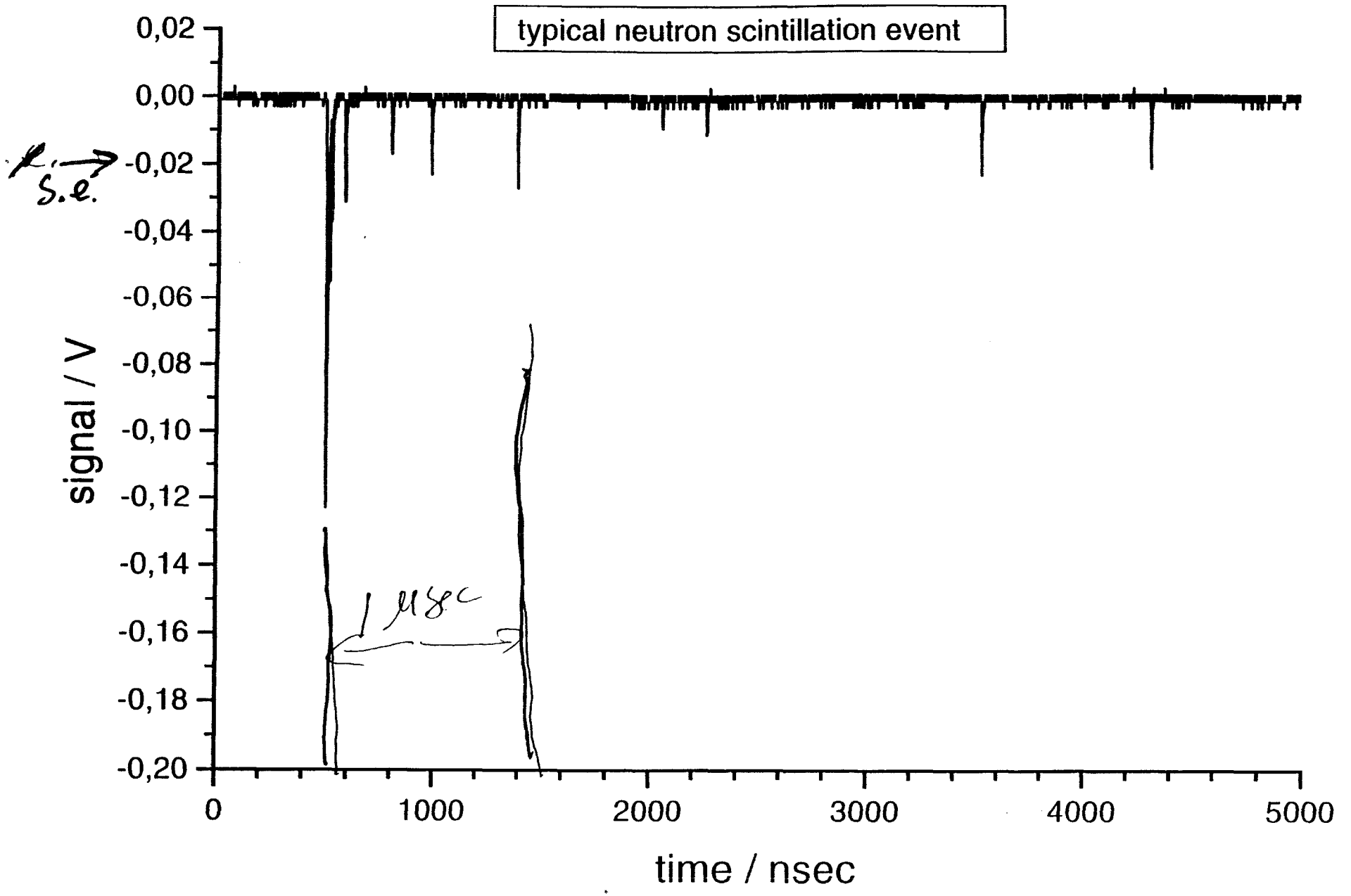
typical neutron scintillation event
0,02
0,00
-0,02
-0,04
-0,06
-0,08
-0,10
-0,12
-0,14
-0,16
-0,18
-0,20
signal / V
0
1000
2000
3000
4000
5000
time / nsec
1 μsec

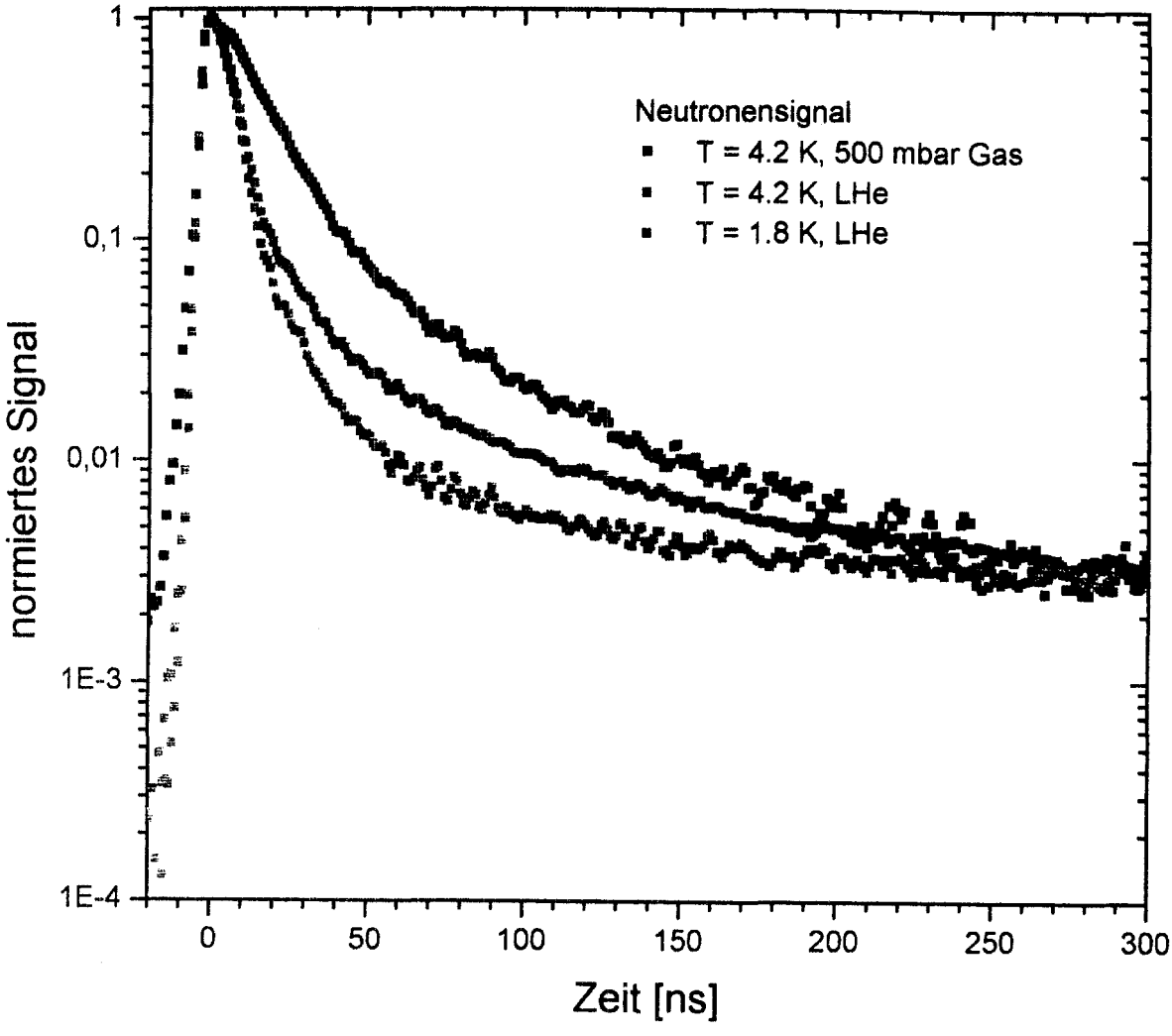
Neutronensignal
T = 4.2 K, 500 mbar Gas
T = 4.2 K, LHe
T = 1.8 K, LHe
normiertes Signal
1
0,1
0,01
1E-3
1E-4
0
50
100
150
200
250
300
Zeit [ns]

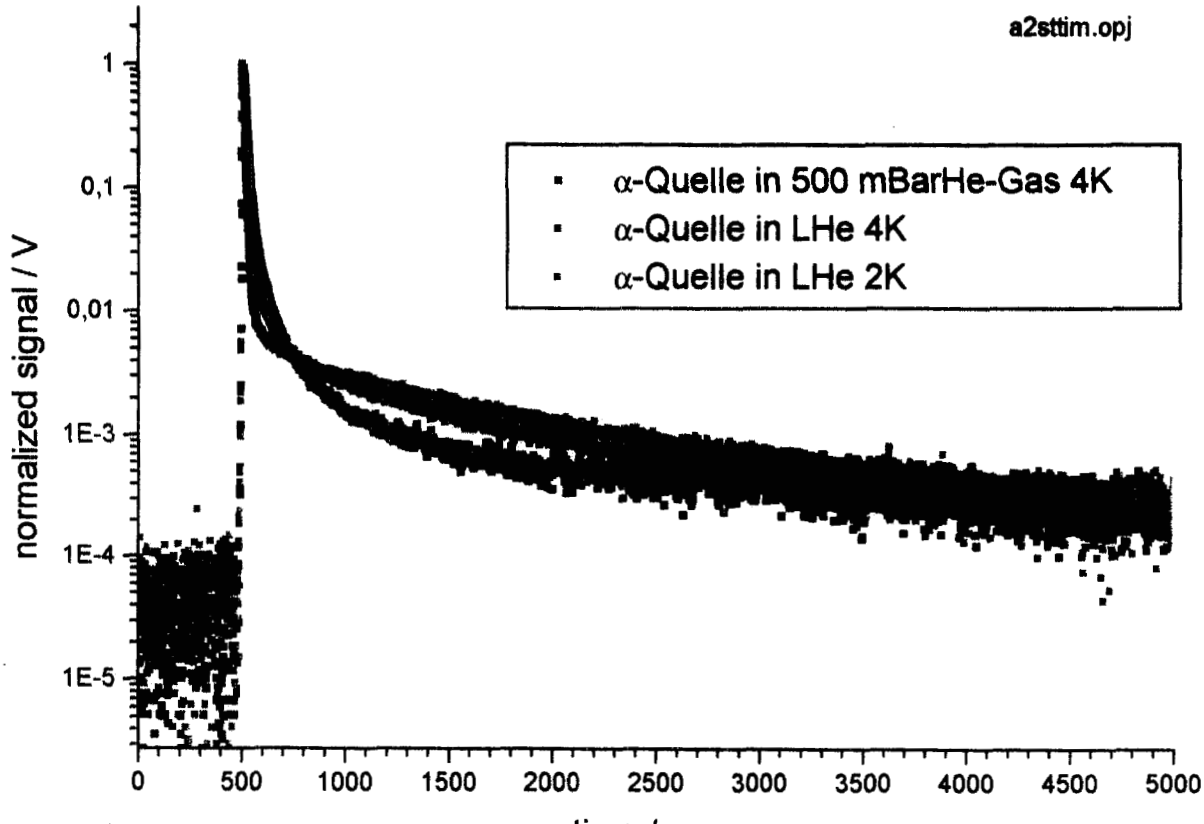

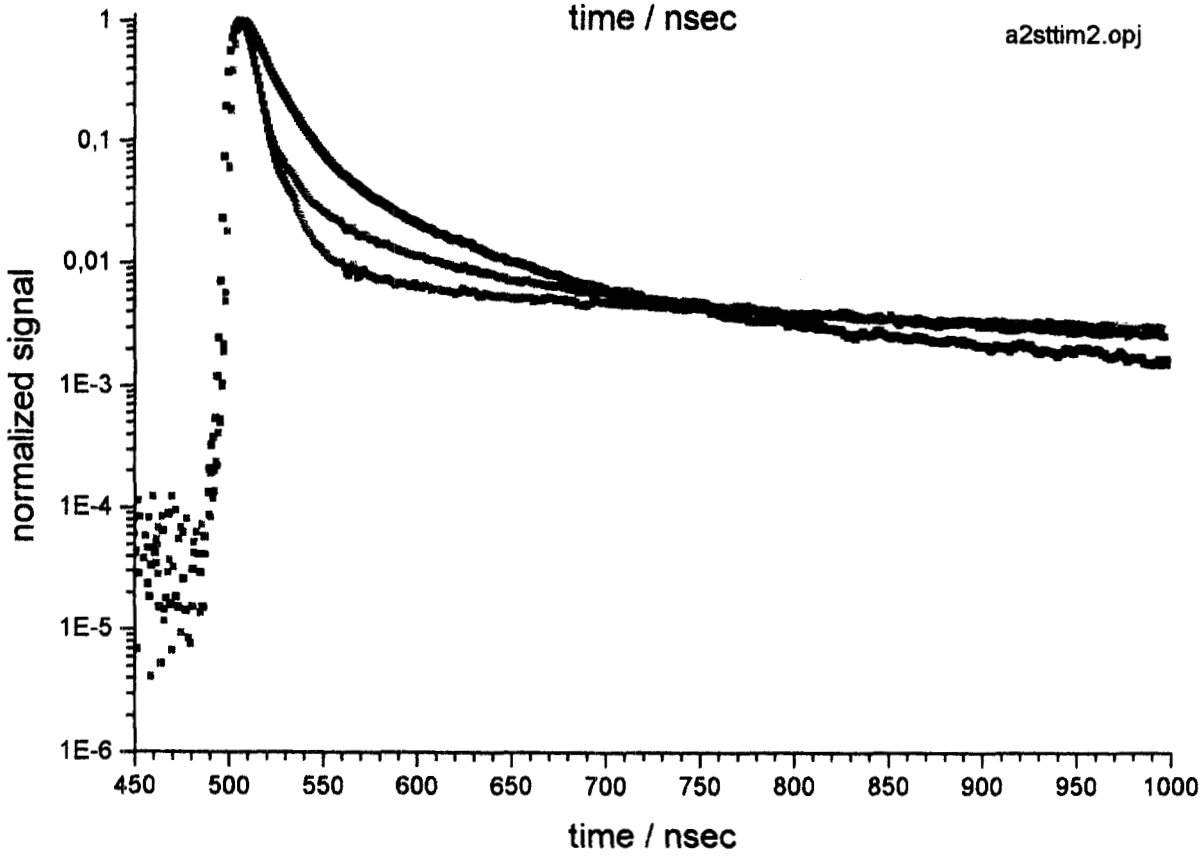

* If long time tail would vanish in gas ⇒ not from TPB

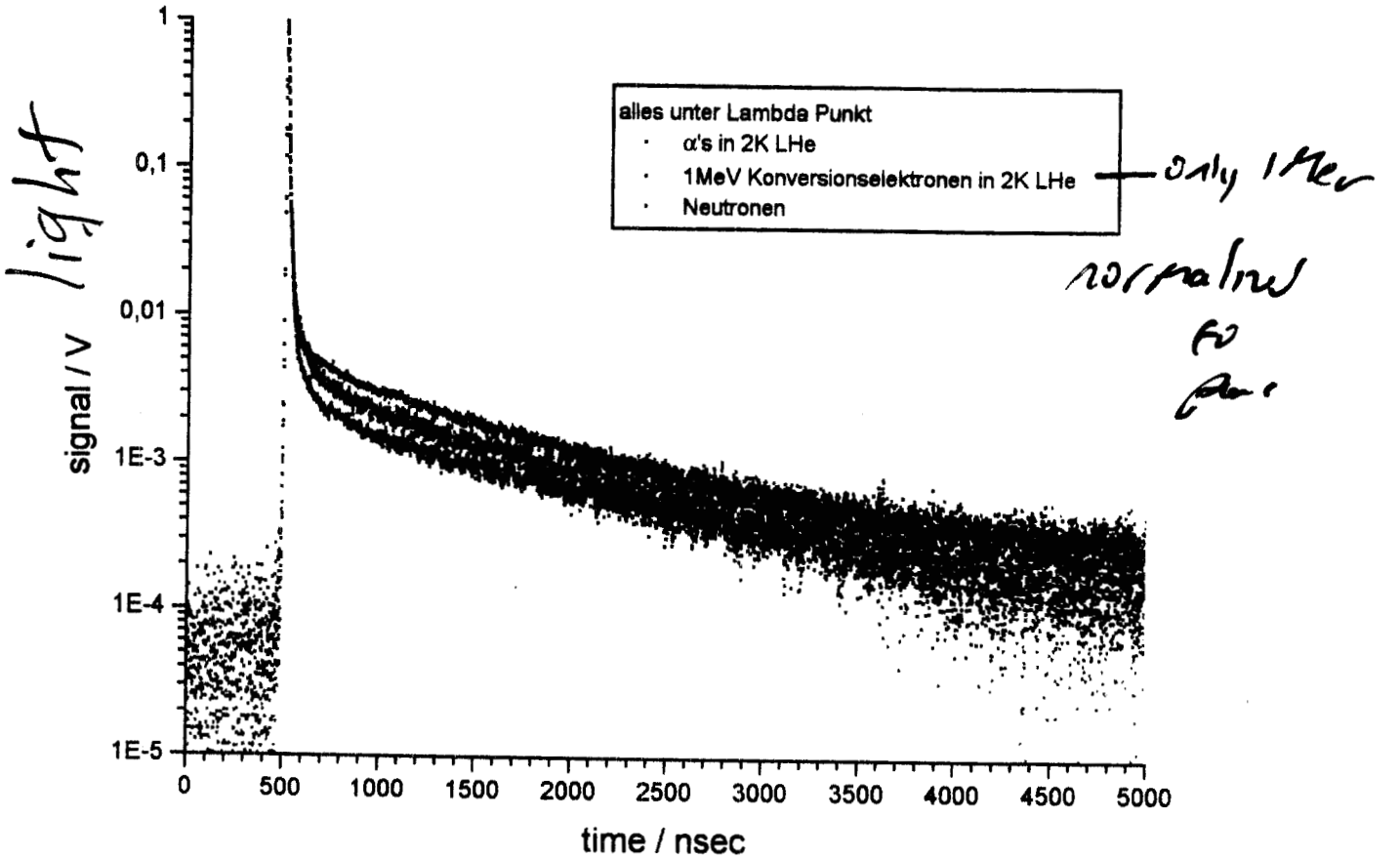

light
signal / V
1
0,1
0,01
1E-3
1E-4
1E-5
0
500
1000
1500
2000
2500
3000
3500
4000
4500
5000
time / nsec
alles unter Lambda Punkt
α's in 2K LHe
1MeV Konversionselektronen in 2K LHe
Neutronen
only 1Mev
normalized
to

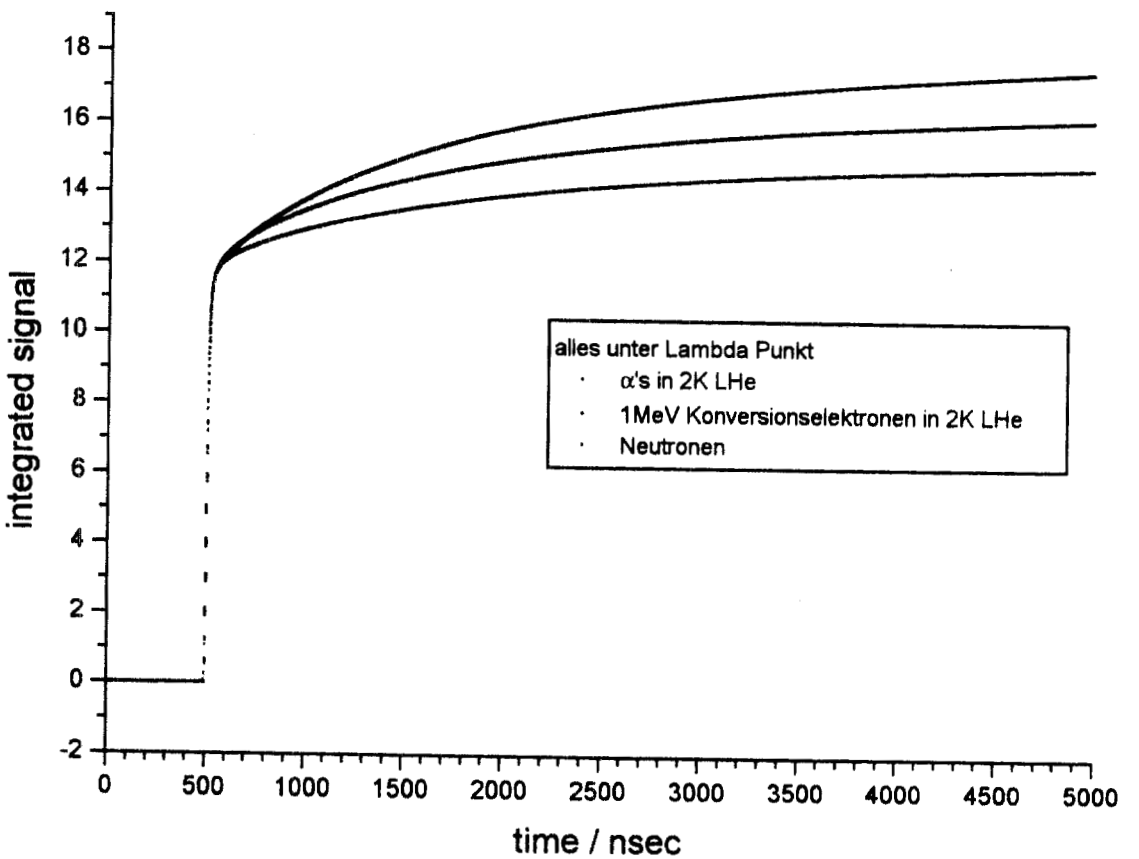

integrated signal
18
16
14
12
10
8
6
4
2
0
-2
0
500
1000
1500
2000
2500
3000
3500
4000
4500
5000
time / nsec
alles unter Lambda Punkt
α's in 2K LHe
1MeV Konversionselektronen in 2K LHe
Neutronen

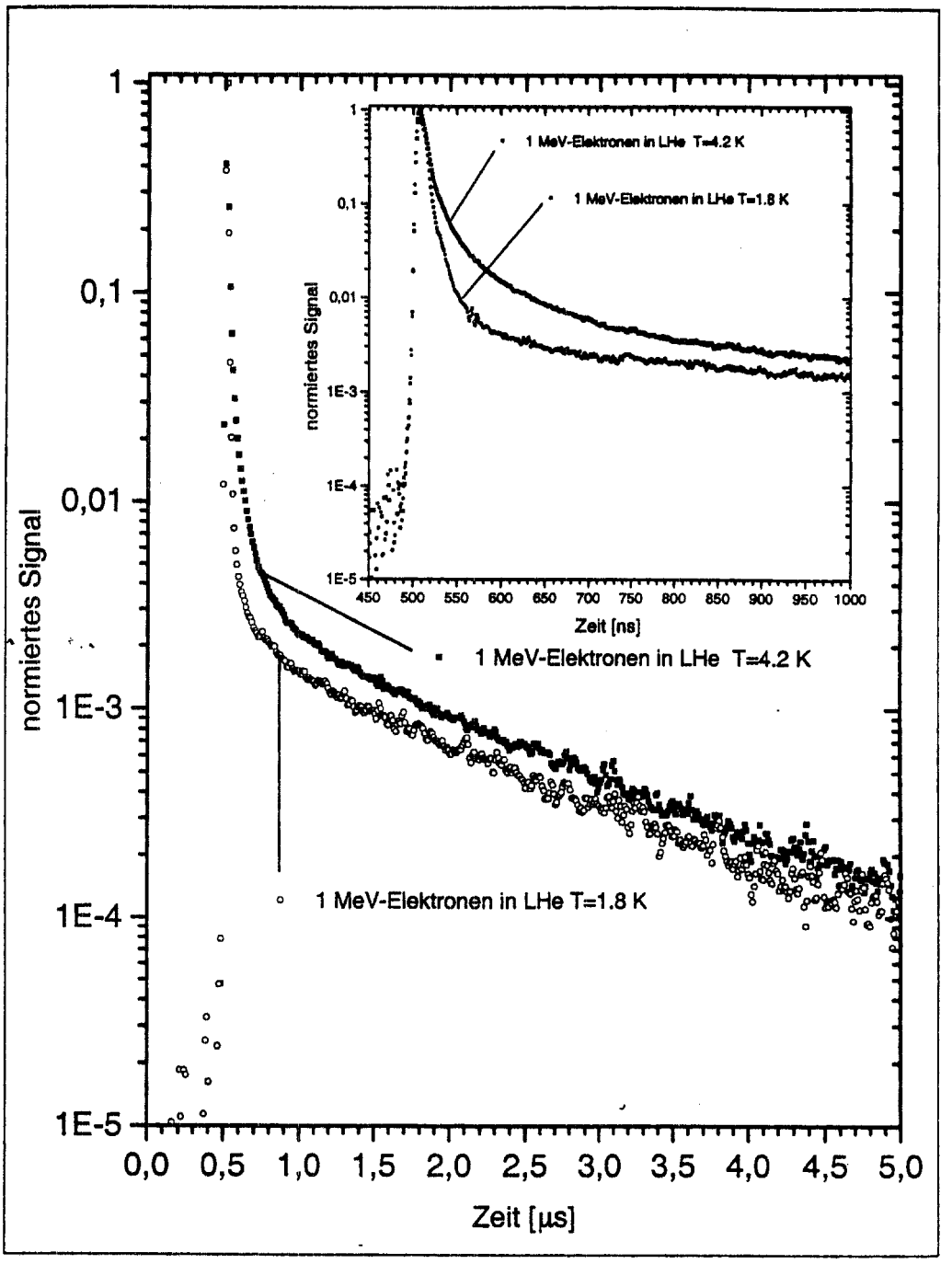

Abb. 4.22: Zeitliches Verhalten des durch monoenergetische Elektronen ($E = 1\ MeV$) induzierten Szintillationssignals innerhalb der ersten 4.5 μs nach dem Signalanstieg für flüssiges Helium bei T= 4.2 K und bei T= 1.8 K. Rechts oben: Zeitskala von 450 ns bis 1 μs. Man beachte, daß das Maximum des Signals bei t=500 ns liegt. Die Signale sind jeweils auf das Maximum normiert.

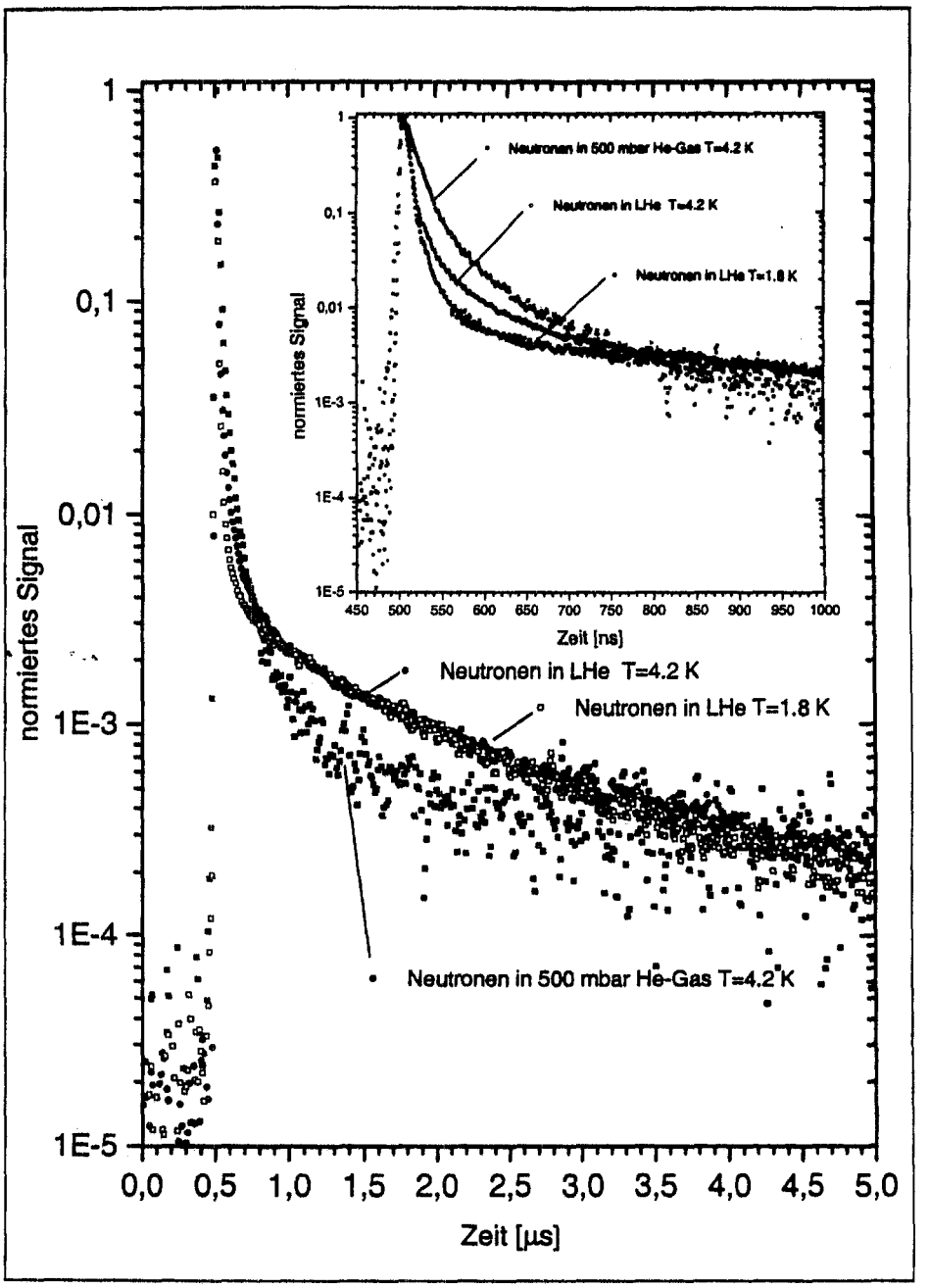

Abb. 4.21: Zeitliches Verhalten des durch Neutronen induzierten Szintillationssignals innerhalb der ersten 4.5 μs nach dem Signalanstieg für 500 mbar He-Gas bei T= 4.2 K, flüssiges Helium bei T= 4.2 K und bei T= 1.8 K. Rechts oben: Zeitskala von 450 ns bis 1 μs. Man beachte, daß das Maximum des Signals bei t=500 ns liegt. Die Signale sind jeweils auf das Maximum normiert. Für die Messung von neutroneninduzierten Szintillationen in der Gasphase wurden nur 2400 Ereignisse gemessen – alle anderen Messungen: 24000 Ereignisse.

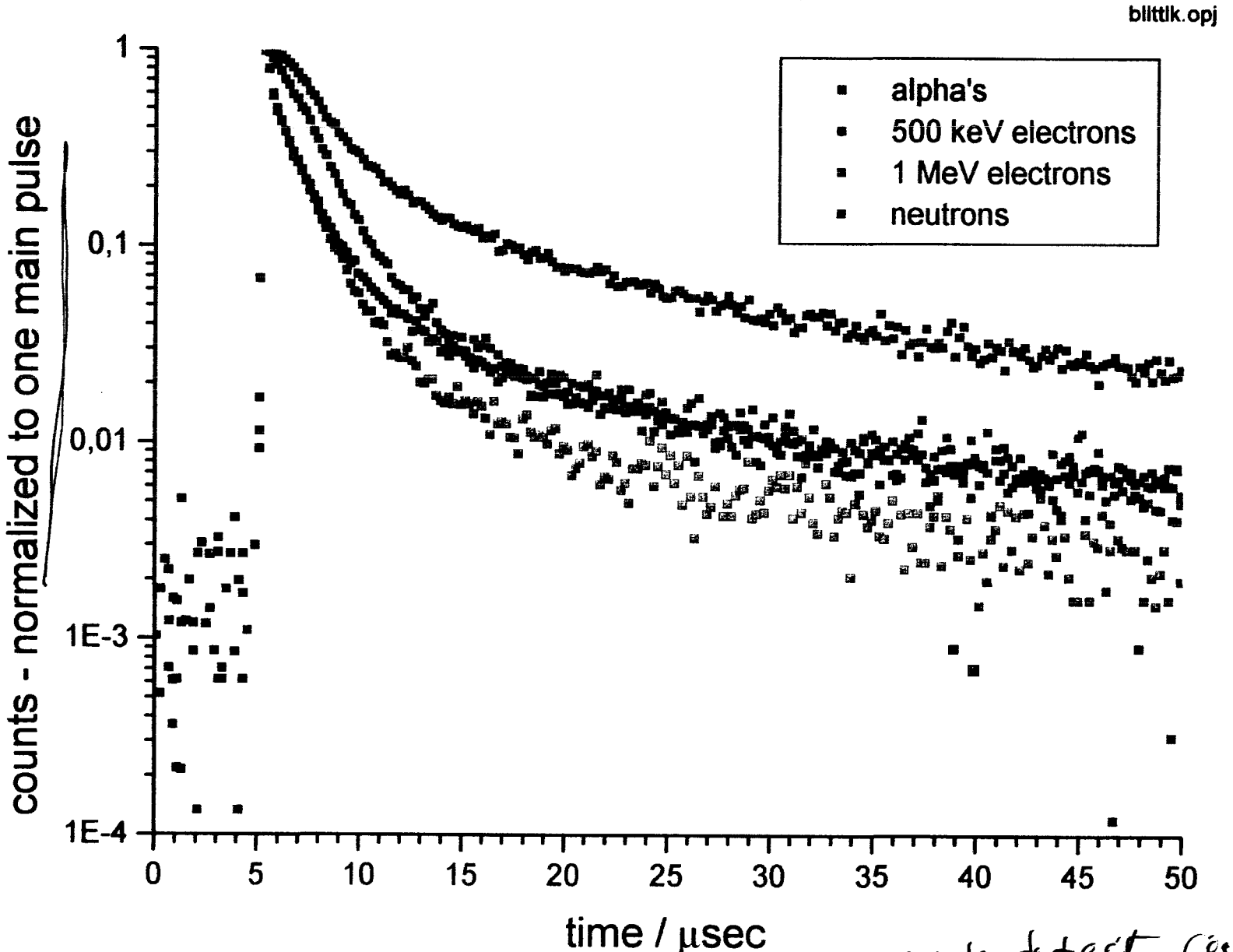

peak detect counts

Normalization nicht zu fassen

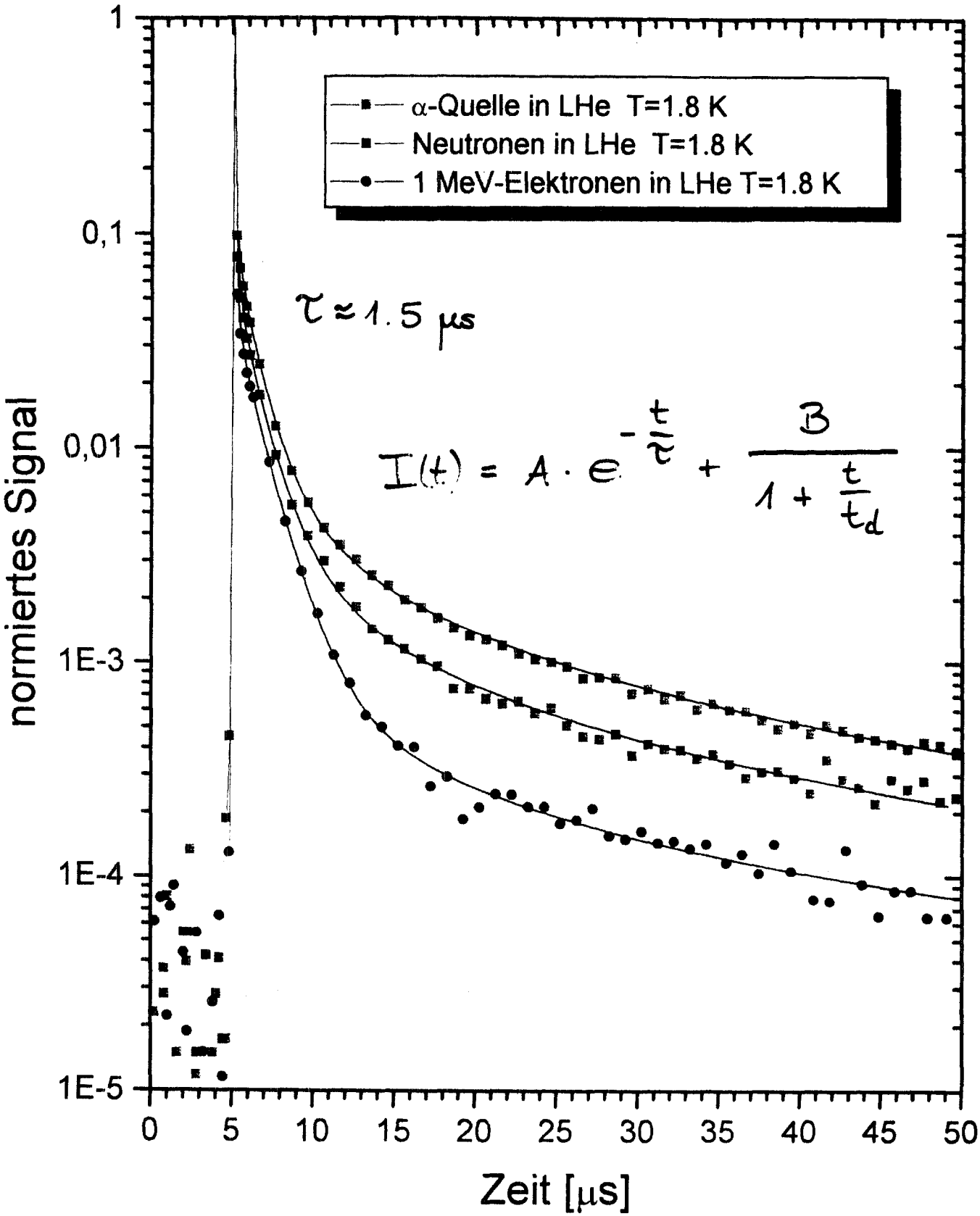
α-Quelle in LHe T=1.8 K
Neutronen in LHe T=1.8 K
1 MeV-Elektronen in LHe T=1.8 K
τ ≈ 1.5 µs
I(t) = A · e^(-t/τ) + B / (1 + t/t_d)
normiertes Signal
Zeit [µs]
1
0,1
0,01
1E-3
1E-4
1E-5
0
5
10
15
20
25
30
35
40
45
50

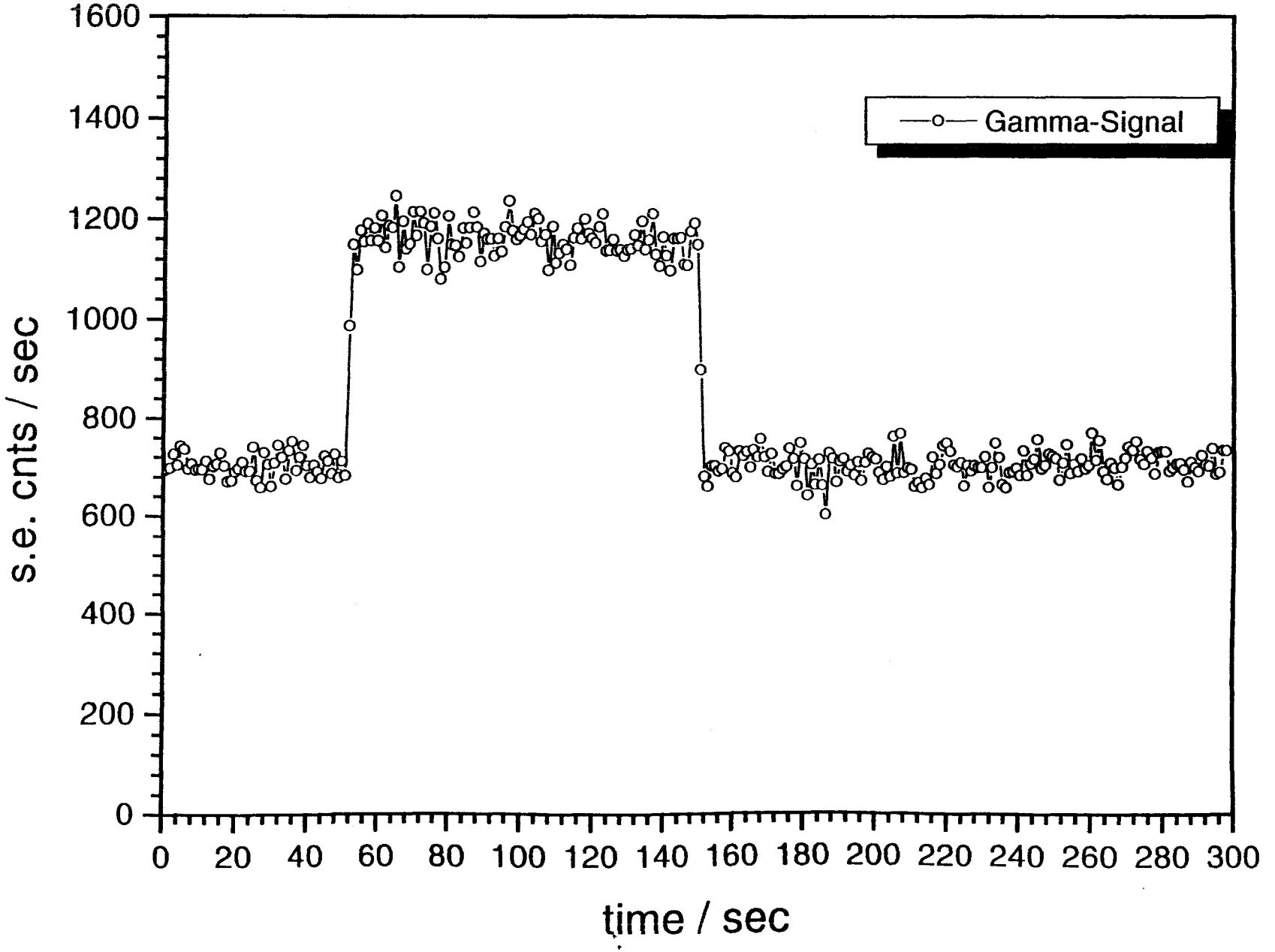
Gamma-Signal
s.e. cnts / sec
time / sec
0
200
400
600
800
1000
1200
1400
1600
0
20
40
60
80
100
120
140
160
180
200
220
240
260
280
300

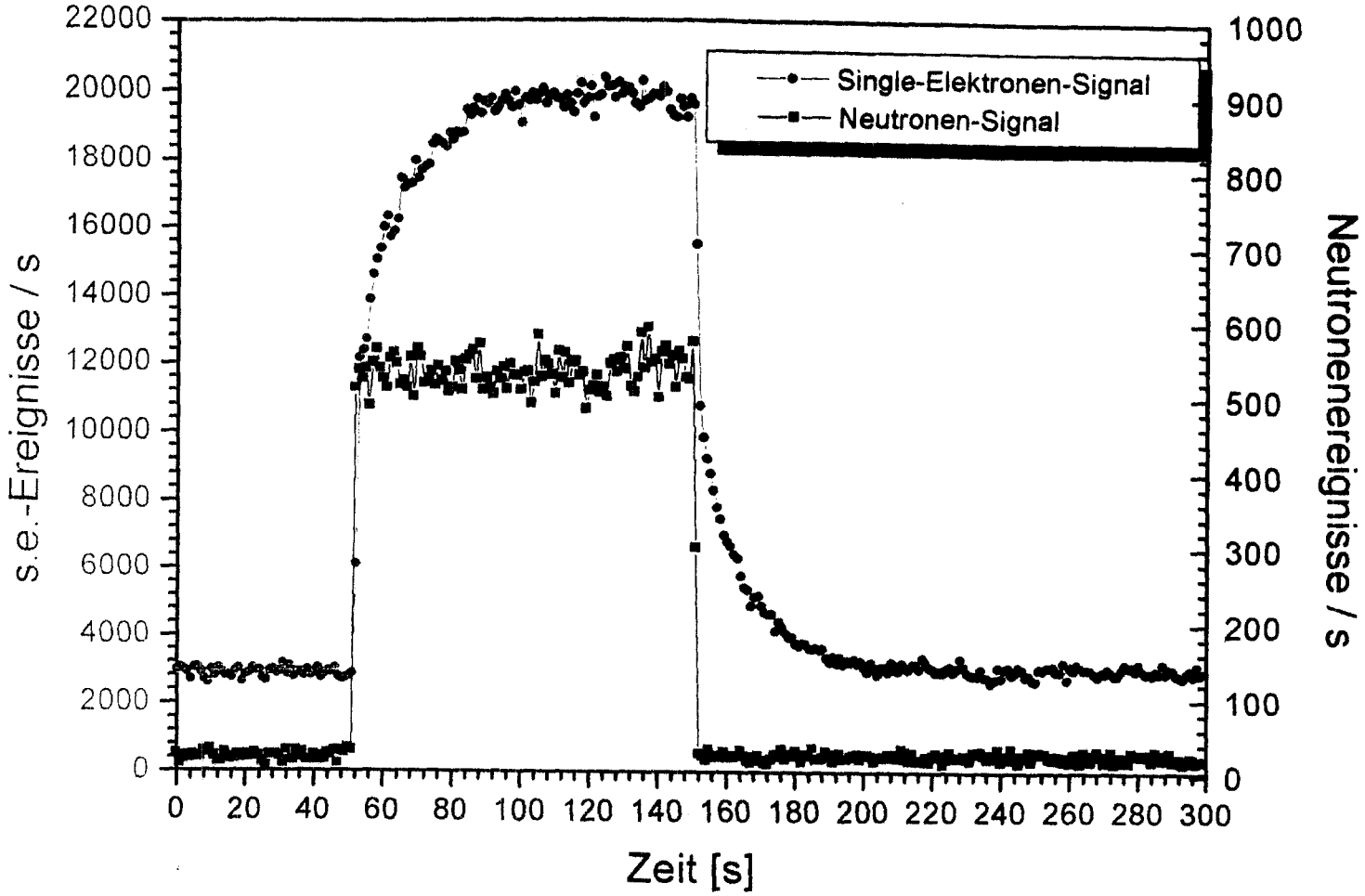
Single-Elektronen-Signal
Neutronen-Signal
s.e.-Ereignisse / s
Neutronenereignisse / s
Zeit [s]

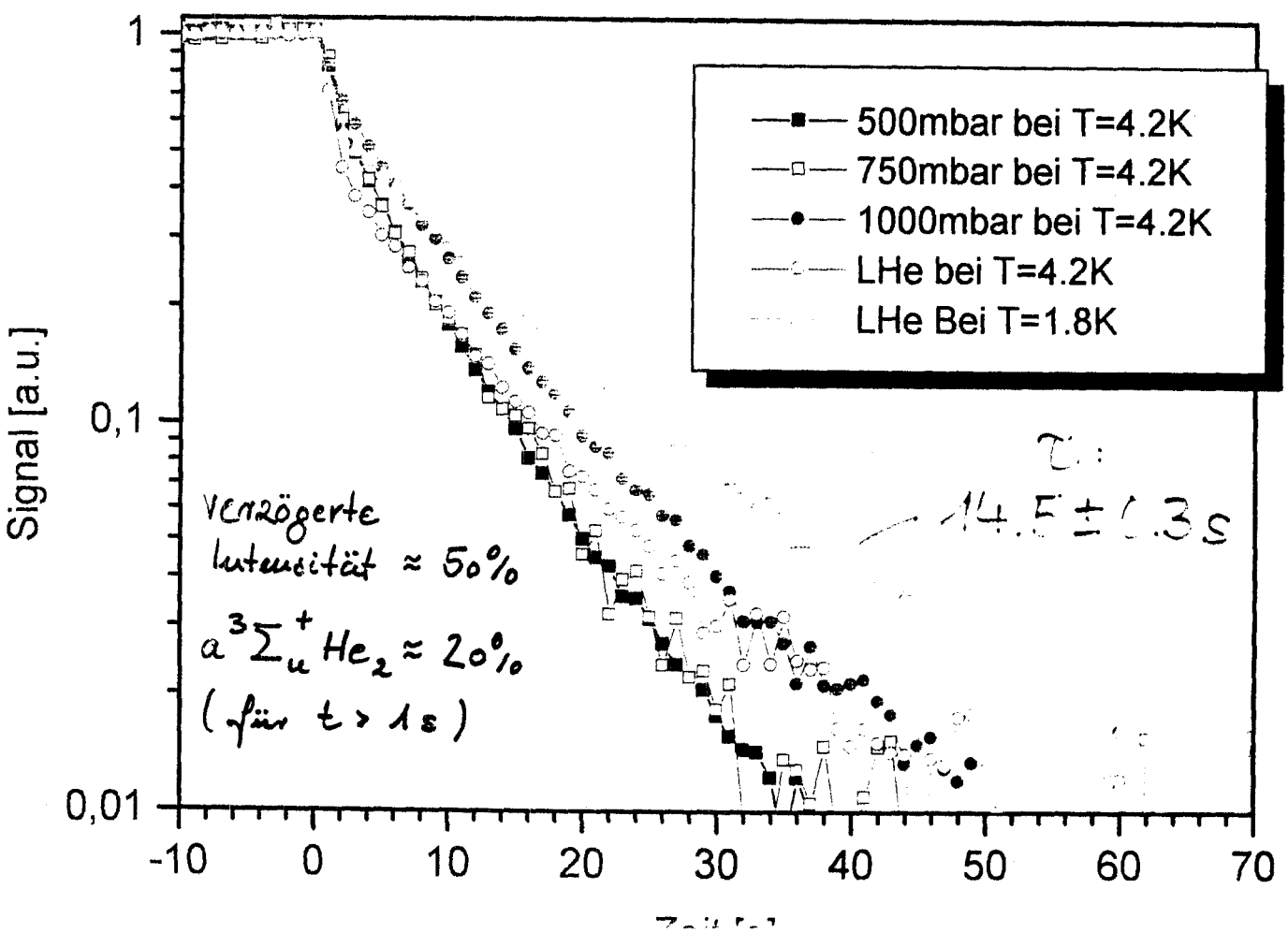
500mbar bei T=4.2K
750mbar bei T=4.2K
1000mbar bei T=4.2K
LHe bei T=4.2K
LHe Bei T=1.8K
Signal [a.u.]
verzögerte Intensität ≈ 50%
$a^3\Sigma_u^+ He_2$ ≈ 20%
(für t > 1s)
τ: 14.5 ± 0.3 s

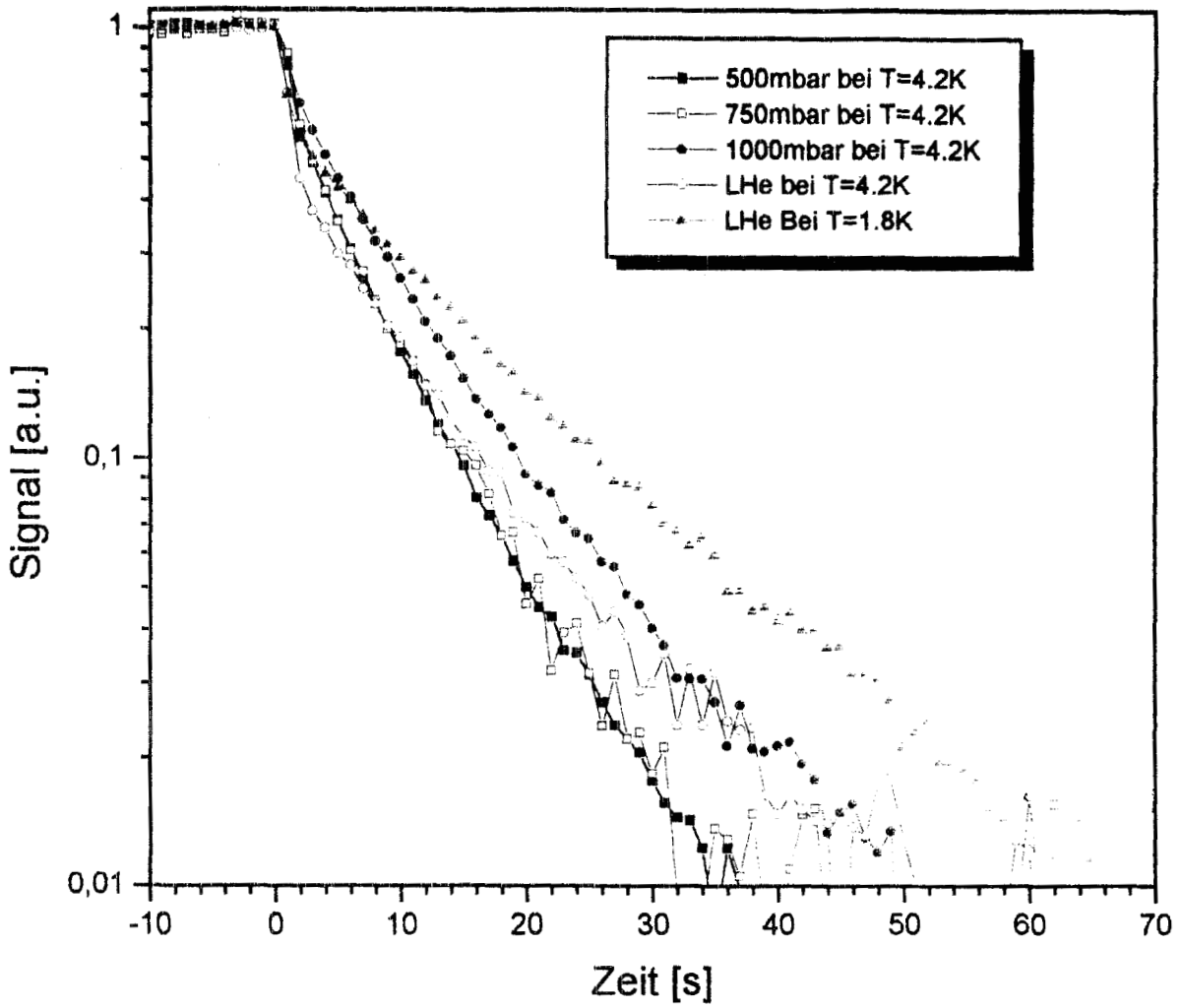

Sample	Temp	number density cm^{-3}	mainpulse p.e.'s/n	afterpulses s.e.'s/n	τ
500 mbar	4.2K	8.6×10^{20}	28	50 ±1	8.0 ± .1
750 mbar	4.2K	1.3×10^{21}	23.5	46	7.9 ± .2
1000 mbar	4.2K	1.7×10^{21}	18.5	43	10.0 ± .2
LHe	4.2K	1.9×10^{22}	31	21	14 ± .1
LHe	1.8K	2.2×10^{22}	25.5	20	14.5 ± .2

γ's : B_4C in beam switch shutter

$$n + {}^3He \rightarrow p + t + 764\ keV$$

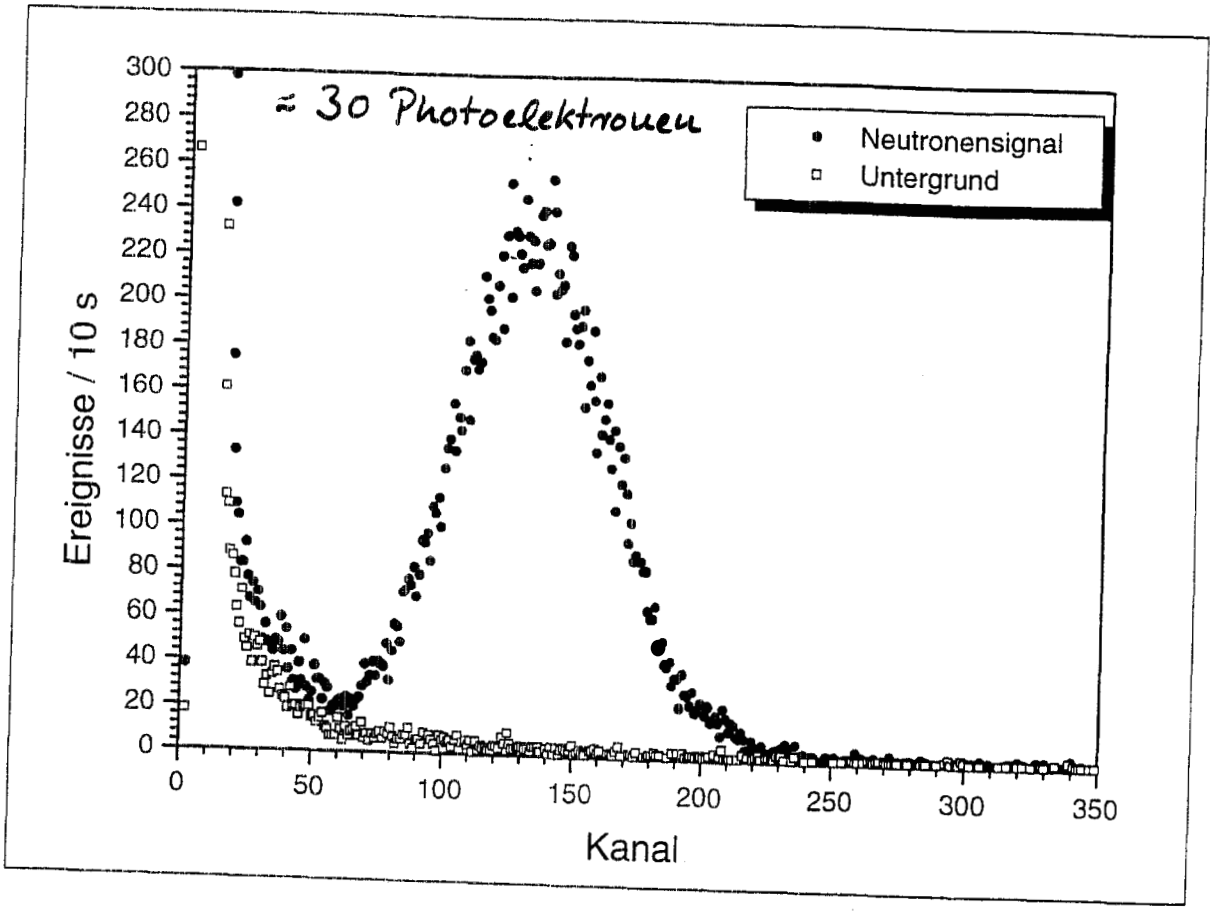

e^- : 0.15 - 0.2 p.e. / keV

α, n : 0.035 - 0.04 p.e. / keV $\approx$ Faktor 4 - 5

$\rightarrow$ Quenching

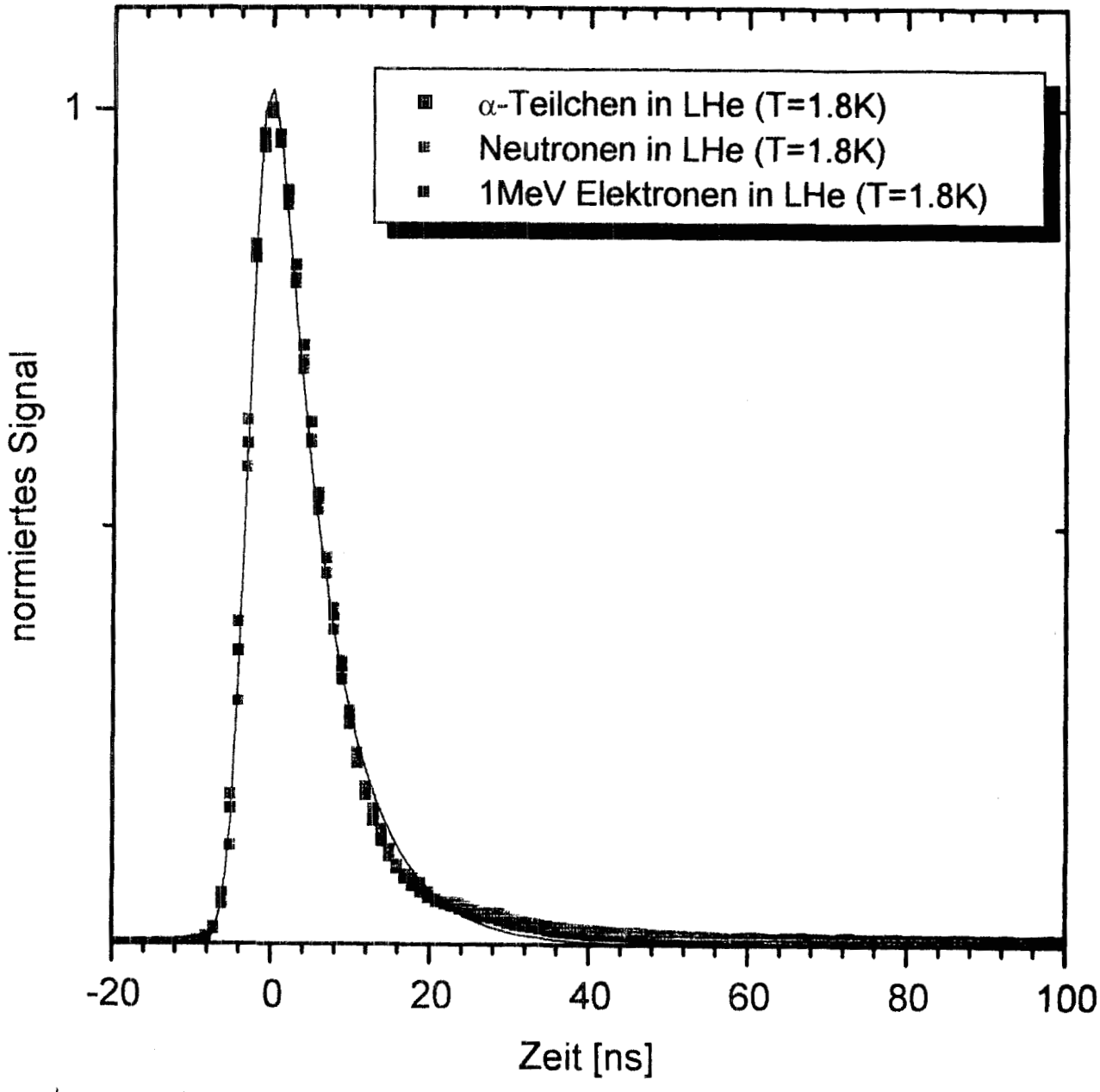

$t_r \approx 4.2$ ns
$t_f \approx 13.6$ ns } für alle Teilchen → PSD ??

Modell: 2 exponentielle Zerfälle,
Zeitauflösung: Gauß-Funktion

FWHM = 3.5 ns

$\tau_1 \approx 2.4$ ns

$\tau_2 \approx$ [illegible] (T = 1.8 K)

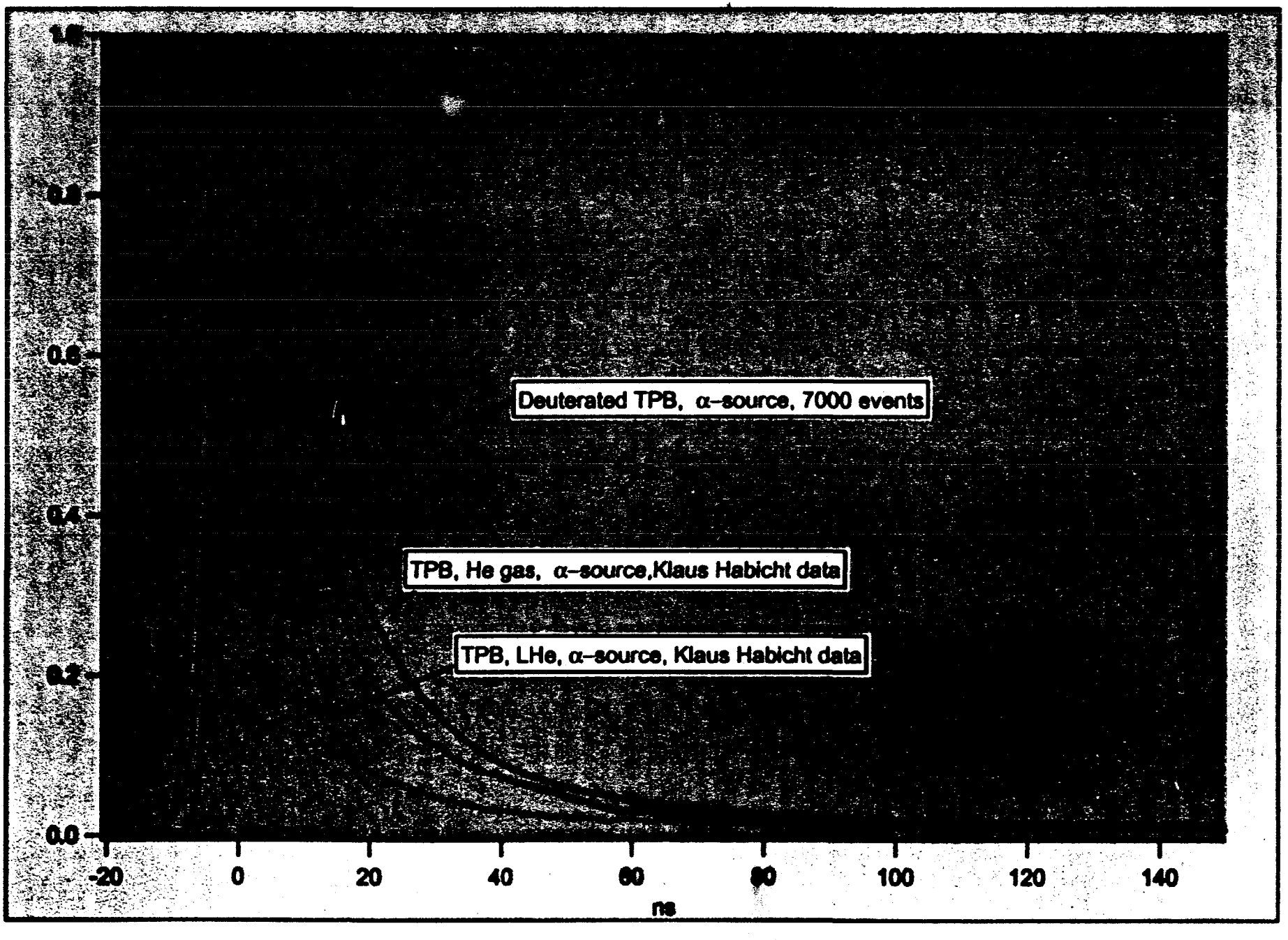
Deuterated TPB, α–source, 7000 events
TPB, He gas, α–source,Klaus Habicht data
TPB, LHe, α–source, Klaus Habicht data
0.0
0.2
0.4
0.6
0.8
1.0
-20
0
20
40
60
80
100
120
140
ns

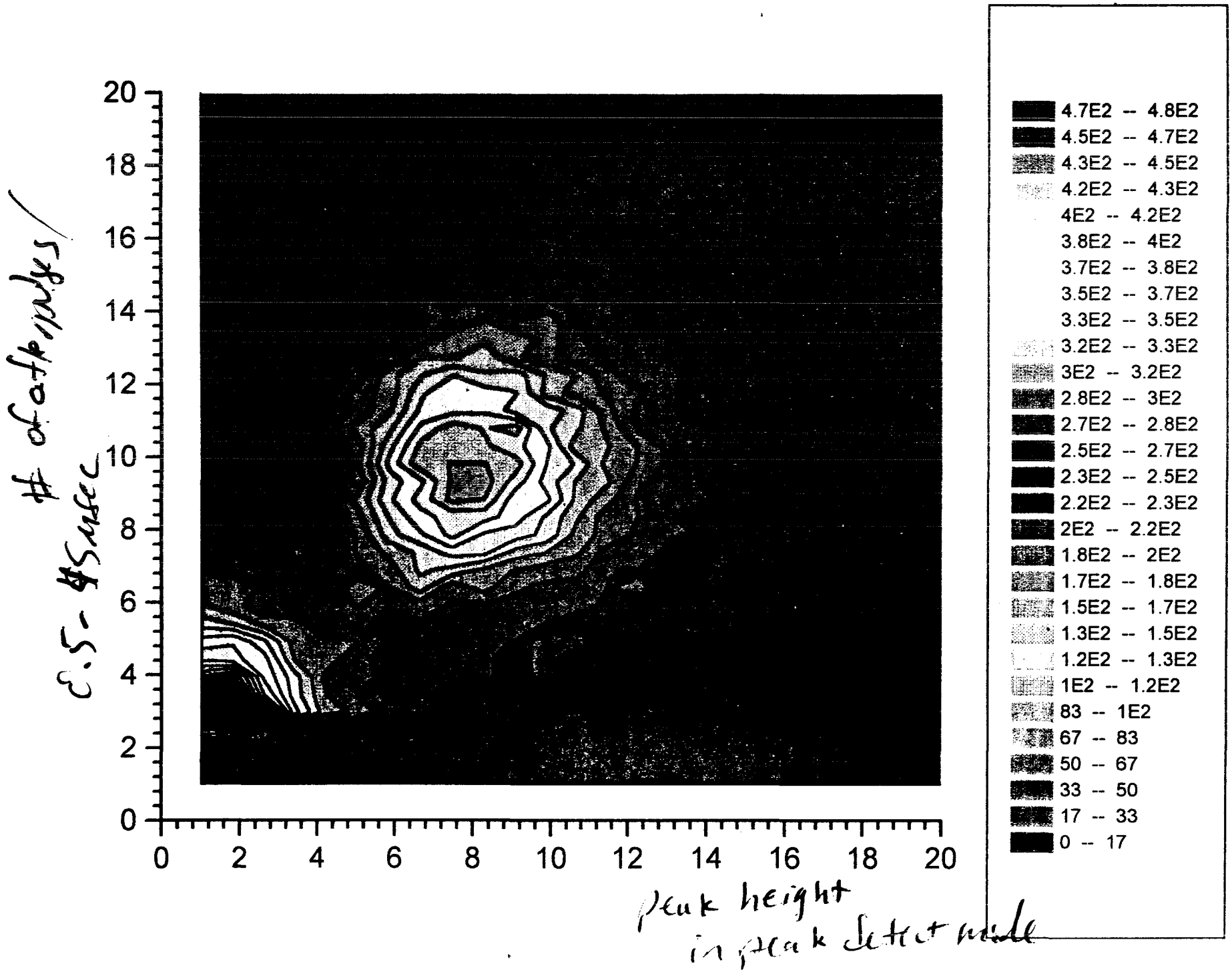

n
VL
4K
peak
det

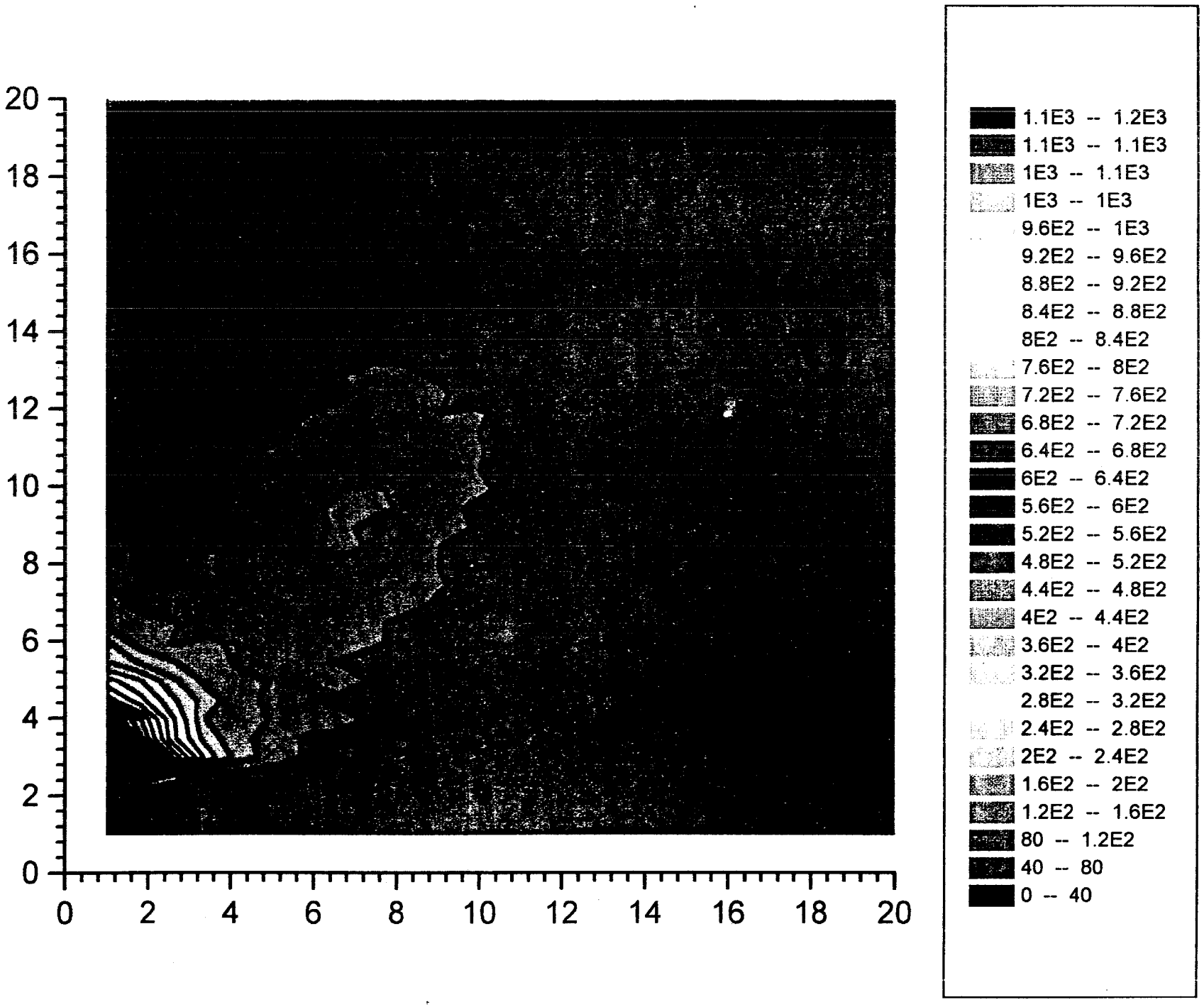
20
18
16
14
12
10
8
6
4
2
0
0
2
4
6
8
10
12
14
16
18
20
1.1E3 -- 1.2E3
1.1E3 -- 1.1E3
1E3 -- 1.1E3
1E3 -- 1E3
9.6E2 -- 1E3
9.2E2 -- 9.6E2
8.8E2 -- 9.2E2
8.4E2 -- 8.8E2
8E2 -- 8.4E2
7.6E2 -- 8E2
7.2E2 -- 7.6E2
6.8E2 -- 7.2E2
6.4E2 -- 6.8E2
6E2 -- 6.4E2
5.6E2 -- 6E2
5.2E2 -- 5.6E2
4.8E2 -- 5.2E2
4.4E2 -- 4.8E2
4E2 -- 4.4E2
3.6E2 -- 4E2
3.2E2 -- 3.6E2
2.8E2 -- 3.2E2
2.4E2 -- 2.8E2
2E2 -- 2.4E2
1.6E2 -- 2E2
1.2E2 -- 1.6E2
80 -- 1.2E2
40 -- 80
0 -- 40

Monte-Carlo studies

Martin Cooper (Los Alamos)

SIGNAL ANALYSIS

Scintillation Signal

$$\Phi = \Phi_B + Ne^{-\Gamma_{AVE}t}\left[\frac{\varepsilon_\beta}{\tau_\beta} + \frac{\varepsilon_3}{\tau_3}\left[1 - P_3P_n e^{-\Gamma_p t}\cos(\omega_r t + \phi)\right]\right]$$

$$+ N_{Al}e^{-t/\tau_{Al}} + N_{Cu}e^{-t/\tau_{Cu}}$$

measured for a time T_M

- How does the error in a least squares fit compare to the proposal?
- How does the error on ω_r depend on other parameters?
- What is the optimal value of T_M?
- What is the optimal value of N_3 that sets τ_3?
- At what level can Φ_B, N_{Al}, and N_{Cu} be ignored?
- What is to be gained by suppressing the β decays, i.e. $\varepsilon_\beta \rightarrow 0$?

SQUID Signal

$$\Phi_S \propto \Phi_{BS} + N_3\left[1 - P_3 e^{-\Gamma_3 t}\cos(\omega_3 t + \phi_3)\right]$$

ν_0 = 3 Hz $N_n = 2 \times 10^6$ σ_{LS} = 1.20 μHz σ_{rms} = 1.25 μHz

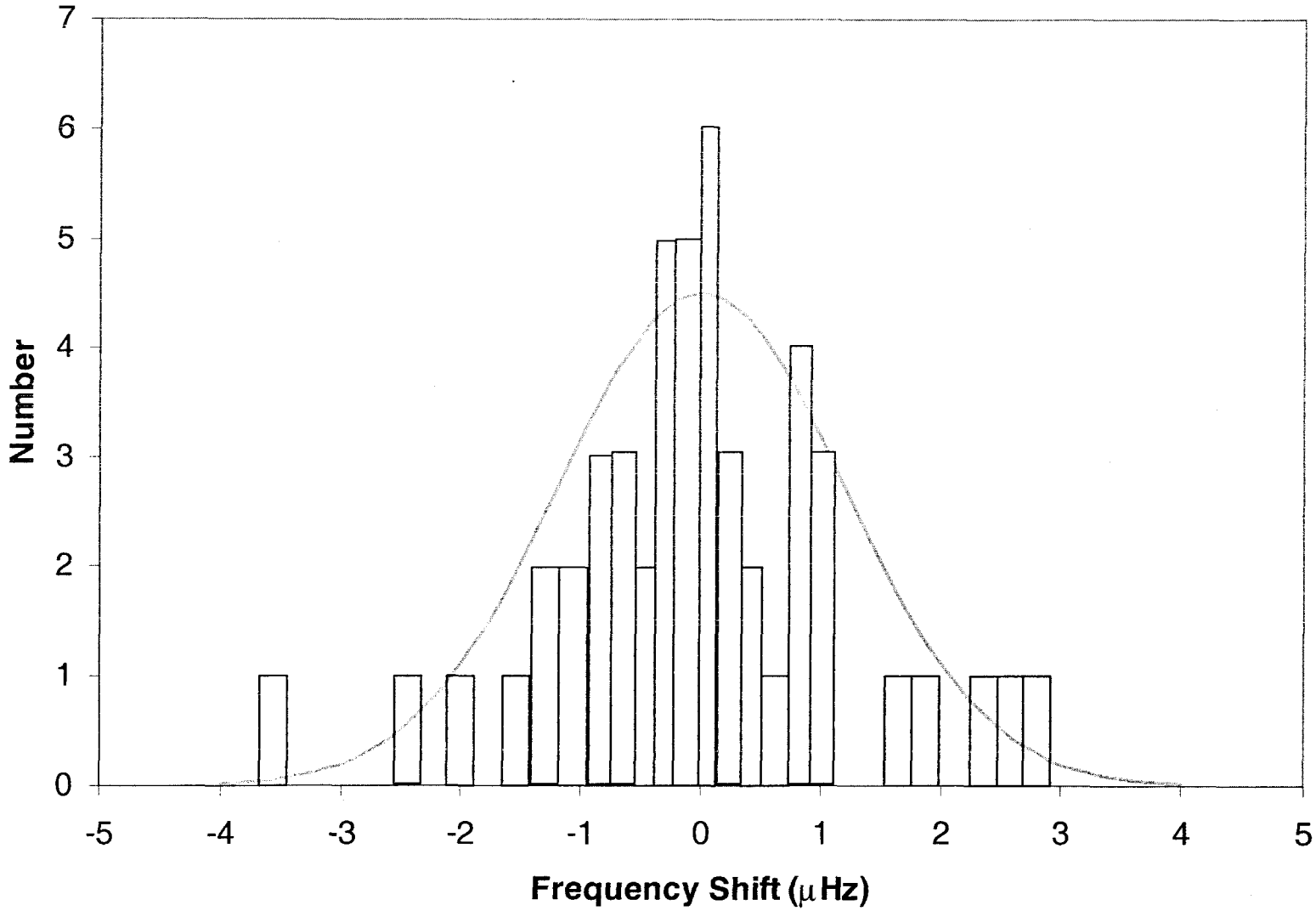

$\nu_0 = 3$ Hz $N_n = 2 \times 10^6$

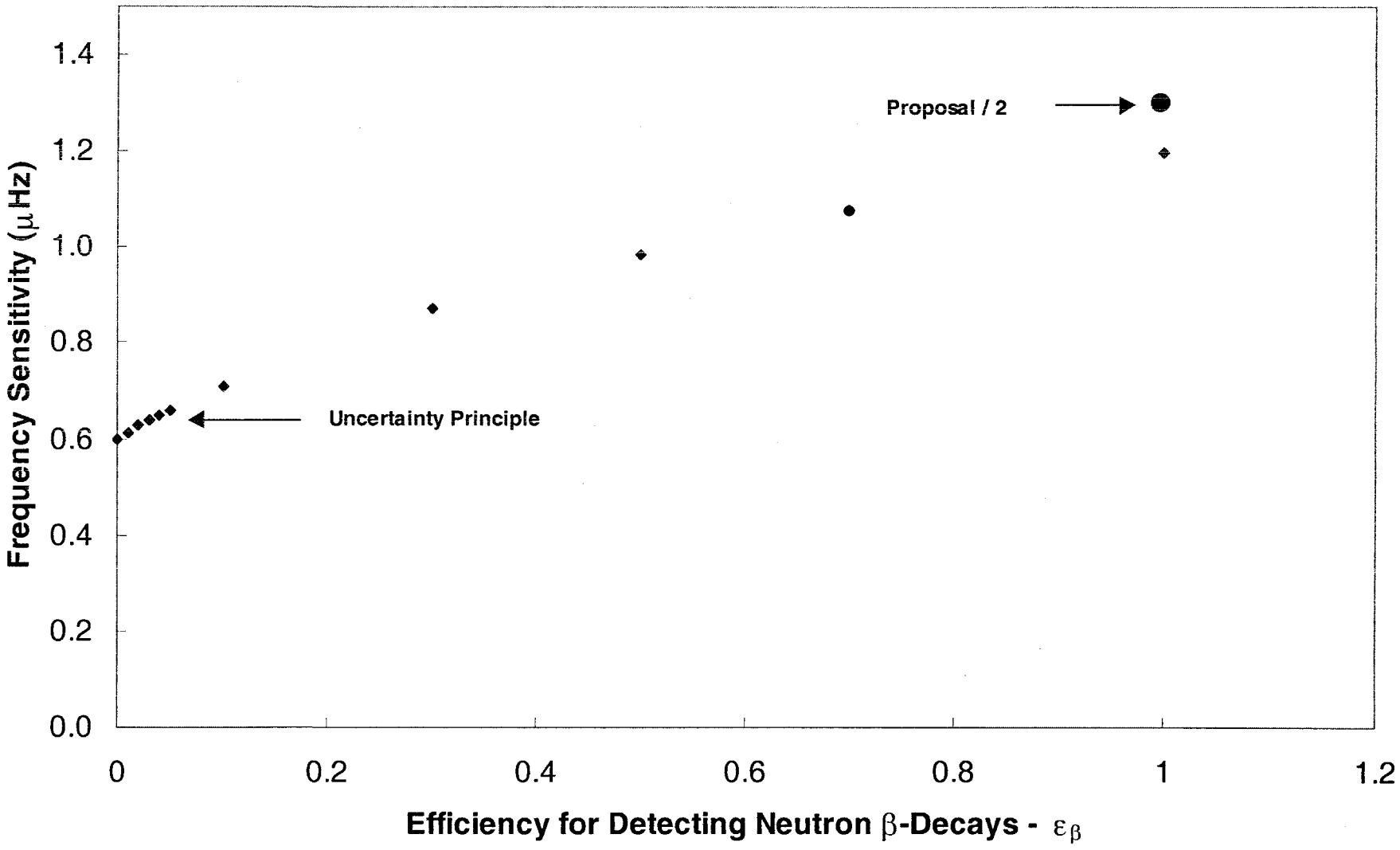

DEPENDENCE ON OTHER PARAMETERS

Free Variables	σ_{LS}
$f_0 = \omega_r/2\pi$	1.2 μHz
f_0, τ	1.2 μHz
f_0, τ, N_n	1.2 μHz
f_0, τ, N_n, ϕ	2.4 μHz

LIGHT COLLECTION

Optimizing the light collection design

- What is the number of photoelectrons expected?
- How many PEs do we get versus integration time?
- How is the number of PEs influenced by compromises associated with HV, activation backgrounds, cryogenics, etc?
- Do fiber optics have a role?

GUIDE7 program as a starting place

Test code against NIST lifetime results

COLD NEUTRON TRANSPORT

Design the beam polarizing beam splitter

- How do we optimize polarization and transmission given the allowed length?
- Do losses in the splitter make backgrounds?

Minimizing beam activation

- Do we need a guide in the cryostat?
- What sort of collimation is useful?
- Do the entrance windows need to be Be?
- How can we minimize the activation on the electrodes?
- How should we dump the beam?

Minimize scattered-neutron activation

- Where do we want to place neutron absorbers?

Problems with trace elements

UCN IN THE TRAP

Should these considerations be part of the light colloection Monte-Carlo?
UV light in the trap also needs to be considered?

SPIN TRANSPORT OF THE ^{3}He INTO THE CELL

Polarization losses in the transport into the cryostat
Polarization losses in the storage volume
Polarization losses in the transport from the storage volume to the measuring cell

Fitting into LANSCE ER-2

Jan Boissevain (Los Alamos)

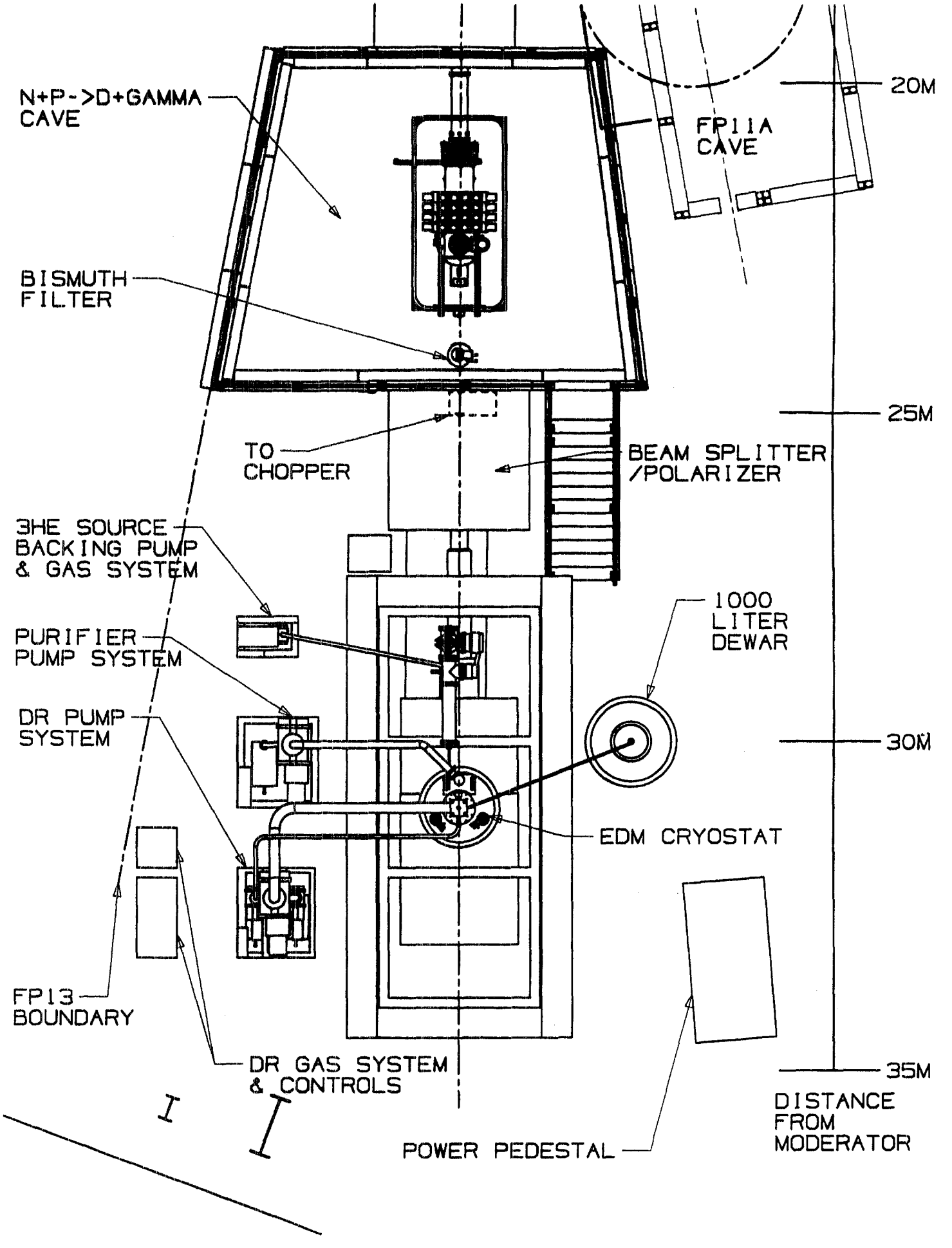
N+P->D+GAMMA
CAVE
BISMUTH
FILTER
FP11A
CAVE
20M
25M
TO
CHOPPER
BEAM SPLITTER
/POLARIZER
3HE SOURCE
BACKING PUMP
& GAS SYSTEM
PURIFIER
PUMP SYSTEM
DR PUMP
SYSTEM
1000
LITER
DEWAR
30M
EDM CRYOSTAT
FP13
BOUNDARY
DR GAS SYSTEM
& CONTROLS
35M
DISTANCE
FROM
MODERATOR
POWER PEDESTAL

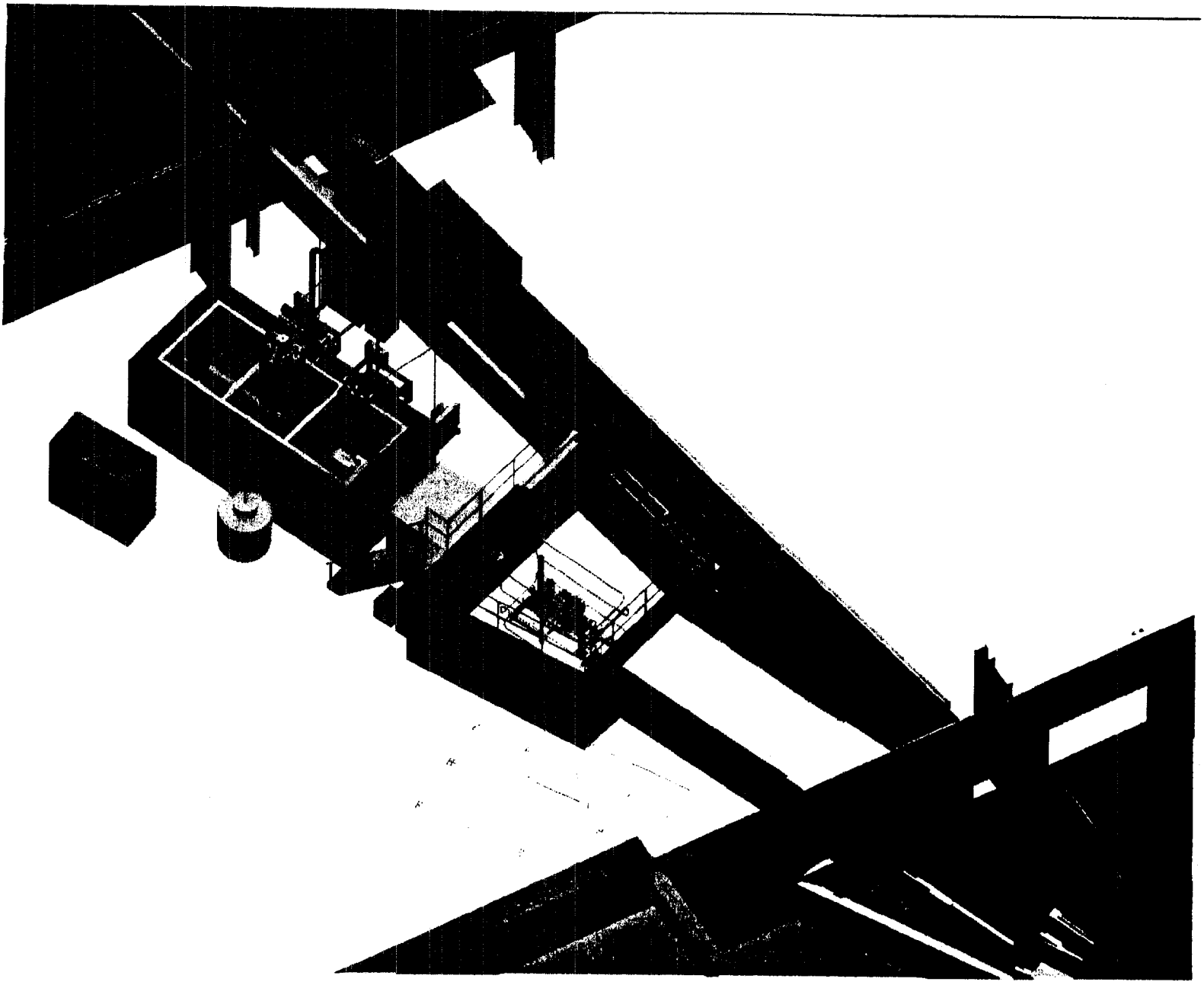

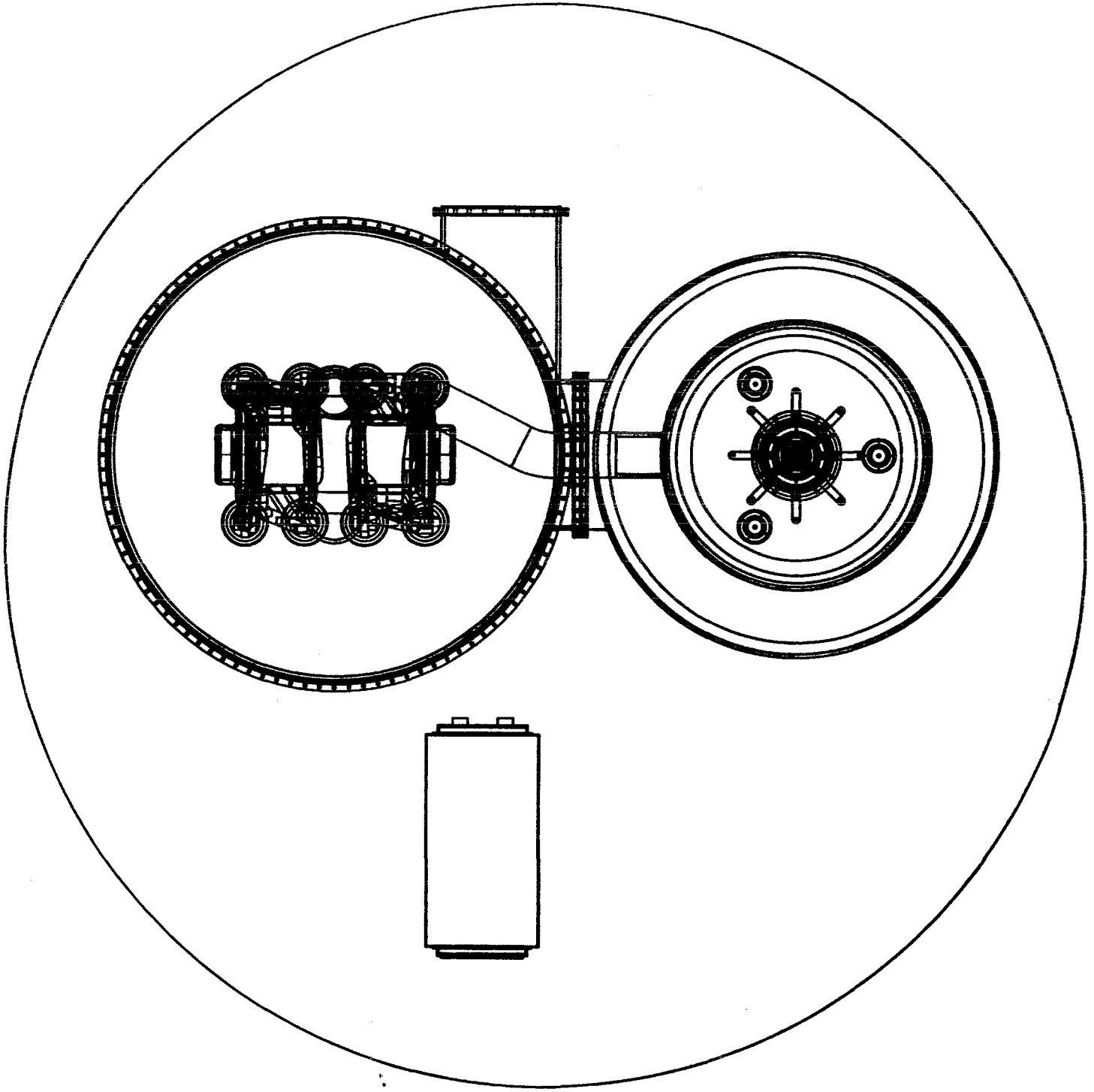

Tour of LANSCE ER-2 and Building 10 Lab

Seppo Penttila (Los Alamos)

Separating the purifier from the dilution refrigerator, an alternate design

Paul Huffman (NIST)
James Butterworth (ILL)

Figure 3.1 The Heat Flush

a) Flushing tube
b) Needle Valve
c) Heater
d) Helium of natural purity
e) Decreasing level of ^3He

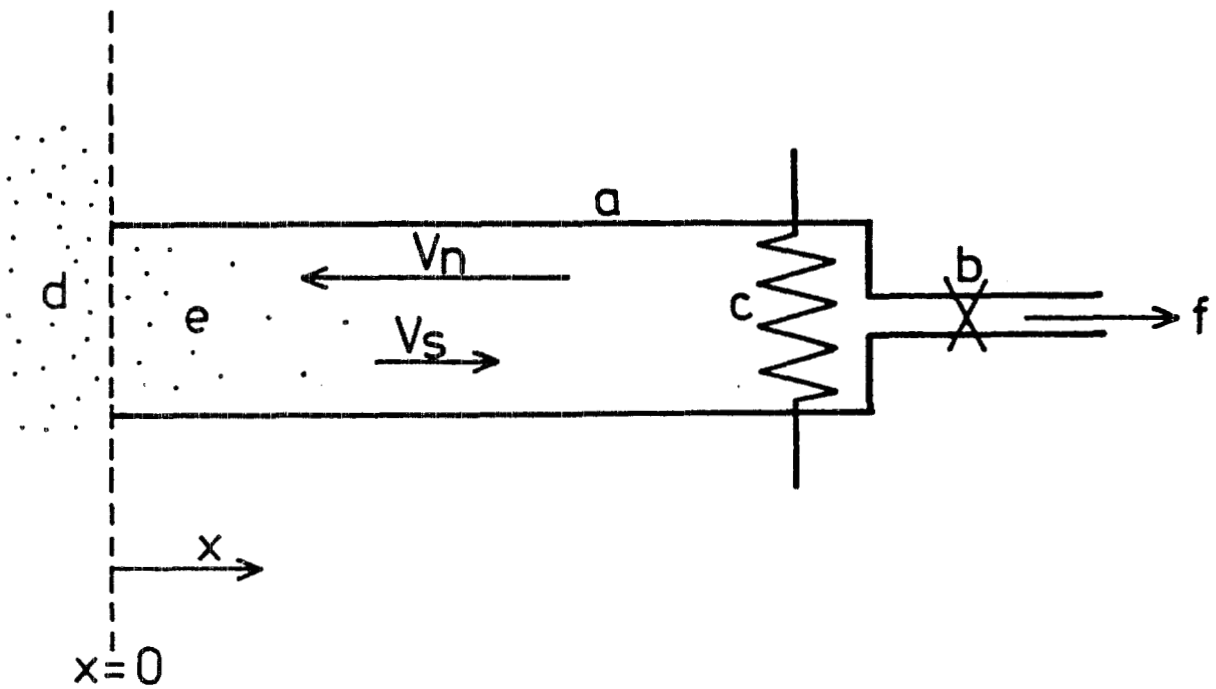

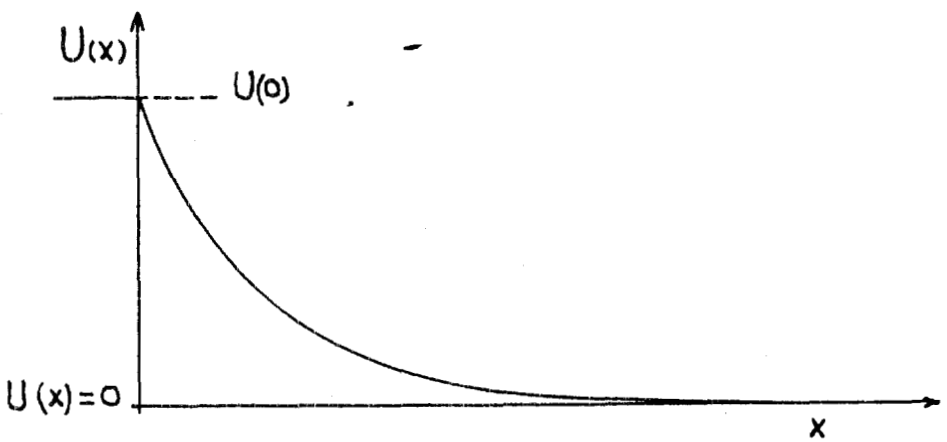

Graph to show ^3He concentration in Flushing tube

P.V.E. McClintock '87

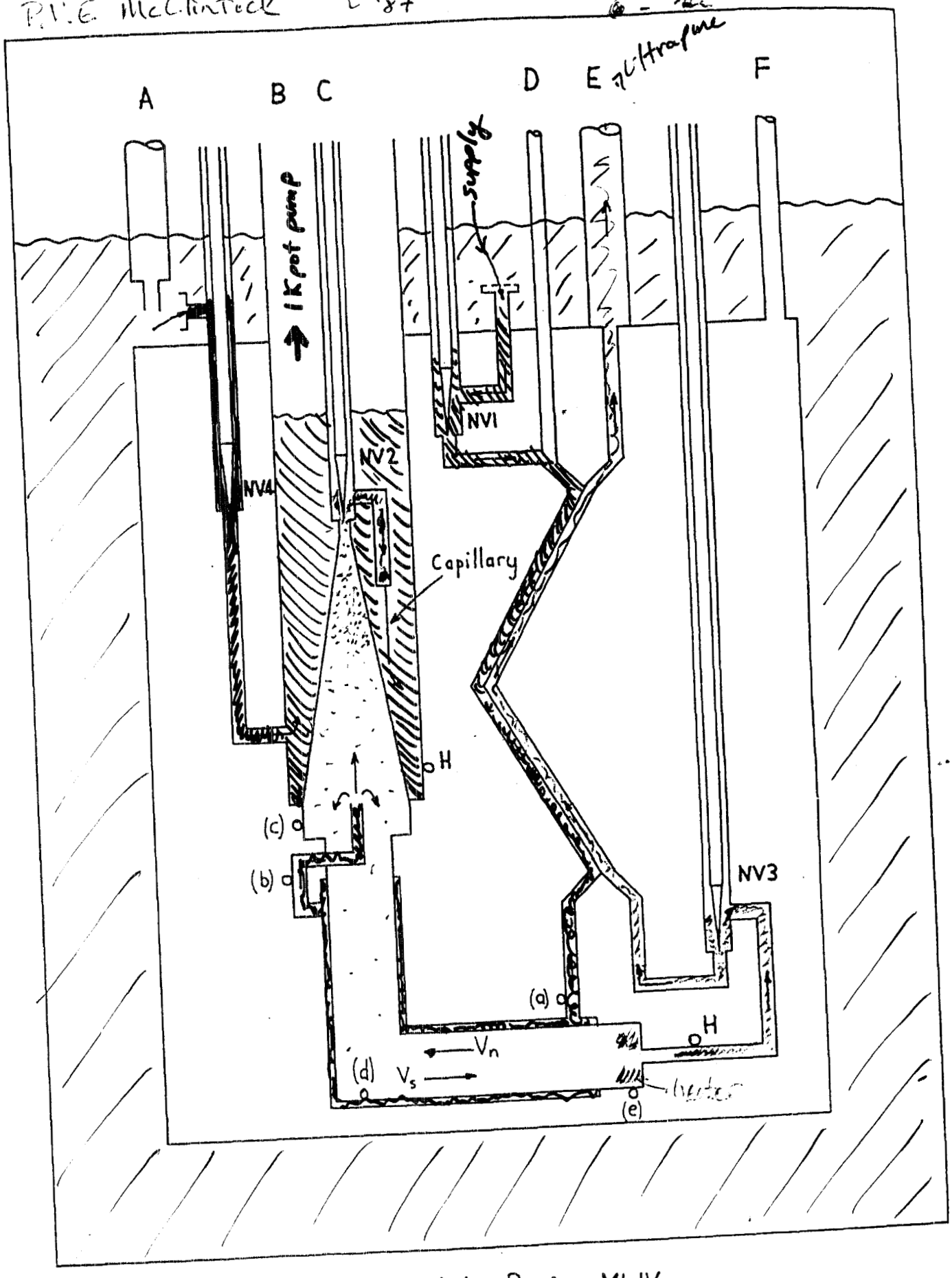

Figure 4.4 Purifier Mk IV

McClintock apparatus

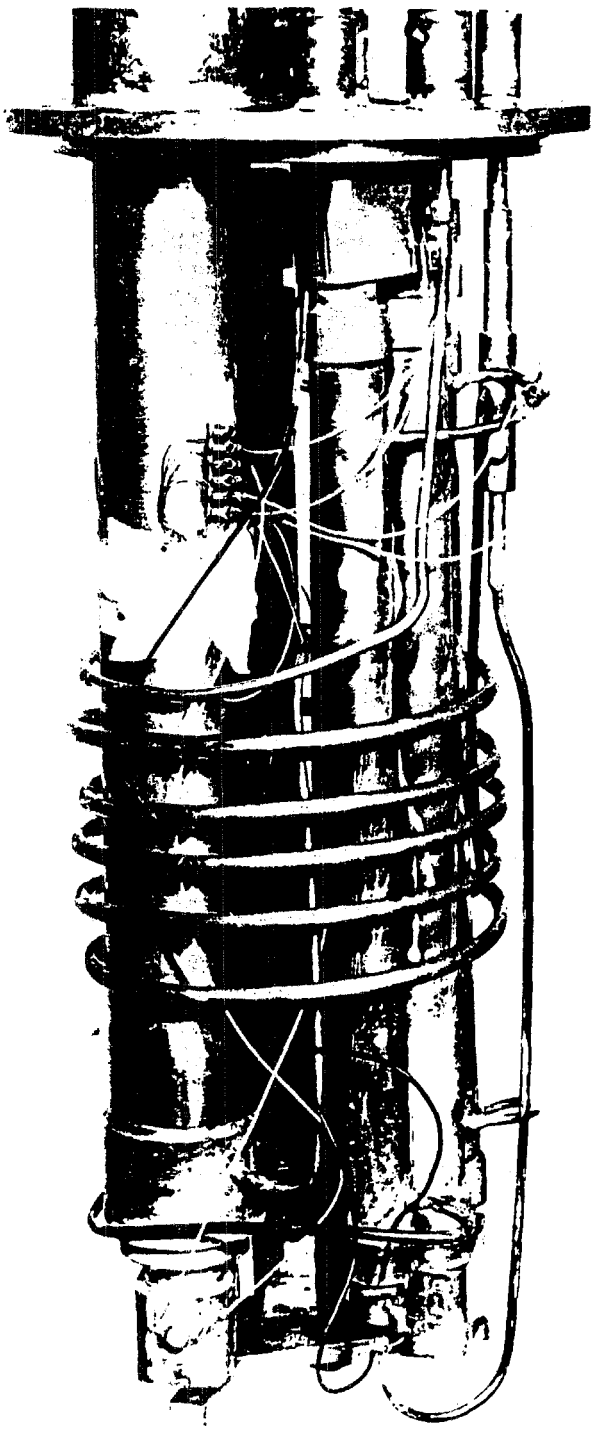

Photo 1 The Purifier Insert

helium out

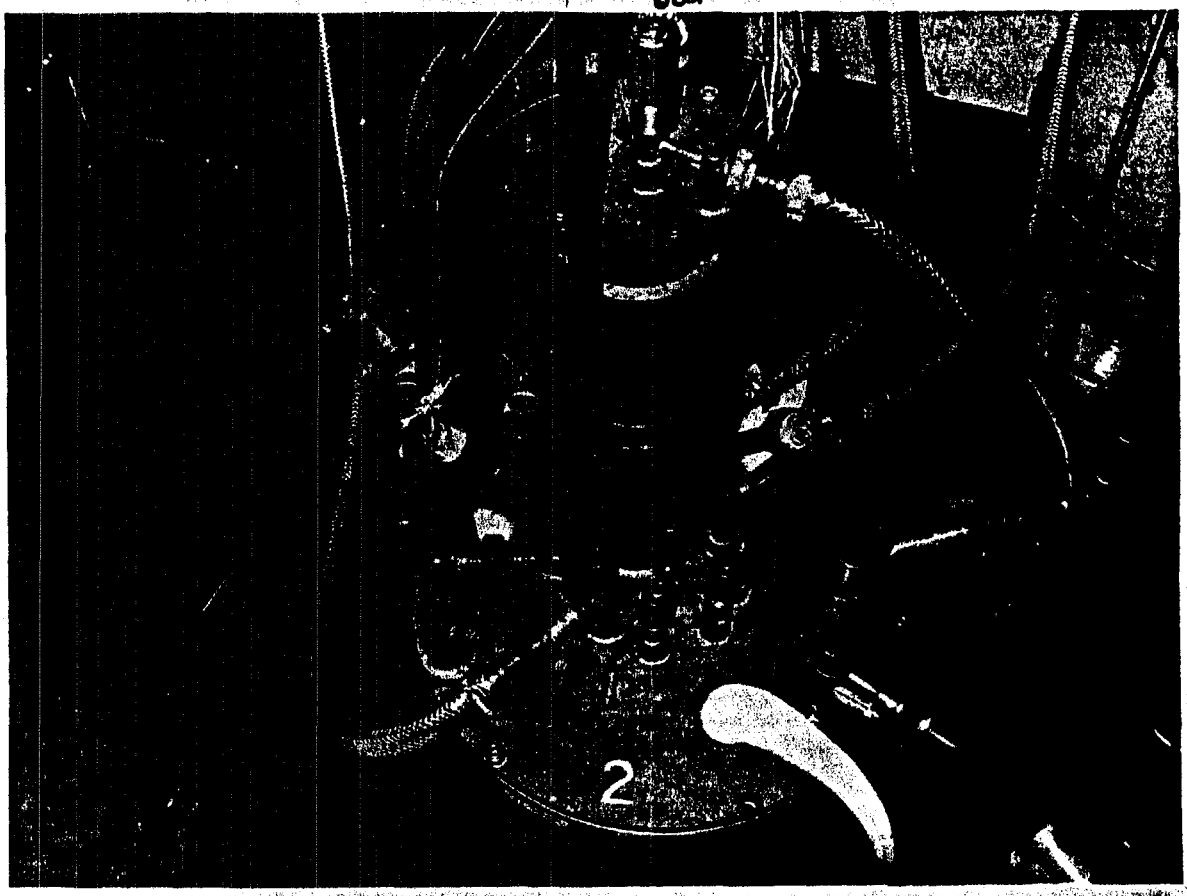

top of cryostat

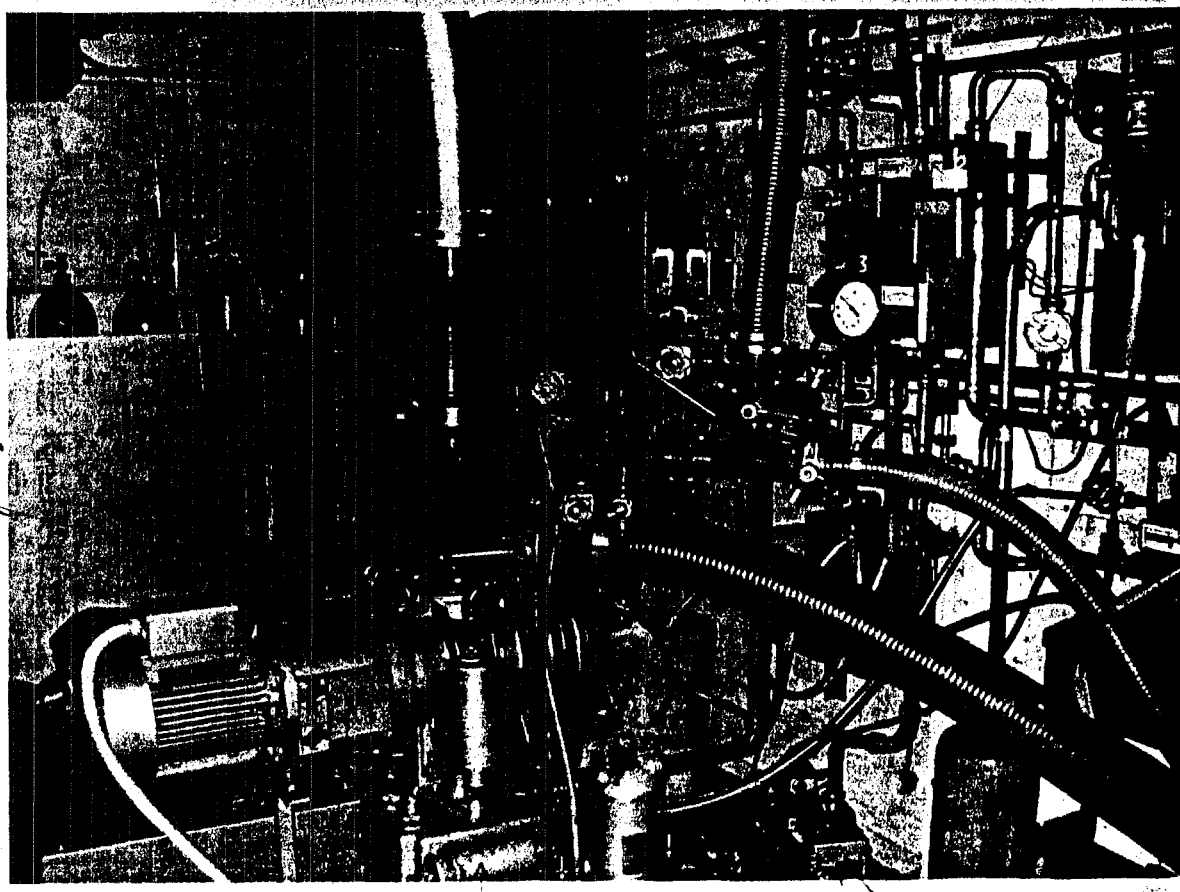

...pressor ...lve)

1K pot pump line

1K pot roots

1K pot mech. pump

Sealed pump for moving

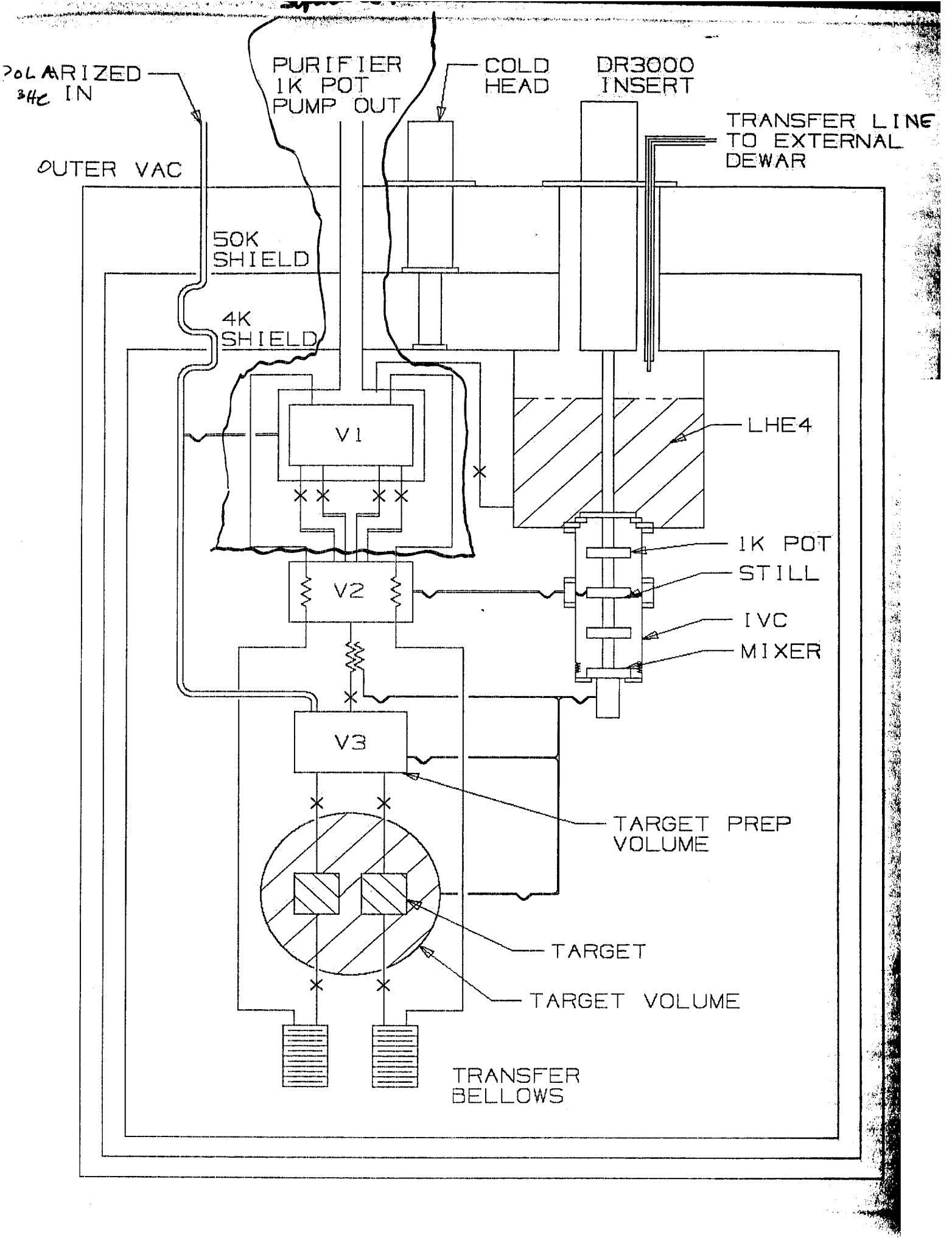
POLARIZED
3He IN
PURIFIER
1K POT
PUMP OUT
COLD
HEAD
DR3000
INSERT
TRANSFER LINE
TO EXTERNAL
DEWAR
OUTER VAC
50K
SHIELD
4K
SHIELD
V1
LHE4
1K POT
STILL
V2
IVC
MIXER
V3
TARGET PREP
VOLUME
TARGET
TARGET VOLUME
TRANSFER
BELLOWS

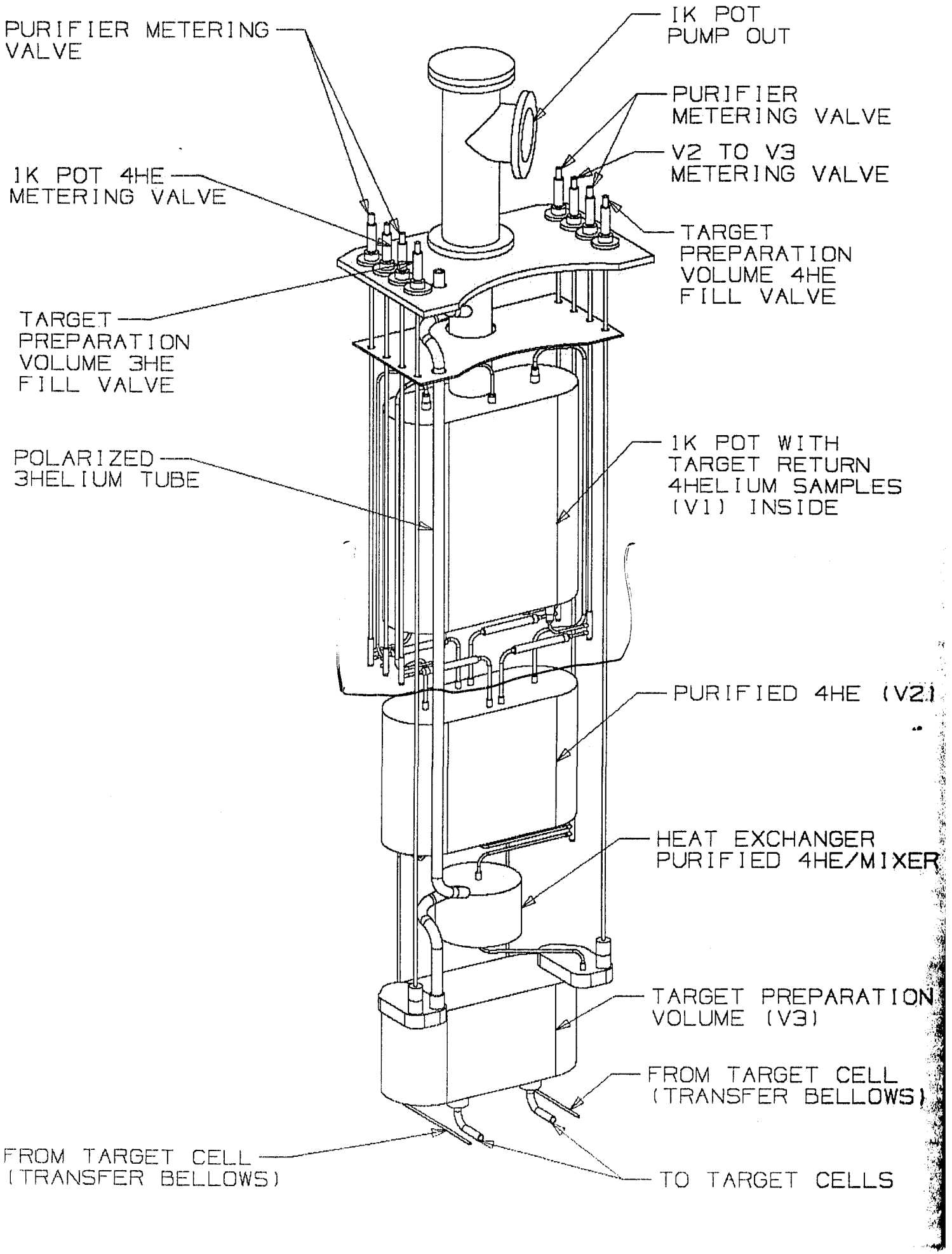
PURIFIER METERING VALVE
1K POT PUMP OUT
PURIFIER METERING VALVE
V2 TO V3 METERING VALVE
1K POT 4HE METERING VALVE
TARGET PREPARATION VOLUME 4HE FILL VALVE
TARGET PREPARATION VOLUME 3HE FILL VALVE
POLARIZED 3HELIUM TUBE
1K POT WITH TARGET RETURN 4HELIUM SAMPLES (V1) INSIDE
PURIFIED 4HE (V2)
HEAT EXCHANGER PURIFIED 4HE/MIXER
TARGET PREPARATION VOLUME (V3)
FROM TARGET CELL (TRANSFER BELLOWS)
FROM TARGET CELL (TRANSFER BELLOWS)
TO TARGET CELLS

EDM CRYOSTAT

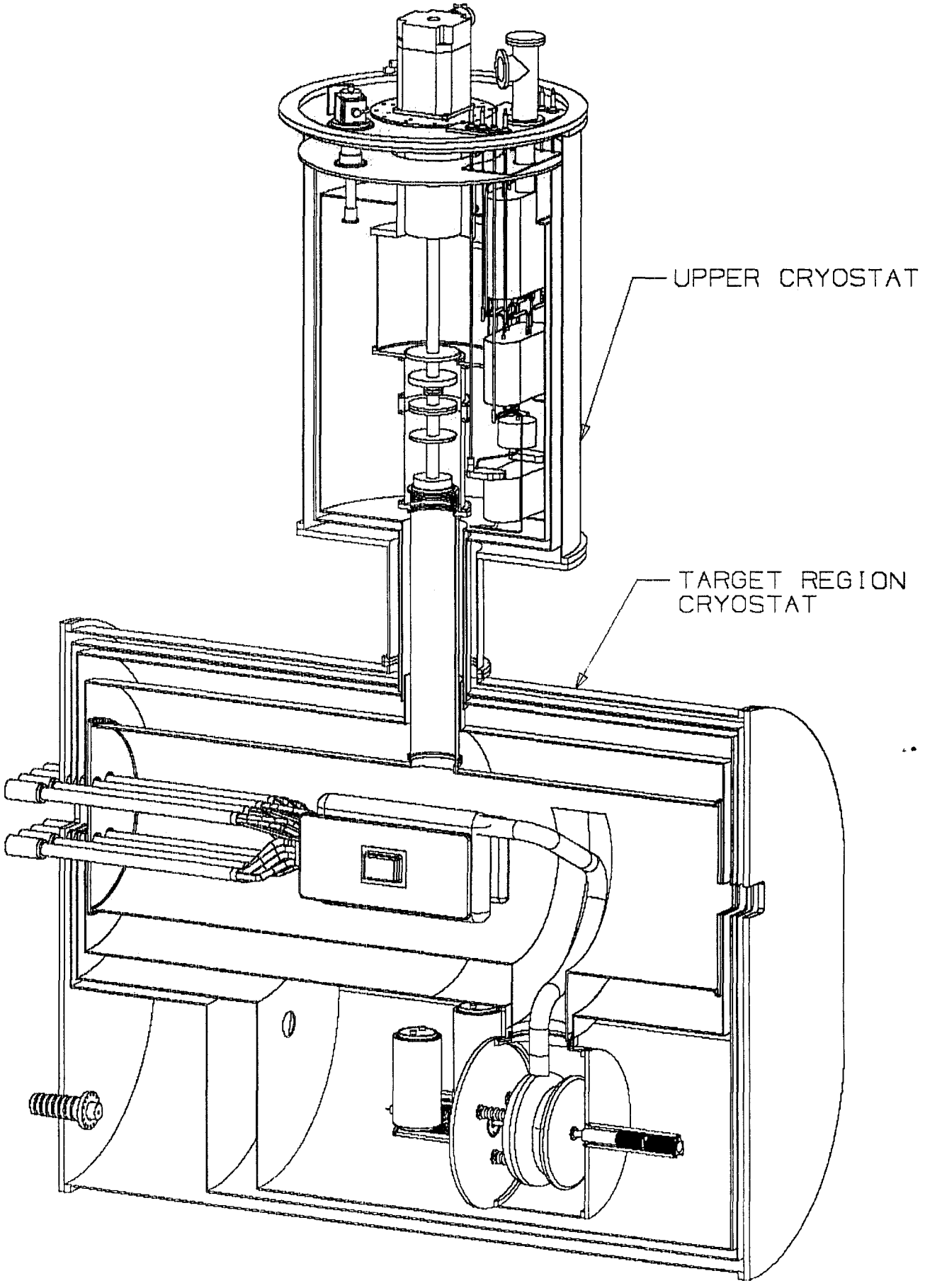

EDM UPPER CRYOSTAT

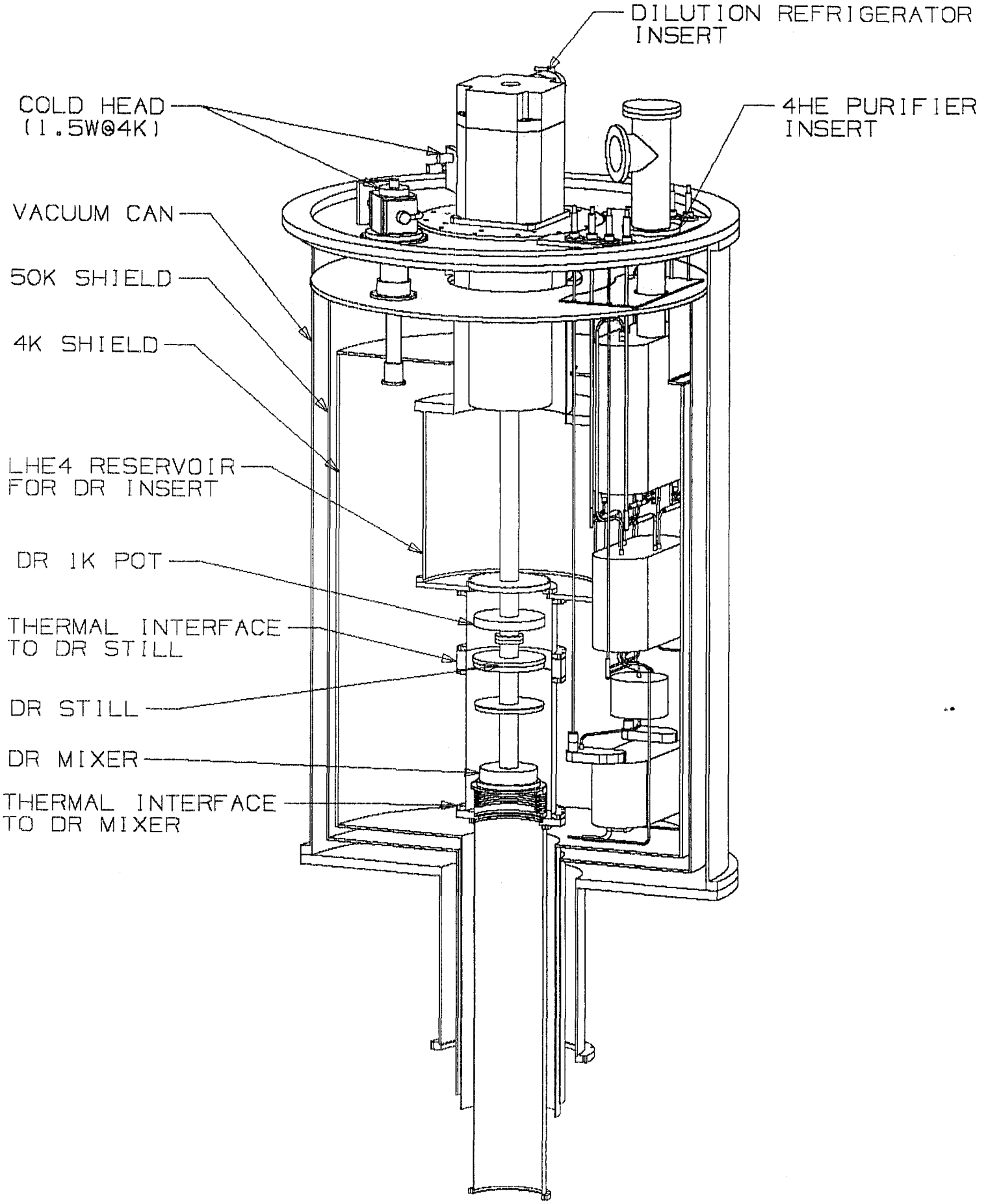

Combined System (proposal design)

Advantages:

- compact design
- minimizes amt. of equipment used
- helium circulated at "low" (<2K) temperature

Disadvantages:

- problem with one system requires warming up both systems. (turnaround for purifier ~ 1 day, for D.R. + compr. ~ 1 week)
- thermal fluctuations in one system may significantly affect the other system
- combining systems after independent development and testing may be difficult
- extra equipment needed during development.

Two independent systems:

Advantages:

- systems can be tested independently
- helium could be accumulated prior to the run (for reserve)
- no interdependence between systems

  instability in one system (OR LEAK) DOES NOT PREVENT OPERATION OF OTHER SYSTEM

DISADVANTAGES:

- recovering used helium difficult
  (using "new" helium would be ~ 1000 L/day)
- incoming helium must be cooled
  (4.2K ⇒ ~9W)
  (2.2K ⇒ ~3W)

Hybrid system: (compromise?)

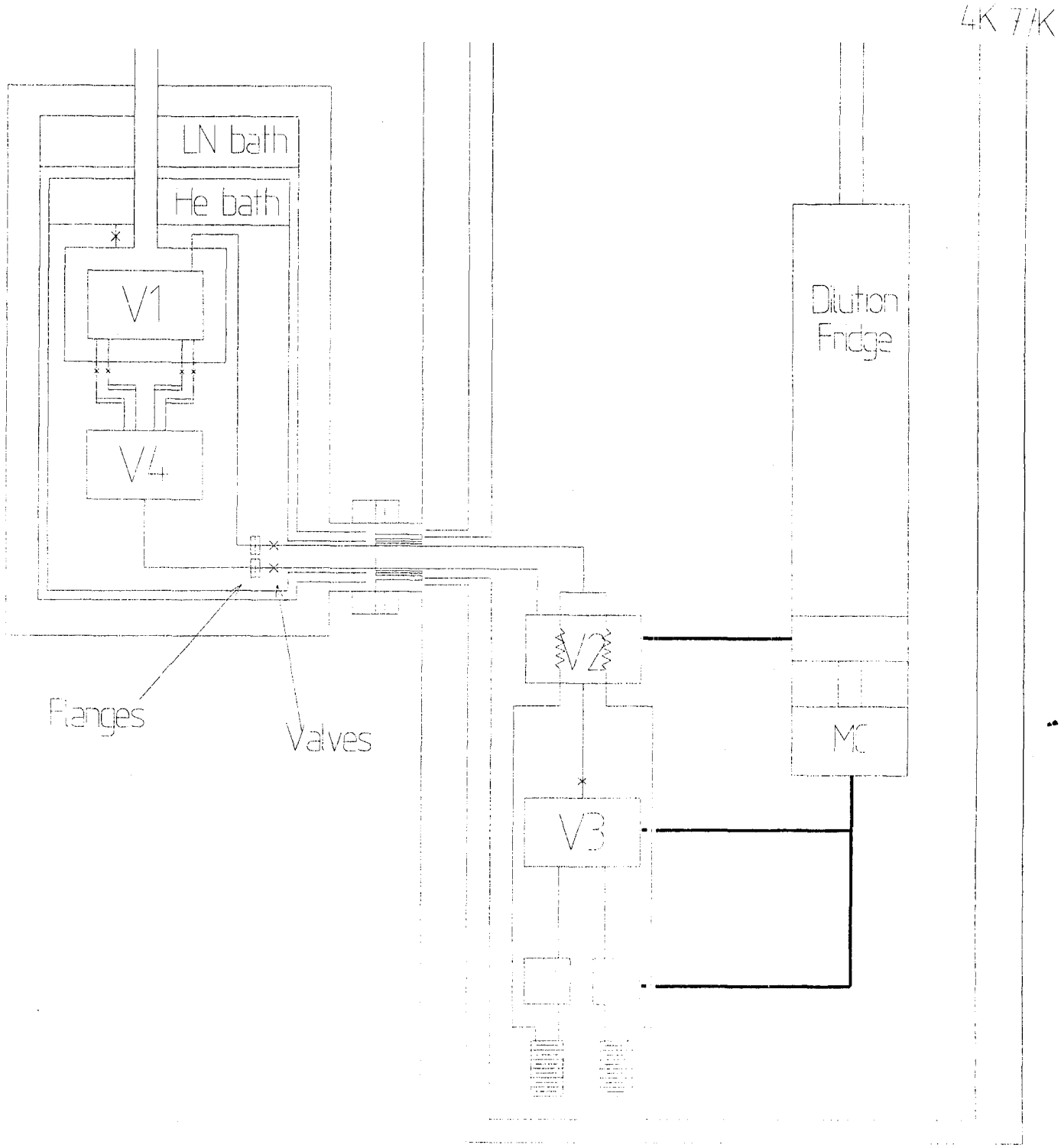

Proposed tests of SQUIDs

Michelle Espy (Los Alamos)

SQUIDs in the nEDM

- Introduction
- Temperature Effects
  - Survey of SQUIDs
- Upcoming tests

Motivation

- 3He comagnetometer reduces systematic errors due to instabilities in the magnetic field.
- SQUIDs provide direct measure of 3He precession frequency, $\nu_3 = \gamma_{3He} B_0$,thus a direct measure of B_0 averaged over cell volume and measurement period.
- SQUIDs could provide a measure of polarization of 3He introduced into the cell during the filling period
- Monitor orientation of 3He magnetization
- *Hopefully* simpler than dressed spin technique (no RF)

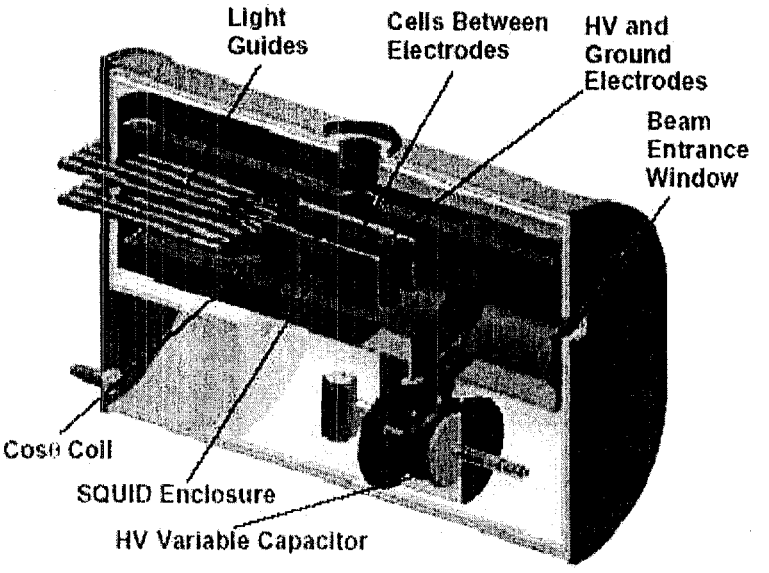

Fig IV-1. Experimental cryostat. length ~ 3.1 m. The neutron beam enters from the right. Two neutron cells are between the three electrodes. Scintillation light from the cells is monitored by the light guides and photomultipliers.

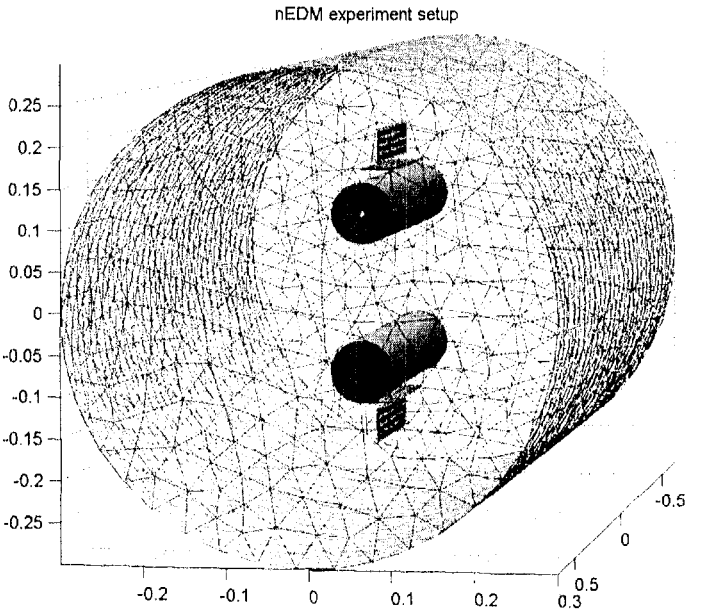

What does the FEM model say?

Without SIS = .002 Φ_o and with SIS = .02 Φ_o .

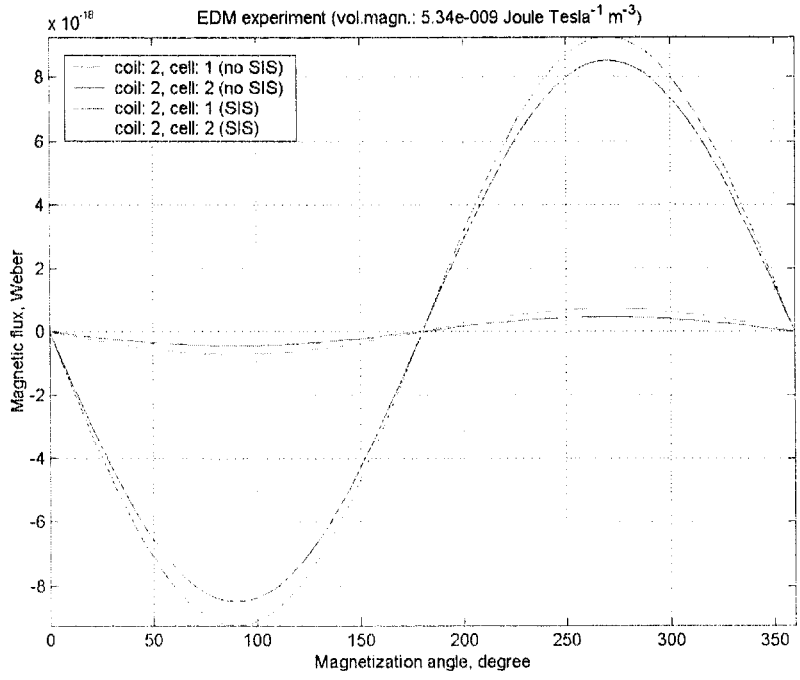

Figure V.F.2. Predicted values of flux in the vertically oriented pick-up coils expected, both with and without the superconducting vessel.

Parameter	Value
SIS Cylinder	
Length	1.34 m
Radius	0.3 m
Target cells	
Length	0.5 m
Inner Radius	0.04 m
Center from SIS axis	+/- 0.1 m
Magnetization	$5e^{-9}$ J/(Tm^3) assuming $1.25e^{15}$ 3He/cell
SQUID pickup coils	
Length	0.25 m
Width	0.04 m
Center from SIS axis	
Coils #1,3 (Horizontal)	+/- 0.145 m
Coils #2,4 (Vertical)	+/- 0.175 m

Assume the target is a uniformly magnetized sphere:
M=magnetization=polarization*magnetic moment/volume
100% polarization
$\mu = 2.127\mu N = 2.127(5.05\text{x}10\text{-}27)$
$1.25e^{15}$ 3He and cell volume (2.5 liters) = $5e^{17}$ $3He/m^3$

$M = 54e\text{-}^{10}$ JT/m^3

$$B_z = \frac{2}{3}\mu_o \frac{a^3}{z^3} M$$

radius of cell a~8.5cm and pick-up coil is z~1cm from surface.

Flux = B-field* area. Assume field constant over $100cm^2$ area.
Peak-to-peak value of flux in pick-up coils: 0.04 Φ_o .

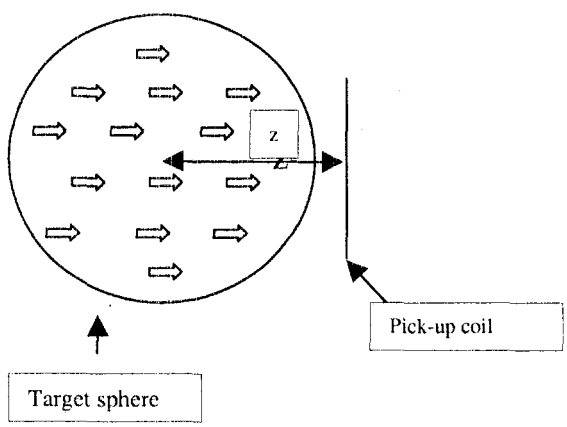

- 100 cm^2 pick-up S=0.02 Φ_0.

- Flux actually coupled to the SQUID is

$$\Phi_s = \frac{\Phi_p M}{(L_p + L_i)}$$

"typical" values M=10 nH, L_i=600 nH, 100 cm^2 loop L_p=1.4 μH.

Roughly 1/100th of the signal gets to the SQUID.

At 4 K: $d\Phi_{SQ}$~3 $\mu\Phi_0/Hz^{1/2}$ (measured) and should scale with sqrt(4K/0.3K).

- Experimental noise needs to be limited to as low as possible

- Possible sources: vibration in B field, leakage current, Johnson noise, magnetic noise through penetrations, non-uniformity in B field.

Noise vs. Temperature

Initial work was at 4 K. The nEDM will be at 0.3 K.

Wellstood, Urbina, Clarke

Appl. Phys. Lett., V**54** (25) 19 June 1989

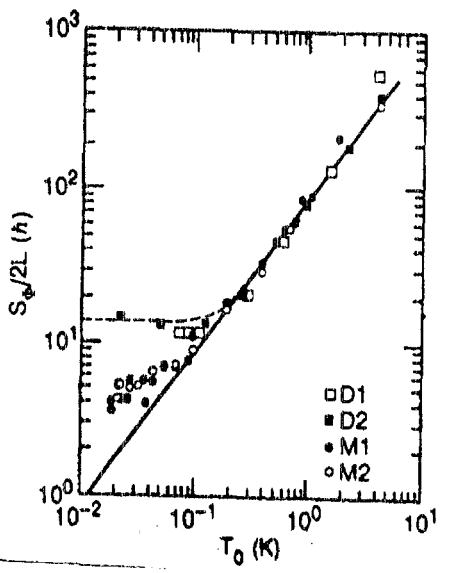

Wellstood, Urbina, Clarke

Appl. Phys. Lett., V**50** (12) 23 March 1987

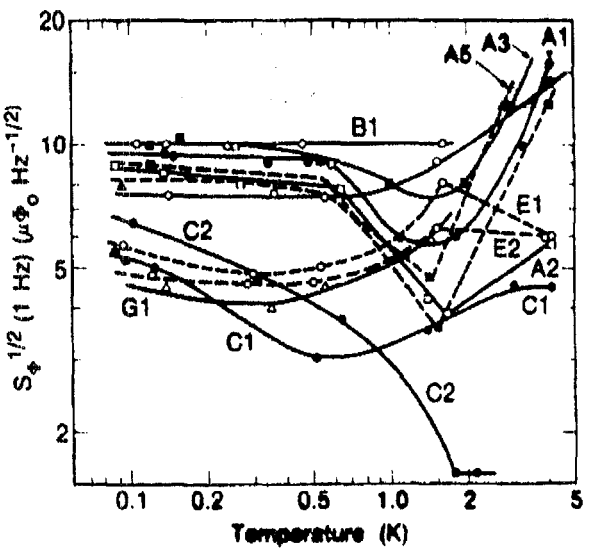

New Picovoltmeter built for tests at low temperatures

Data taken at NHMFL '01-'02

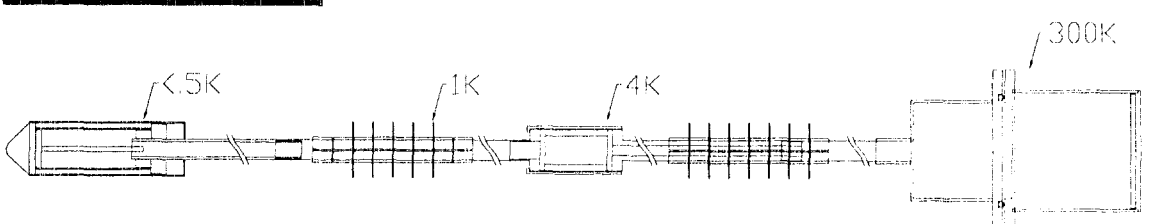

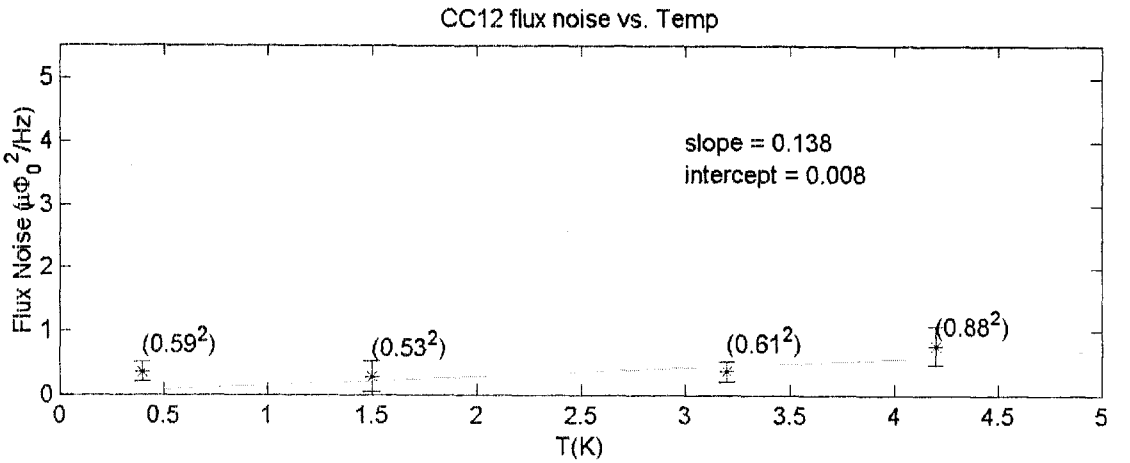
CC12 flux noise vs. Temp
Flux Noise ($\mu\Phi_0^2$/Hz)
T(K)
slope = 0.138
intercept = 0.008
(0.59^2)
(0.53^2)
(0.61^2)
(0.88^2)

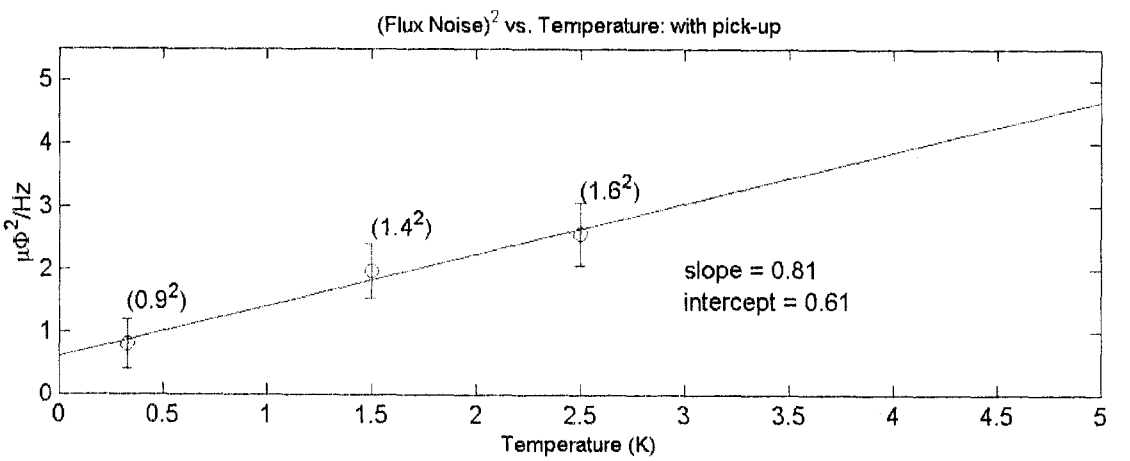
(Flux Noise)^2 vs. Temperature: with pick-up
$\mu\Phi^2$/Hz
Temperature (K)
slope = 0.81
intercept = 0.61
(0.9^2)
(1.4^2)
(1.6^2)

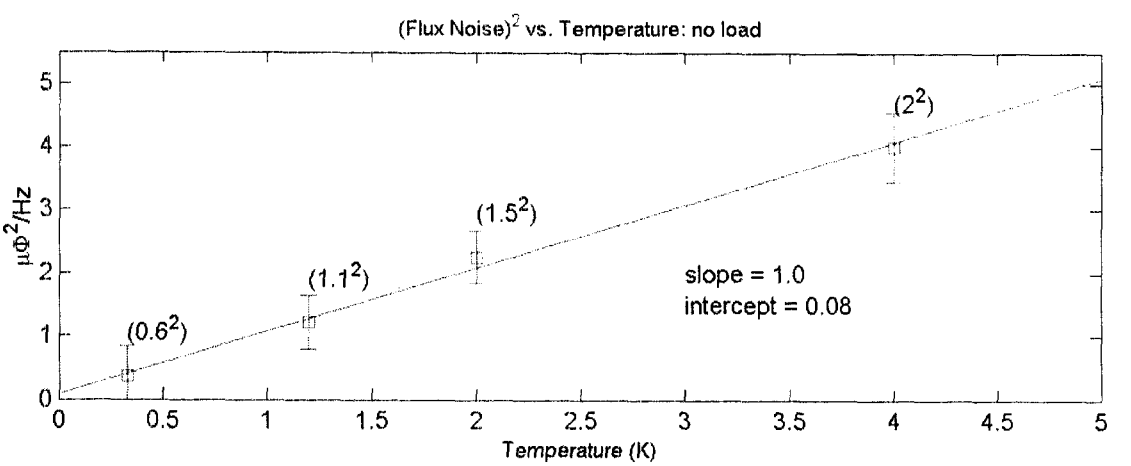
(Flux Noise)^2 vs. Temperature: no load
$\mu\Phi^2$/Hz
Temperature (K)
slope = 1.0
intercept = 0.08
(0.6^2)
(1.1^2)
(1.5^2)
(2^2)

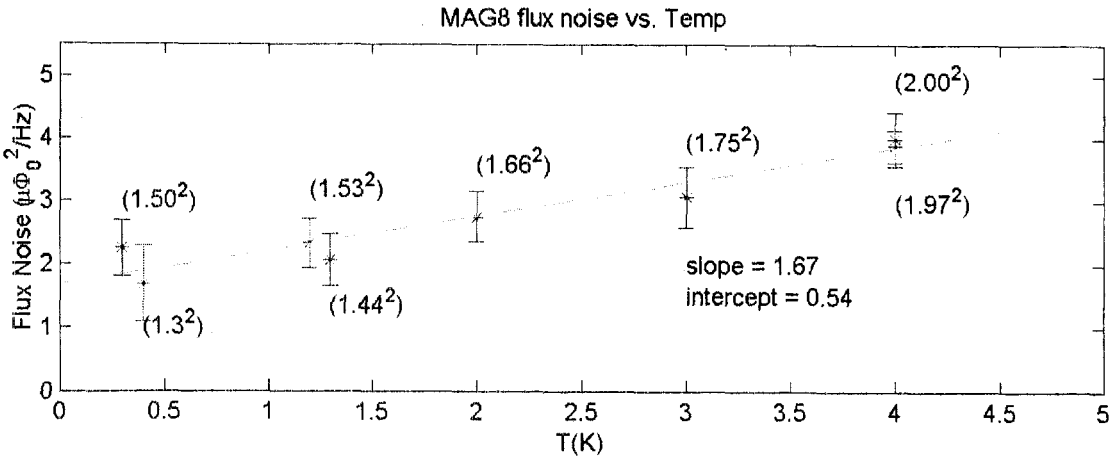

Same SQUID as in full head MEG system.
Effective area is 2.5 mm^2

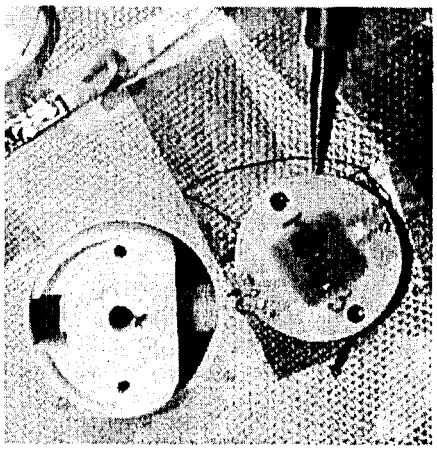

Mag 8

.84nT/ Φ_0 and 2×10^{15} Tm^2 in flux quantum

2.4 mm^2 effective area

SQUID with big coil

.02nT/ Φ_0 and 2×10^{15} Tm^2 in flux quantum

100 mm^2 effective area

The ratio of areas is 40.

$200\ \mu\Phi_0 / 40 = 5\ \mu\Phi_0$

The signal-to-noise goes as sqrt(# of SQUIDs)

Upcoming Tests

No plans to test SQUIDs in HV at this time

tests of gradiometer as function of temperature at NHMFL (from 4K to at least 1K)

Additional FEM modeling for optimization of SQUID position

detection of 3He

High voltage issues (constraints on leakage current)

1nA produces 10^{-15} T at 10cm

- Johnson Noise
  - Electrodes can't superconduct
  - Must be high resistance material

$$\langle I^2 \rangle = \frac{4kT\Delta f}{R}$$

- Protection of SQUIDs
  - SQUIDs in some sort of Faraday cage?

Try a large area gradiometer.

We have obtained a 1st order gradiometer from IHPT Jena

Each coil is 19mm x 19mm

The chip is 60mm x 20mm x 5mm

Effective area (for one coil) is 7.5 mm^2

(sensitivity $0.28 nT/\Phi_0$)

Modify FEM to reflect new coils and optimize their location

Petr Volegov UNM

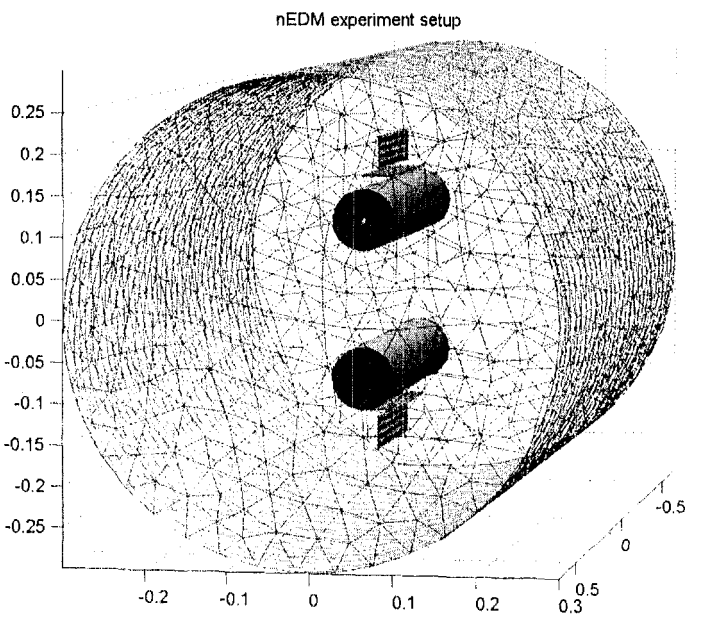

Detection of ^{3}He

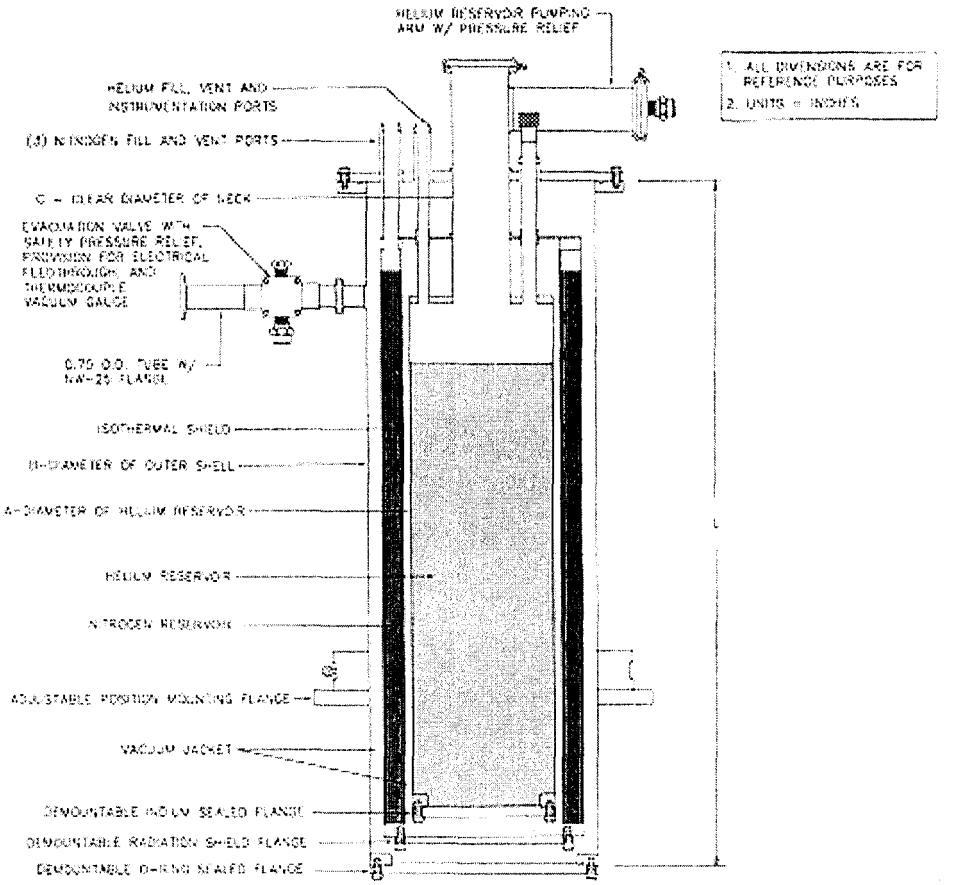

Shortening the magnet by better matching of boundary conditions; magnetic shielding issues

Brad Filippone (Caltech)

EDM Magnetic Fields & Shielding:

Issues/Challenges:

- Will Superconducting Shield work?
  - → "No" EDM exp. has used inner SC shield
    - Possible uncontrolled trapped flux
    - Trapped flux may vary randomly
      - ⇔ increased $\vec{B}$ noise

- Can Ferromagnetic Shield work?
  - → Standard Mag. materials perform poorly at low T
    - Reduced μ, T cycling worsens?
  - → Ferro. shield may allow smaller volume
    - Boundary Conds. give better uniformity than SC shield

- Will external $\vec{B}$ leakage through penetrations compromise SQUIDs?

Present Baseline Design

Target region with magnet coil

Specs:

$|\vec{B}| \sim mG$

Uniformity $\lesssim 10^{-3}$

Time stab. $< 10^{-6}/s$

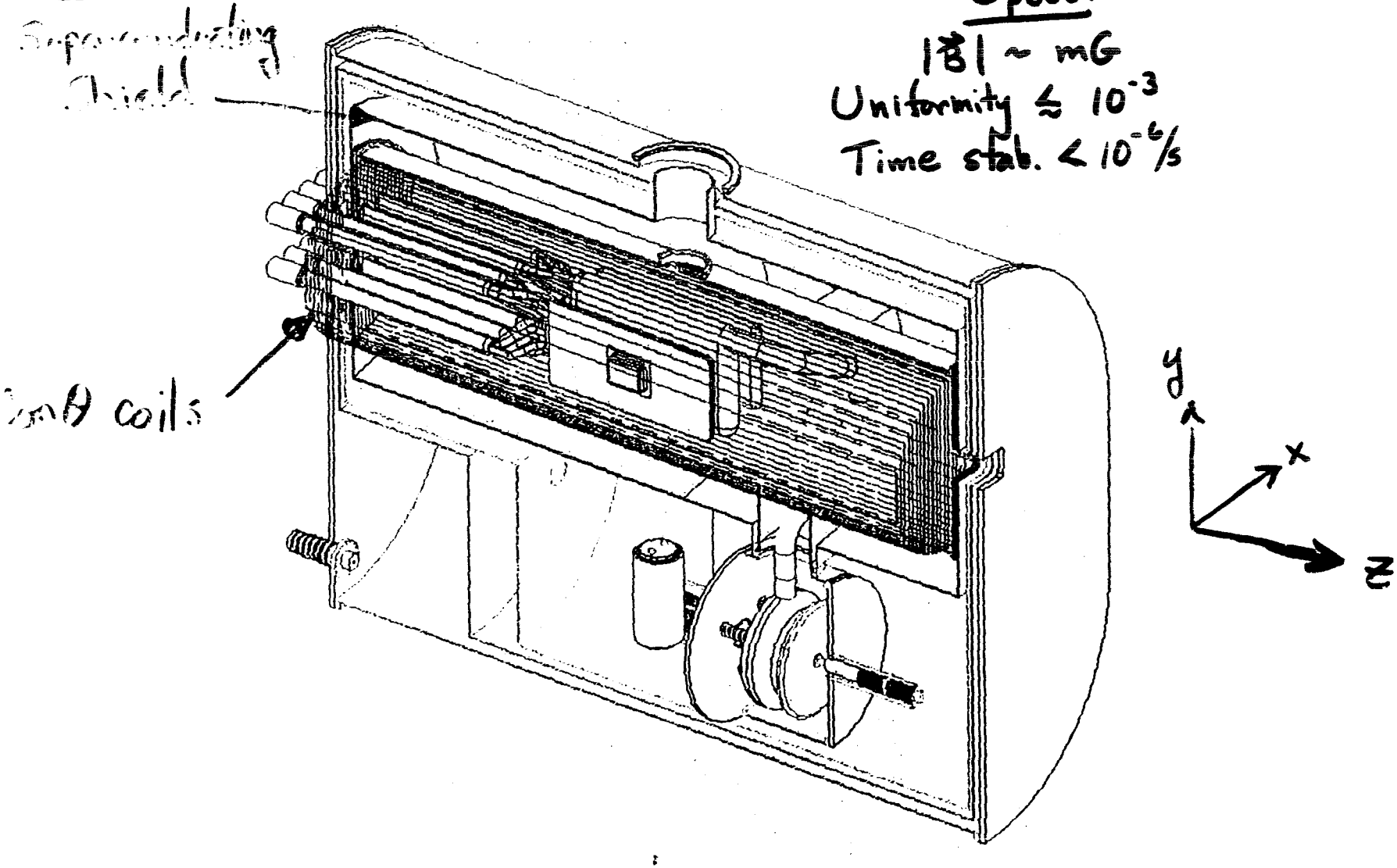

Ferromag. vs. SuperCond. Shield

Boundary Conds. favor Ferromag.

Ferromag.

$\mu \to \infty$

$B_{\parallel} = 0$ at Surface

SC

$\mu = 0$

$B_{\perp} = 0$ at Surface

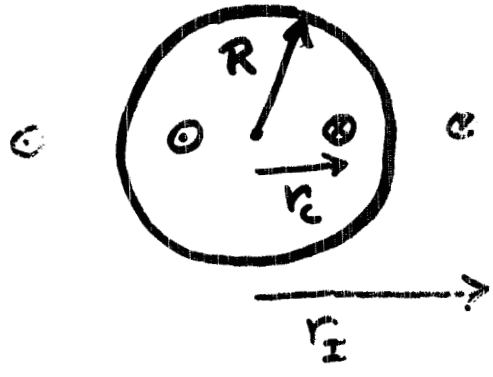

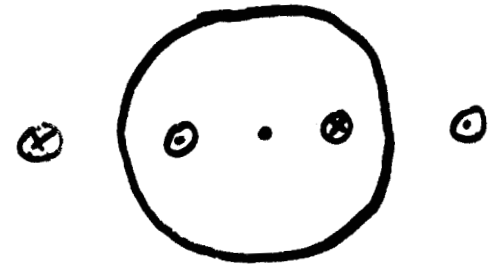

Image Currents

$r_I = \left(\frac{R}{r_c}\right) R$

$I_I = I_c$

As $r_c \to R$ image current adds to coil

$r_I = \left(\frac{R}{r_c}\right) R$

$I_I = -I_c$

As $r_c \to R$ image current cancels coil I

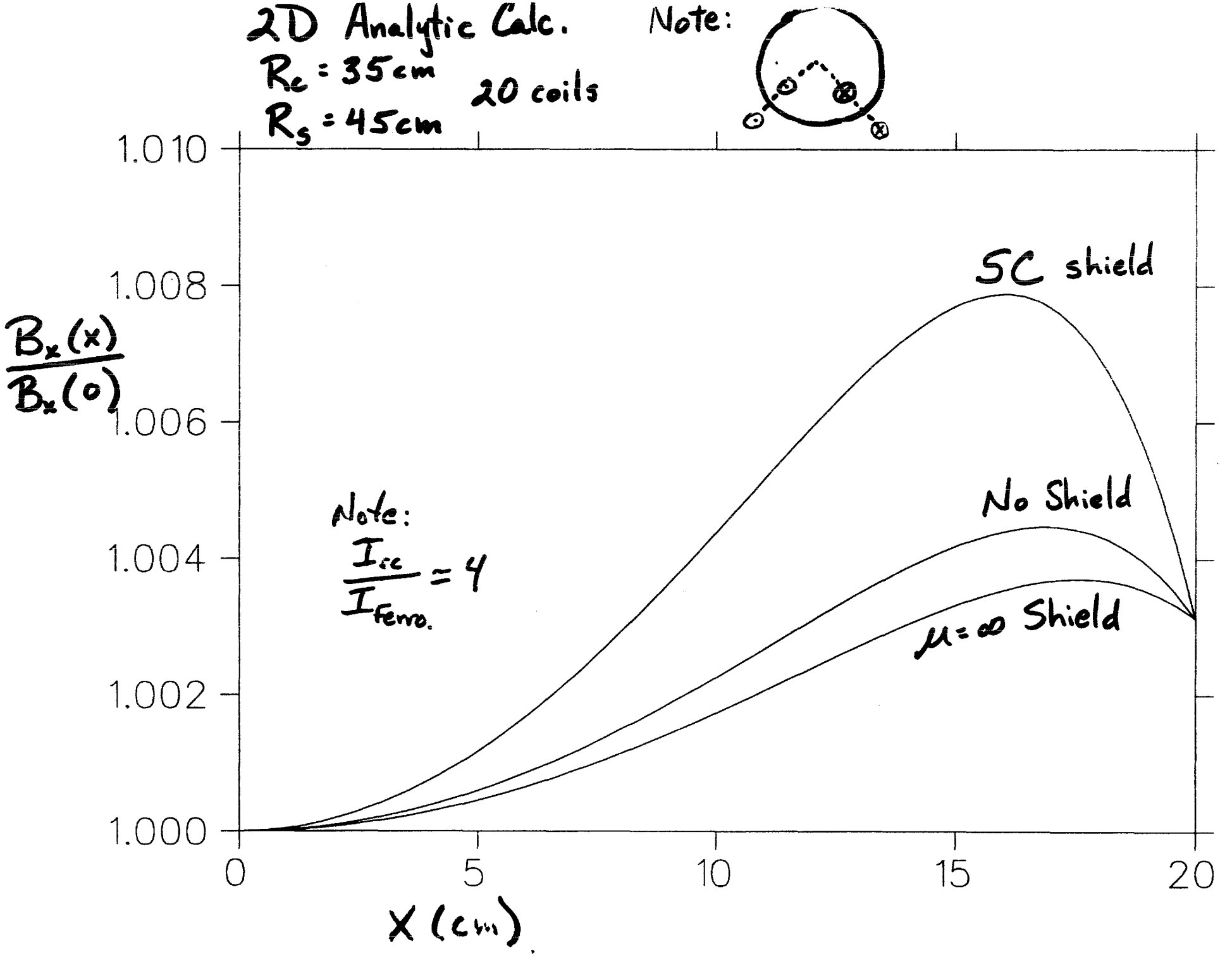
2D Analytic Calc.
$R_c = 35$ cm
$R_s = 45$ cm
20 coils
Note:
SC shield
No Shield
$\mu = \infty$ Shield
Note:
$\frac{I_{sc}}{I_{Ferro.}} = 4$
$\frac{B_x(x)}{B_x(0)}$
1.010
1.008
1.006
1.004
1.002
1.000
0
5
10
15
20
X (cm)

∴ • Ferromag. shield may allow smaller cryo volume + meet uniformity spec.

• Also no trapped flux problems

⇒ Glenn Strycker & Jan B. (LANL) working on ANSYS calc. of ferromag. shield

But ...

Low T favors SC shield

SC <u>only</u> works at Low T

Ferromag. may not work at low T

Low T Ferromag. performance:

- "Mu metal has $\mu \sim 3500$ at 4 K"
  ↳ Anneal

  (Problems w/ T cycling ?)

- Other materials may be promising

  Cryoperm 10 (high Ni)
  Claimed μ at 4K $\simeq$ 75,000
  (M. Snow IUCF studying)

  Metglas
  Amorphous metal (metal glass)
  Formed via rapid solidification $\sim 10^6$ C/s

  2705M looks interesting
  ↳ anti-theft tags

  (Steve L. has some of this ribbon)

metglas® SOLUTIONS

www.metglas.com

Magnetic Alloy 2705M (Cobalt-based) Technical Bulletin

Applications

- Flexible electromagnetic shielding
- Magnetic sensors
- High frequency cores

Benefits

- Near-zero magnetostriction
- High DC permeability at low fields without annealing
- High tensile strength

Typical DC Hysteresis Loop

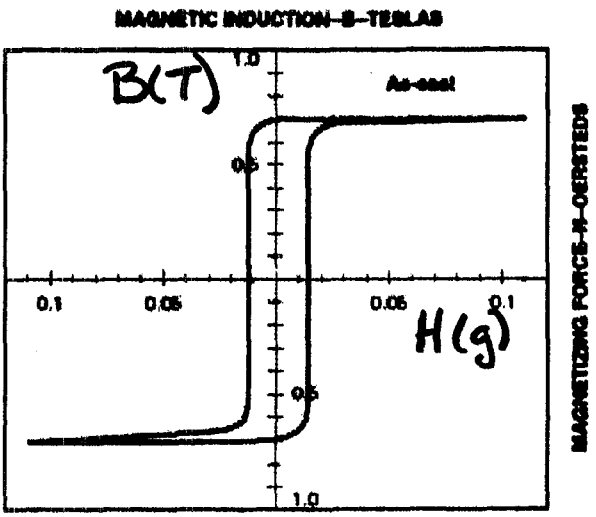

Typical Impedance Permeability Curves, Longitudinal Field Anneal

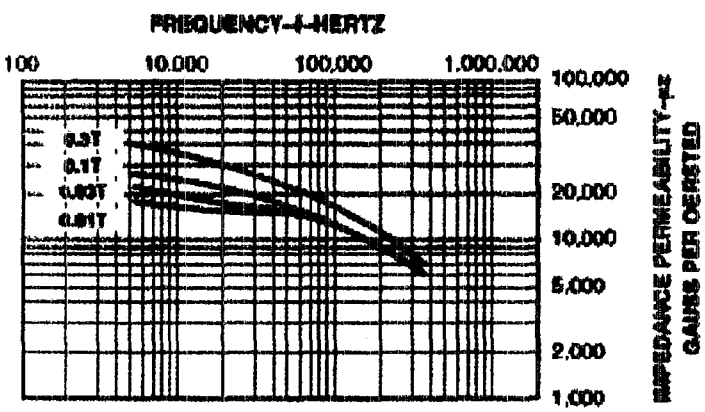

Physical Properties

Density (g/cc)	7.80
Vicker's Hardness (50g load)	900
Tensil Strength (GPa)	1-2
Elastic Modulus (GPa)	100-110
Lamination Factor (%)	>75
Thermal Expansion (ppm/°C)	12.1
Crystallization Temperature (°C)	520
Continuous Service Temp. (°C)	90

Magnetic Properties

Saturation Induction (Tesla)	0.77
Maximum D.C. Permeability (μ):	
Annealed	600,000
As Cast	290,000
Saturation Magnetostriction (ppm)	<<1
Electrical Resistivity (μ-Ω-cm)	136
Curie Temperature (°C)	365

If suitable Ferromag. material can be identified, perhaps optimal soln. is

"Compact" Coil - Ferromag. - SC set

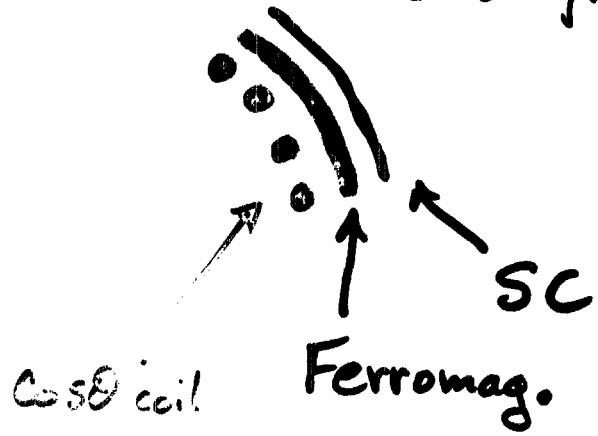

UIUC Cryostat (D. Beck)

KD 527

Proposed Vapor-Shielded Liquid Helium Dewar

R. Giannetta
Princeton University
609-452-4390

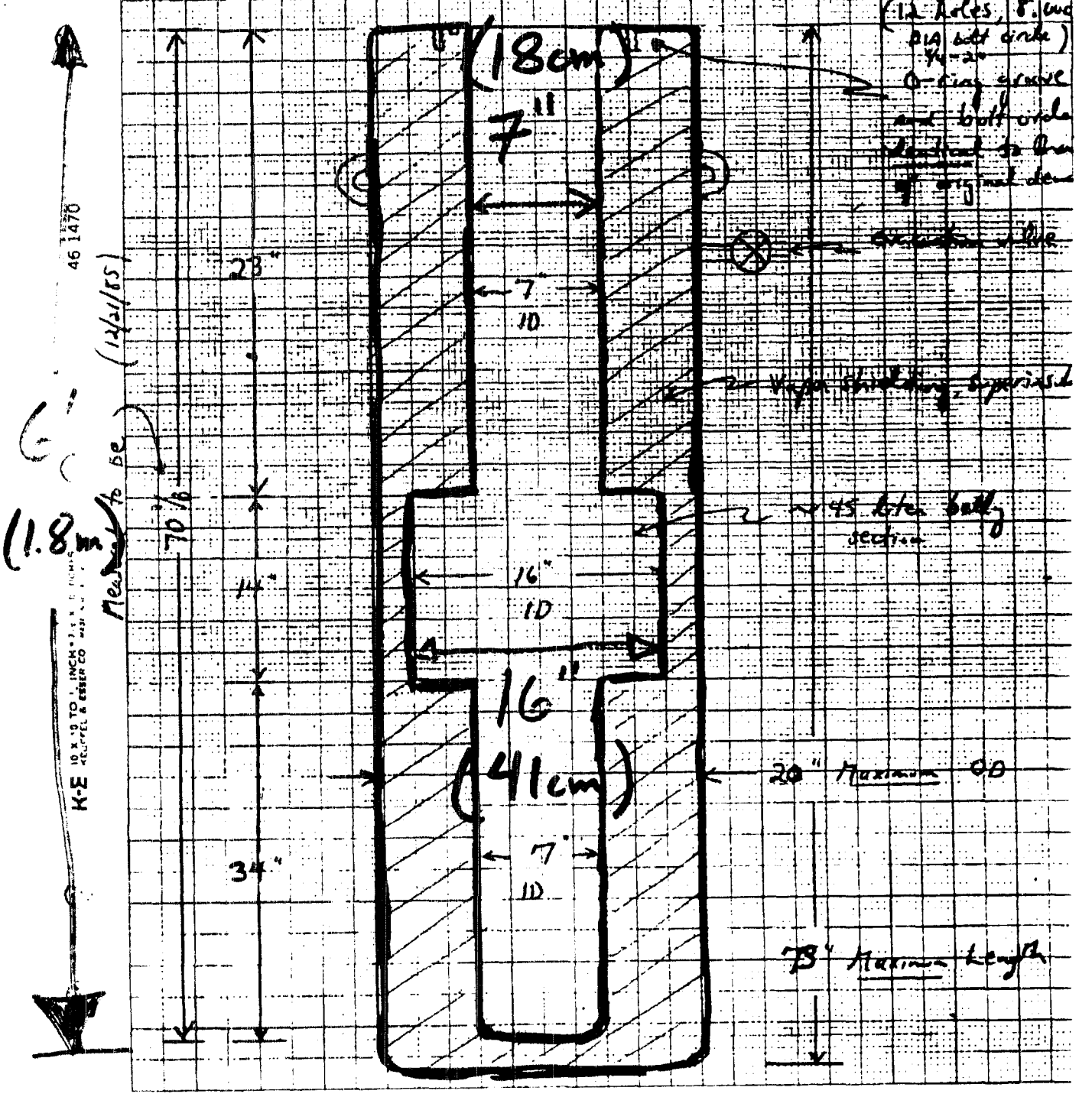

Possible Task List for next 1.5 yrs.

- Full 3D calc. of $\cos\theta$ coil + Ferromag. Shield

- Study Low T behavior of Ferromag. materials

- Build scaled (~ 1/4) prototypes?
  - → Borrow cryostat (UIUC, LANL, ...?)
    ↳ PIC
  - → Wind Coil
  - → Make shields
  - → Install SQUID's/NMR

Fiscal/Manpower Impact

$\simeq$ 1 FTE + 10-20k\$

Modifications of the apparatus to incorporate the dressed-spin technique

Bob Golub (HMI)

Polarization of UCN

$$He^3 + n \rightarrow H^3 + p$$
$$(He^4)$$

$$\vec{J} = \vec{I}_{He^3} + \vec{S}_n$$

experimentally ($J=0$ resonance in He^4)

$$\frac{\sigma_{J=0}}{\sigma_{tot}} = 1.01 \pm .03$$

$$\therefore \vec{I} \parallel \vec{S} \Rightarrow \sigma_{He^3} = 0$$

<u>polarized He^3</u>

$$\sigma_{S_n=+} = 0 \qquad \sigma_{S_n=-} = 2\sigma_0$$

$$\frac{1}{\tau_\pm} = \frac{1}{\tau_w} + (1 \mp P_3)\left[N_3 \sigma_0 v_{UCN}\right] \Rightarrow 1/\tau_{He}$$

$$\rho_\pm = \frac{\phi_p}{2}\tau_\pm$$

ϕ_p = UCN prod rate

$$= \int \phi(E)\, \Sigma(E-E_{UCN})\, dE$$

$$P_{UCN} = \frac{P_3}{1 + \tau_{He}/\tau_w}$$

For Polarized UCN

$$1/\tau_{abs} = N \sigma_0 v (1 - \vec{P}_N \cdot \vec{P}_3)$$

Absorptions $\Longrightarrow$ Scintillations

He^3 co-magnetometer

Scintillation rate

$$= \frac{\rho_{n\alpha} V}{\tau_{abs}} \sim (1 - \vec{P}_n \cdot \vec{P}_3)$$

$$(1 - P_n P_3 \cos \theta_{n3}(t))$$

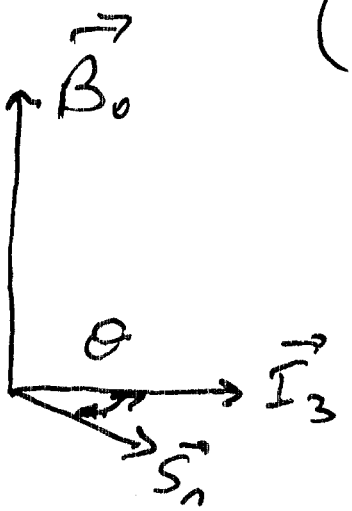

$$\theta = (\gamma_n - \gamma_3) B_0 t \pm \frac{e d_n E}{\hbar} t$$

$$\gamma_3 = 1.1 \gamma_n$$

$\omega_{eff} = .1 \gamma_n B_0$ factor of 10 reduction in field sensitivity

Scintillation rate

measures field

shows edm

Further Development

Dressed Neutron (Muskat, Dubbers, Schärpf

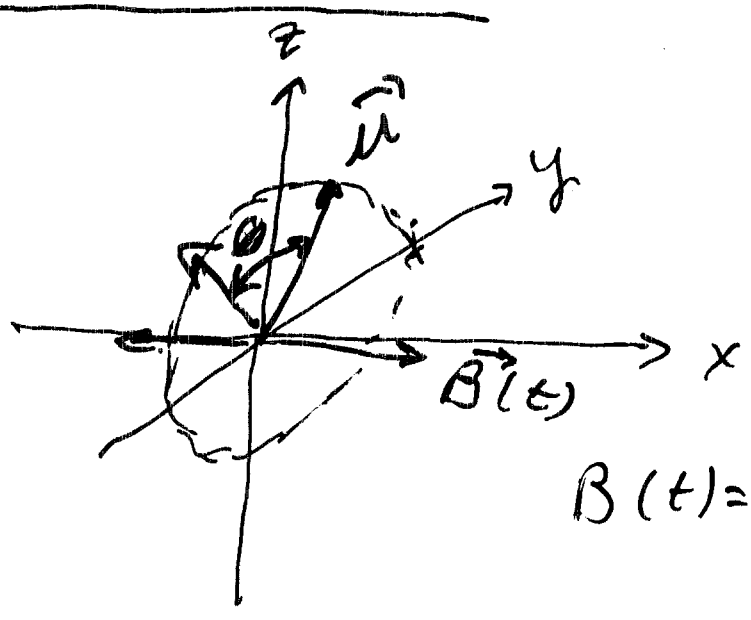

$$B(t) = B_d \sin \omega_d t$$

$$\omega_{prec} = \gamma B(t) = \dot{\theta}(t)$$

$$\theta = \frac{\gamma B_d}{\omega_d} \cos \omega_d t$$

$$\langle \cos\theta \rangle = \frac{1}{T} \int_T dt \cos\left[\frac{\gamma B_d}{\omega_d} \cos \omega_d t\right]$$

$$= J_0\left(\frac{\gamma B_d}{\omega_d}\right) = J_0(x) = \gamma_{eff}$$

$x =$ dressing parameter

$= \gamma B_d / \ldots$

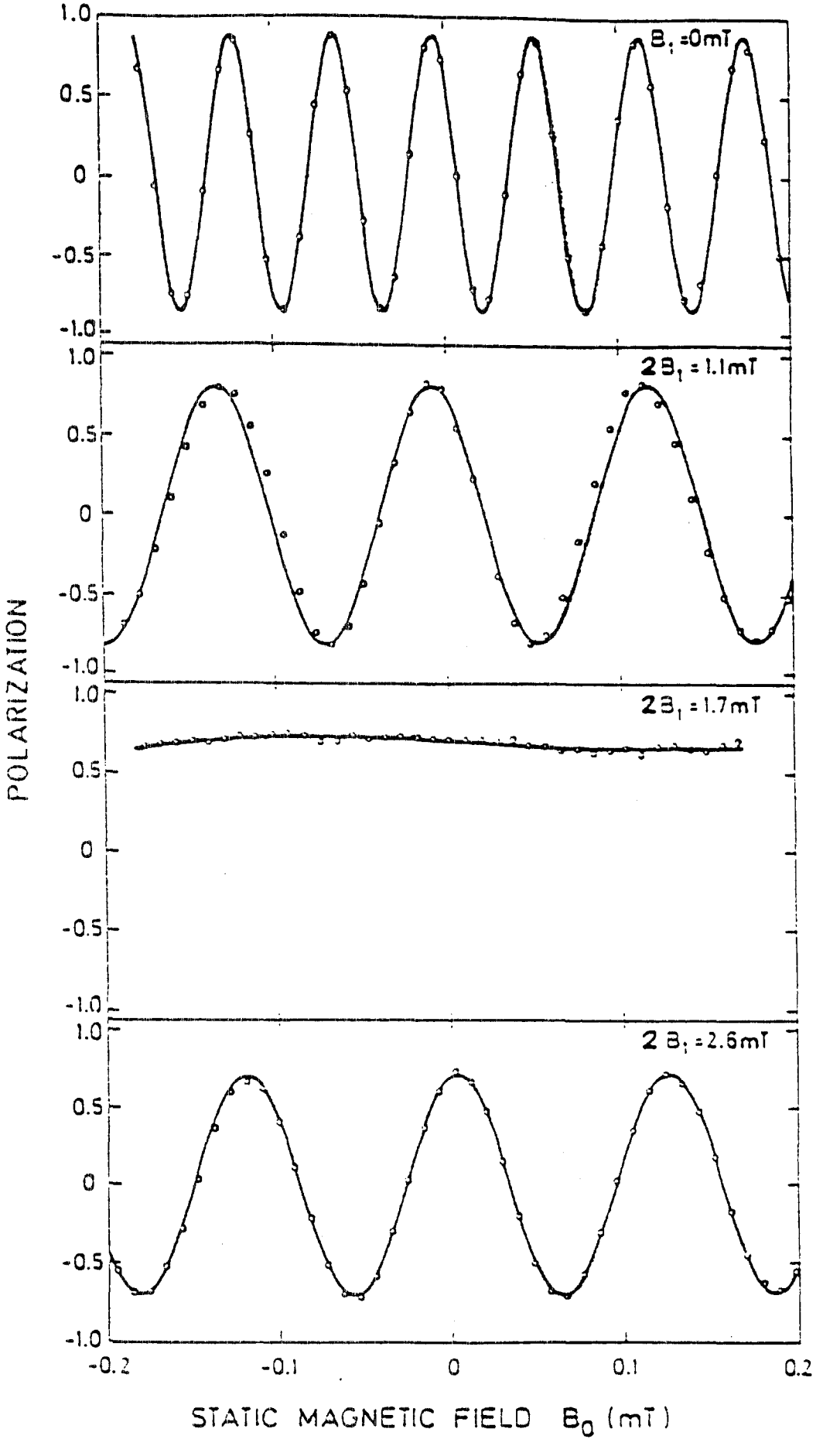

FIG. 3. Spin-precession measurements with dressed neutrons. At the critical rf-field strength $2B_1 = 1.7$ mT the g

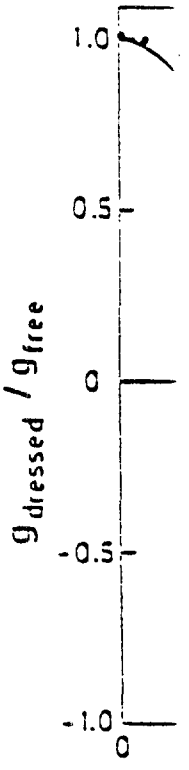

FIG. 4.
field streng

Dressec
the conte
searches.
earth's m
tween ne
neutrons
effective
not help
decouple
ly reestat
ing B_0 so
gy diagr
again be
discussec
basis, wh
the disc
neutron
sight.

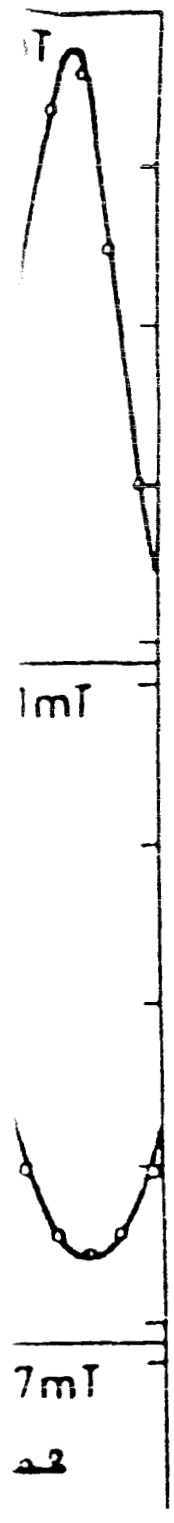

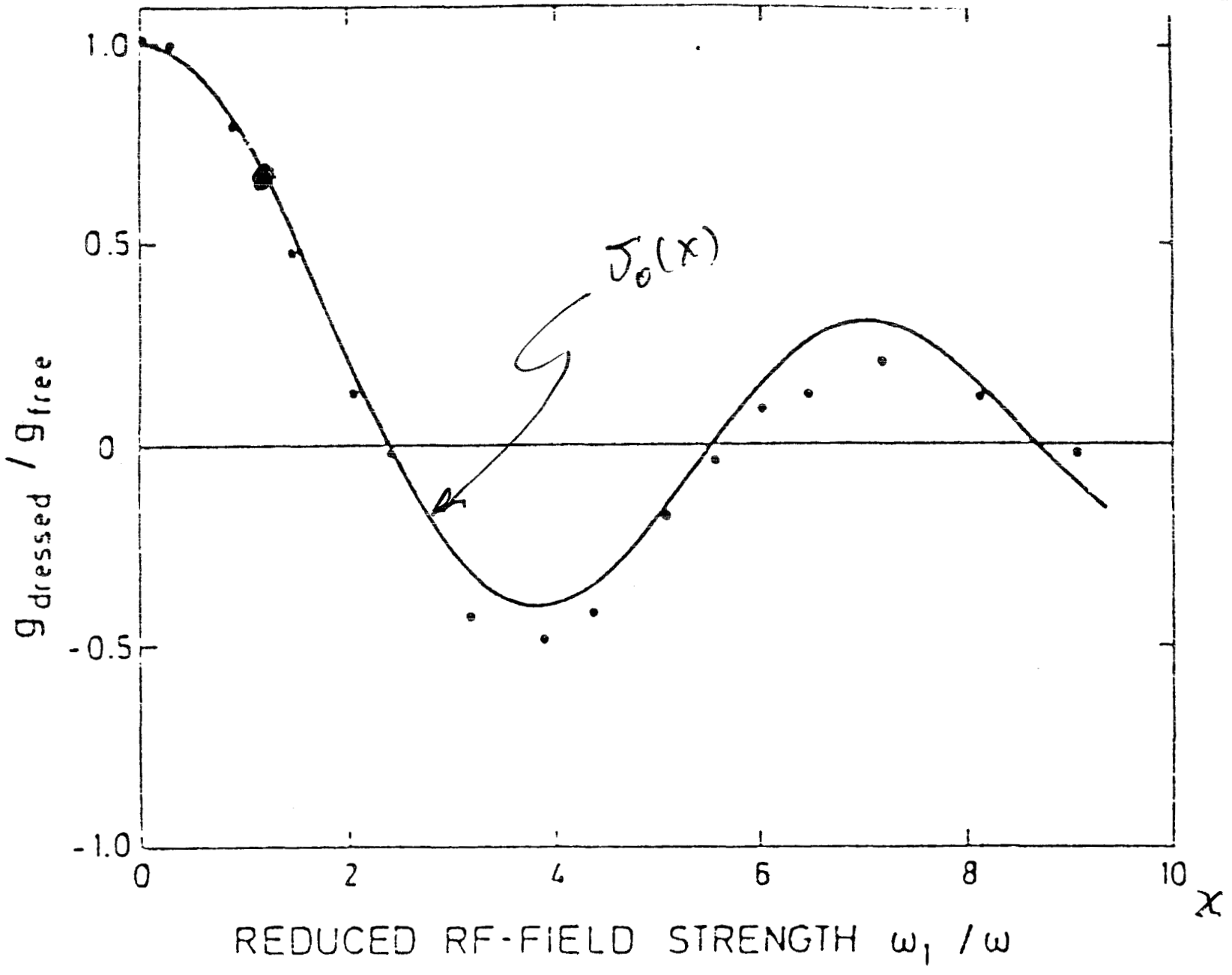

FIG. 5. Variation of the dressed-neutron's g factor with rf-field strength ($\omega_1 = \gamma B_1$).

Magnetic Moment Dressing

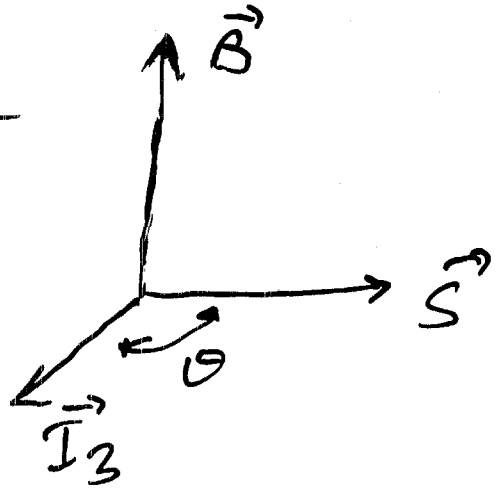

$$\omega = \left(\gamma_3^{eff} - \gamma_n^{eff}\right) B_0 \qquad \gamma_i^{eff} = J_0(x_i)\gamma_i$$

$$x_i = \gamma_i B_d / \omega_d$$

$$\gamma_3/\gamma_n = 1.1$$

$$\left[\gamma_3 J_0(x_3) - \gamma_n J_0(x_n)\right] \stackrel{?}{=} 0$$

$$1.1\, J_0(1.1 x_c) = J_0(x_c) \quad ?$$

Yes!

$$x_c = 1.19$$

<u>critical dressing</u> $\Rightarrow$

constant scintillation rate independent of DC magnetic field

corrections $\sim \dfrac{B_{DC}}{B_d}$

edm

apply electric field

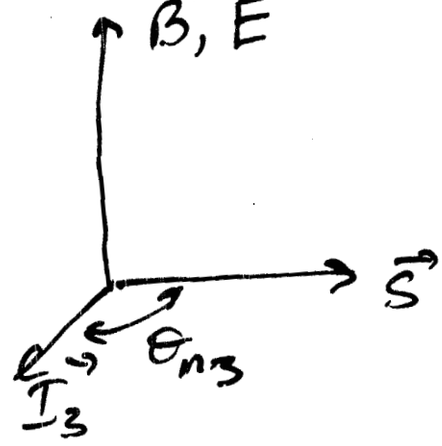

$$\omega_n = \gamma_{eff} B_0 \pm e \frac{d_n}{\hbar} E J_0(x_c)$$

$$\theta_{n3} = e \frac{d_n E t}{\hbar}$$ } shows up in scintillation rate.

---

with $\vec{S}, \vec{I}$ parallel

absorption ~ 0

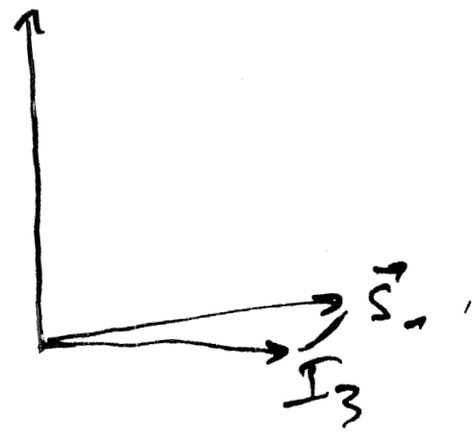

modulate x

$$x(t) = x_c + \epsilon \cos \omega_m t$$

$$\delta \omega_{n3} \sim \epsilon \cos \omega_m t \pm k \tilde{d}_n E$$

$$\delta \theta \sim \frac{\epsilon}{\omega_m} \sin \omega_m t \pm k \tilde{d}_n E t$$

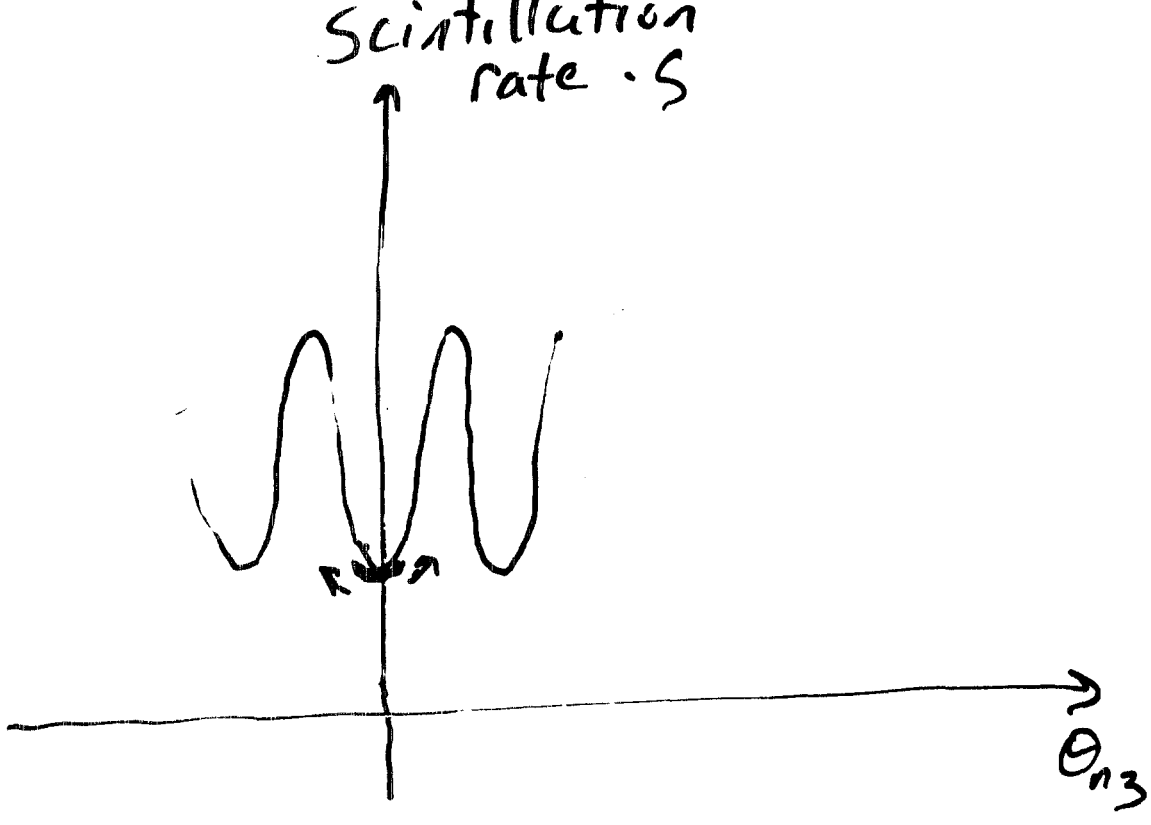

$$\frac{\partial S}{\partial \theta_{n3}} = 0 \Rightarrow \text{2nd harmonic}$$

$$\sim (\delta\theta)^2$$

$$\delta\theta = \delta\theta_0(\omega_m t) \pm k \tilde{d}_n E t$$

$$(\delta\theta)^2 \sim \pm \delta\theta_0(\omega_m t)\, k \tilde{d}_n E t$$

1st harmonic.
growing with time.

$\Longrightarrow$ EDM!

2nd Harmonic for calibration

$B_{DC} = 10^{-3}$ gauss $\quad \nu_0 = 3\ Hz \quad \omega_0 = 20$ rad/sec

$\omega_1 = \gamma B_{rf} \quad x = \frac{\omega_1}{\omega_{rf}} = 1.19 = x_c$

$\omega_1 >> \omega_0 \qquad \omega_1 \sim 200$ rad/sec

2000 rad/sec

$B_{rf} = 10^{-2}$ g (30 Hz)

10^{-1} g (300 Hz)

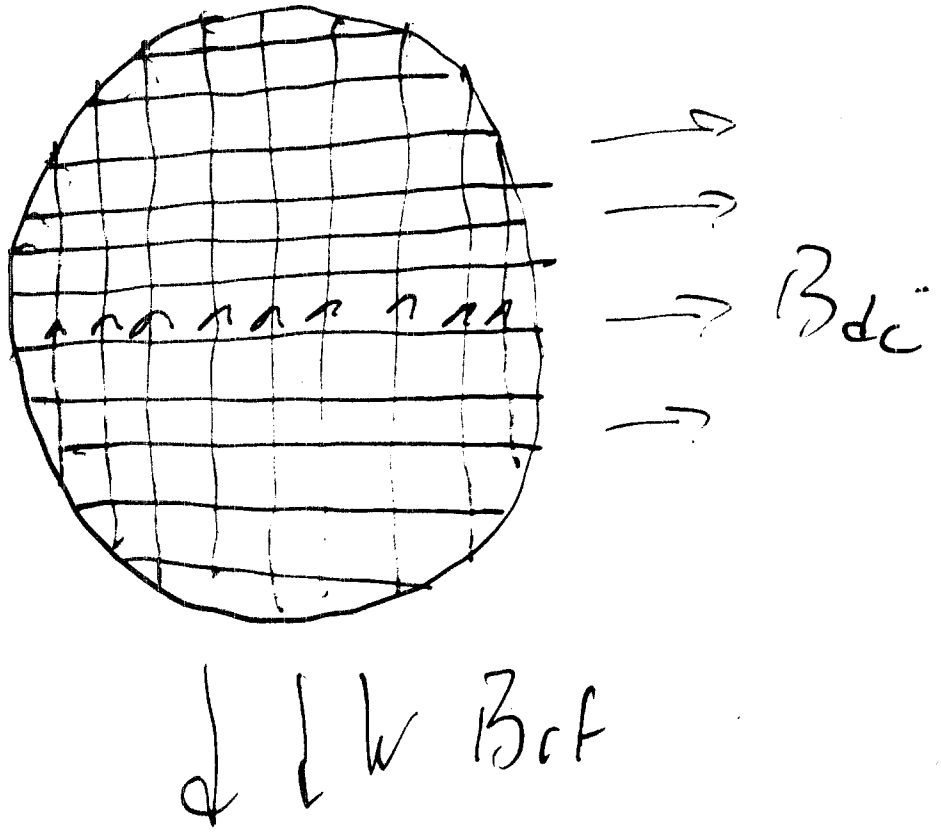

shaking field

Shaking - Keep domains moving

$\mu_{shake} >> \mu_{static}$

material	field	freq
μ-metal	50 mg	50 Hz
Metglas 2705M	30 mg	1 kHz (B_{in} = 1600g)
	25 mg	200 Hz
multilayer shield	10 mg	200 Hz
	25 mg	536 Hz

up to 50 kHz OSC

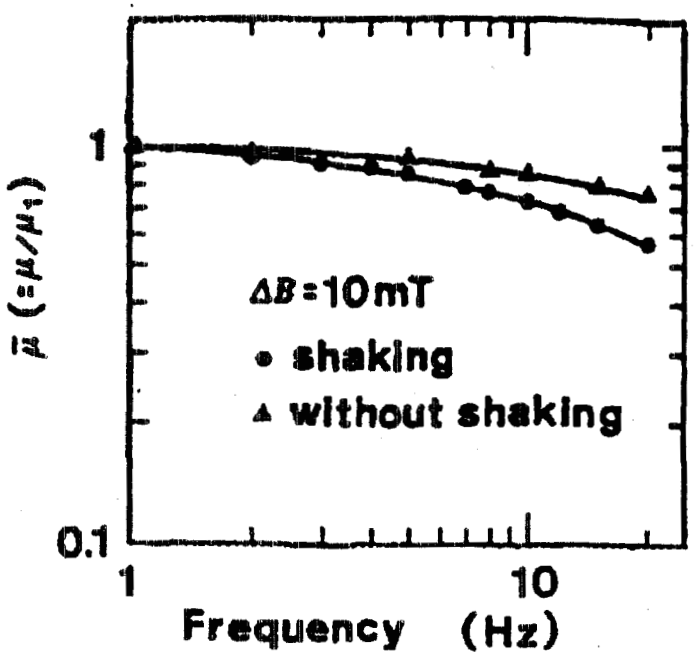

5×10^5

3.4×10^4

FIG. 1. Frequency dependence of the permeability, where values are normalized by μ_1 (permeability at 1 Hz); $\mu_1 = 5.27 \times 10^5$ under magnetic shaking, $\mu_1 = 3.41 \times 10^4$ under normal condition.

Metglas 2705M

2.1×10^{-4} J/kg/cycle

$\times 500$ Hz

$\Rightarrow 100$ mW/kg

say 1 watt

2.1×10^{-4} J

$\times 500$ H

Downloaded 09 Jul 2002 to 134.30.119.56. Redistribution subject

6cm φ
X10cm/ons

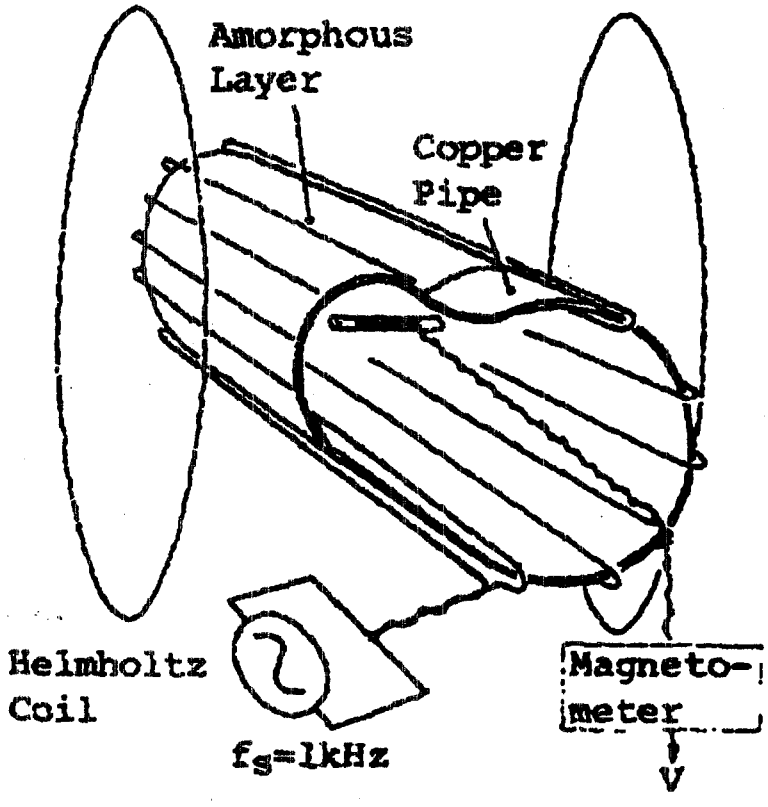

FIG. 2. Experimental setup for measuring the shielding factor under shaking.

was used to cancel the horizontal component of the earth's field. Before each measurement, the shielding case was demagnetized using the shaking coil.

RESULTS AND DISCUSSION

It was found that the leakage field into the shielded space increased gradually after applying the disturbing field and then reached steady state. The increase in leakage field was at most 14% within 2 h of observation. However, this phenomenon is not taken into account in the following data.

and shows a broad peak for $H_s = 2.0$–3.0 A/m. The effec
value decreases with decreasing ΔH, however, it is still h
The maximum value even for $\Delta H = 0.002$ A/m (rms
higher than 3.5×10^5. The maximum value, for example,
tained with Mumetal by shaking is 8.9×10^4 under no dc
field.[2] In that case, the value goes down to almost one-
when a dc bias field increases up to 0.5 A/m. A similar p
nomenon was also found with the Metglas 2705M ribb
however, the decrease in the effective permeability due to

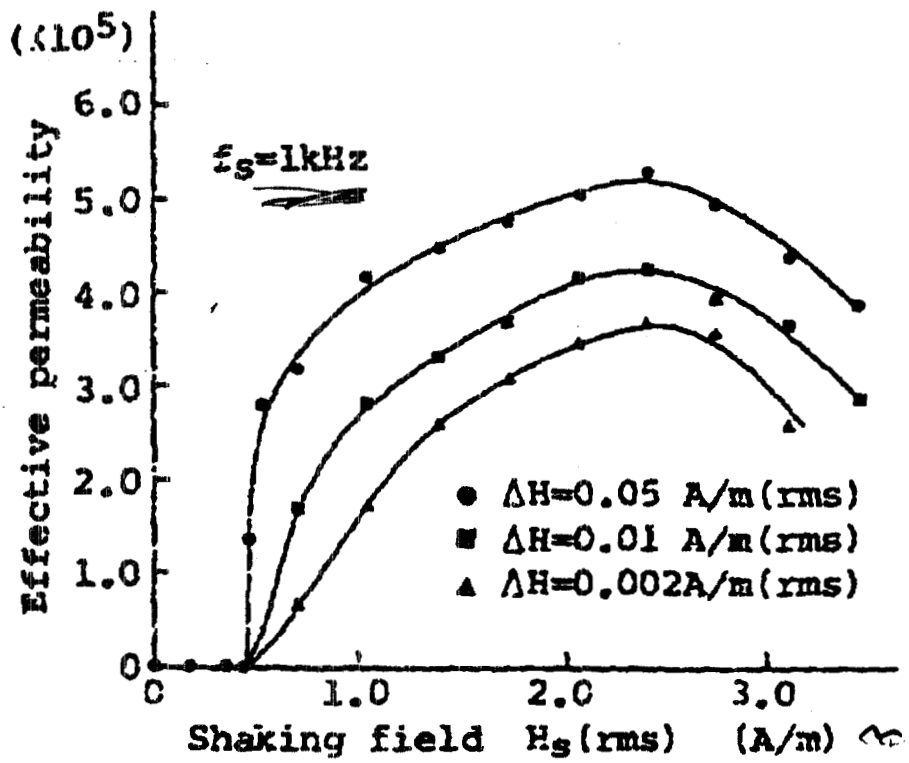

≈ 10mG

FIG. 3. Effective permeability vs shaking field strength (single layer).

Downloaded 09 Jul 2002 to 134.30.119.56. Redistribution subje

ing magnetic field leaking from shells #1–#4. The total weight of the tapes used was 15 kg. Nominal diameters of the shells are 56 cm for #1, 55.3 cm for #2, 54.6 cm for #3, 52.6 cm for #4, and 52 cm for #5. Numbers of turns were 50 for shaking coils #1 and #2 and 20 for the demagnetizing coil

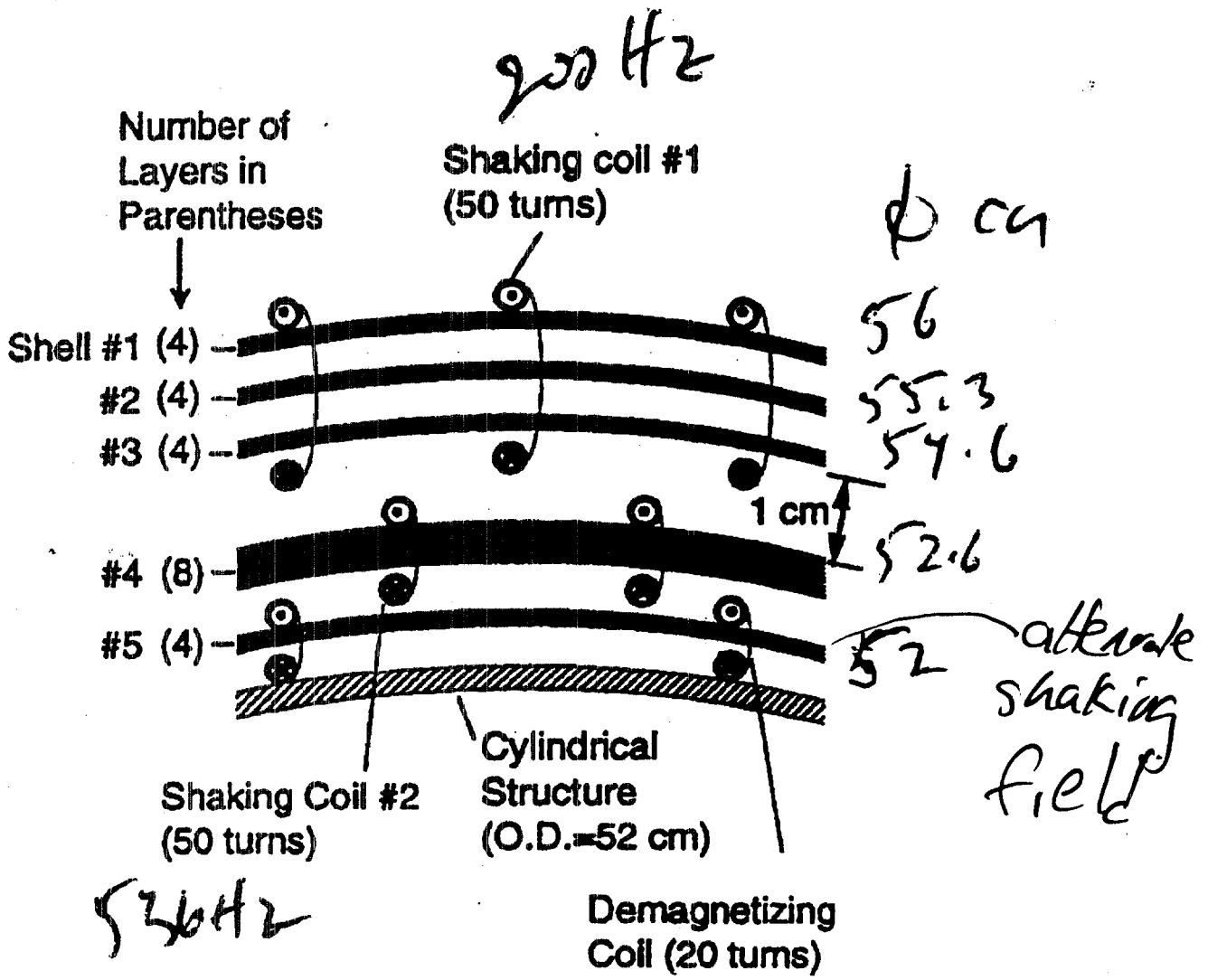

FIG. 1. Cross sectional view of thin multiple-structure. Spacings between shells are about 3.5 mm, unless otherwise indicated.

96/79(8)/5490/3/$10.00 © 1996 American Institute of Physics

ubject¬to¬AIP¬copyright,¬see¬http://ojps.aip.org/japo/japcpyrts.html.

sists of n magnetic shells. In our case, the order of the polynomial function is 4 because shells #1–#4 are subjected to magnetic shaking. The permeability of shell #5 is treated as a constant equal to 2000. When the distances between the neighboring shells are small, coefficients of higher order terms become small. Therefore, when the permeability is low, higher order terms do not affect a resulting shielding factor. In other words, a thin multiple-shell structure behaves as a single shell with the same total thickness when the permeability is low. On the other hand, when the permeability is sufficiently large, higher order terms with small coefficients become substantial, so a thin multiple-shell does work to increase shielding factor.

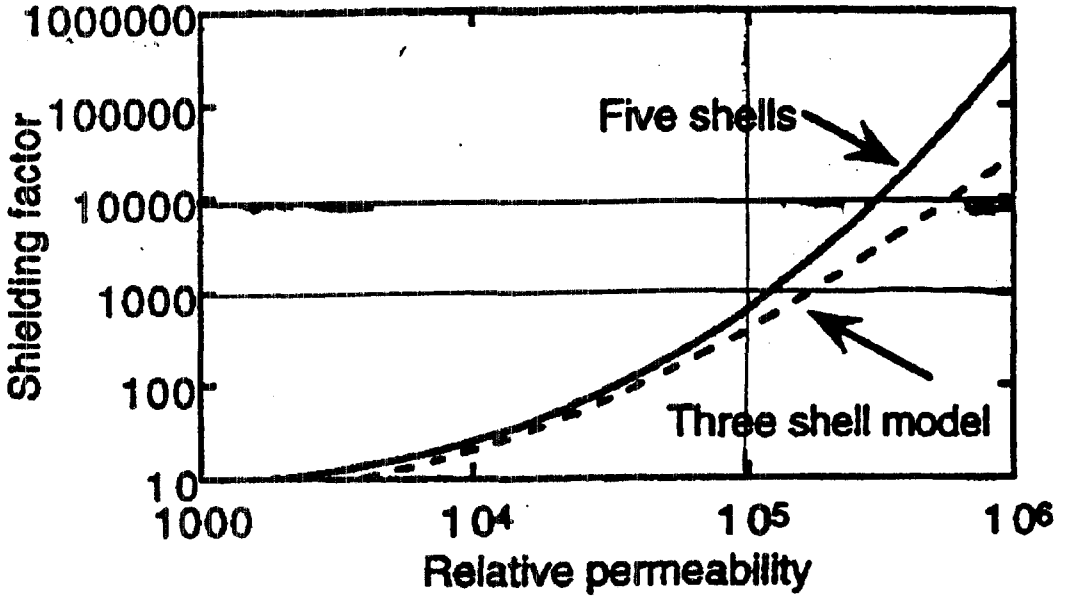

FIG. 4. Relationship between shielding factors and relative permeability.

subject to AIP copyright, see http://ojps.aip.org/japo/japcpyrts.html.

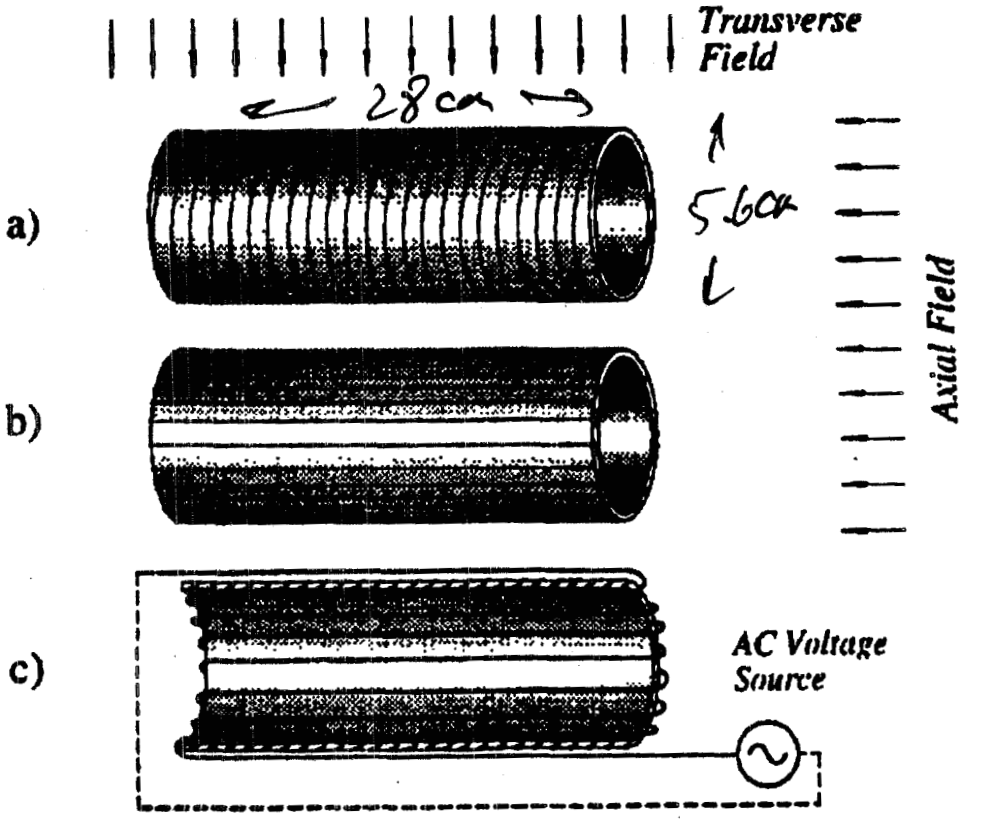

FIG. 1. Open-ended cylindrical shields employing Metglas ribbons. (a) Cylinder consisting of a helical structure of the ribbons. (b) Cylinder consisting of an axial structure of the ribbons. (c) Magnetic shaking by a toroidal coil.

sured at the shield centers by a miniature magnetoresistive sensor of the HMC 1022 type, manufactured by Honeywell. The shielding characteristics measured (the shielding factors versus the shaking field) are shown in Fig. 3 and the ASF and TSF are shown in Table I. In order to investigate the effect of the shaking field direction on shielding enhancement, magnetic shaking by solenoidal coils

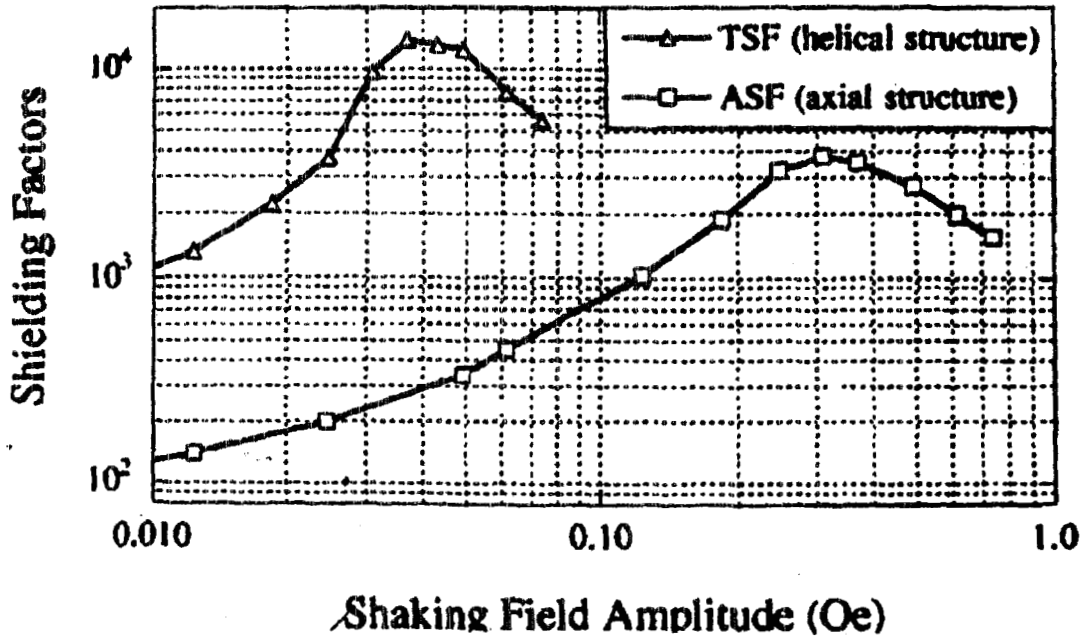

FIG. 3. Shielding characteristics: Transverse and axial shielding factor vs shaking field intensity.

cylindrical shields (length, outer diameter, thickness: 283 ×56×0.31 mm) consisting of helical [Fig. 1(a)] and axial [Fig. 1(b)] structures of Metglas 2705M amorphous ribbons were built for this purpose. The shielding factors were measured at the centers of these shields by a flux-gate magnetometer of the MAG-03 MC type, manufactured by Bartington, and are listed in Table I. The shaking field intensities, corresponding to maximum shaking enhancement of the shielding factors, are approximately equal to corresponding values of the same parameter obtained for miniature shields: ~50 mOe for the TSF and ~320 mOe for the ASF (see Fig. 3). The data in Table I shows that magnetic shaking provides an

rmly shielded area is extended toward the opening by

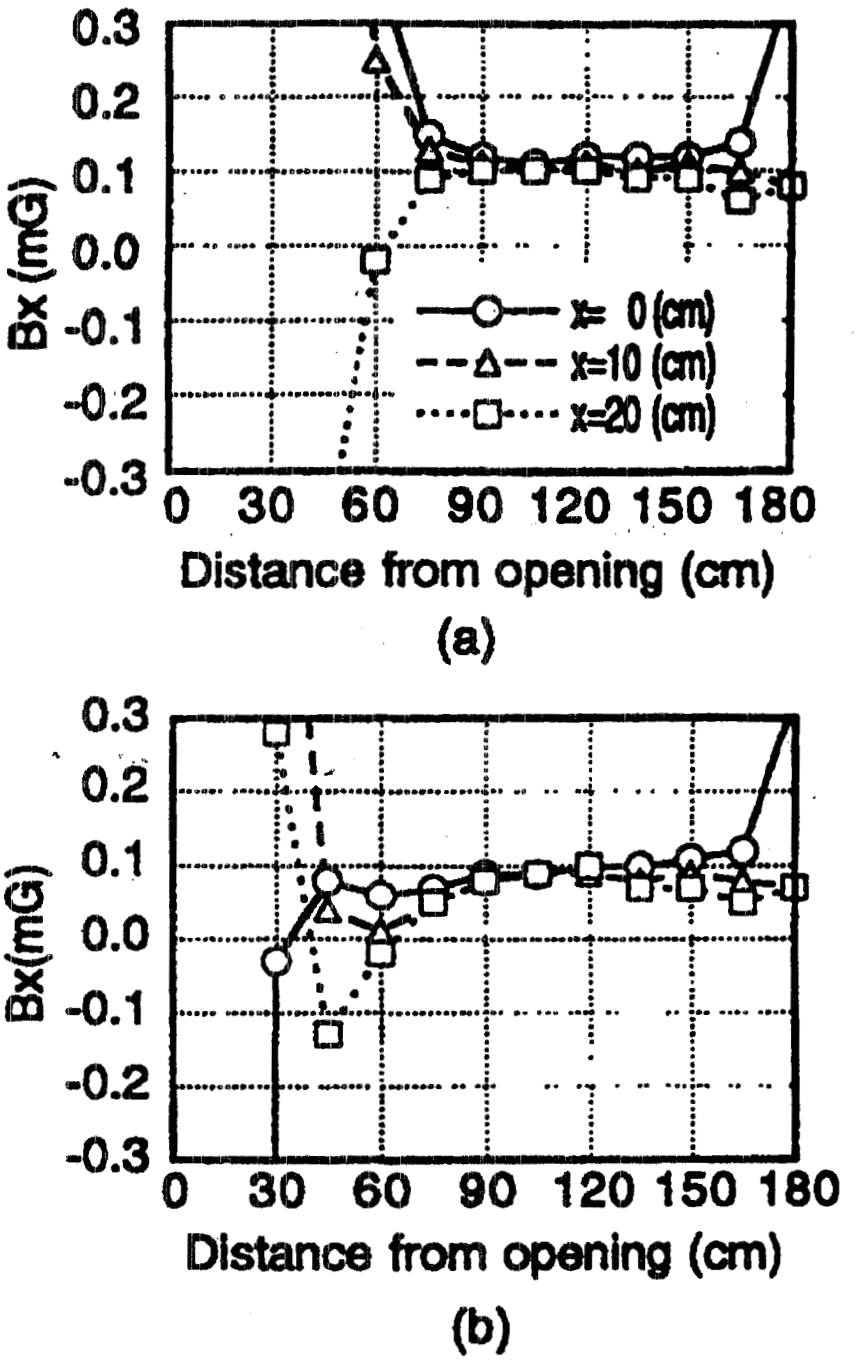

FIG. 4. Distributions of Bx, where the opening compensation is off in (a) and on in (b).

to AIP copyright, see http://ojps.aip.org/japo/japcpyrts.html.

Update on the HV-test apparatus

Debbie Clark (Los Alamos)

EDM High Voltage Test

A. Purpose of Experiment.

B. Describe System.

C. Tests and their Significance.

D. Schedule.

E. Remaining Design Issues.

F. Questions.

EDM High Voltage Test

A. **Purpose of Experiment.**
   a. Learn High-voltage behavior.
   b. Liquid Helium behavior at ~1 K.
   c. Magnetic field issues.
   d. Failure points
      i. Mechanical, electrical leakage, sparks.
   e. Is 50kV possible?

B. **Describe System.**
   a. Vacuum shell, nitrogen shell, LHe chamber.
   b. Electrodes, actuators, bellows.

C. **Tests and their Significance.**
   a. Can we assemble this?
   b. Mechanical failure of components and seals.
   c. Are heat loads acceptable?
   d. Does variable capacitor work as designed?
   e. Measure dielectric constant of materials.
   f. Measure dielectric strength of LHe at 1K.
   g. Measure E Field with Kerr effect.
      i. Source, laser
   h. Effect of E Field on scintillation process.
      i. Phototube.
   i. Potentially use Squid to see Johnson effect, leakage current.

D. **Schedule.**
   a. Order parts starting in September 2002.
   b. Assembly begins November 2002.

E. **Remaining Design Issues.**
   a. Large wire seal flanges.
   b. Cam system.

F. **Questions.**

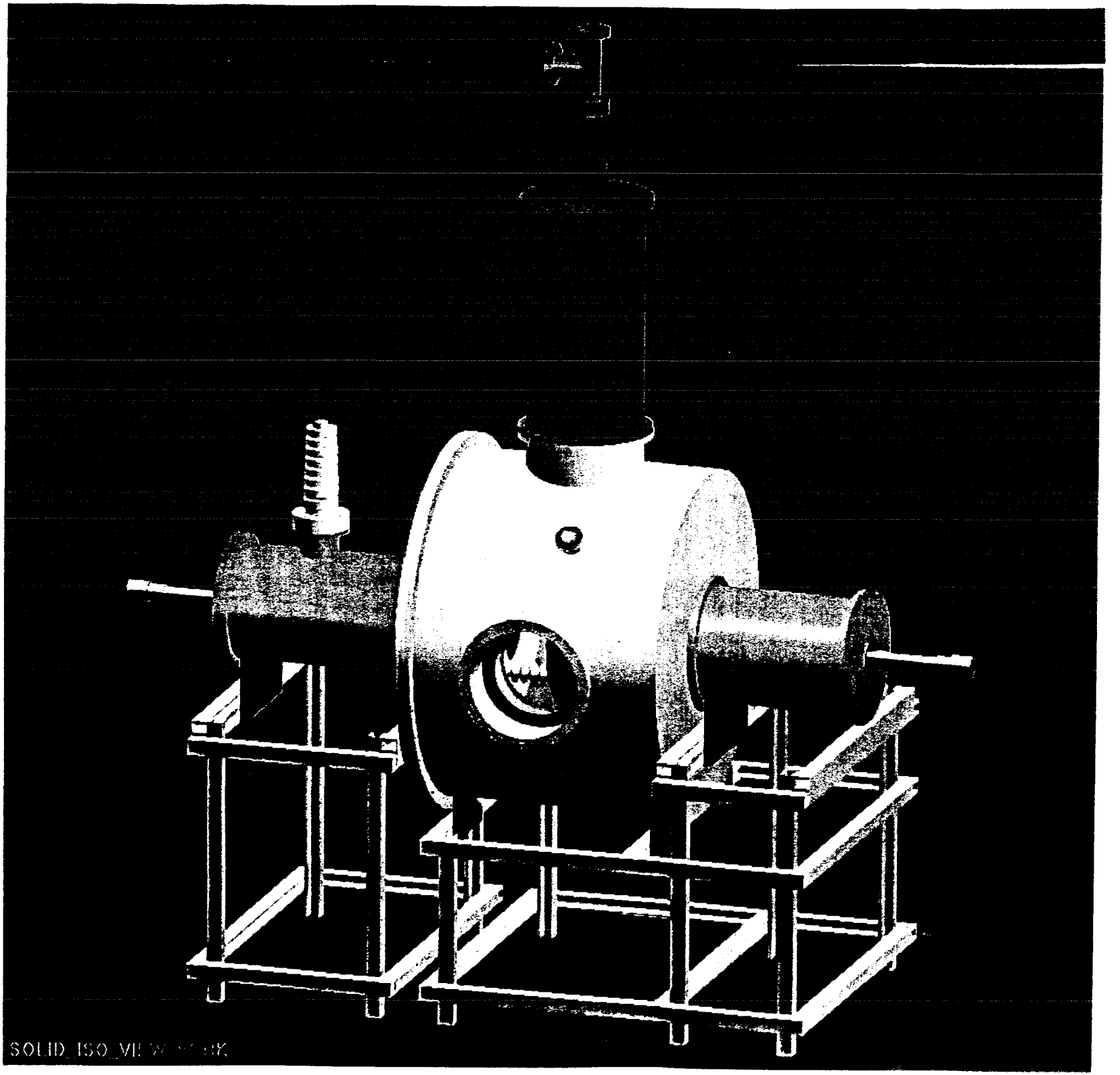
SOLID_ISO_VIEW

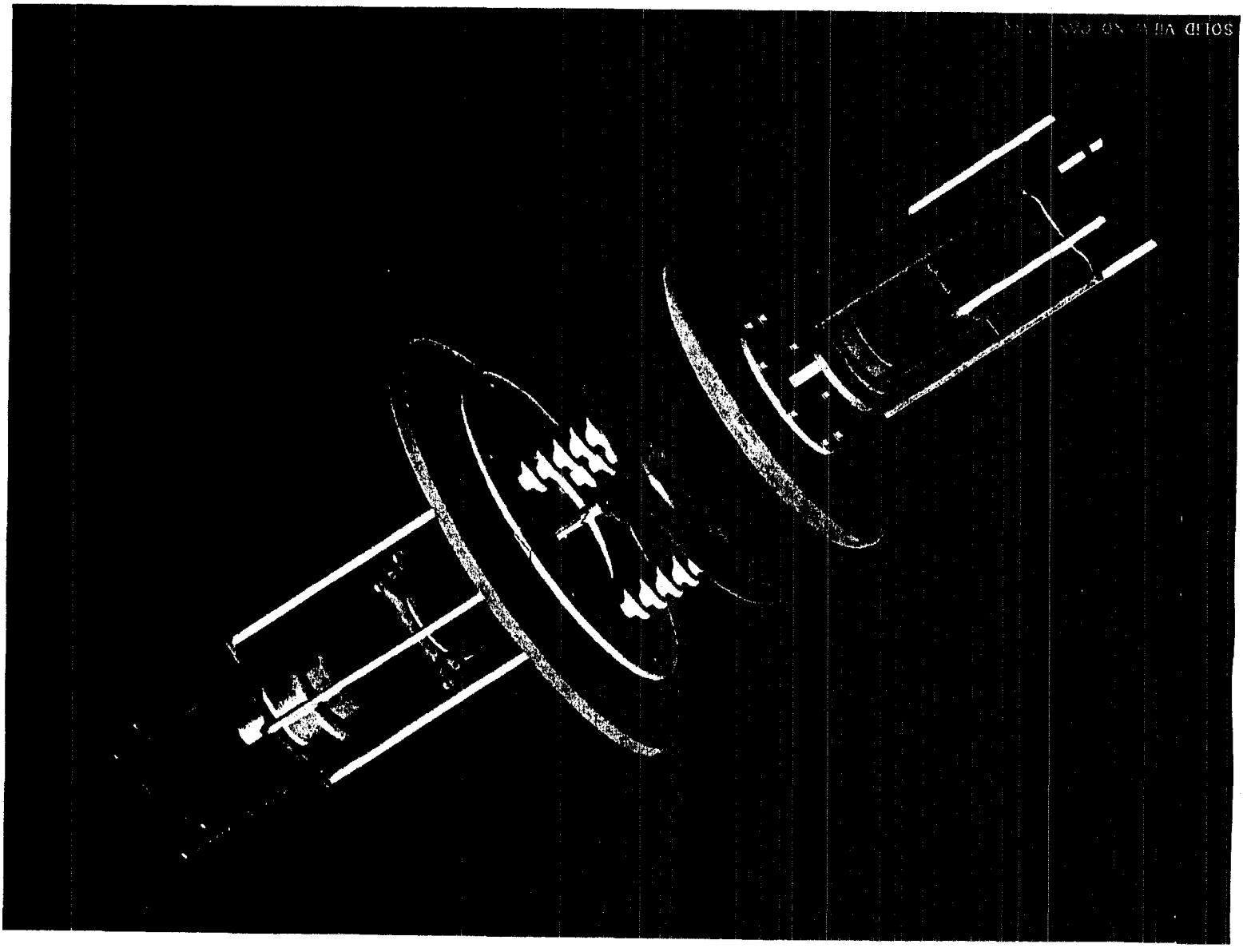

High Voltage Test Assembly

estimated June, 2002 D. Clark

Hunt. Linear Actuator & Cont. (2)	$ 7000	
Outer Vac Can Assy Alum A&B	16325	
Nitro Shield Cu Assy A&B	4850	
Andonian Modification	3025	
Inner He4 Copper Can A&B	20500	(+$2000)
G-10 Dbl Bearing Assy (2)	725	
Bellows/Flg. Weldment (4) Uses # 501	6000	(+$3000)
High Volt. End Actuator Assy (w/ 2 #500)	3685	
Ground End Actuator Assy (uses 2 #500)	2325	
Unistrut Stand Assy A&B	2000	
TOTAL	$ 66435	(+$ 5000 spares)

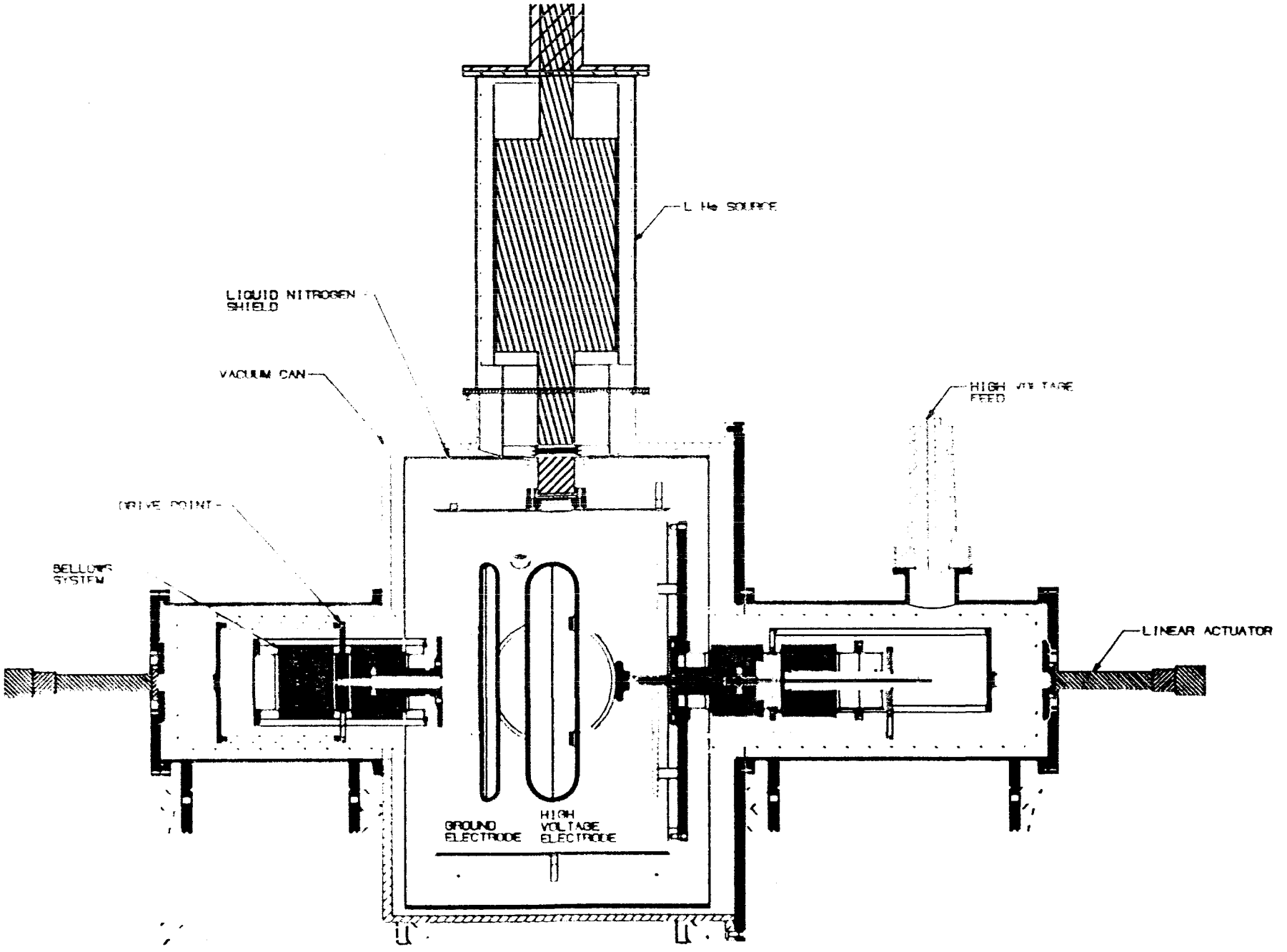
L He SOURCE
LIQUID NITROGEN SHIELD
VACUUM CAN
HIGH VOLTAGE FEED
DRIVE POINT
BELLOWS SYSTEM
LINEAR ACTUATOR
GROUND ELECTRODE
HIGH VOLTAGE ELECTRODE

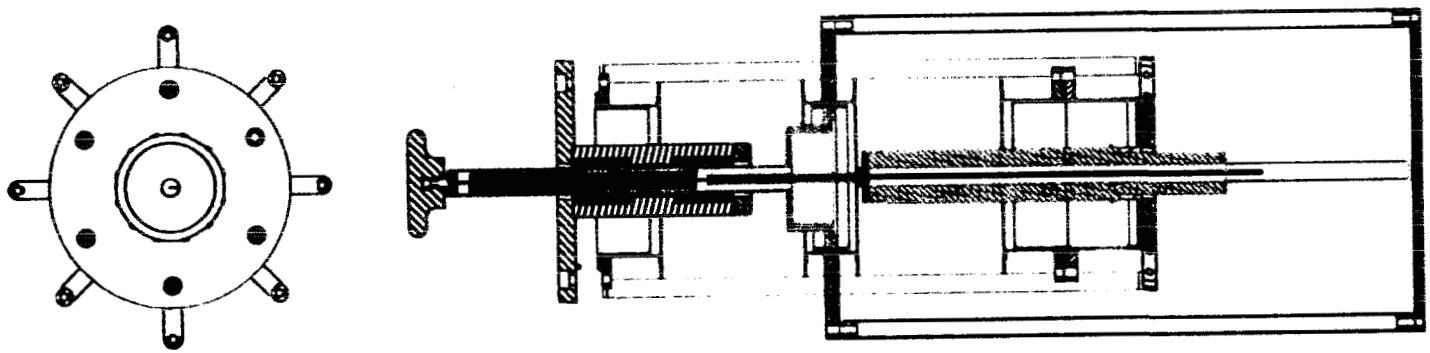

HIGH VOLTAGE END PLUNGER ASSEMBLY

CLARK 7/02 P-25

HIGH VOLTAGE EXP.

HIGH VOLTAGE END PLUNGER ASSEMBLY

.5 12BY-287819

Discussion of test objectives

1. Confirm viability of engineering design

   acceptable heat loads

   cold HV feedthrough survives

   flanges remain sealed

2. Validate variable capacitor design

3. Measure cryogenic properties of materials

   testbed for engineering issues

   measure dielectric constant of cell materials

4. HV properties of LHe

   determine dielectric strength

5. Develop E field measurement with Kerr effect

6. Investigate effect of E field on scintillation process

7. Study performance of SQUIDS in test environment

Measuring the Kerr effect at crogenic temperatures

Alex Sushkov (UC-Berkeley)

Kerr Effect-based Measurement of the Electric Field

Alex Sushkov
Dima Budker
Valeriy Yashchuk
(UC Berkeley)

Precision Measurement of Electric Fields

- **Kerr effect**: appearance of uniaxial anisotropy in an initially isotropic medium, induced by an applied external electric field:

$$\Delta n = n_{\parallel} - n_{\perp} = K\lambda E^2$$

- For input light polarized at 45° to E, the induced ellipticity:

$$\epsilon = \pi l \Delta n/\lambda = \pi l K E^2$$

- Circular analyzer: $\delta\epsilon \approx 10^{-8}$ rad $Hz^{-1/2}$ (shot)

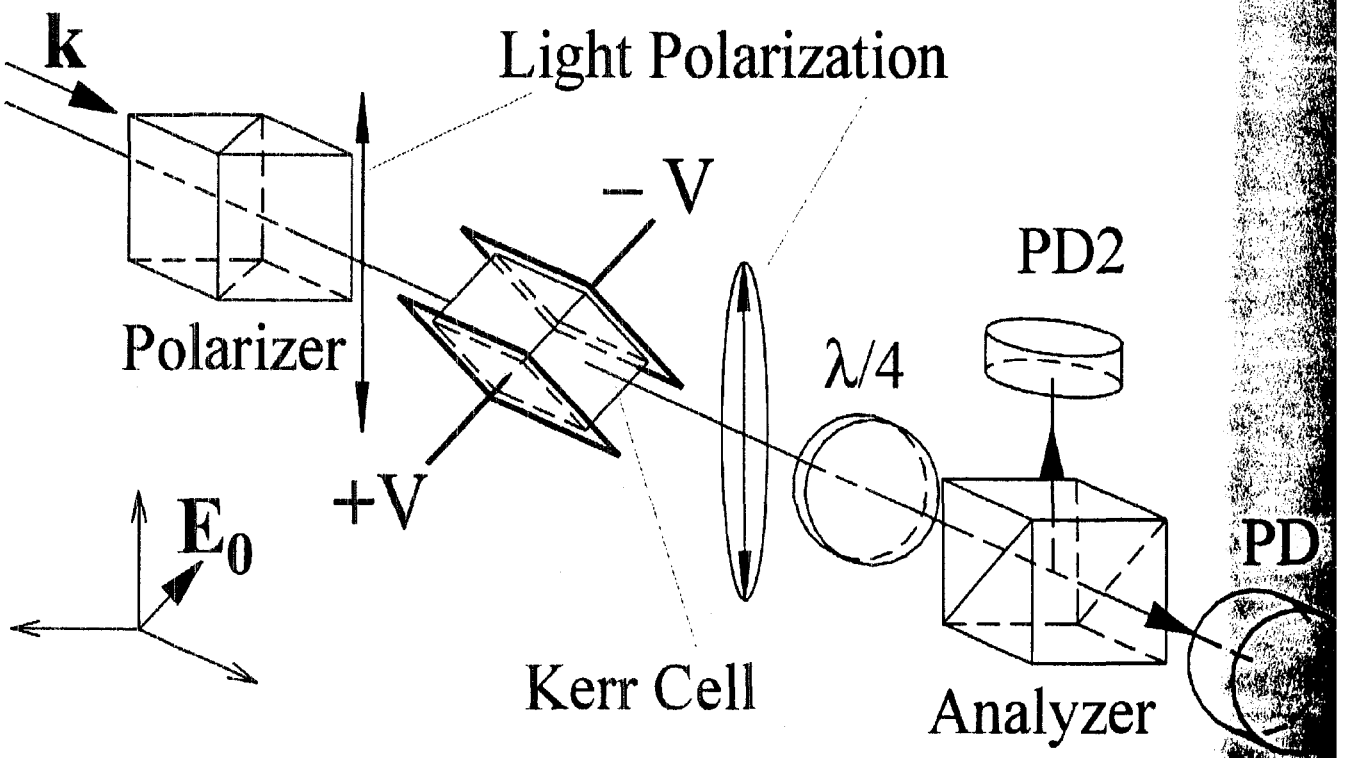

Kerr Effect in LHe: Electric Field Measurement Sensitivity

- **Parameters of the neutron EDM experiment:**
  - Electric field: E = 50kV/cm
  - Sample length: l = 10cm
  - LHe Kerr constant inferred from He gas hyperpolarizability at T=300K: $K = 1.7\times10^{-16}$ cm/V^2
- **Resulting shot-noise sensitivity:**
  - Induced ellipticity: $\epsilon \approx 10^{-5}$rad
  - A 1s measurement gives sensitivity:

$$\delta E/E \approx 5\times10^{-4}$$

Experimental Setup: Polarimeter

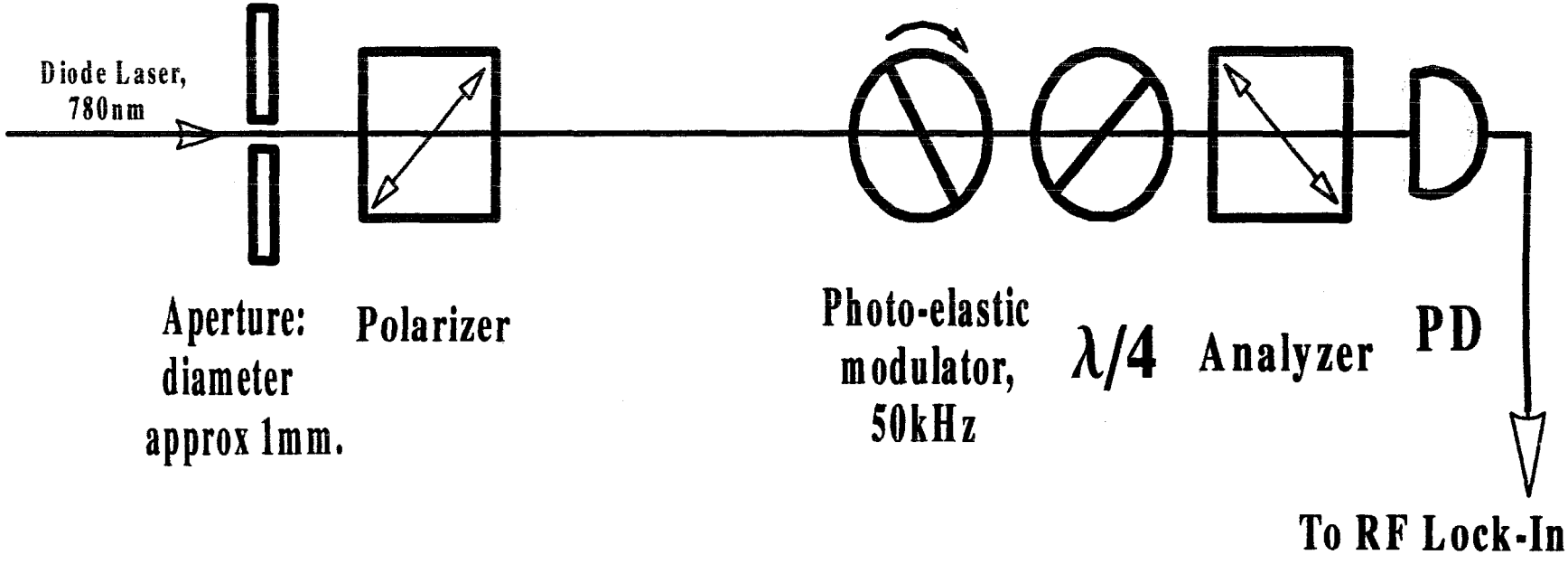

Results: Polarimeter

- **Optimized performance:**
  $$\delta\epsilon = 10^{-7}\ \mathrm{rad/Hz^{1/2}}$$
  (lock-in input noise)
- Laser power: P = 0.1 mW, corresponding to shot noise of: $5\times10^{-8}\ \mathrm{rad/Hz^{1/2}}$

Experimental Setup: Kerr Effect in LN_2

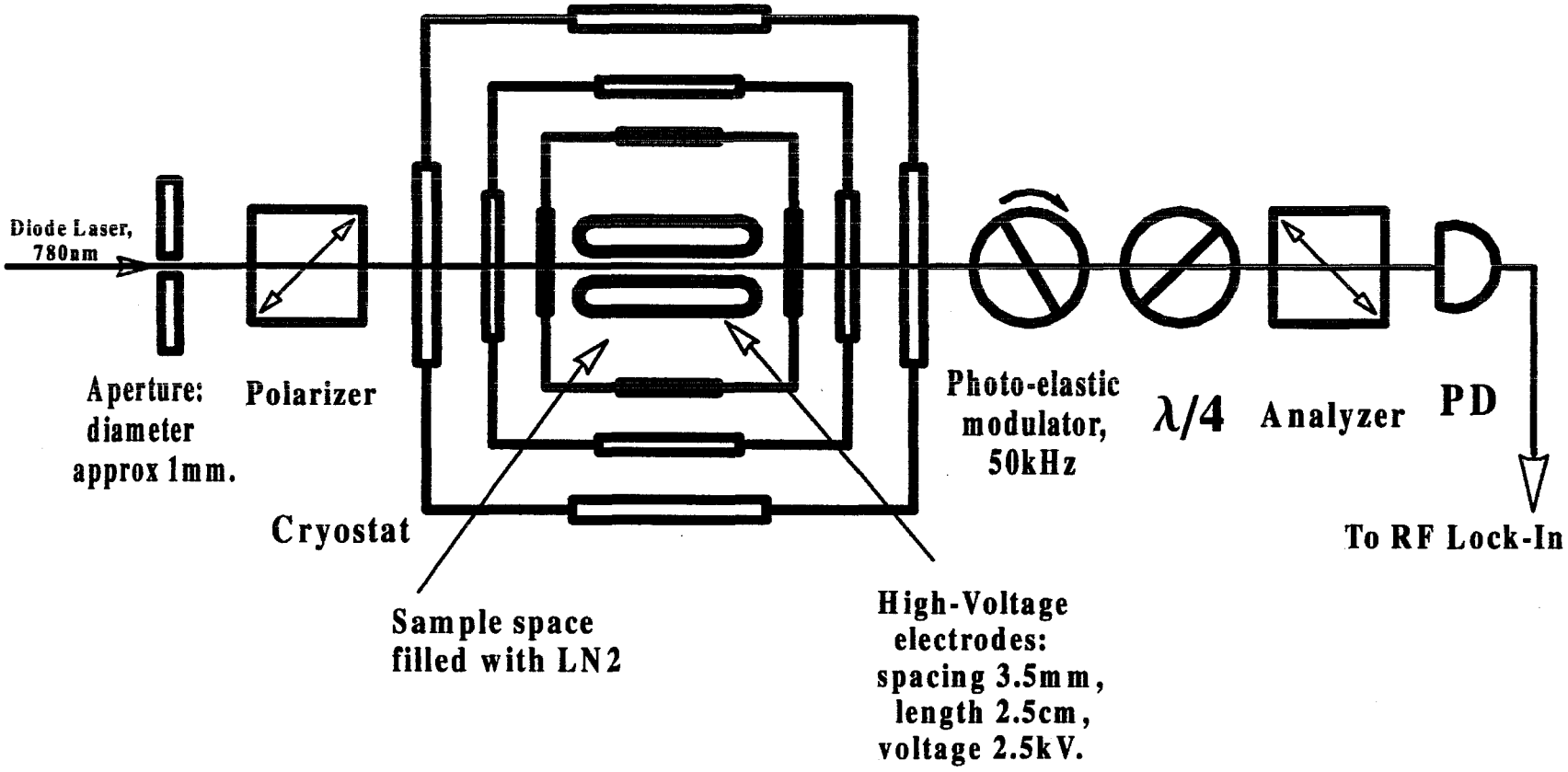

Results: LN_2

- Measured Kerr constant for LN_2:
  $K = (7.1 \pm 1.7) \times 10^{-14}\ cm/V^2$
- Published value: (K.Imai et. al., Proceedings of the 3rd Int. Conf. On Prop. and App. Of Diel. Mat., 1991 Japan)
  $K = 6.3 \times 10^{-14}\ cm/V^2$

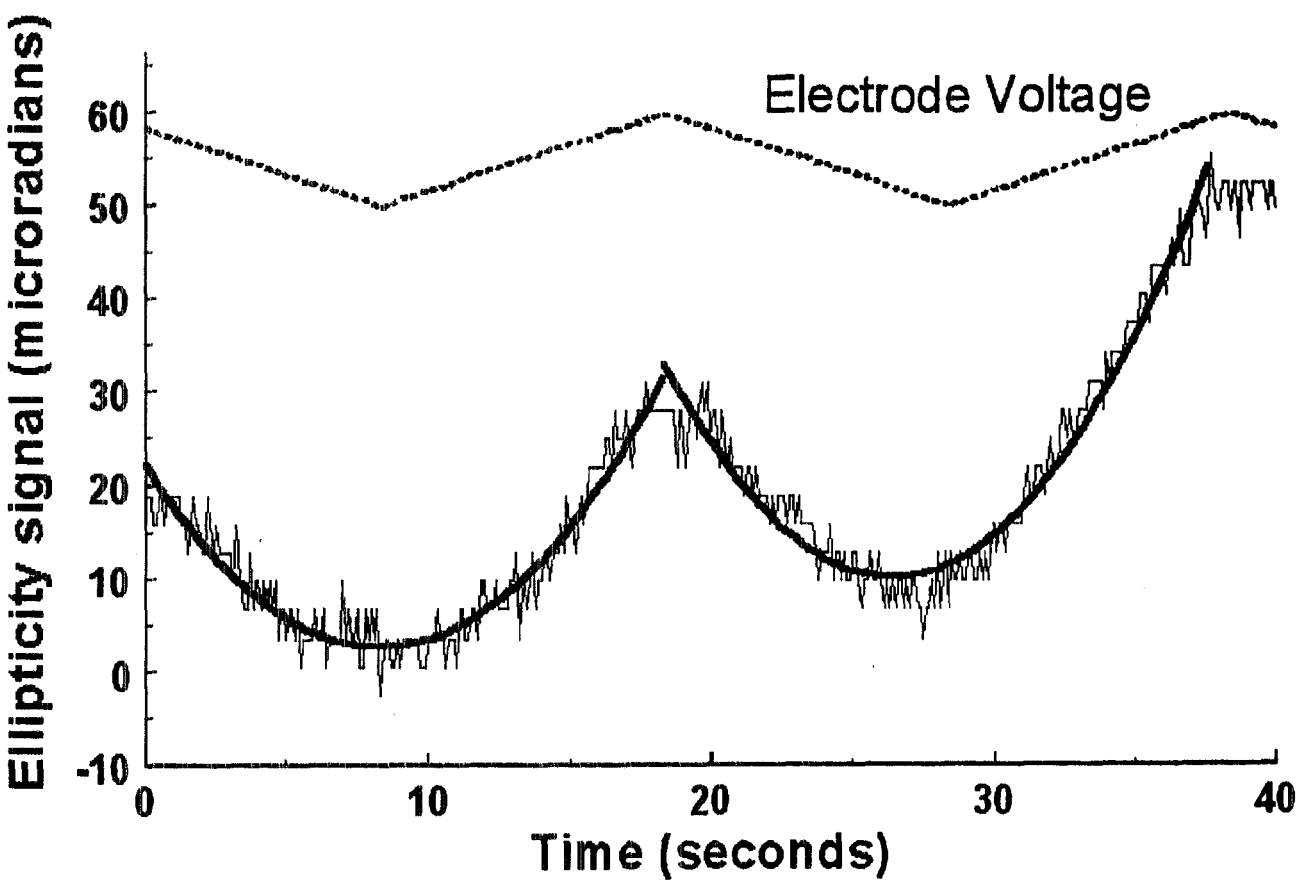

Troubleshooting

- Cryostat window birefringence, induced by stresses and temperature gradients $\Longrightarrow$ large drifts in the ellipticity signal
- Find better cryostat windows!

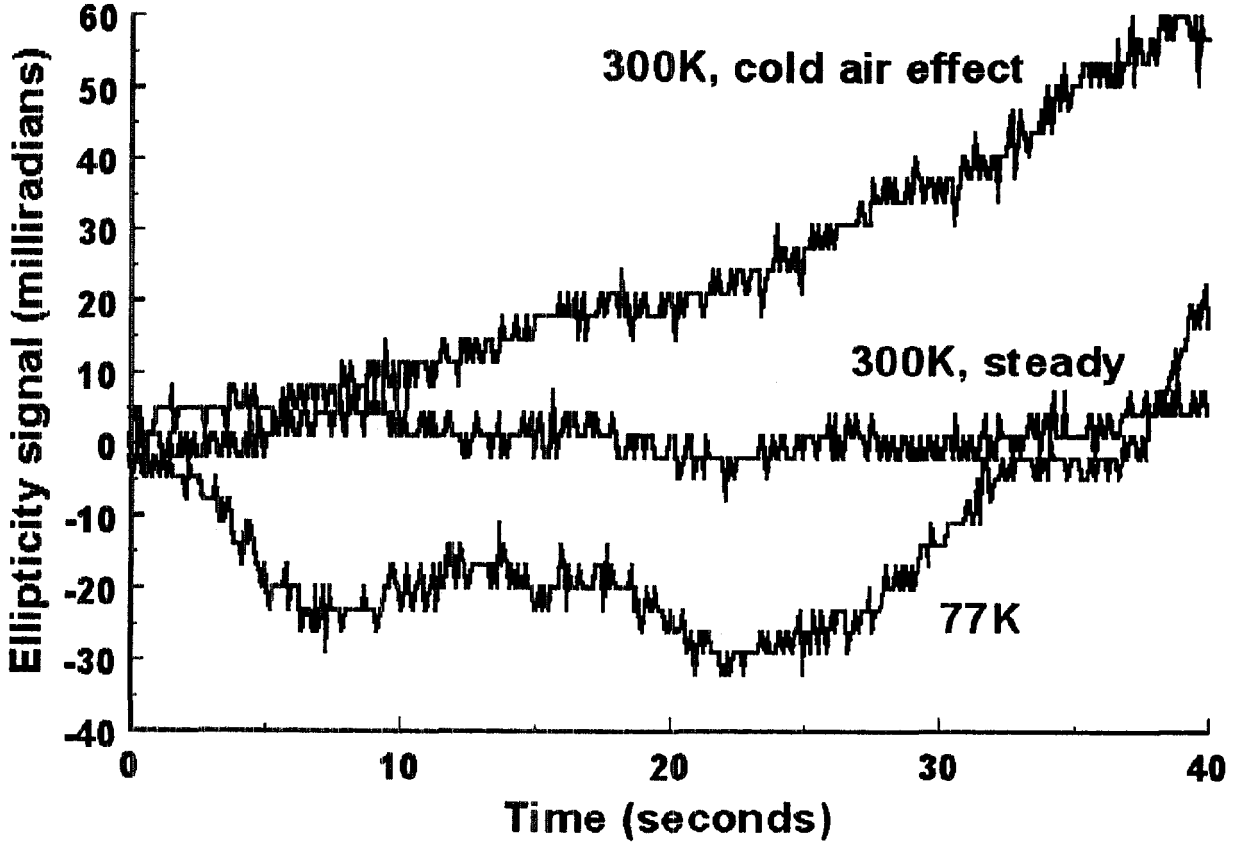

What's next?

1. Sort out the cryostat windows birefringence drifts.
2. Measure the LN_2 Kerr constant
3. Measure the LHe Kerr constant (UCBerkeley & LANL).
4. Evaluate the possibility of monitoring the EDM E-field using the Kerr effect.

Update on the polarized 3He source

Justin Torgerson (LANL)

^{3}He polarization

Requirements

- $P_3 \approx 1$
- $\sim 10^{12}$ ^{3}He/cm^3 $\quad (\chi_3 \sim 10^{-10})$
  $\longrightarrow 10^{16}$ in 8 L $\quad$ (collect in 1000 s)

Quadrupole state selector

- $P_3 > 0.99$ initially
- $I_0 > 10^{14}$/s

Experimental uncertainty

- $\delta f \propto 1/P_3$ $\qquad P_3, P_n \approx 1$
- $\delta f \propto 1/{P_3}^2$ $\qquad P_n \approx 0$
- $\delta f \propto 1/{P_3}^m$ $\qquad P_3, P_n \neq 1$

Our Approach

Exploit $\vec{F} = \mu(\hat{s}\cdot\vec{\nabla})\vec{B}$

Quadrupole Field

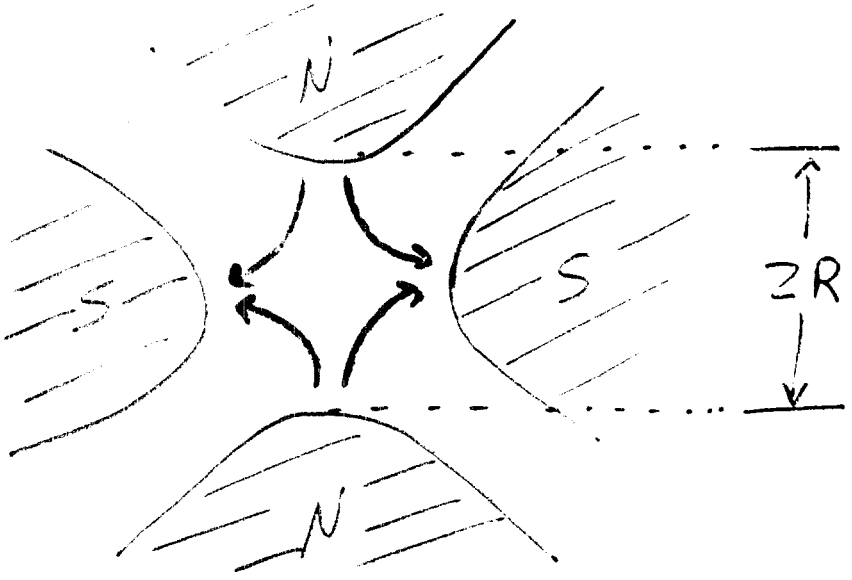

$$\vec{F} = \pm\mu\frac{B_0}{R}\hat{r}$$

(assuming adiabatic following)

Simple Calculation of ^3He Flux

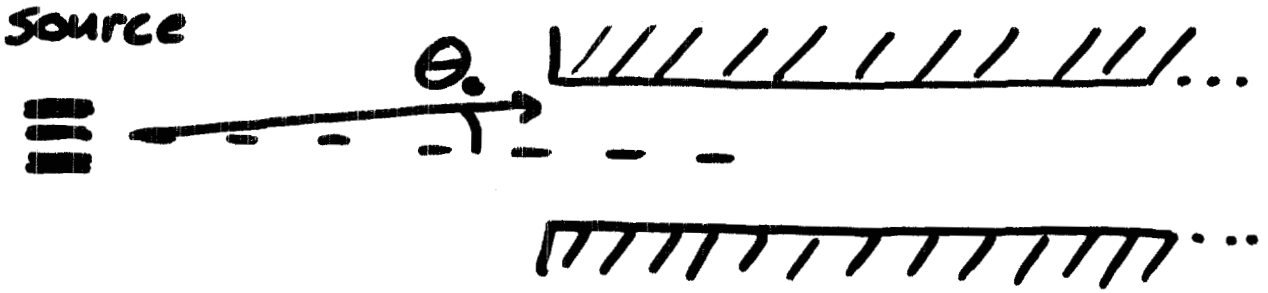

Maximum acceptance

$$\sin(\theta_0) \approx \sqrt{\frac{\mu B_0}{4kT}} \approx 0.9°$$

for $B_0 = 0.75$ Tesla
$T = 0.6$ K

Maximum source pressure

$$\lambda_s \geq \rho_s = 0.35\,mm$$

$$p \leq kT/\sqrt{2}\,\rho_s \sigma \approx 10^{-4}\,torr$$

Maximum flux

$$I_0 = \frac{1}{2} \cdot 2\sqrt{\frac{kT}{m}} \cdot \frac{p}{kT} \cdot A_s \sin^2\theta_0 \approx \underline{\underline{10^{15}/s}}$$

for $A_s = 1\,cm^2$

Numerical Analysis

$$\vec{F}_B = \pm \mu \frac{B_0}{R} \frac{1}{\sqrt{1+(B_z R/B_0 r)^2}} \hat{r}$$

$$\vec{F}_g = -m\left(g + \frac{v_z^2}{R_f}\right)\left(\sin\phi\, \hat{r} + \cos\phi\, \hat{\phi}\right)$$

$$\vec{F}_B + \vec{F}_g = m\ddot{\vec{r}}$$

$$\ddot{\vec{r}} = \left(\ddot{r} - r\dot{\phi}^2\right)\hat{r} + \left(r\ddot{\phi} + 2\dot{r}\dot{\phi}\right)\hat{\phi}$$

Also,

$$I(v) \propto v^3 e^{-\frac{mv^2}{2kT}}$$

$$I(\theta) \propto \cos\theta$$

Source 22 cm from Polarizer

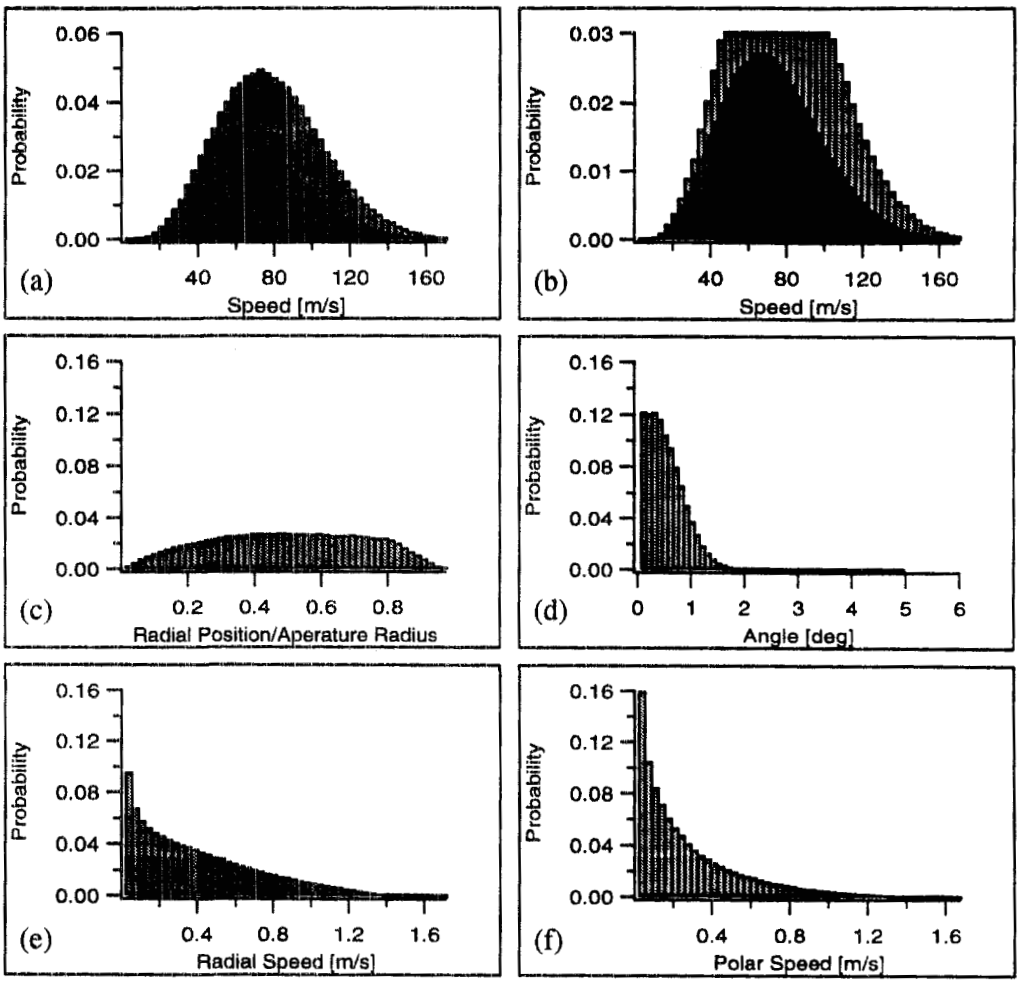

Figure 2: The light gray bars in (a) represent the velocity distribution of atoms which enter the aperture of the polarizer and the dark gray represents the subset that successfully traverses the polarizer. Panel (b) shows the same results as (a) with a different vertical scale. Panels (c-f) show the distributions of various initial conditions for atoms which successfully traverse the polarizer.

$$\begin{cases} t_\uparrow = 0.53 \\ t_\downarrow = 0.0004 \end{cases} \qquad P_3 = 0.998$$

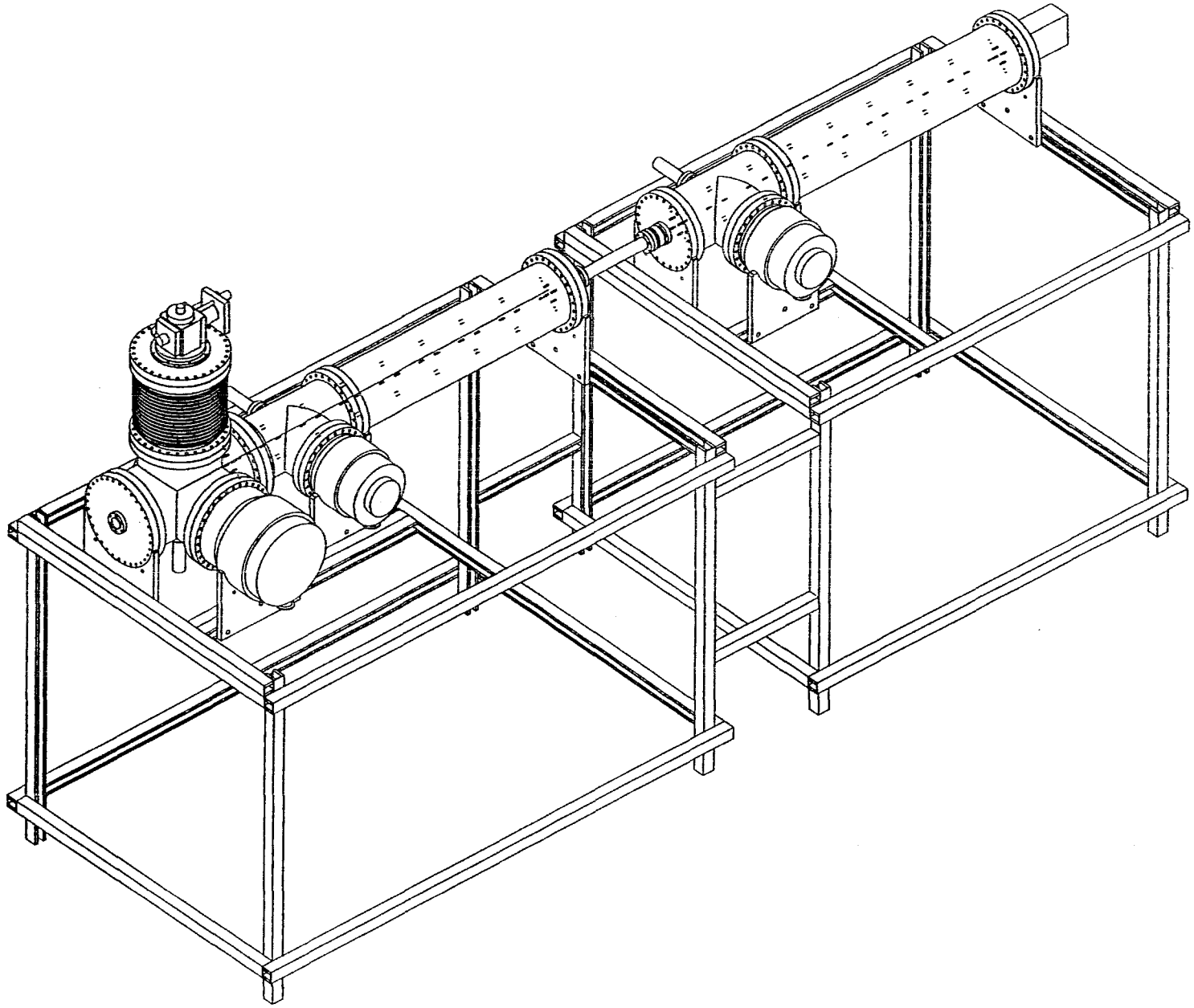

3He Polarized Source

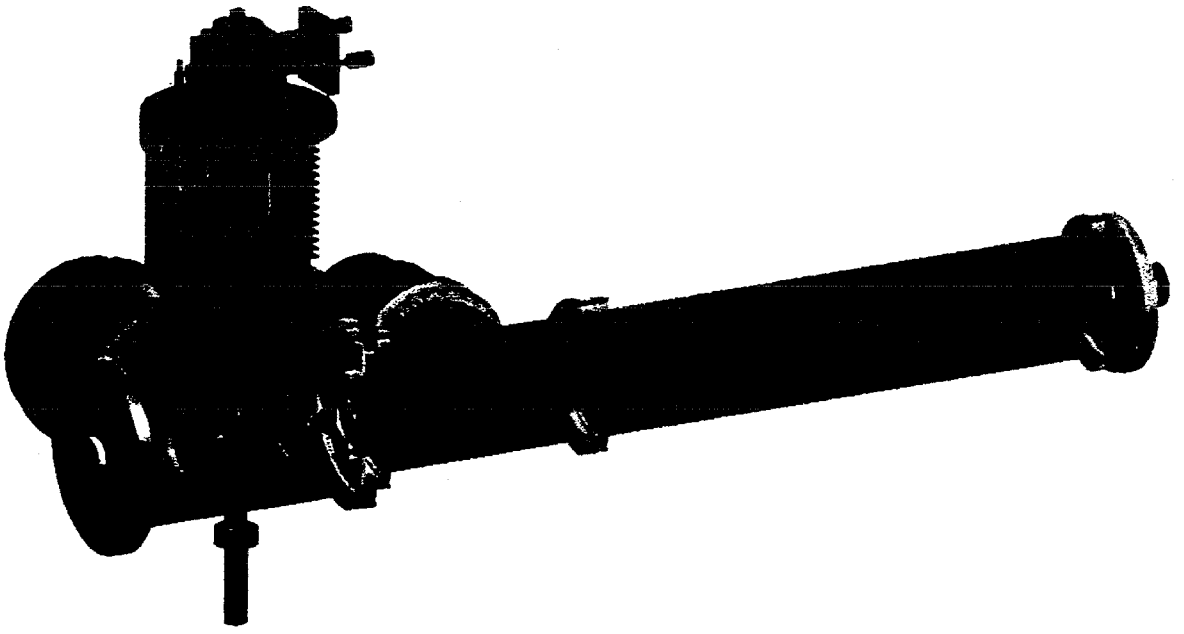

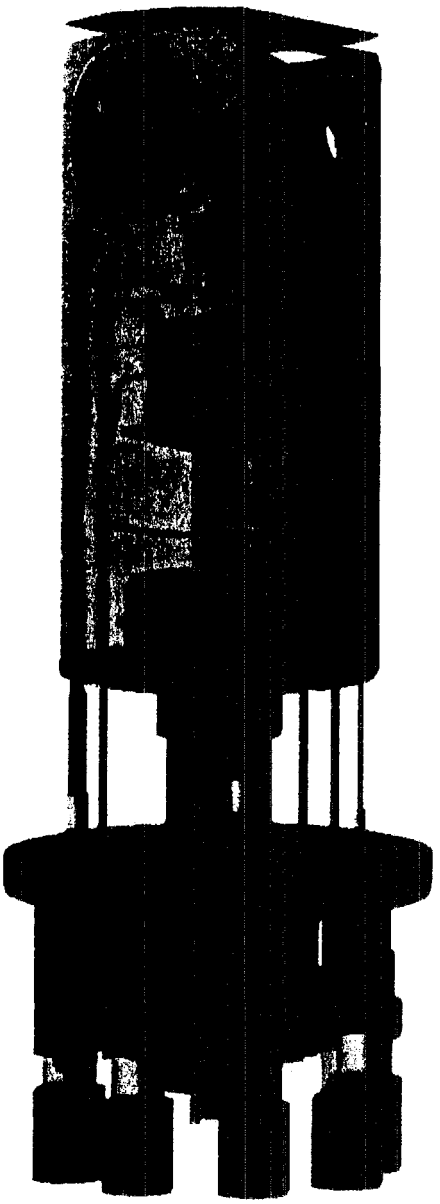

Transport of $\uparrow^3$He

Magnetic field issues

- Gradient at quadrupole exit
- Reduce field before experimental volume
- Bent ^{3}He guide (horizontal polarizer)
- Higher ^{3}He temperatures (300 K) and field gradients

Gradient at quadrupole exit

$$\left|\frac{dB/dt}{B}\right| \ll \mu B$$

$$\frac{dB}{dt} = \frac{dB}{dz} v_z$$

- $B(z) \simeq B_0{}' \frac{R_0{}^4}{z^4}$
- $B \gg B(z)$ at $z = (\frac{1}{4}\frac{\mu}{v_z} B_0{}' R_0{}^4)^{\frac{1}{3}}$
- $B_0{}' \approx \frac{1}{30} B_0$ (from calculation)

$$B >> 200\,\mathrm{mG}$$

for $B_0 = 0.75\,\mathrm{T}$ and $R_0 = 7.5\mathrm{mm}$

Bent ^{3}He guide

(horizontal polarizer)

- $B_z = B_0 \cos(\theta)$ and $v_z = v \cos(\theta)$

- $|\frac{dB}{dz}| = B_0 \frac{z}{R^2} / \cos(\theta)$

- assuming $|B| = B_0$ everywhere

$$B_0 \gg \frac{z}{R^2}\frac{v}{\mu} \gg \frac{v}{R\mu}$$

$$B_0 \cdot R >> 100\,\text{mG·m at } 300\,\text{K}$$

$$B_0 \cdot R >> 3\,\text{mG·m at } 0.6\,\text{K}$$

Reducing B field before experiment

- $\frac{dB}{dz} \ll \frac{\mu}{v_z} B^2$

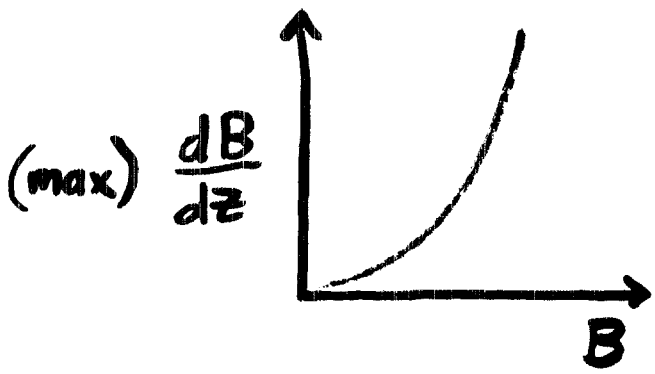

$$\frac{dB}{dz} \ll 100\,\mathrm{mG/m}$$

for 300 K and $B = 100$ mG

$B \longrightarrow 10$ mG is very difficult at 300 K

Experiences with hexapole state selectors

Janos Fuzi (Budapest)

Experiences with hexapole state selectors

Füzi János

Hungarian Academy of Sciences
Research Institute for Solid State Physics and Optics

Particles with magnetic moment in inhomogeneous magnetic field

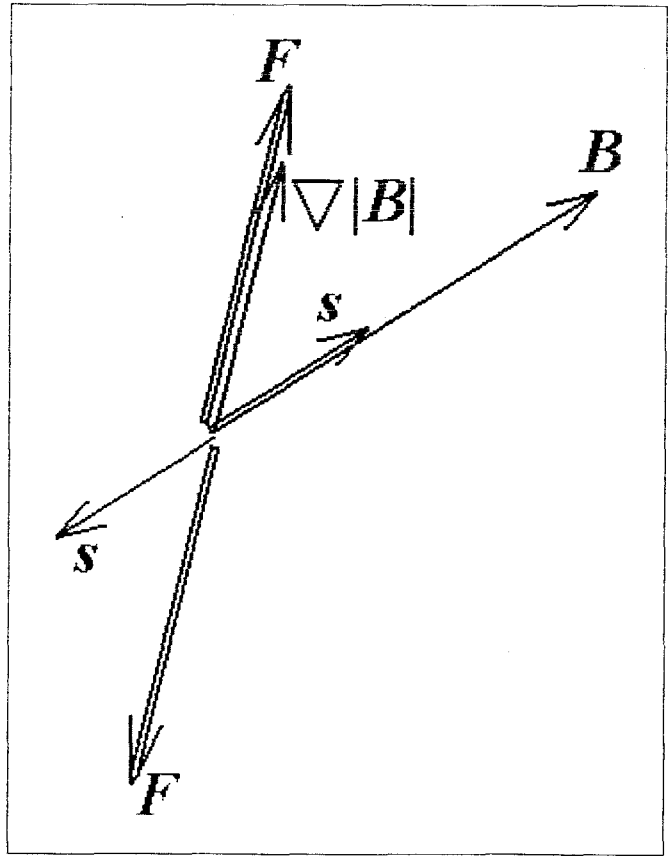

$$\boxed{\boldsymbol{s} = \gamma \boldsymbol{L}}$$

$$\boxed{\boldsymbol{F} = (\boldsymbol{s} \cdot \nabla)\boldsymbol{B} \quad ; \quad \boldsymbol{T} = \boldsymbol{s} \times \boldsymbol{B}}$$

$$\boxed{\boldsymbol{F} = m\frac{\mathrm{d}^2 \boldsymbol{r}}{\mathrm{d}t^2} \quad ; \quad \boldsymbol{T} = \frac{\mathrm{d}\boldsymbol{L}}{\mathrm{d}t} = \boldsymbol{w} \times \boldsymbol{L}}$$

$$\boxed{\Psi = Cr^n \cos n\varphi}$$

$$\boxed{\boldsymbol{B} = \mu_0 Cnr^{n-1}\left(-\cos n\varphi \boldsymbol{e}_r + \sin n\varphi \boldsymbol{e}_\varphi\right)}$$

$$\boxed{\boldsymbol{F} = s_r \frac{\partial \boldsymbol{B}}{\partial r} + s_\varphi \frac{1}{r}\frac{\partial \boldsymbol{B}}{\partial \varphi}}$$

$$\boxed{\boldsymbol{F} = \nabla(\boldsymbol{s} \cdot \boldsymbol{B}) = \pm s \nabla |\boldsymbol{B}|}$$

Quadrupole versus hexapole field configurations

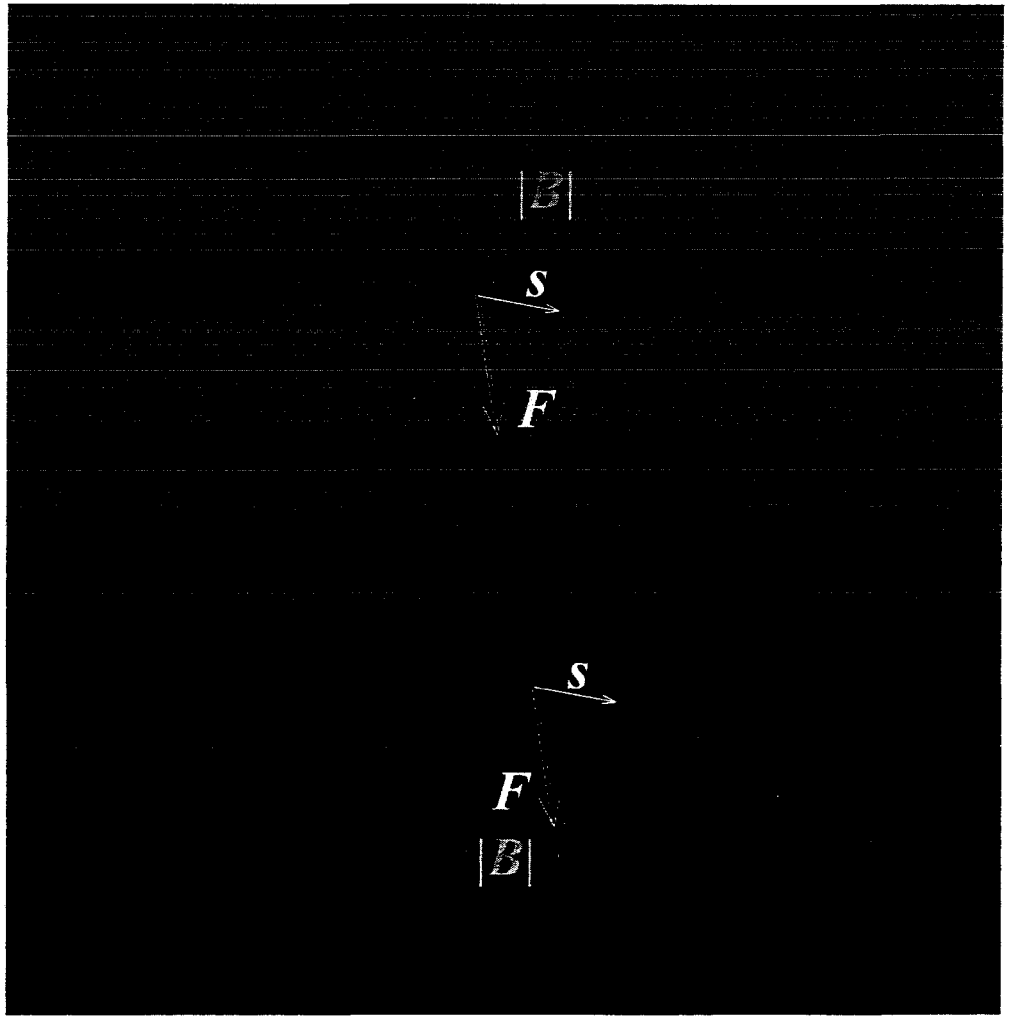

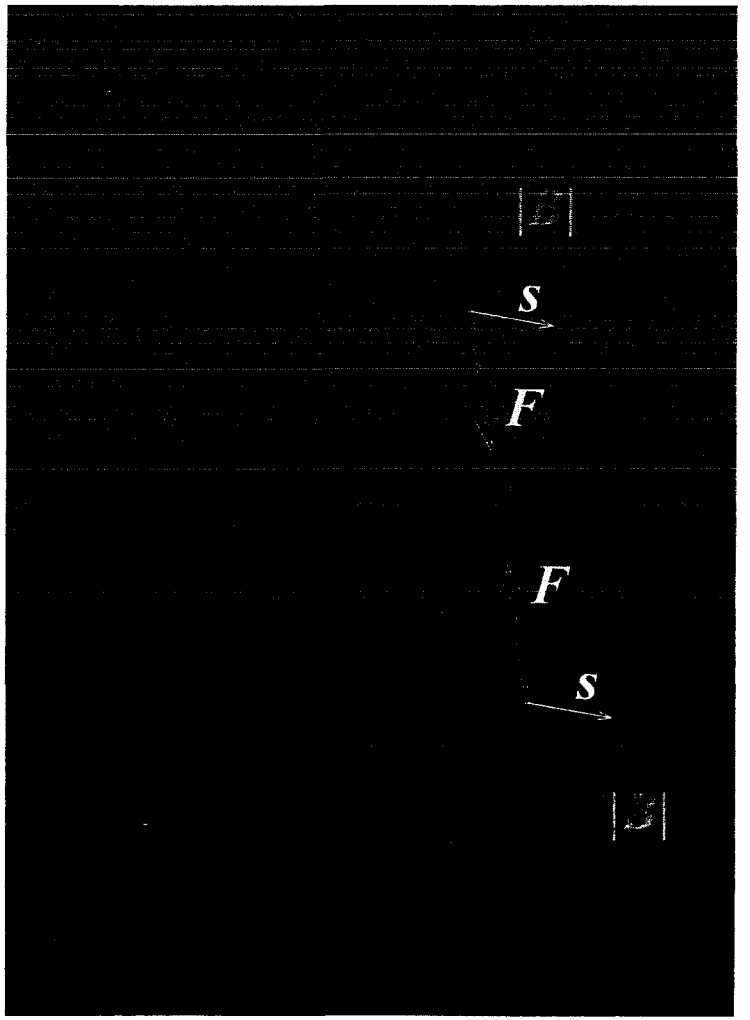

Hexapole neutron lens electromagnet

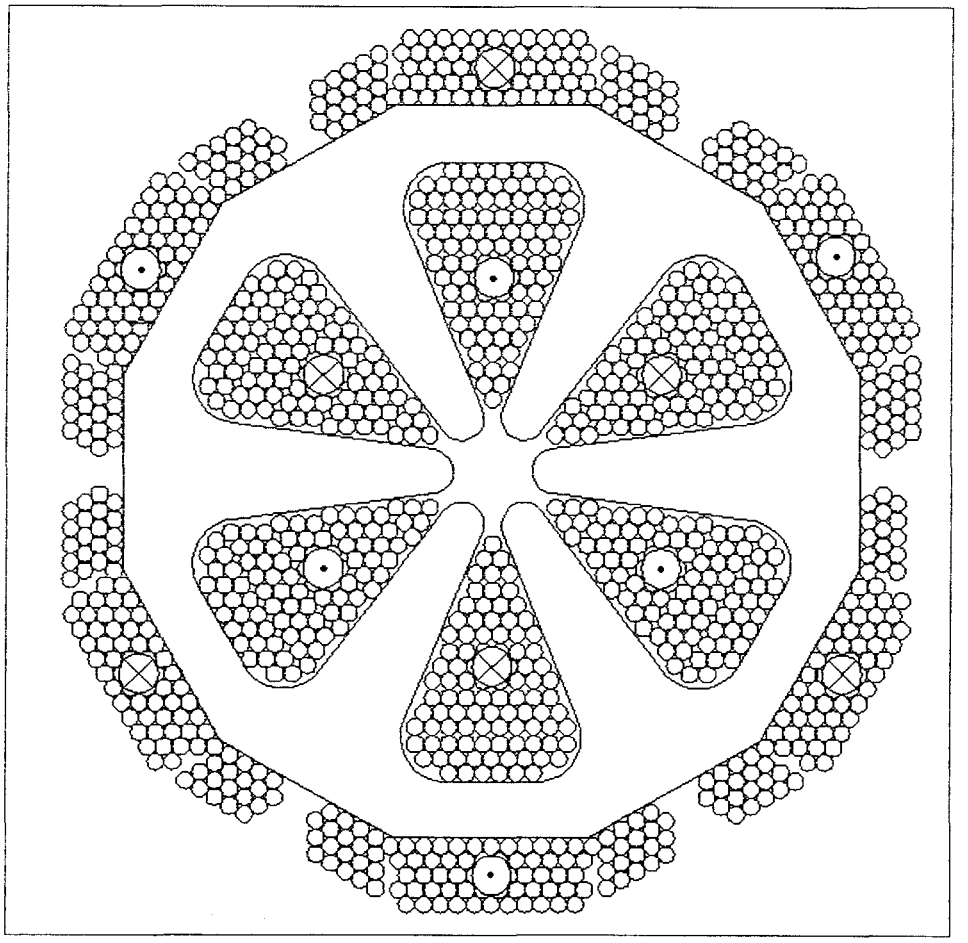

Cross-section

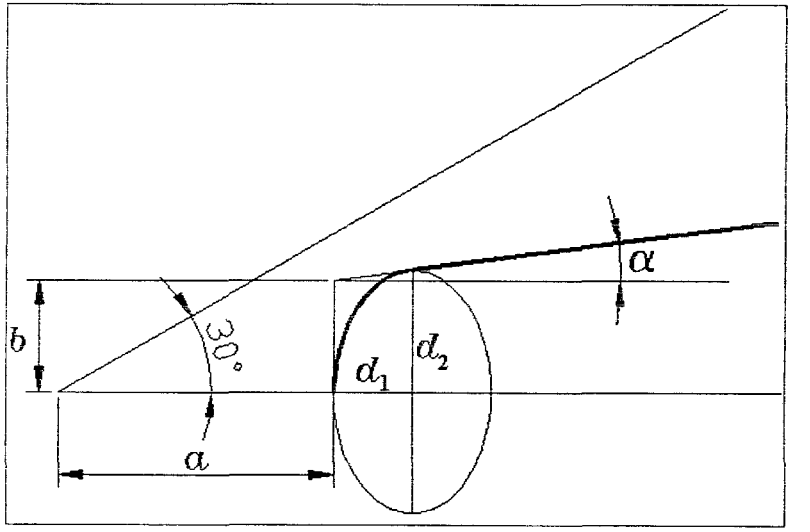

Definition of pole geometry

Boundary conditions:

$b < a / \sqrt{3}$

$\alpha < 30°$.

Magnetic field computation

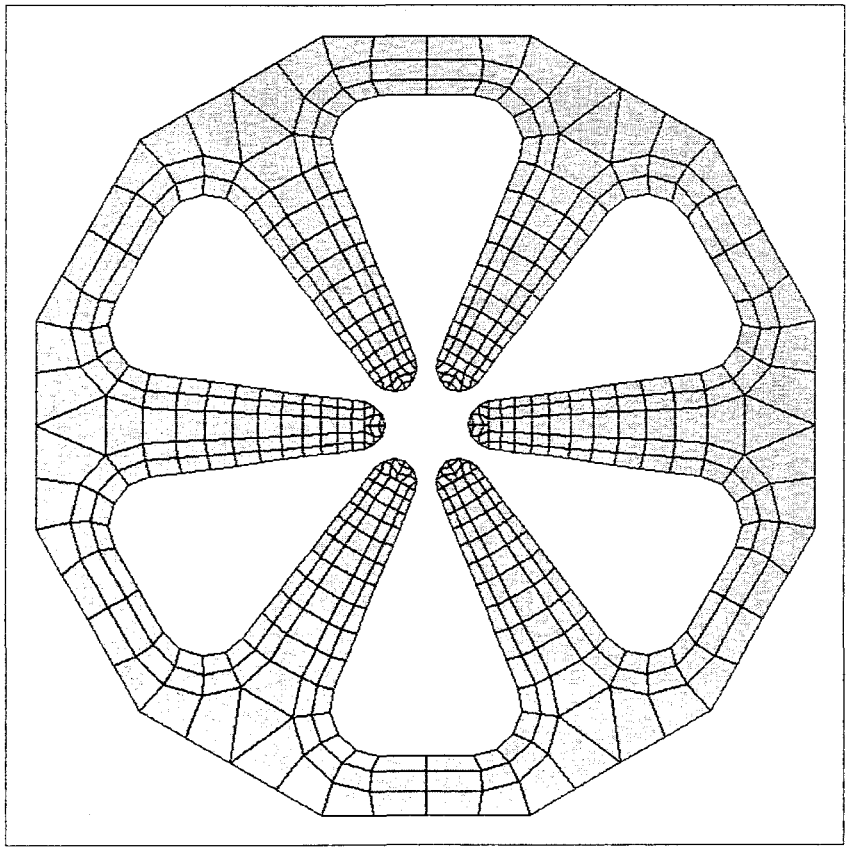

Division of iron core cross-section

$$\boldsymbol{H}_f = -\frac{1}{2\pi}\iint_{A_s}\left(M_x \nabla_f \frac{x_f - x_s}{r^2} + M_y \nabla_f \frac{y_f - y_s}{r^2}\right)\mathrm{d}A$$

$$\boldsymbol{H}_f = \left(C_{xx}M_x + C_{xy}M_y\right)\boldsymbol{i} + \left(C_{yx}M_x + C_{yy}M_y\right)\boldsymbol{j}$$

$$C_{xx} = \frac{1}{2\pi}\iint_{A_s}\frac{2\left(x_f - x_s\right)^2 - r^2}{r^4}\mathrm{d}A$$

$$C_{xy} = C_{yx} = \frac{1}{2\pi}\iint_{A_s}\frac{\left(x_f - x_s\right)\left(y_f - y_s\right)}{r^4}\mathrm{d}A$$

$$C_{yy} = \frac{1}{2\pi}\iint_{A_s}\frac{2\left(y_f - y_s\right)^2 - r^2}{r^4}\mathrm{d}A$$

Singularity exclusion

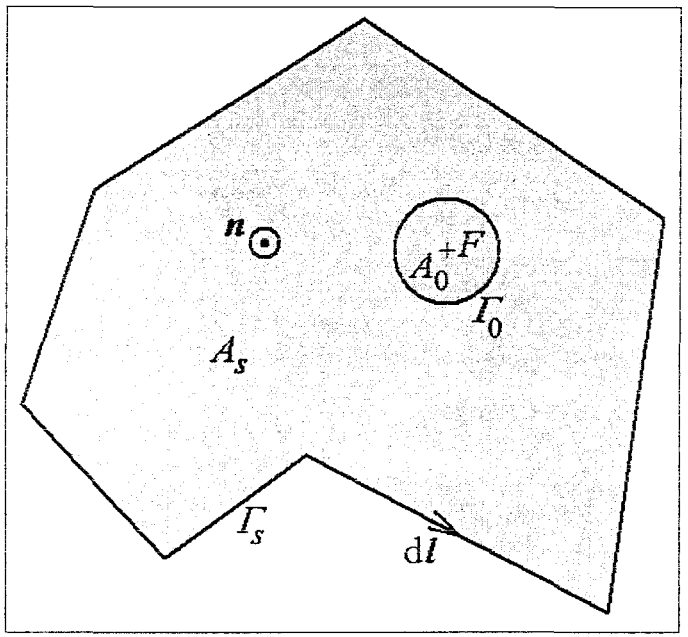

$$\nabla_s \times \left(\frac{y_f - y_s}{2r^2}\boldsymbol{i} + \frac{x_f - x_s}{2r^2}\boldsymbol{j} \right) = \frac{2(x_f - x_s)^2 - r^2}{r^4}\boldsymbol{k}$$

$$\nabla_s \times \left(-\frac{x_f - x_s}{2r^2}\boldsymbol{i} + \frac{y_f - y_s}{2r^2}\boldsymbol{j} \right) = \frac{2(x_f - x_s)(y_f - y_s)}{r^4}\boldsymbol{k}$$

$$\nabla_s \times \left(-\frac{y_f - y_s}{2r^2}\boldsymbol{i} - \frac{x_f - x_s}{2r^2}\boldsymbol{j} \right) = \frac{2(y_f - y_s)^2 - r^2}{r^4}\boldsymbol{k}$$

$$\iint_{A_0} \frac{2(x_f - x_s)^2 - r^2}{r^4}\mathrm{d}A = 0$$

$$\iint_{A_0} \frac{(x_f - x_s)(y_f - y_s)}{r^4}\mathrm{d}A = 0$$

$$\iint_{A_0} \frac{2(y_f - y_s)^2 - r^2}{r^4}\mathrm{d}A = 0$$

$$C_{xx} = \frac{1}{2\pi}\iint_{A_s} \frac{2(x_f - x_s)^2 - r^2}{r^4}\mathrm{d}A =$$

$$= \frac{1}{2\pi}\iint_{A_s - A_0} \frac{2(x_f - x_s)^2 - r^2}{r^4}\mathrm{d}A + \frac{1}{2\pi}\iint_{A_0} \frac{2(x_f - x_s)^2 - r^2}{r^4}\mathrm{d}A =$$

$$= \frac{1}{4\pi}\oint_{\Gamma_s} \frac{(y_f - y_s)\boldsymbol{i} + (x_f - x_s)\boldsymbol{j}}{r^2}\mathrm{d}\boldsymbol{l} - \frac{1}{4\pi}\oint_{\Gamma_0} \frac{(y_f - y_s)\boldsymbol{i} + (x_f - x_s)\boldsymbol{j}}{r^2}\mathrm{d}\boldsymbol{l} =$$

$$= \frac{1}{4\pi}\oint_{\Gamma_s} \frac{(y_f - y_s)\boldsymbol{i} + (x_f - x_s)\boldsymbol{j}}{r^2}\mathrm{d}\boldsymbol{l} - \frac{1}{2}$$

Magnetic field computation

$$C_{xx} = \begin{cases} -\dfrac{1}{2} + \dfrac{1}{4\pi} \displaystyle\oint_{\Gamma_s} \dfrac{(y_f - y_s)\boldsymbol{i} + (x_f - x_s)\boldsymbol{j}}{r^2} \mathrm{d}\boldsymbol{l} \text{ if } (x_f, y_f) \in A_s \\ \dfrac{1}{4\pi} \displaystyle\oint_{\Gamma_s} \dfrac{(y_f - y_s)\boldsymbol{i} + (x_f - x_s)\boldsymbol{j}}{r^2} \mathrm{d}\boldsymbol{l} \text{ if } (x_f, y_f) \notin A_s \end{cases}$$

$$C_{xy} = C_{yx} = \frac{1}{4\pi} \oint_{\Gamma_s} \frac{-(x_f - x_s)\boldsymbol{i} + (y_f - y_s)\boldsymbol{j}}{r^2} \mathrm{d}\boldsymbol{l}$$

$$C_{yy} = \begin{cases} -1 - C_{xx} & \text{if } (x_f, y_f) \in A_s \\ -C_{xx} & \text{if } (x_f, y_f) \notin A_s \end{cases}$$

Magnetic field computation

$$\boldsymbol{H}_k = \boldsymbol{H}_0(i) + \sum_{l=1}^{N} [\mathbf{C}_{kl}] \boldsymbol{M}_l$$

$$k = 1,\ldots,N$$

$$\mu_0 \tilde{\boldsymbol{M}} = \frac{\boldsymbol{H}}{H} \sum_{k=1}^{n} m_k \tan^{-1}(a_k H)$$

Error minimization

$$\varepsilon = \sum_{k=1}^{N} \left| \boldsymbol{M}_k - \tilde{\boldsymbol{M}}_k \right|^2 \rightarrow \min$$

Contraction iteration

$$\boldsymbol{M}_k^{i+1} = \tau \boldsymbol{M}_k^i + (1-\tau) \tilde{\boldsymbol{M}}_k^i \quad ; \quad 0 < \tau << 1$$

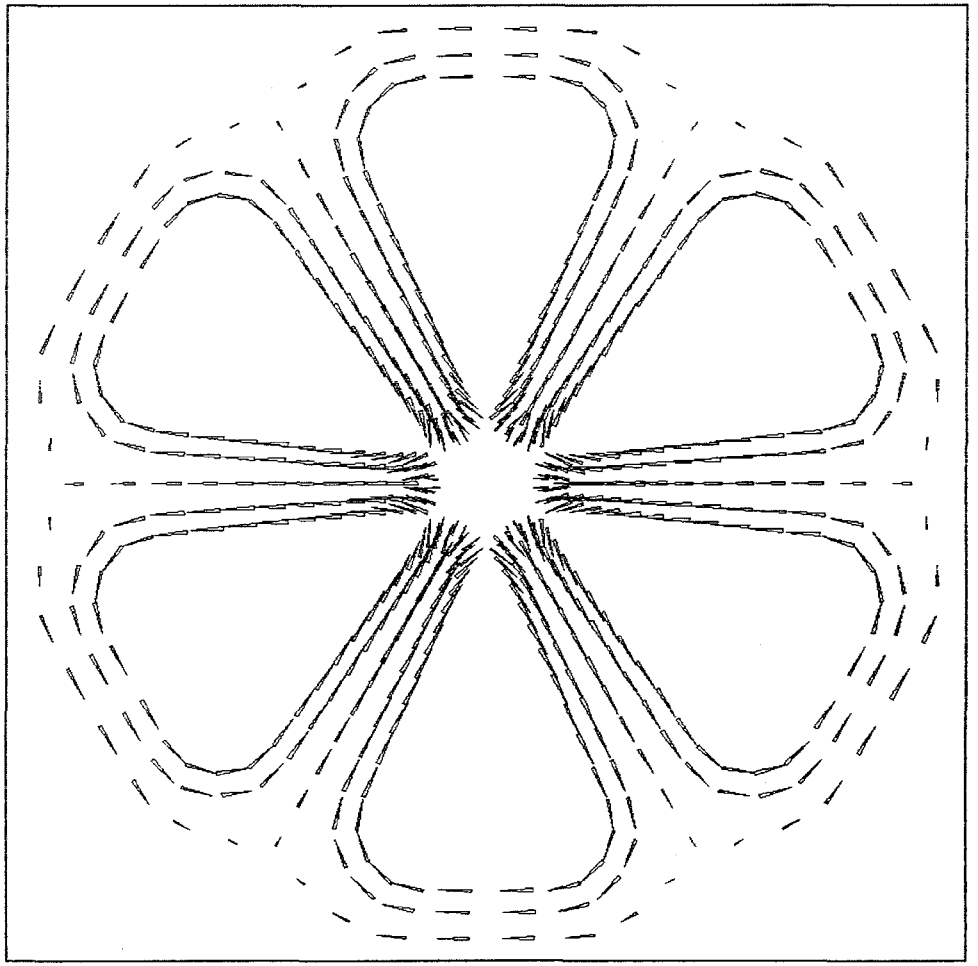

Magnetization vectors of surface elements

Results of the magnetic field computation

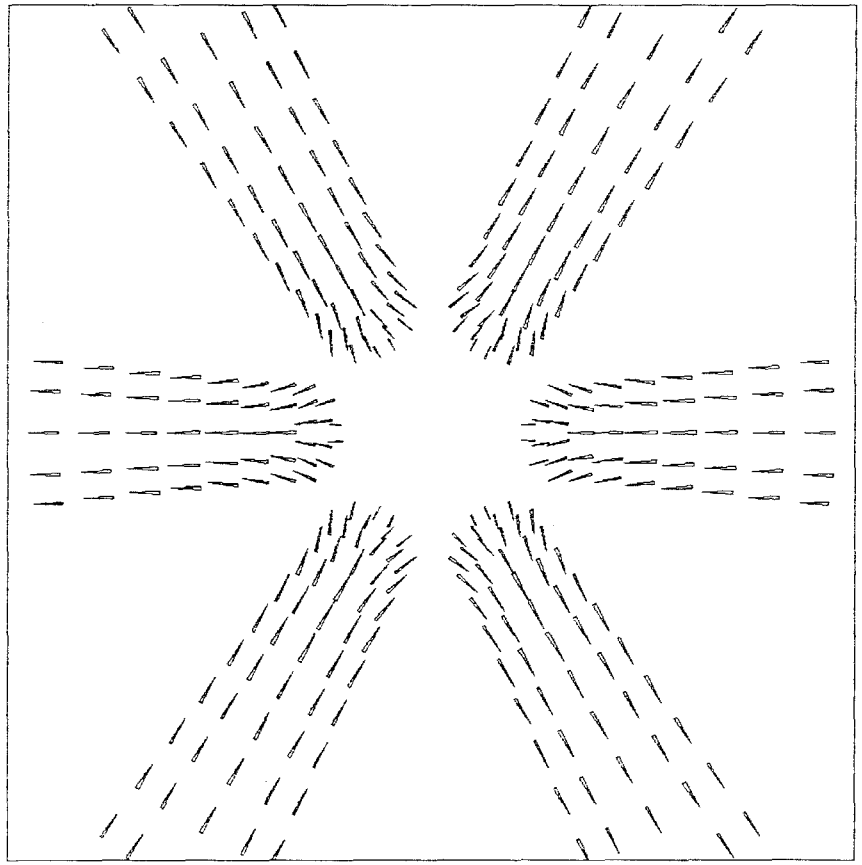

Magnetization vectors of surface elements in the vicinity of the aperture

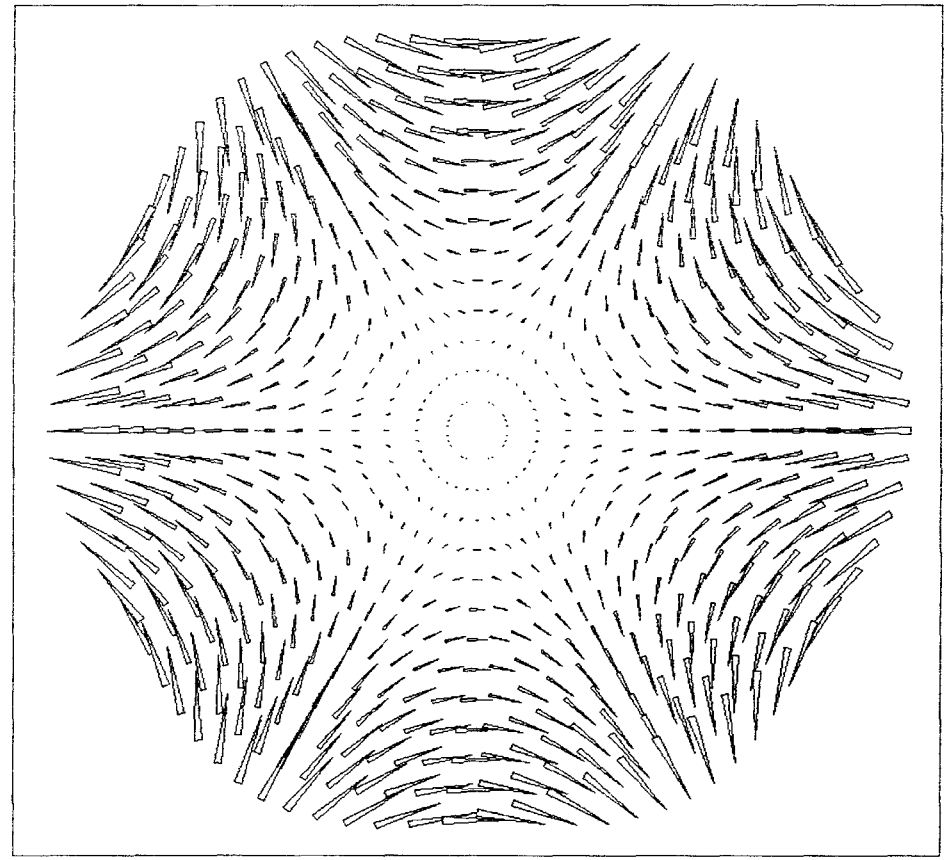

Magnetic flux density vectors in the aperture

Measurement results

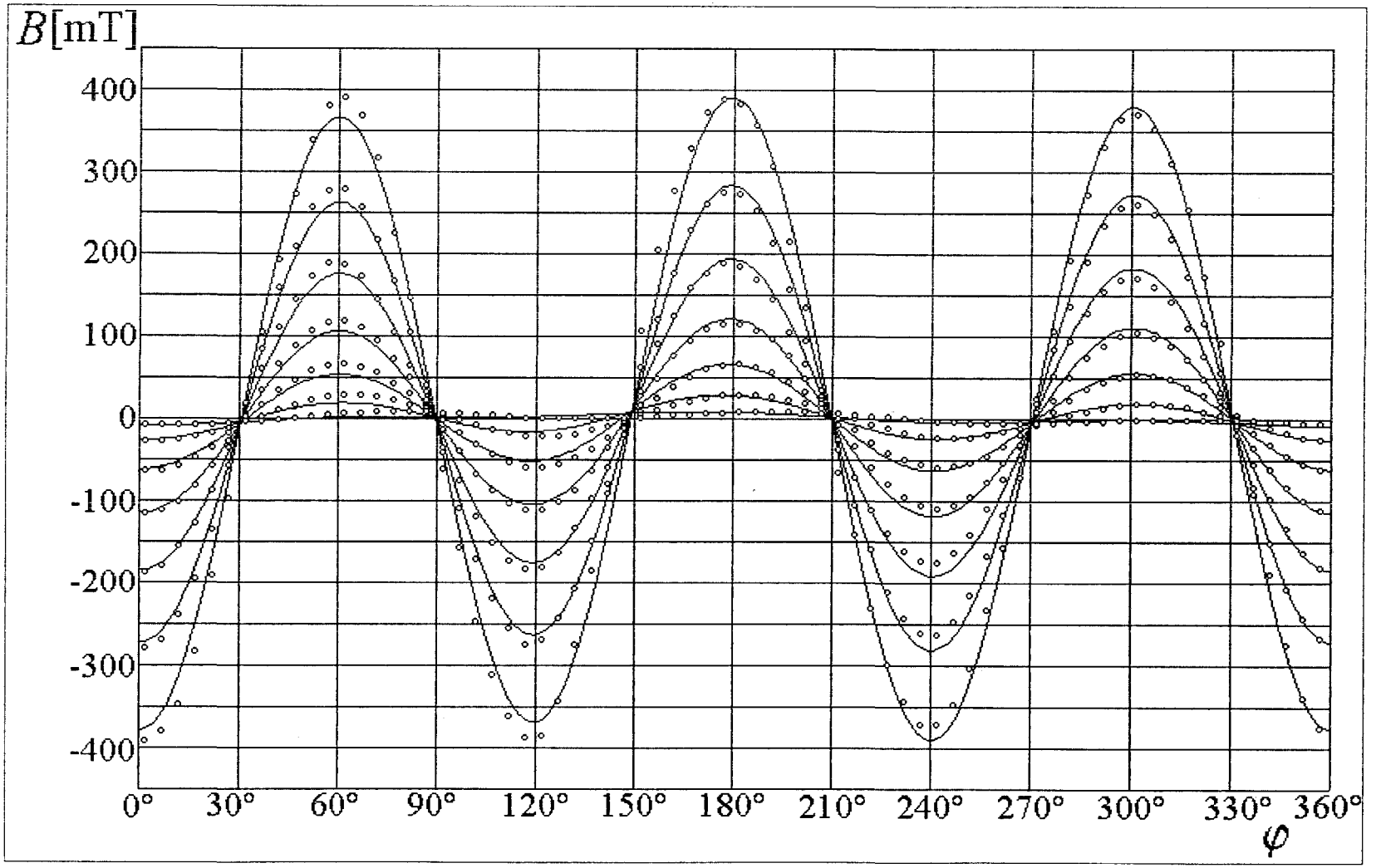

Measurement results

$$\boldsymbol{B} = \left[C_1 \cos(\varphi - \varphi_1) - C_3 r^2 \cos 3(\varphi - \varphi_3)\right]\boldsymbol{e}_r + \left[-C_1 \sin(\varphi - \varphi_1) + C_3 r^2 \sin 3(\varphi - \varphi_3)\right]\boldsymbol{e}_\varphi$$

$C_1 = B_1 = 5.8$ mT $\quad \varphi_1 = 120°$

$C_3 = B_3 / r_p^{\,2} = 34810$ T/m^2 $\quad \varphi_3 = 0$

$r_p = 5.5$ mm

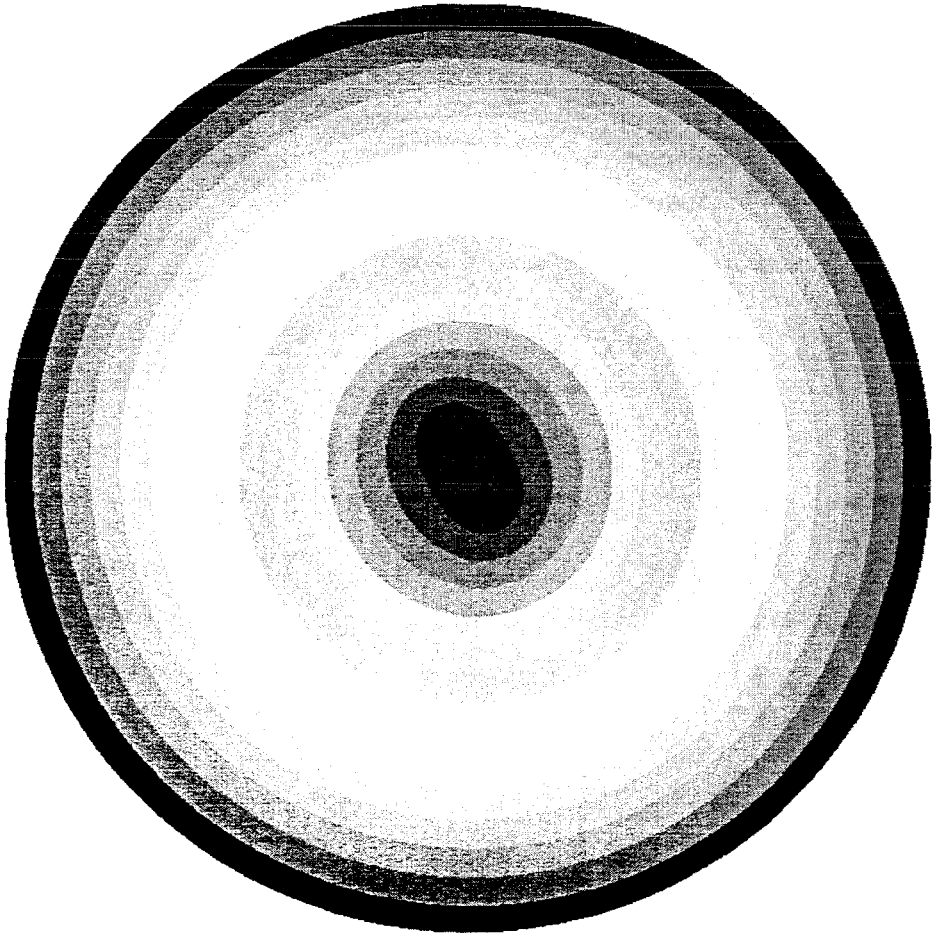

Contour plot of magnetic flux density magnitude in the aperture (parabolic scale, 5 mm radius plotted).

Neutron optical simulation

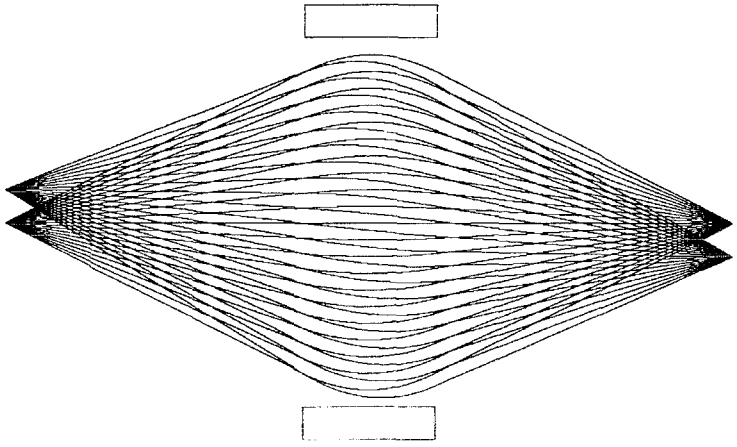

Panim.exe

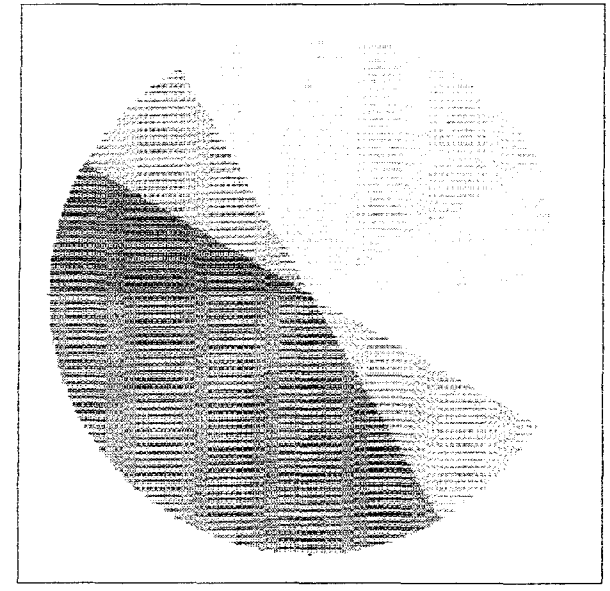

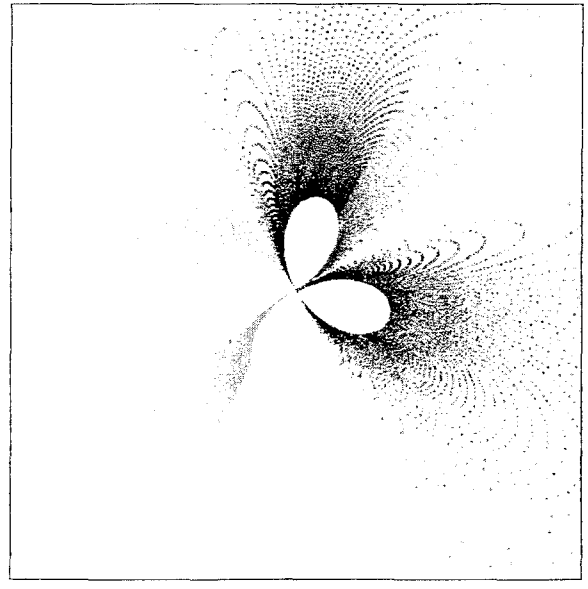

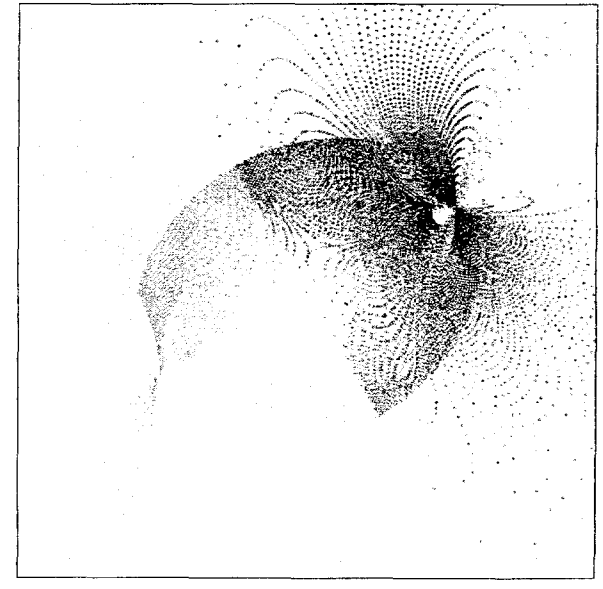

Permanent magnet neutron lens

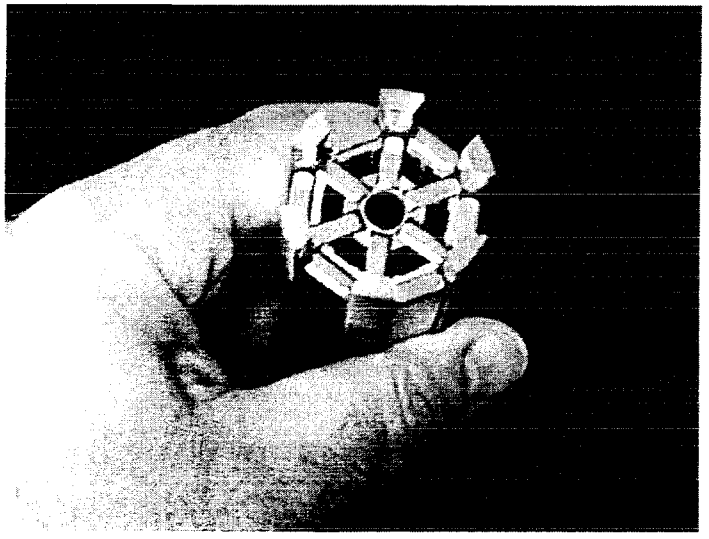

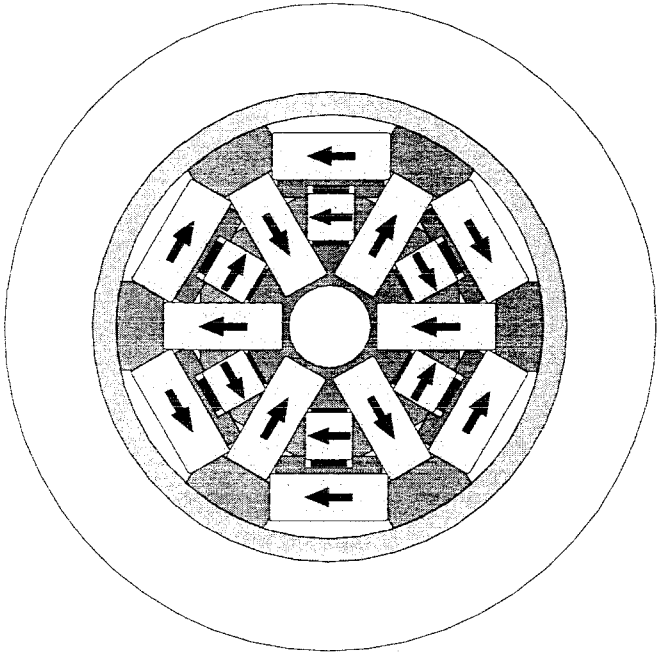

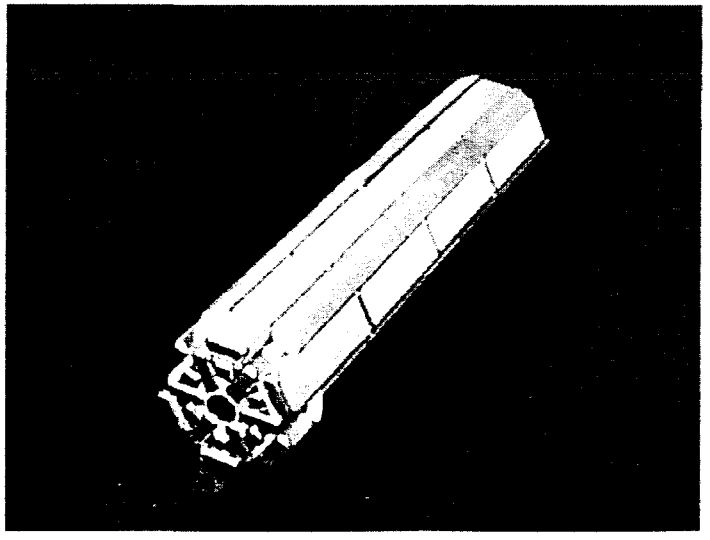

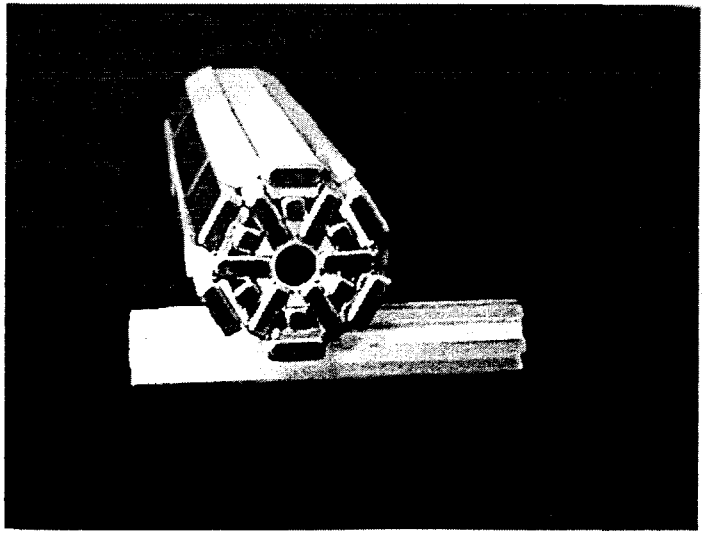

Permanent magnet neutron lens

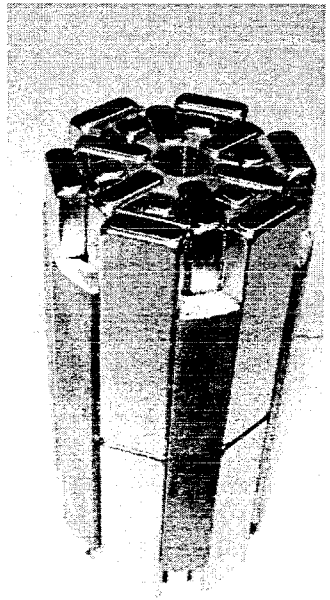

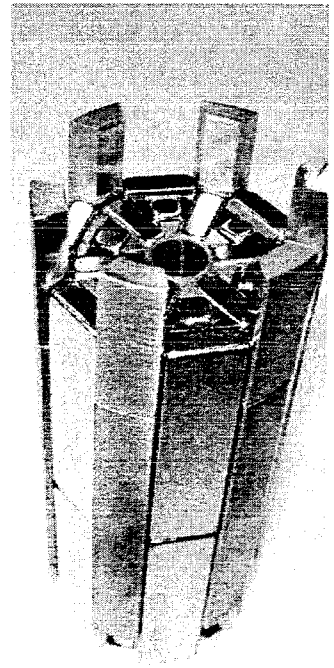

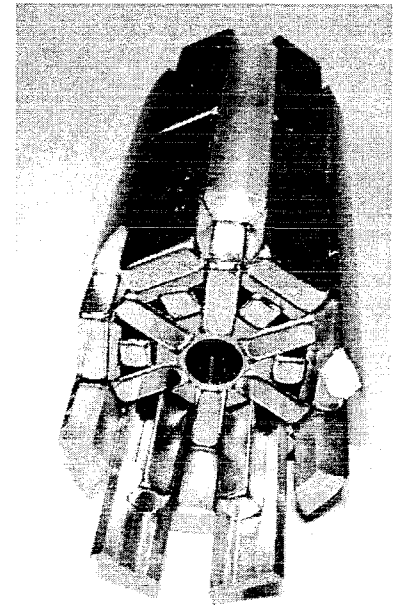

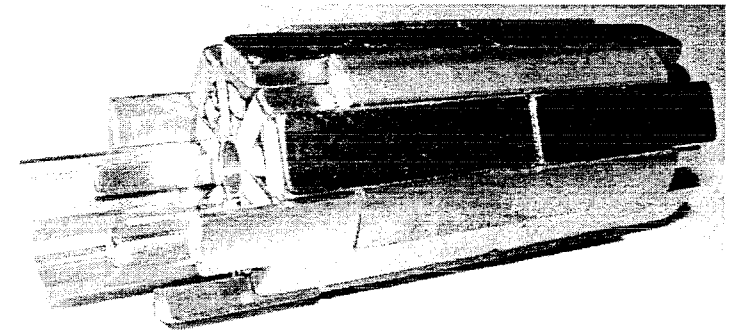

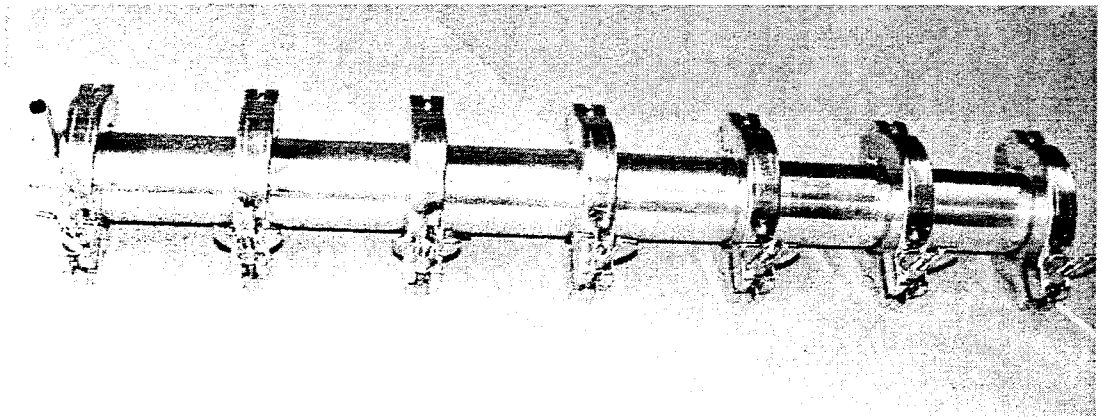

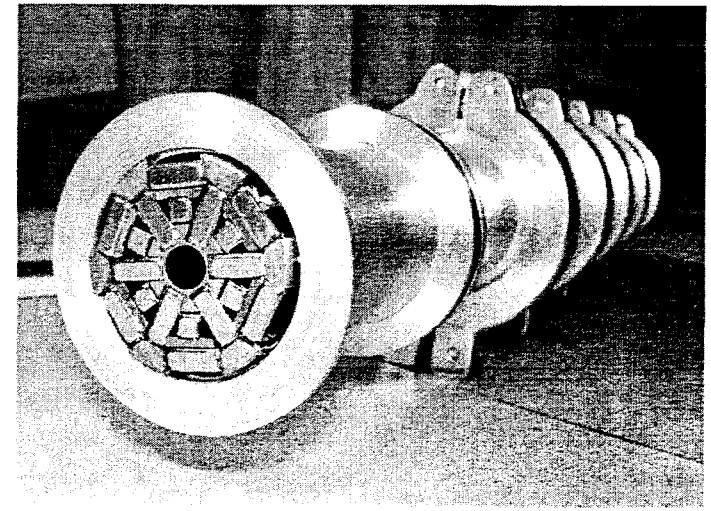

Beam divergence: 15'
Wavelength: 6 Å
Magnet length: 900 mm
Hexapole field constant: 40 000 T/m^2
Dipole field: 20 mT (same orientation in each segment)

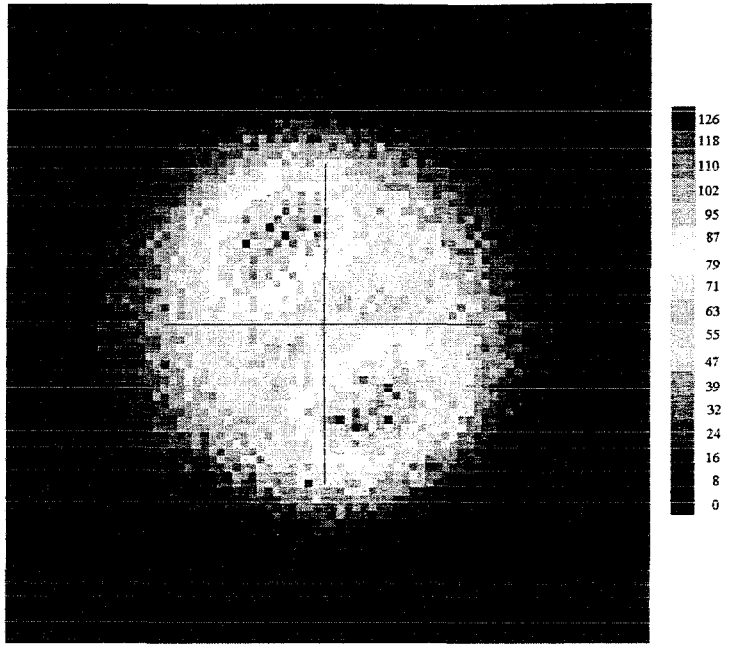

Pkollmag1

Pkollhex2

Pkolliquad2

1120 mm

Pkollmag2

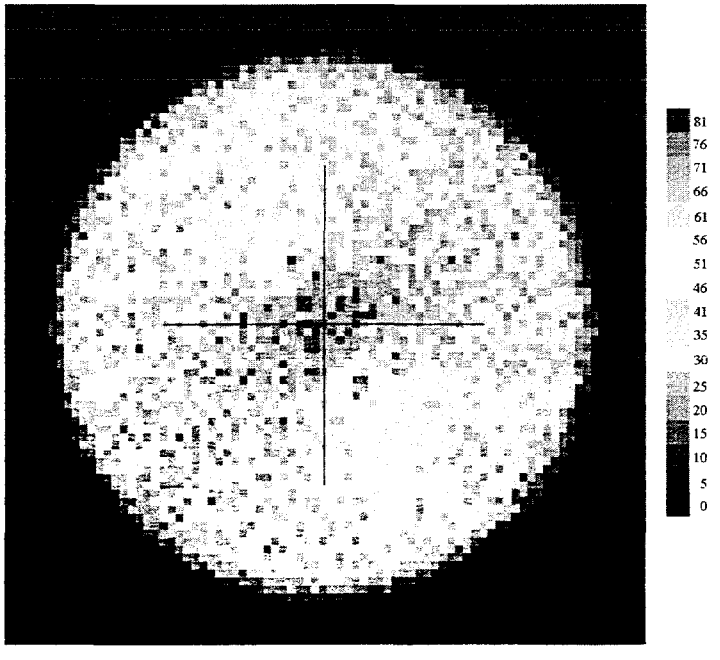

At magnet exit

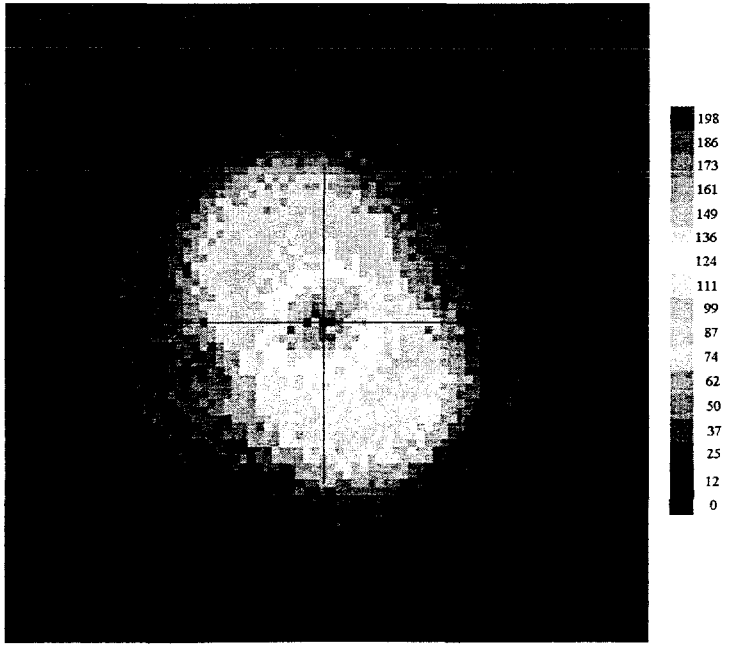

1810 mm (focal plane)

Beam divergence: 15'
Wavelength: 6 Å
Magnet length: 900 mm
Hexapole field constant: 40 000 T/m^2
Dipole field: 20 mT (different orientation in different segments)

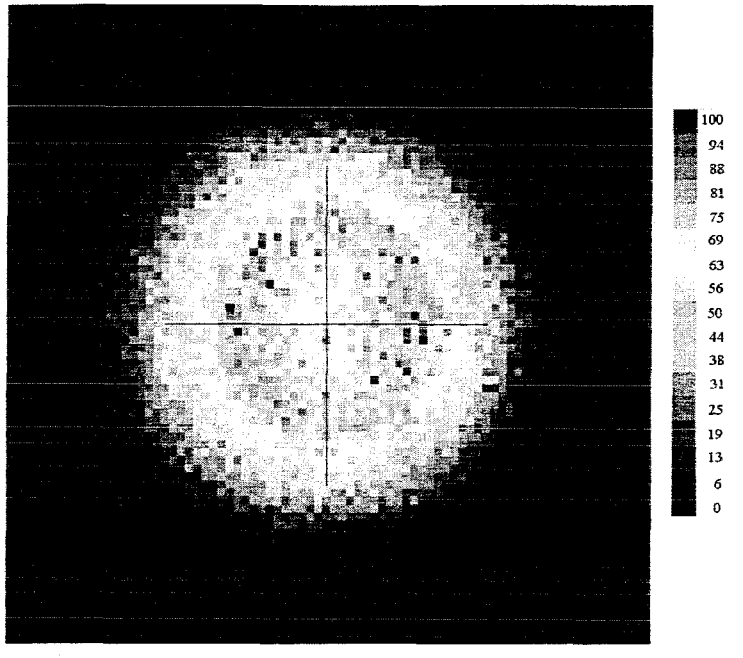

Pkollmag4

Pkollhex3

1120 mm

Pkollmag3

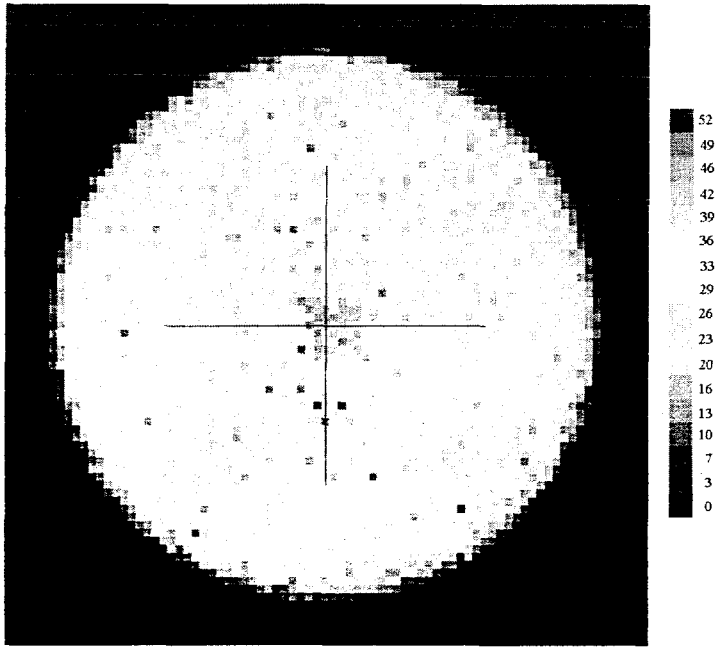

Mágnes végén

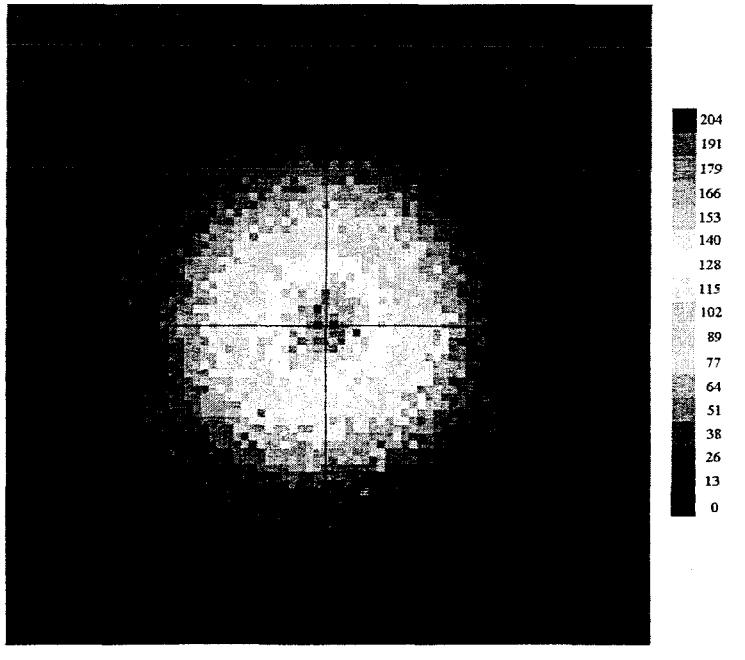

1810 mm
(fókuszsík)

First beam experiment

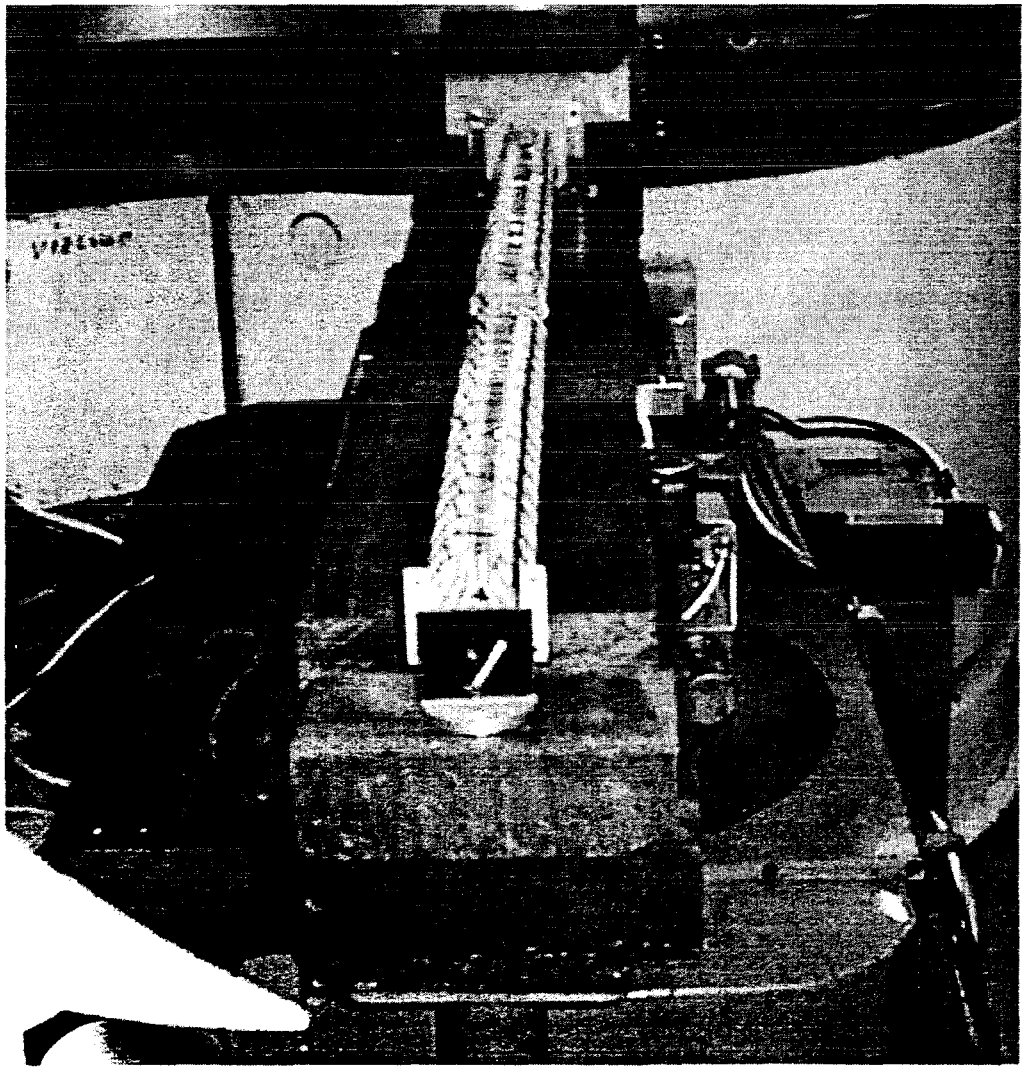

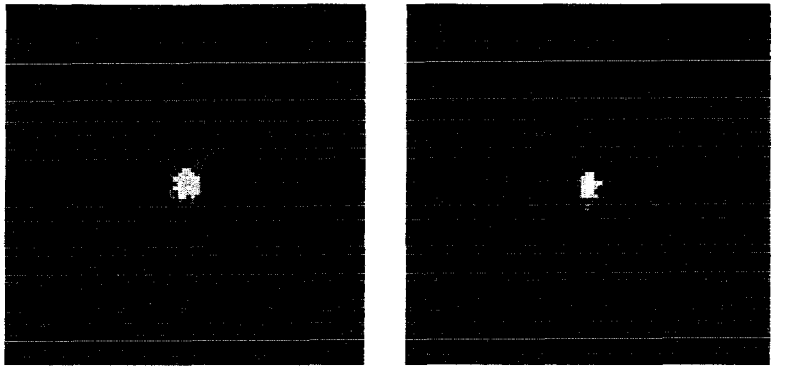

one lens two lenses
330 cm from magnet end

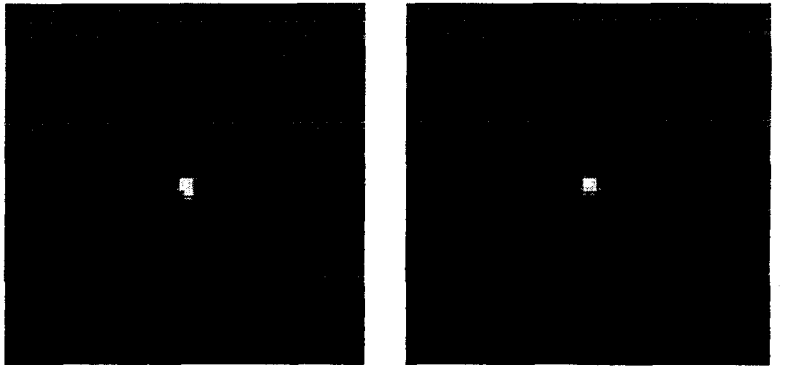

one lens two lenses
120 cm from magnet end

Permanent magnet ^{3}He spin state separators

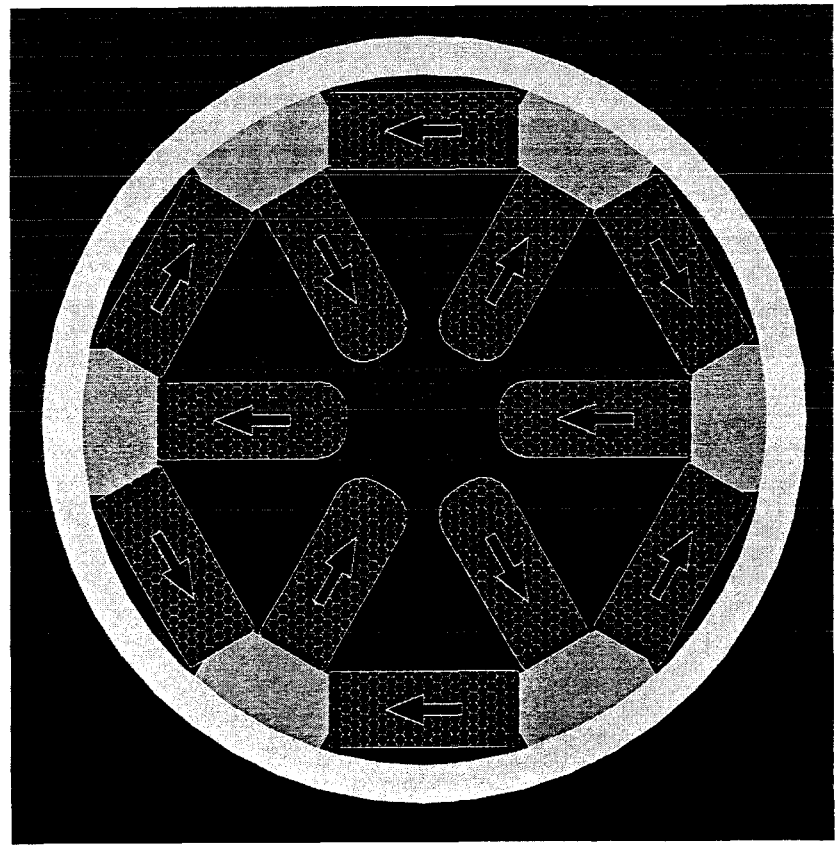

Quadrupole

Hexapole1

Hexapole2

Conclusions

Hexapole magnets are efficient tools both for neutron beam focusing and ^{3}He spin state separation. From all possible inaccuracies, the most disturbing is the presence of a dipole component (it affects the neutron optical characteristics and causes spin flips and reduces the efficiency of spin state separators).

Hexapole ^{3}He spin state separators can be more efficient than quadrupole ones. The performance of the latter can be significantly improved by the use of a thin axial rod which hinders the crossing of the low field area where spin flips occur.

Since the very low temperature is given, it would be worth considering the use of superconducting hexapole electromagnets.

Issues to be adressed:

- permanent magnet characteristics at very low temperature;
- optimal permanent magnet hexapole design to allow exit of atoms in the wrong spin state;
- measures to minimize the dipolar field component to avoid unwanted spin flips.

Thank you for your attention

Experiments relavent to transporting 3He into the superfluid He and the 3He polarization lifetime

Mike Hayden (Simon-Fraser)

Issues relevant to getting the ^{3}He into the liquid, moving it about, and keeping it polarized ...

Mike Hayden
Simon Fraser University

Outline:

- source of polarized ^{3}He?
- liquid-vapour exchange
- motion of ^{3}He within the liquid
- wall relaxation
- experiments

Polarized Atomic Beam Source

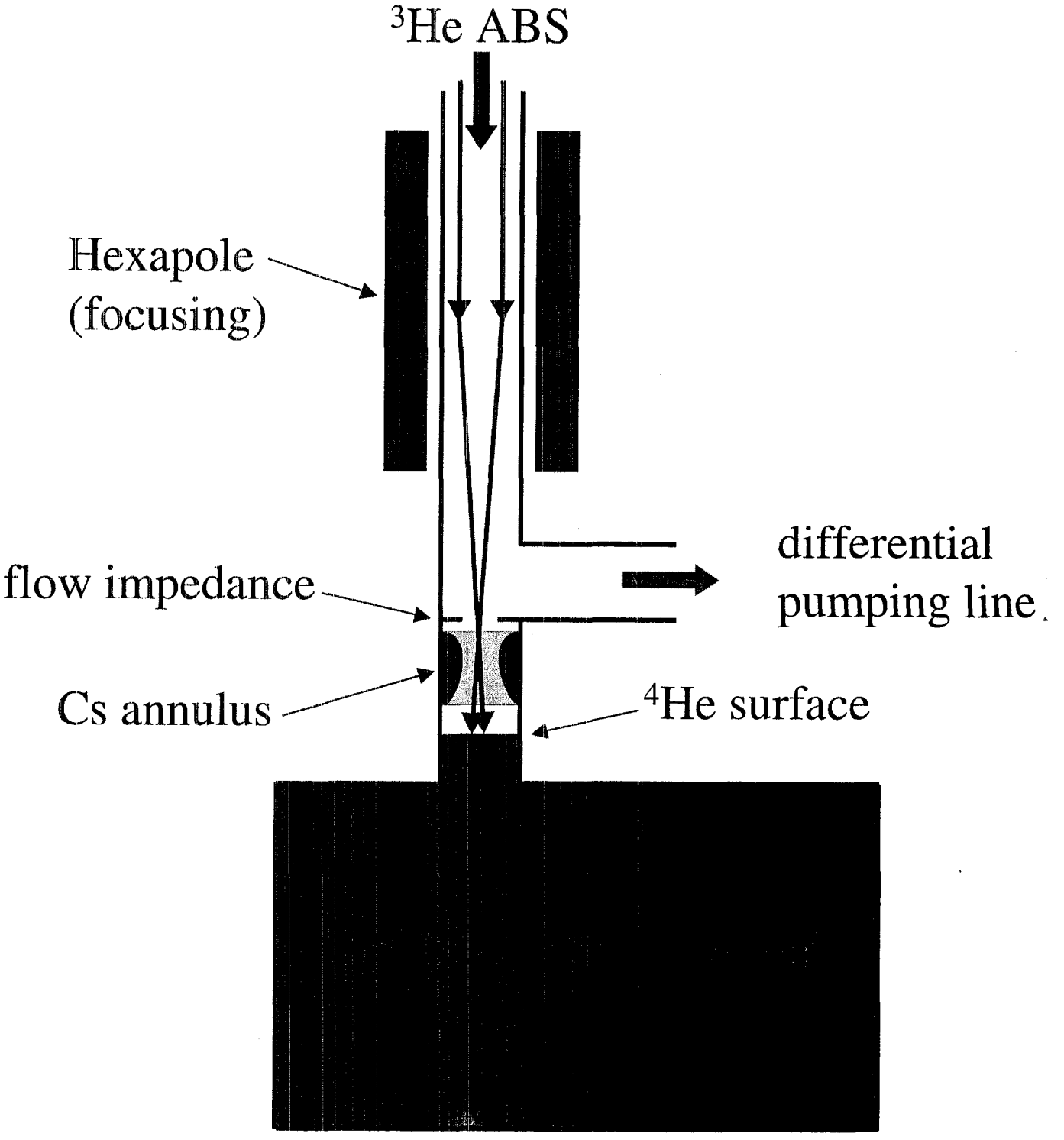

Apparatus for Production of High Nuclear Polarization in Liquid ^3He-^4He Mixtures

Phys. Rev. Lett. **73**, 2587 (1994)

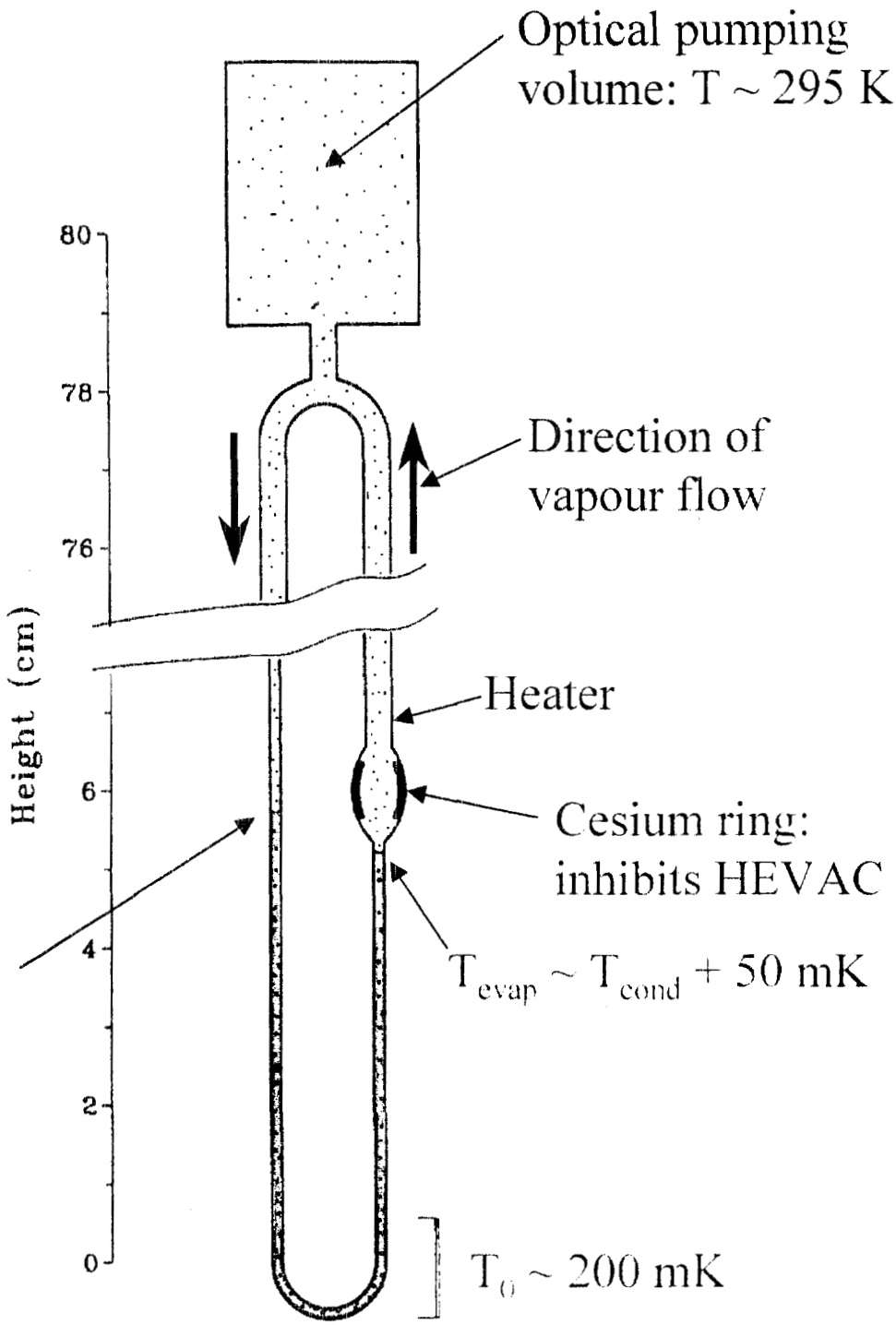

HEVAC Effect

JLTP **97** 417, 1994
Physica B **194-6** 677, 1994

(Helium Vapour Compression)

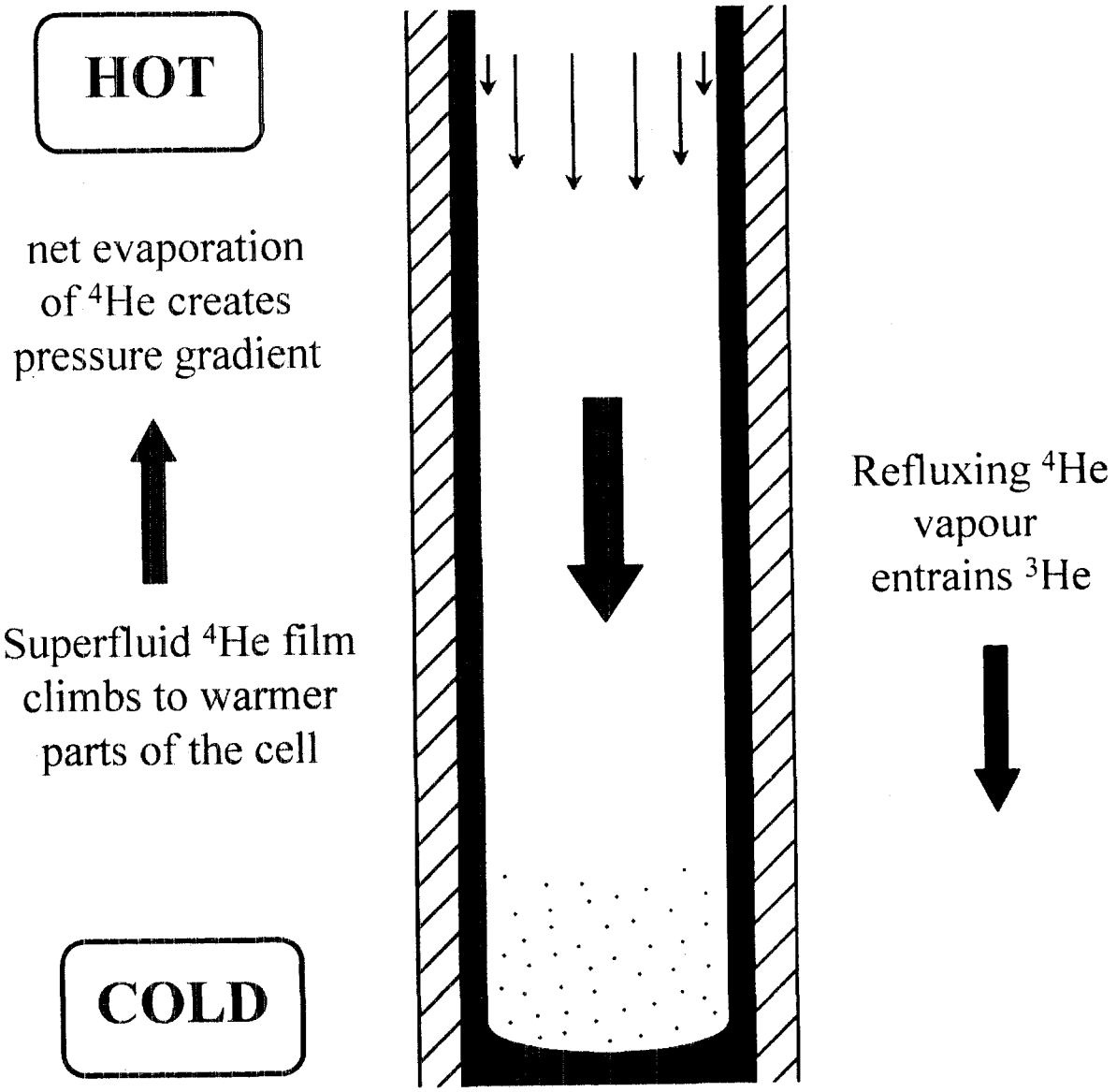

^{3}He Evaporation Rate

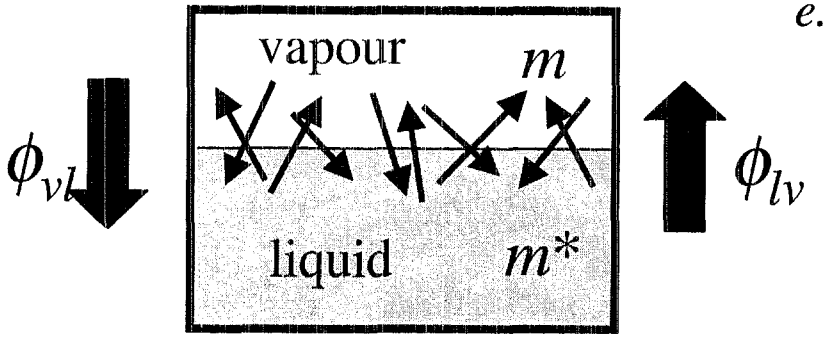

e.g. JLTP **99,** 787 (1995) and *JLTP* **84,** 87 (1991)

$$\dot{n}^* = -\frac{A\phi_{lv}}{V}$$

$$\phi_{lv} = \frac{1}{4} n^* \bar{v} \sqrt{\frac{m}{m^*}} \alpha_{lv}$$

$$\phi_{lv} = \frac{1}{4} n \bar{v} \alpha_{vl}$$

$$\Lambda = \sqrt{\frac{2\pi\hbar^2}{mkT}}$$

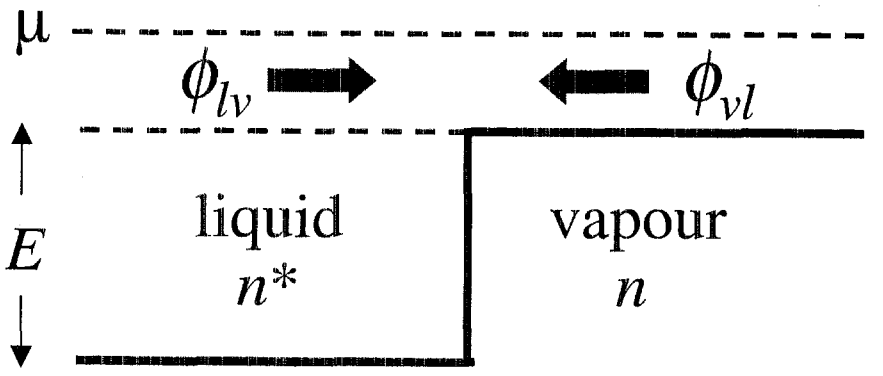

$$\text{require} \begin{cases} \phi_{lv} = \phi_{vl} \\ kT\ln\left[n\Lambda^3\right] = kT\ln\left[n^*\left(\frac{m}{m^*}\right)^{\frac{3}{2}}\Lambda^3\right] - E \end{cases}$$

$$\text{leads to} \begin{cases} \alpha_{lv} = \alpha_{vl}\frac{m}{m^*}\exp\left(\frac{-E}{kT}\right) \\ n = n^*\left(\frac{m^*}{m}\right)^{-\frac{3}{2}}\exp\left(\frac{-E}{kT}\right) \end{cases}$$

time constant

$$\tau = \frac{4V}{A\bar{v}\alpha_{vl}}\left(\frac{m^*}{m}\right)^{\frac{3}{2}}\exp\left(\frac{E}{kT}\right)$$

Reflection Coefficients

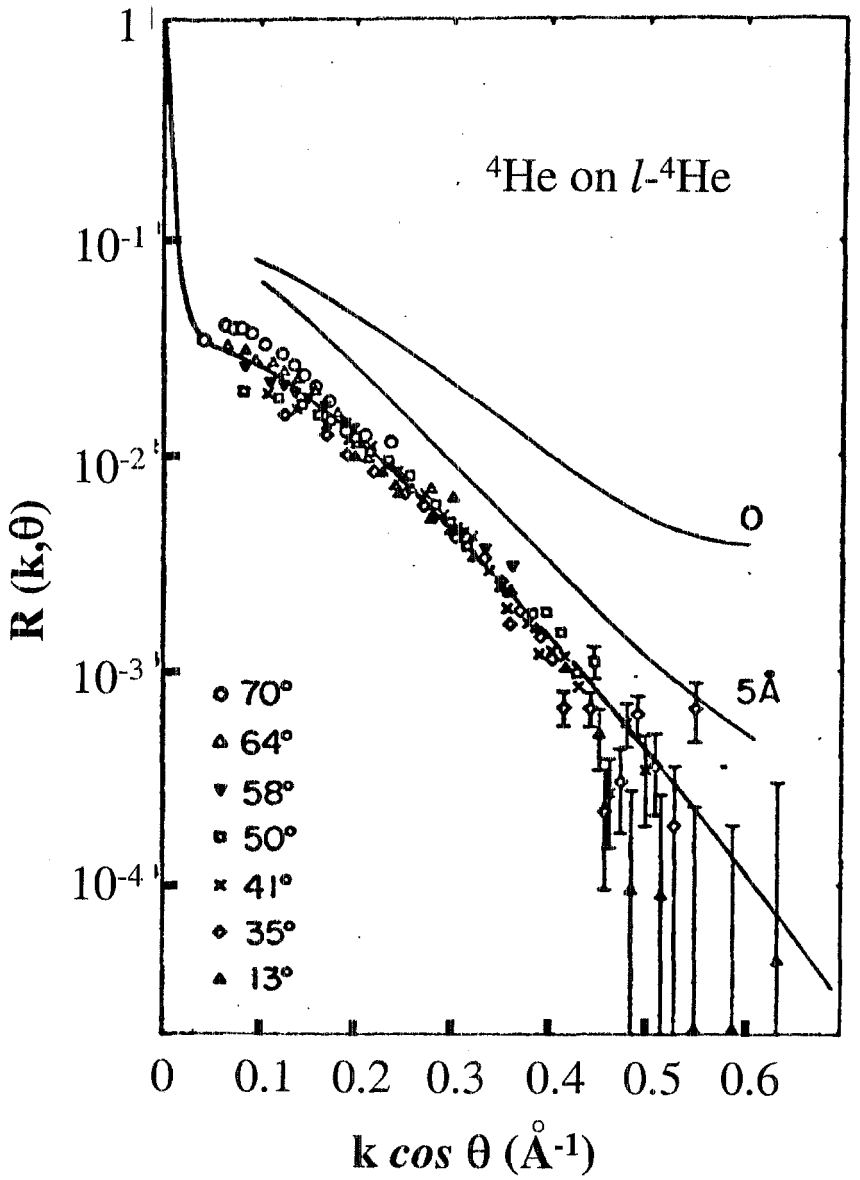

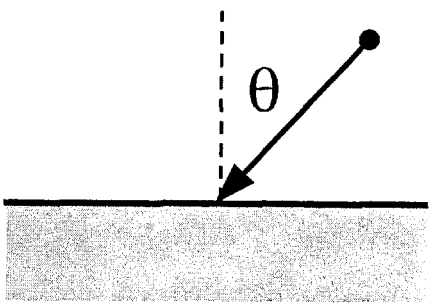

For ^{3}He:

$$\Lambda \sim \frac{1\ \text{nm}\cdot\text{K}^{1/2}}{\text{T}^{1/2}}$$

$$k \cos\theta \sim (0.6\ \text{Å/K}^{1/2})\ \text{T}^{1/2}$$

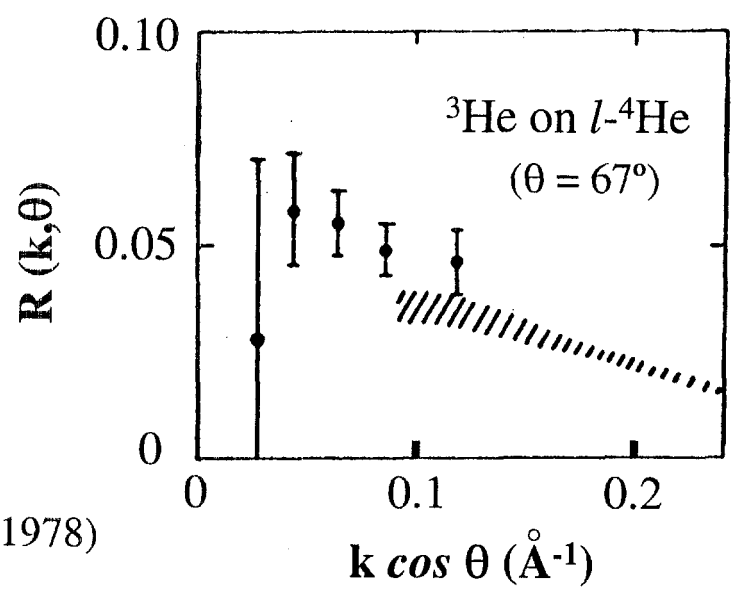

See Edwards and Saam,
Prog. Low. Temp. Phys. VIIA,
D.F. Brewer ed, North-Holland (1978)

Saturated Vapour Pressure of l-^{4}He

e.g. Rusby and Durieux, Cryogenics **24**, 363 (1984)

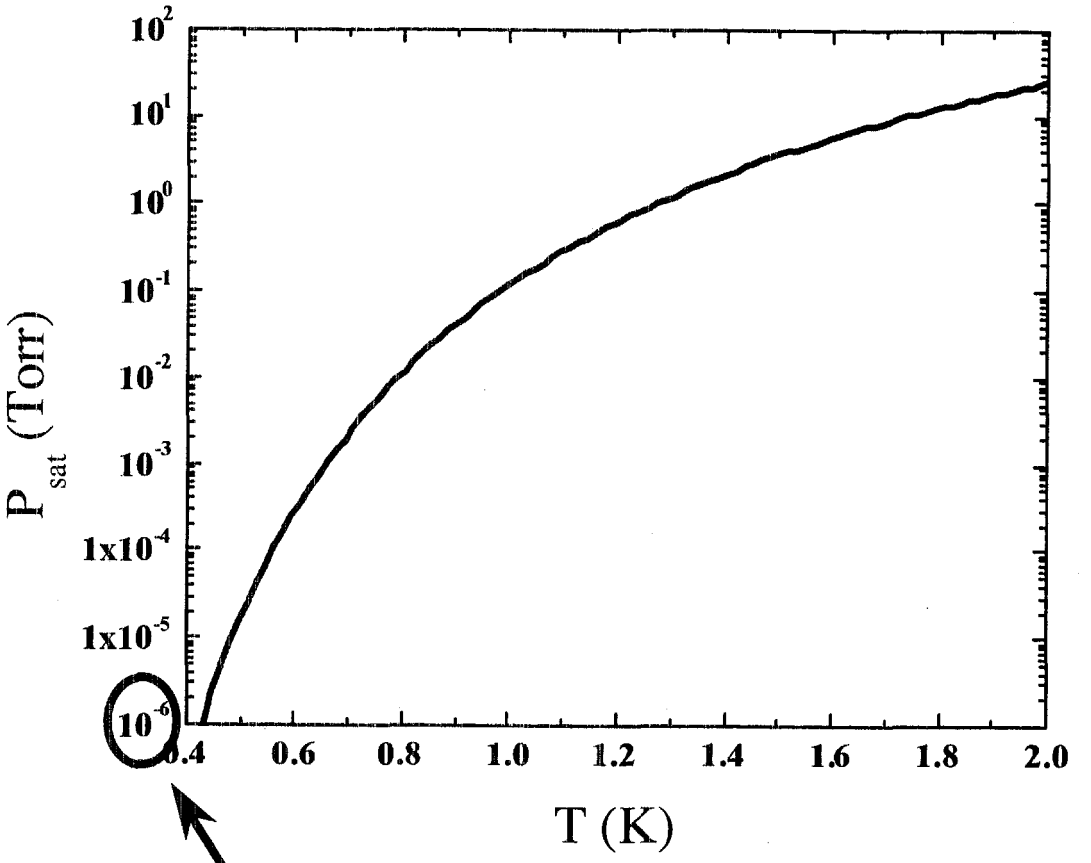

design goal for pressure
in magnet region of ABS!

^{3}He 'Escape' Rate

$$\tau = \frac{4V}{A\bar{v}\alpha_{vl}}\left(\frac{m^*}{m}\right)^{\frac{3}{2}} \exp\left(\frac{E}{kT}\right)$$

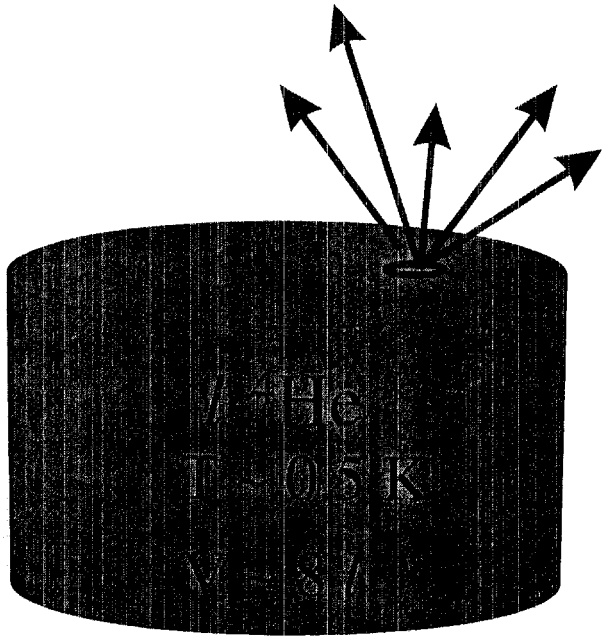

(internal diffusion fast)

$E_s \sim 2.8$ K

$\frac{m_3{}^*}{m_3} \sim 2.4$

$\alpha_{vl} \sim 1$

$\bar{v}_3 = (83.8\text{m/s})\sqrt{\frac{T}{1K}}$

(in vapour)

a 1cm ϕ hole gives $\tau \sim 2$ h at 0.5K

...but a 30cm ϕ free surface gives an exchange time $\tau \sim 10$ s!

T_1 Relaxation: Influence of Diffusion

c.f. Schearer and Walters *Phys. Rev.* **139** A1398 (1965).

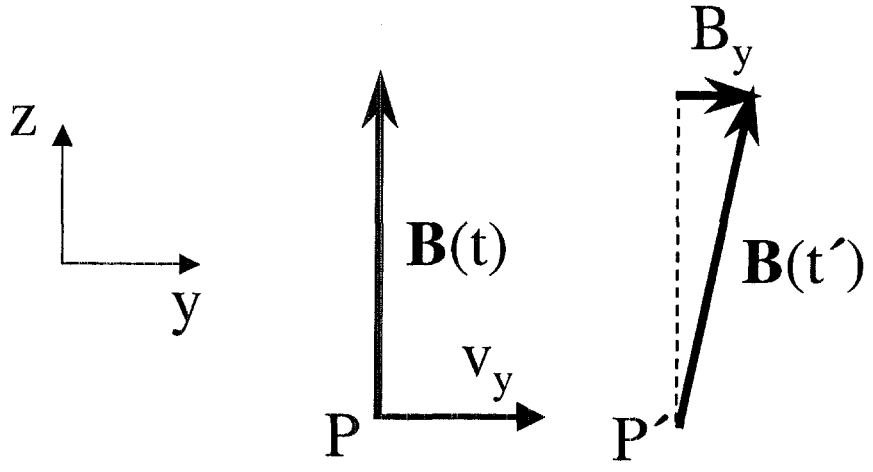

^{3}He atoms see a fluctuating magnetic field as they undergo Brownian motion in the presence of a field gradient

As long as their mfp << container dimensions …

$$\frac{1}{T_1} = \frac{2}{3}\left(\frac{G}{B}\right)^2 \langle v^2 \rangle \frac{\tau_c}{1+\omega_0{}^2\tau_c{}^2}$$

mean time between collisions

$$D = \frac{\langle v^2 \rangle \tau_c}{3}$$

mean-squared velocity

or

$$\frac{1}{T_1} = 2D\left(\frac{G}{B}\right)^2 \left[1+\left(\frac{3\gamma BD}{\langle v^2 \rangle}\right)^2\right]^{-1}$$

… T_1 depends on the *relative* field gradient

Diffusion Coefficients

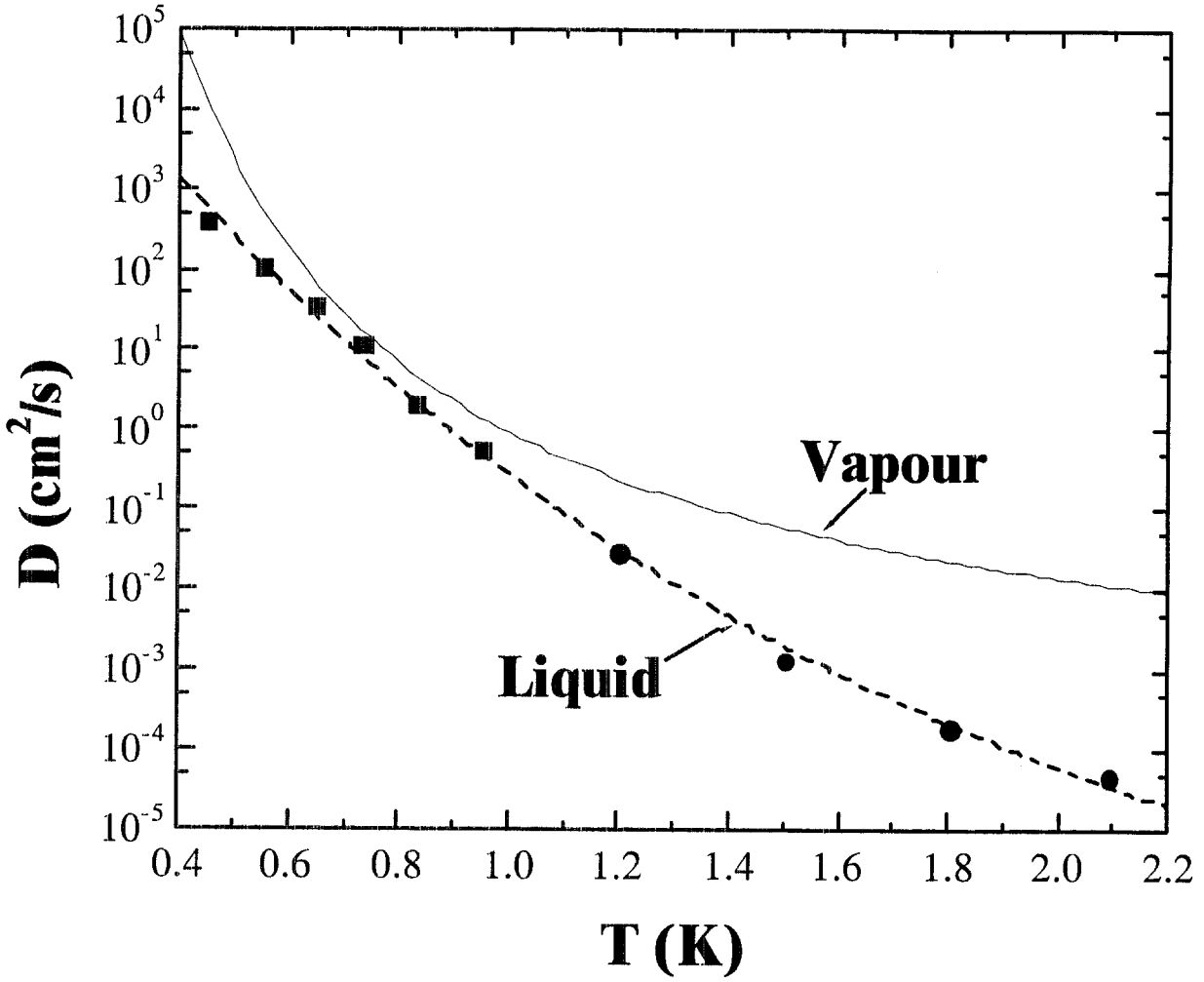

Liquid: Lamoreaux et al. EPL **58**, 718 (2002).
Beenaker et al. Physica **18**, 433 (1952).

Vapour: $D_{34} = 1.463 \times 10^{-3} \dfrac{T^{1.65}}{P}$ (MKS units)

- see *JLTP* **97**, 417 (1994).

Expect maximum sensitivity to
relative fluctuations in **B** near T=0.6 K

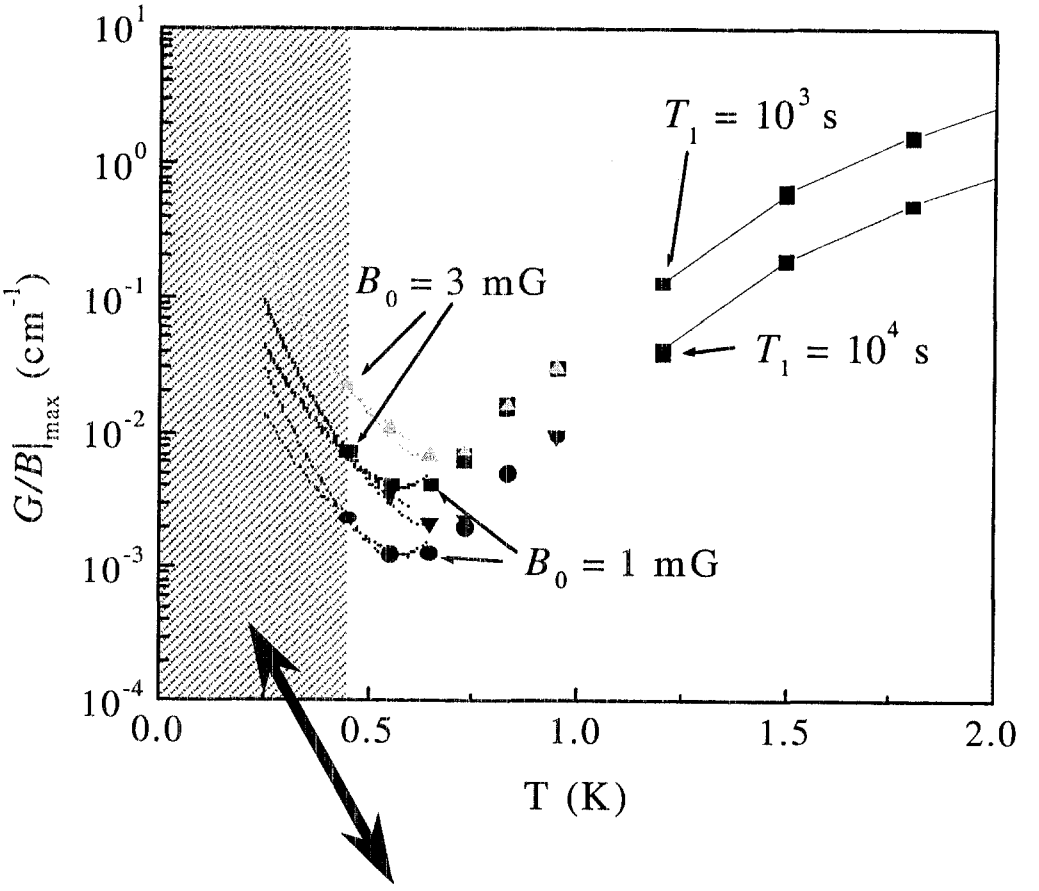

Absolute field gradients become important
when mfp > container dimensions

$$\frac{1}{T_1} \sim \frac{1}{2} \frac{\gamma G^2 L^3 / < v >}{1 + \left(\frac{\gamma BL}{2 < v >} \right)^4}$$

c.f. Kleppner *et al. Phys. Rev.* **126**, 603 (1962).

This regime is not as well understood …
… rough estimate gives $G_{max} \sim 1$ μG/cm
for $T_1 \sim 10^5$ s and T ~ 0.4 K

Maximum Permissible Gradients in $\boldsymbol{B}$ are limited by relaxation rate $1/T_2$

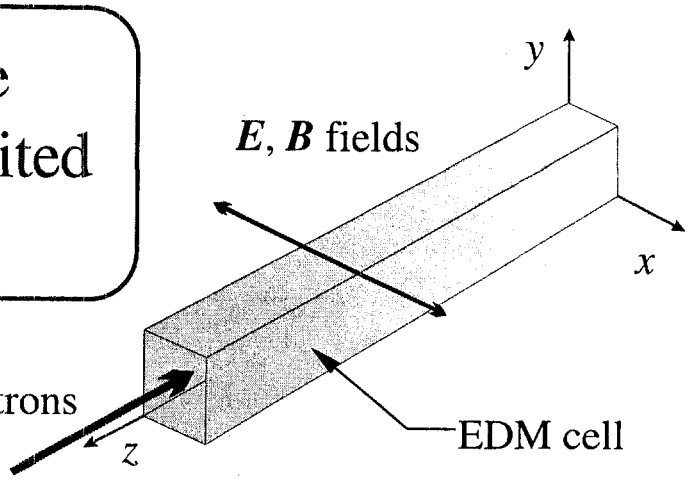

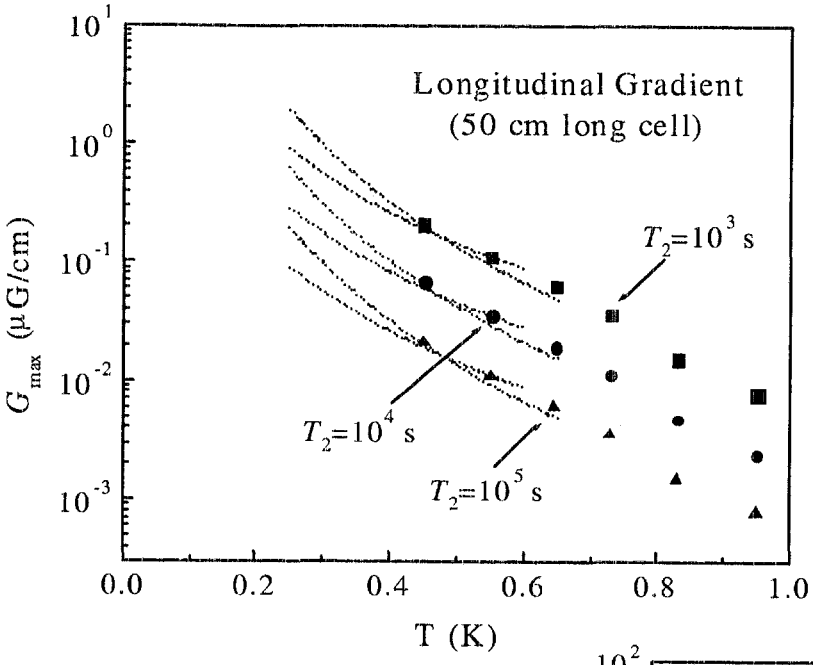

$$\frac{1}{T_2} = \frac{\gamma^2 J_0^{\,2}(x_c) G^2 L^4}{120 D}$$

critical dressing parameter

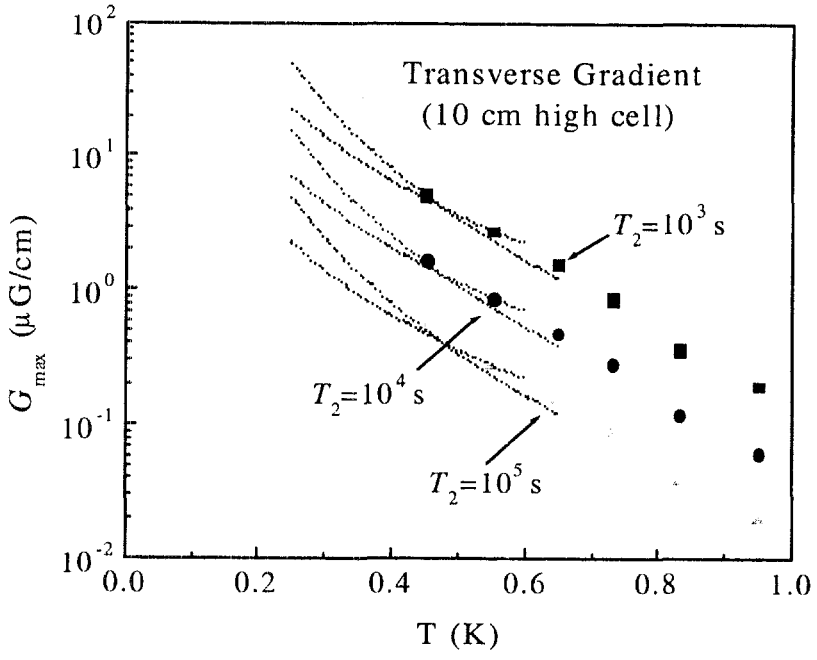

Data and extrapolations are derived from recent measurements of D

Wall Relaxation

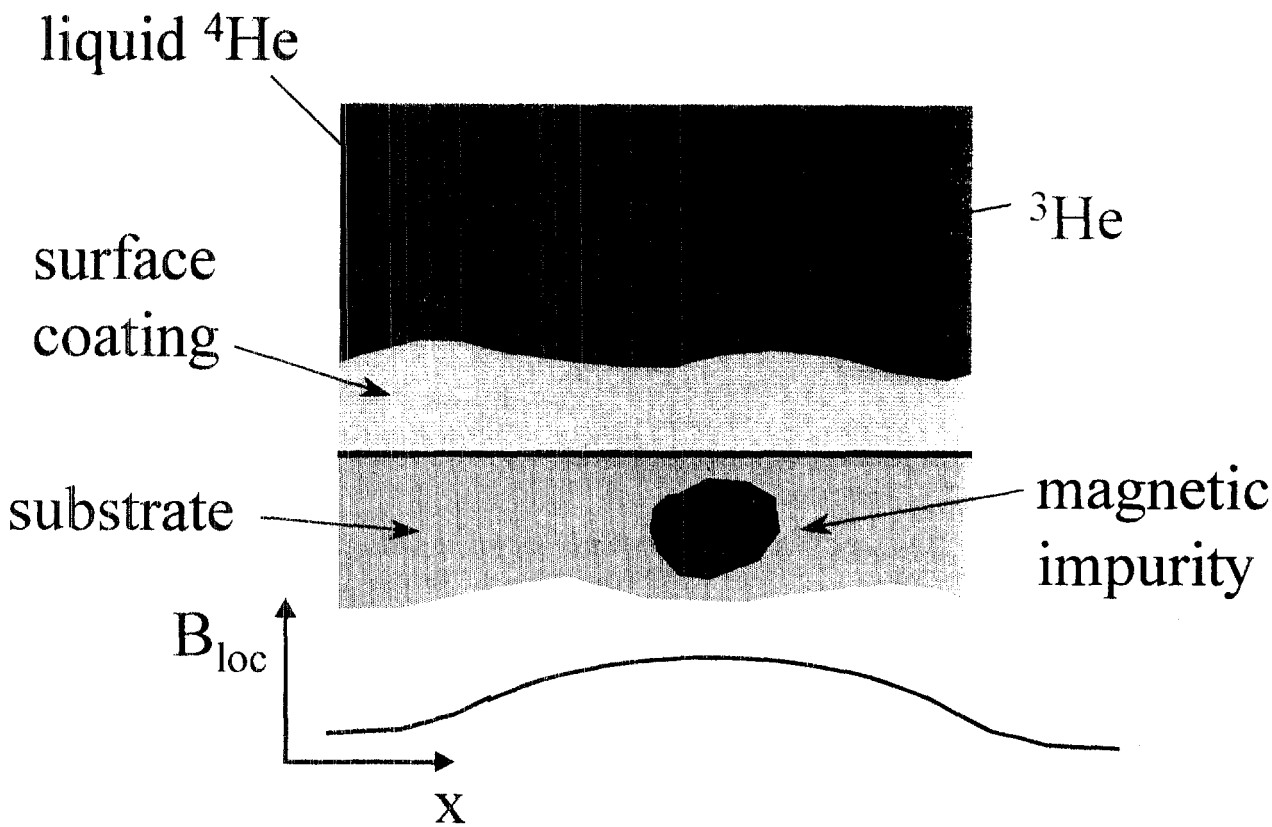

Cs on Pyrex: • very long T_1^w
• not compatible with neutrons
• useful in accumulation cell and "plumbing"

H_2 on Pyrex and Stycast 1266: • long T_1^w
• not compatible with neutrons, but D_2 coatings might work

^{3}He Mean Free Path

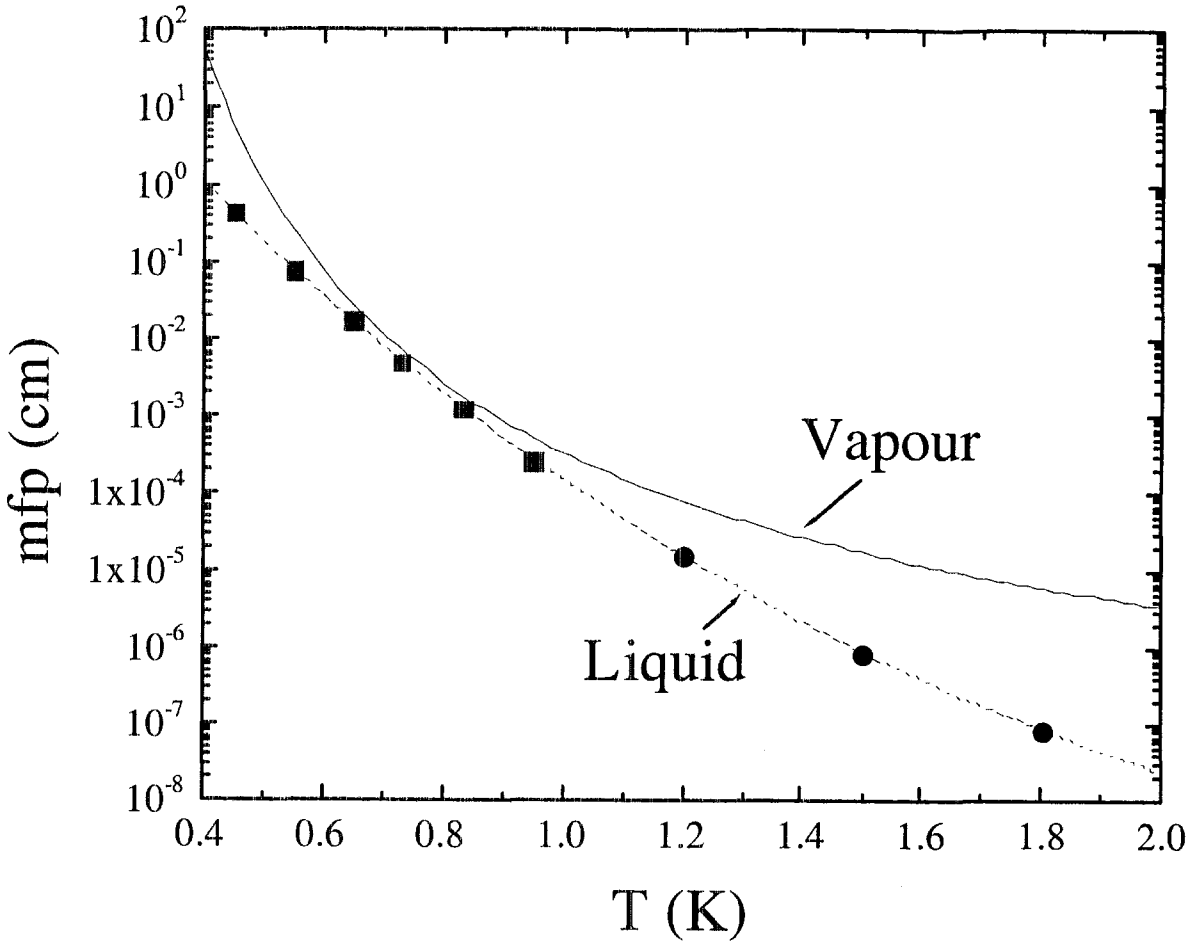

"Cesiated" Glass Substrates

Room temp Heil et al. Phys. Lett. A 201 337 (1995)

- relaxation occurs in bulk Cs and underlying substrate

Low temp pure ^{3}He Tastevin JLTP 89 669 (1992)

- relaxation due to dipolar interactions in bulk liquid

^{3}He - ^{4}He mixtures PRL 73 2587 (1994)

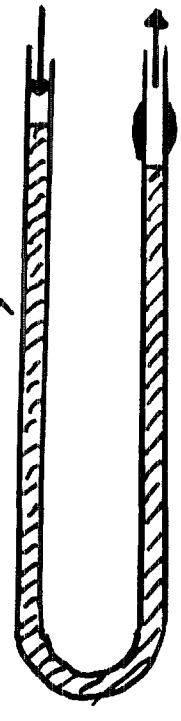

Closed Circulation Loop

T~1K

$T_1 > 5000s$
$A/V \sim 66 cm^{-1}$

Implies $T_1^W > 180h$ for EDM expt.

T~200mK

Benefit: gettering action of Cs tends to passivate paramagnetic O_2

Issues: Compatability with substrates other than pyrex unknown

Risk of contamination in an "open" geometry

H_2-coated Substrates

- evidence that T_1 improves out to ~10 layers of H_2

I Experiments with unsaturated ℓ-^4He films

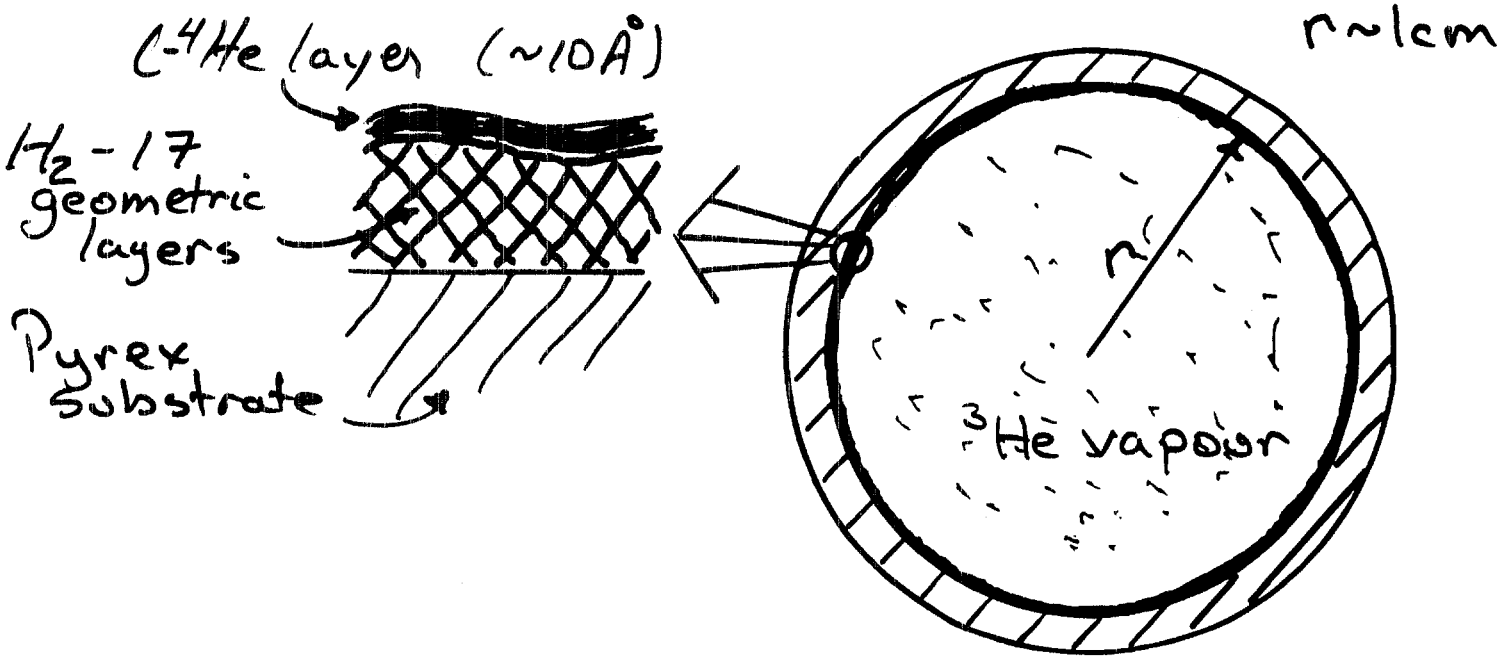

Pyrex: "Clean"-baked at 470°C (10^{-6} Torr) + r.f. discharge cleaning

For T ~ 0.5 K

Sussex Lusher et al JLTP 72, 71 (1988)

$T_1 \sim 10^4$ s at 2.5 KG

ENS Himbert + Dupont-Roc JLTP 76 435 (1989)

$T_1 \sim 10^{-3}$ s at 14 G

Postulate difference due spectral densities of correlation function for perturbation

$$\frac{1}{T_1} \sim \frac{1}{1+\omega^2\tau_c^2}$$

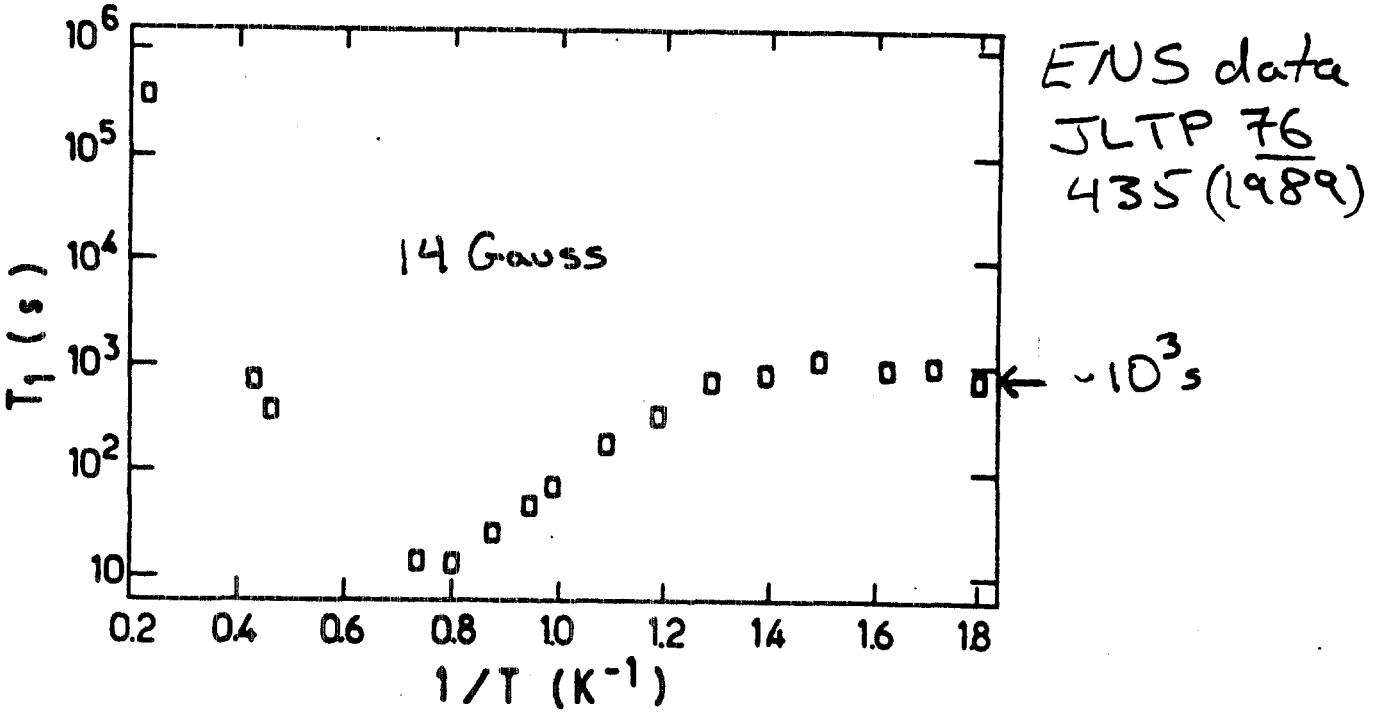

Fig. 2. Longitudinal relaxation time T_1 (logarithmic scale) versus the inverse temperature between 4.2 K and 0.5 K for a particular cell. Lower temperatures are on the right part of the figure.

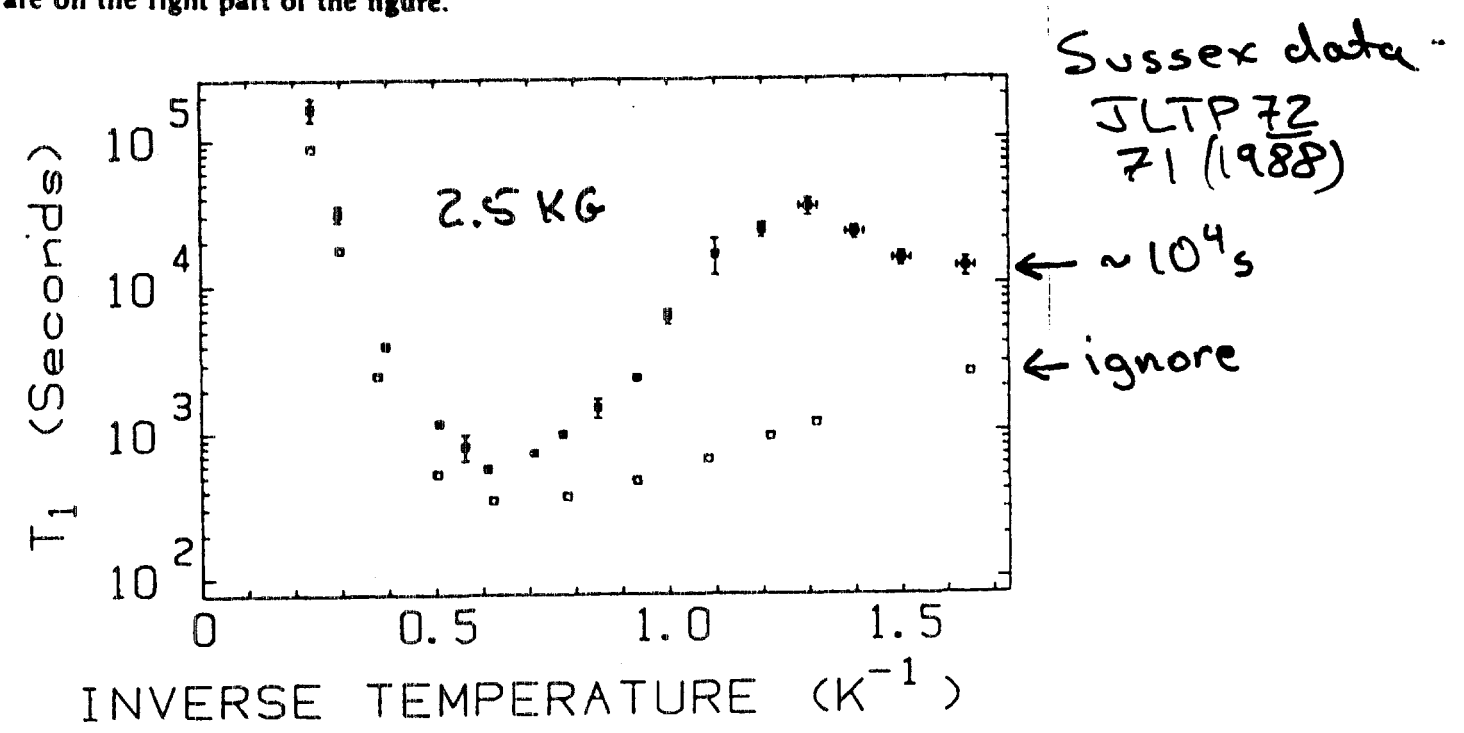

Fig. 4. Values of T_1 measured at 7.7 MHz in sealed Pyrex cells containing ^3He-^4He-H_2 mixtures. (■) $n_3 = 3.3 \times 10^{23}$ m^{-3}, $^3He:^4He = 5:1$; (□) $n_3 = 9.8 \times 10^{23}$ m^{-3}, $^3He:^4He \approx 100:1$.

Estimate $\tau_c \sim 6 \times 10^{-8}$ s ... long!

$\tau_c \gg$ transit time through film

~ exchange time in solid ^{3}He ??

(suggests relaxation near H_2 - l^4He bdy.)

II Experiments with bulk liquid ^{3}He-^{4}He mixtures

UBC PRL 67 839 (1991)

→ Condenser of ^{3}He-^{4}He distillation column for producing polarized ^{3}He

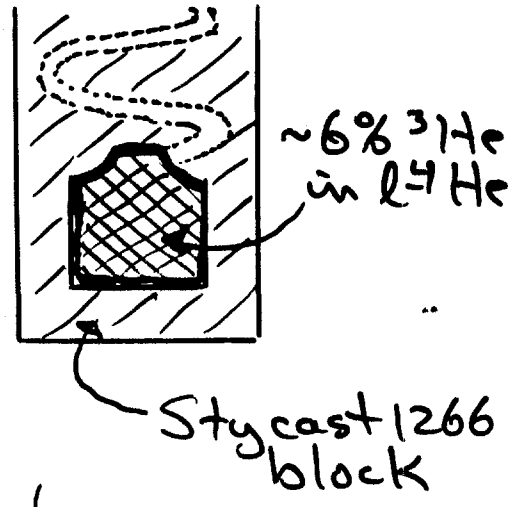

$T_1 \sim 1$ min at 47 KG on bare Stycast

~ 4000 s at 47 KG on H_2-coated Stycast.

Relevance to EDM Expt.

What happens to T_1 as the bulb is filled by adding ℓ-^{4}He ??

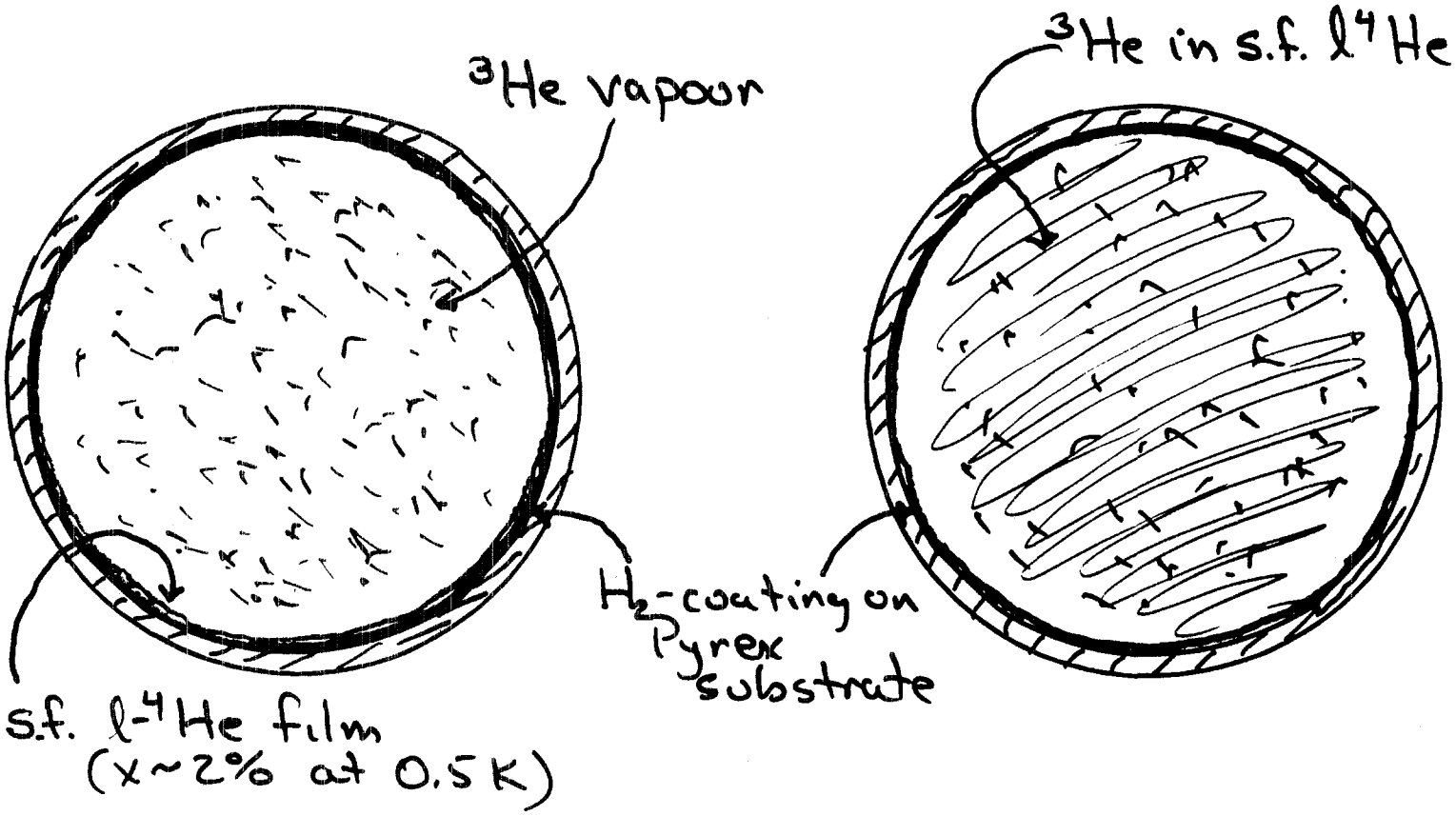

$T_1 \sim 10^3$ s (ENS Expt)

$T_1 \sim$?

Pesimistic viewpoint: $1/T_1 \sim \frac{A}{V}$

ENS expt $A/V \sim 3\,cm^{-1}$
EDM expt $A/V \sim 0.5\,cm^{-1}$
} factor 6 to be gained

(Overly) optimistic viewpoint: concentration of ^{3}He near wall is also diluted by a factor

$$\frac{n^*}{n} = \left(\frac{m^*}{m}\right)^{3/2} \exp\left(E_s/kT\right) \sim 10^3 \text{ at } 0.5\,K$$

Reality: Not enough experimental data!

Experiments

H_2 / D_2 coatings: crucial to demonstrat T_1 adequate for EDM experiment

"open geometry" will be a challenge.

No data on D_2

Cs coatings: Pyrex works as a substrate but nothing else has been tried!

durability of coating will be an issue for open geometries
accum. + meas. cell can't communicate at room T!

ABS of pol. ^3He: delicate balance between mfp, orifice diameter, differential pumping rate, temp. gradients, l-^4He level may be required to keep ^3He in liquid - demonstration needed!

Field Gradients: tightly linked to design*, but the long mfp regime is not as well understood as short mfp regime.

- analogy to H masers ... wall shift if sticking times on D_2 are long?

Basic Science

↓ Simultaneous measurement of mass and spin diffusion coefficients?

ABS may be a great tool for studies of $R(\kappa, \Theta)$

* refine design criteria to reflect $\frac{1}{T_1}, \frac{1}{T_2} \sim G^2$?

Determining the projects to be undertaken at each institution
moderated by Steve Lamoreaux (Los Alamos)

To Do – Prioritized List

1. T_1, T_2 ^3He in realistic cells

   A. Polarized ^3He production

   B. Transport – theory, apparatus

   C. Test Cells Room temp, superfluid helium filled, etc.

Experiment # 1

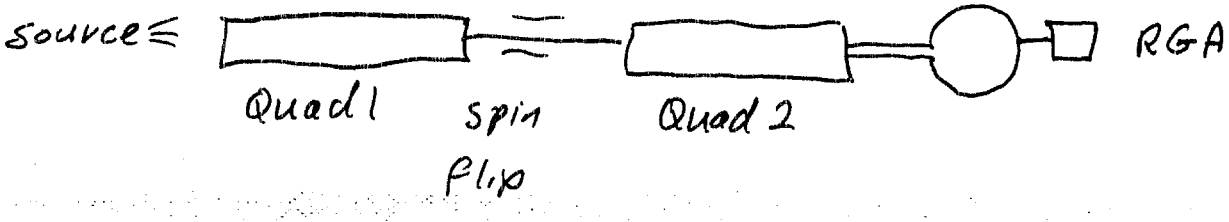

Bulb, 20 cm diameter

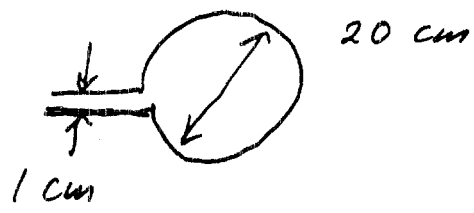

$\gamma = \frac{A_h}{4V} v = 5\ sec^{-1}$

$v = 10^5\ cm/s$ 300K

$\frac{10^{14}/sec}{\gamma} = 2 \times 10^{13}$

$\approx 10^{-7}$ torr

$(5 \times 10^9/cc)$

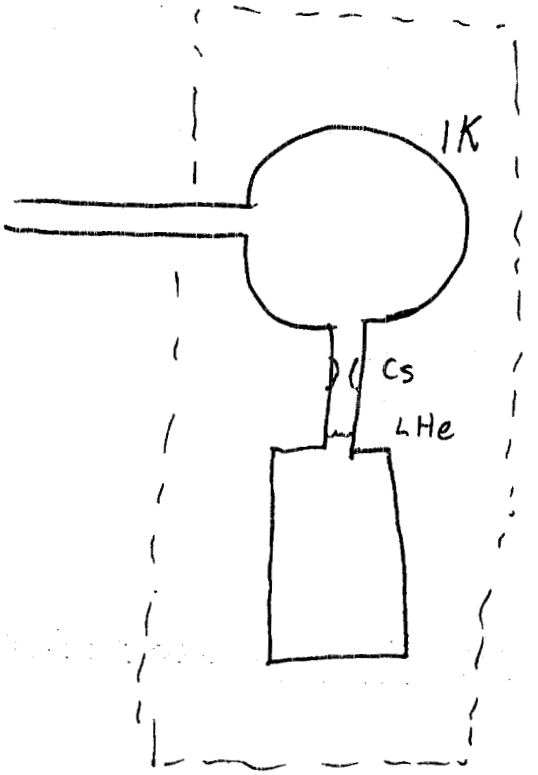

or 300K

1.5 years

time scale

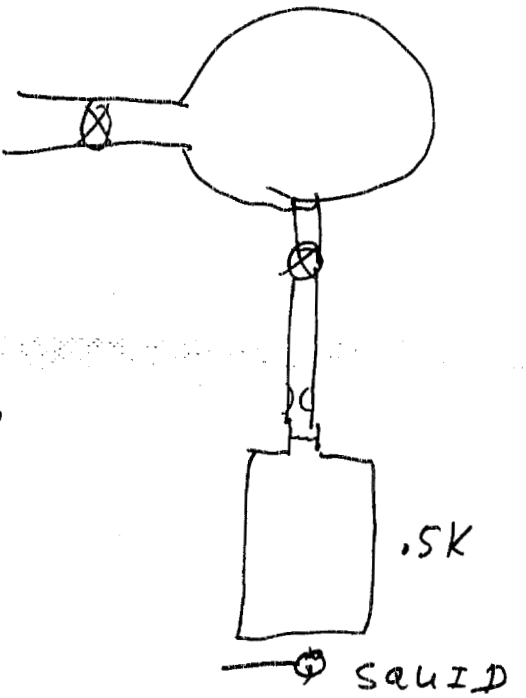

or lower

Transport, Quad.

LANL
SFU

Cell Study w/ optical pump.

UIUC, NIST
SFF, CalTech
MIT

~~SFU~~

~~LANL~~

~~NIST~~

2. High Voltage tests UCB/LANL

A. Background light

B. Capacitive multiplier

C. Damage

D. Kerr effect for in situ measurements UCB

E. Review LANL design

3. Couple 1 & 2
HV effects on lifetime

4. Field Modelling

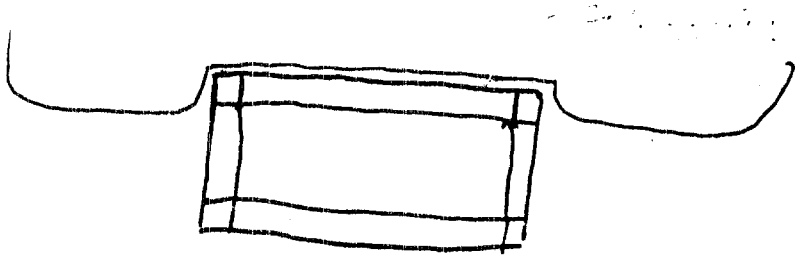

5. Light collection tests & Modeling
Maryland - ... NIST, UIUC
Fibers LANL, MIT

Heat pulse due to RF spin reorientation pulse

If dressing is used, penetration <u>not</u> in optimal region for static or RF field.

Need 3-d calculations with Eddy currents

Measurements of low temp properties of Metglas, cryoperm.

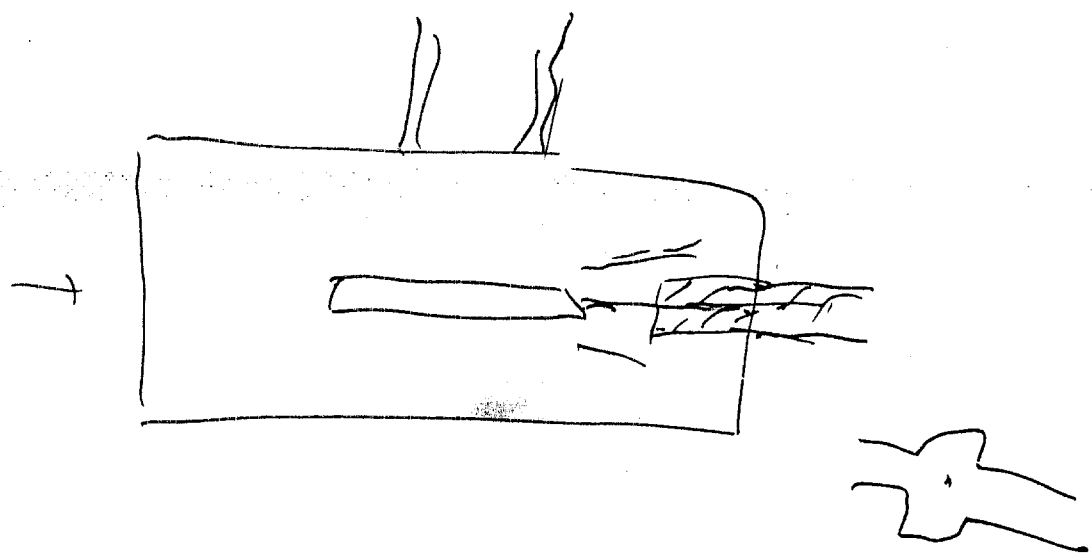

6. Materials selection

A. Johnson noise theory.

UCB Espy 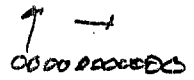 $\frac{1}{r}$.

B. Ferromagnetic shielding
   a. Shaking
   b. dressing

Caltech Materials, field design study

Need hyteresis loops to get power dissipation HMI

Metglas, Cryoperm acrylic

Plastic cryostat ?

B/H Curves, conductivity

C. Eddy currents from dressing, shaking HMI
   a. Barkhausen noise

   b. need $1/10^3$ homogenity of dressing field.

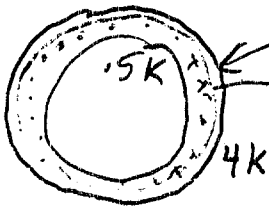

Super ferro $\rho \approx .01\,\Omega\cdot m$

Skin depth

thickess

δ; $t/\delta = 10^{-3}$

$f = 1\,KHz$

$\rho = \sim .01\,\Omega\cdot m$

7. Purification

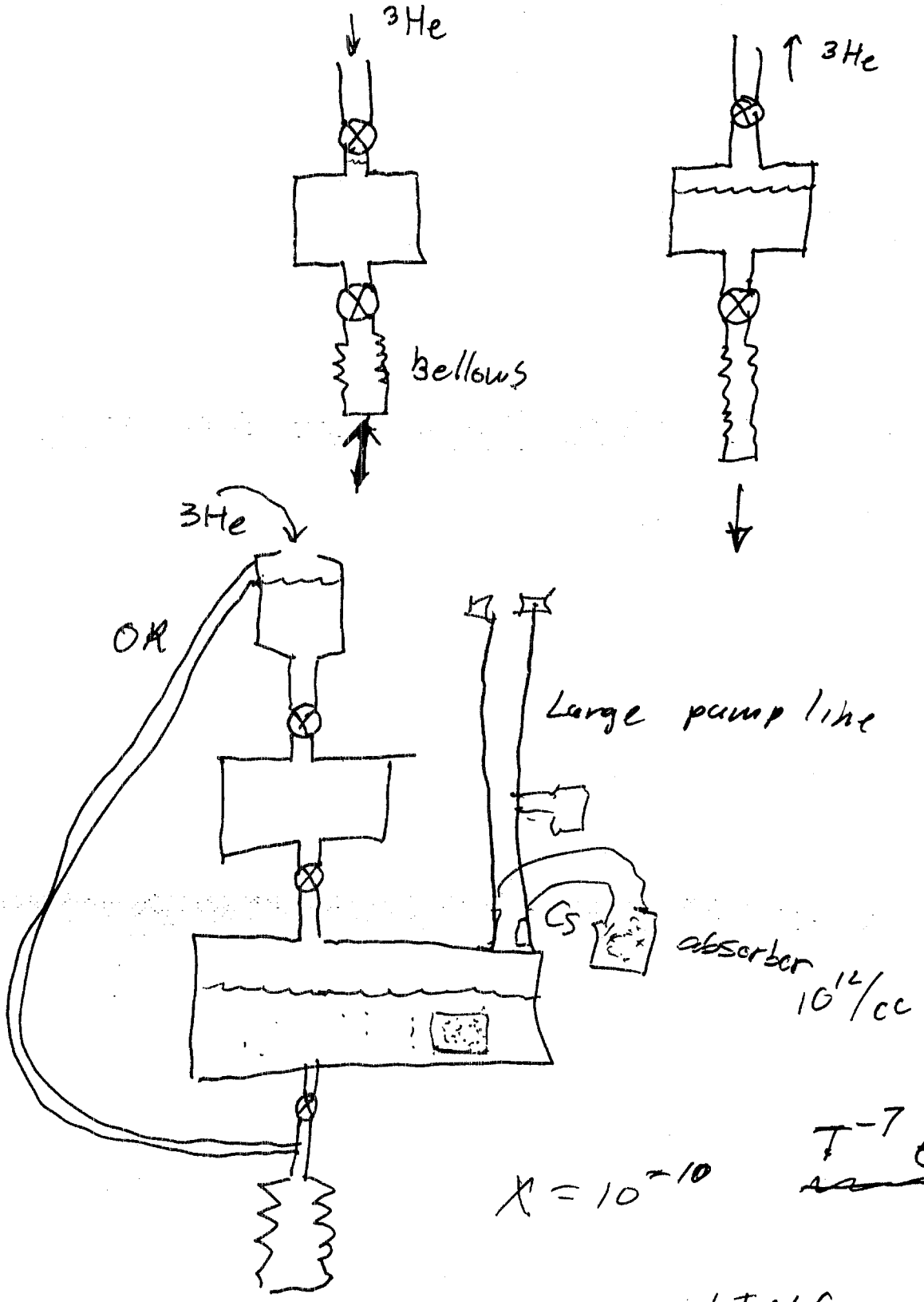

$\chi = 10^{-10}$ $\quad T^{-7} e^{-E/kT} T^{1/2}$

* High Priority

UIUC

SFU

~~UCB~~

8. Monte Carlo Studies

A. Activation

B. Polarizer

C. Light Collection

Maryland

LANL

9. UCN Test - NIST

HMI / NIST

LANL

10. Proposal

Peter Barnes

Future telephone conference calls
moderated by Martin Cooper (Los Alamos)

Development of a financial strategy moderated by Martin Cooper (Los Alamos)

DEVELOPMENT OF A FINANCIAL STRATEGY

Funding for equipment to carry out the R&D plan
Funding for people to carry out the R&D plan
Final experiment funding from non-DOE Nuclear Physics
  Breaking the experiment into distinct pieces